EXPERIMENTAL STUDY ON ICE MANAGEMENT THROUGH THE USE OF PODDED PROPELLER WASH

JENNA MADELINE FERRIERI

Experimental Study on Ice Management through the use of Podded Propeller Wash

by

© Jenna Madeline Ferrieri

A thesis submitted to the School of Graduate Studies

in partial fulfillment of the requirements for the degree of

Master's of Engineering

Naval Architecture and Ocean Engineering

Memorial University of Newfoundland

December 2012

St. John's, Newfoundland

ABSTRACT

Propeller wake wash phenomena were investigated as a means of clearing pack ice, as used during ice breaking and ice management operations. Experiments were performed to model the propeller wash and data were collected in order to quantify the capacity of a propeller to clear pack ice under a range of operating and environmental conditions. The work focused on the interaction between operating and environmental conditions using a central composite experiment design with four factors: propeller shaft speed, inclination angle, initial ice concentration, and distance to the ice edge. It was found that the propeller shaft speed was the most significant factor and that increasing propeller rotation speed increased ice clearing most effectively. In order to clear ice far downstream of the propeller, it was found that directing the propeller wash at the water's surface imparts more energy to the ice pieces, causing them to travel farther.

ACKNOWLEDGEMENTS

I would like to extend my gratitude to all those who have helped in the completion of this Master's thesis. First and foremost, I would like to thank Dr. Brian Veitch and Dr. Ayhan Akinturk for their invaluable help and guidance as my advisors throughout my time at Memorial University of Newfoundland. I would also like extend my thanks to the ABS Harsh Environment Technology Centre for funding a portion of this research and the additional funding from NSERC. Finally, I would like to acknowledge Timo Särkkä as well as the staff of the National Research Council Ocean, Coastal, and River Engineering (OCRE), especially Jungyong Wang, Chris Meadus, Collin Keats, Jim Williams, Mike Walsh, and Wayne Pearson, for their support during the experiment program.

TABLE OF CONTENTS

LIST OF TABLES

LIST OF FIGURES

LIST OF APPENDICES

NOMENCLATURE

A	Propeller Disk Area
ABS	American Bureau of Shipping
BEM	Blade Element Method
c	Chordlength of Blade Element
c_d	Drag Coefficient
c_l	Lift Coefficient
CAD	Computer Aided Design
C_t	Propeller Thrust Coefficient
d	Difference Between Calculated and Measured Force
D_p	Propeller Diameter
D_h	Hub Diameter
GDAC	General Display and Control
k	Number of Data Points in Calibration Set
L_m	Length Term Dependent on Blade Area Ratio
m	Order of Calibration Equation Polynomial Plus One
$\dot{m}$	Mass Flow per Unit Time
n	Propeller Rotational Speed
N	Blade Number
NRC	National Research Council
NSERC	Natural Sciences and Engineering Research Council
OCRE	Ocean, Coastal, River Engineering

P_d	Delivered Power
Q	Propeller Torque
r	Radius to Blade Element
Re_{flow}	Flow Reynolds Number
Re_{prop}	Propeller Reynolds Number
RPM	Revolutions per Minute
RPS	Revolutions per Second
T	Propeller Thrust
U	Expanded Uncertainty
u_c	Combined Uncertainty
u_f	Uncertainty Associated with Applied Force
u_r	Uncertainty Associated with Assuming Linear Fit
V_0	Efflux Velocity
V_A	Upstream Flow Velocity
V_B	Downstream Flow Velocity
W	Incident Velocity on Blade Section
x_1	Factor 1 – Propeller RPS
x_{1p}	Factor 1 – Delivered Power
x_2	Factor 2 – Inclination Angle
x_3	Factor 3 – Distance to the Ice Edge
x_4	Factor 4 – Degree of Ice Cover
Y_{R1}	Response for Area 1

Y_{R2}	Response for Area 2
Y_{R3}	Response for Area 3
Y_{R4}	Response for Area 4
Z	Number of Propeller Blades
ZEF	Zone of Established Flow
ZFE	Zone of Flow Establishment
β	Blade Area Ratio
β_a	Advance Angle
η_s	Shaft Transmission Efficiency
λ	Scaling Factor
ν	Viscosity of Water
ρ	Density of Water

CHAPTER 1 – INTRODUCTION

ICE MANAGEMENT

As the offshore industries expand farther into Arctic waters, the environmental threats pose a challenge to robust offshore structure design. Arctic offshore structures are built to withstand ice loads as required by classification societies, but must also either rely on ice management techniques or disconnect to move away from ice threats. The ISO 19906:2010(E) International Standard defines ice management as involving "various operational procedures that can be used to reduce global and local design ice actions." Eik (2008) explains that ice management includes ice detection, tracking, and forecasting, threat evaluation, icebreaking, ice clearing, and offshore structure disconnection procedures.

Physical ice management can significantly reduce the severity of ice-structure interactions (Taylor et al. 2012). This procedure involves breaking up ice floes that are imposing on offshore drilling and exploration operations before the ice threatens to stop the operation. One method of accomplishing this is involves the use of two different size ice breakers. The more powerful icebreaker is positioned farther upstream of the offshore structure. This vessel breaks the initial incoming ice floe by manoeuvring in a zigzag pattern. The less powerful icebreaker breaks the ice floes into even smaller pieces by operating in the same manner (Edmond et al. 2011). Figure 1 shows this idealized concept of ice management with two icebreakers.

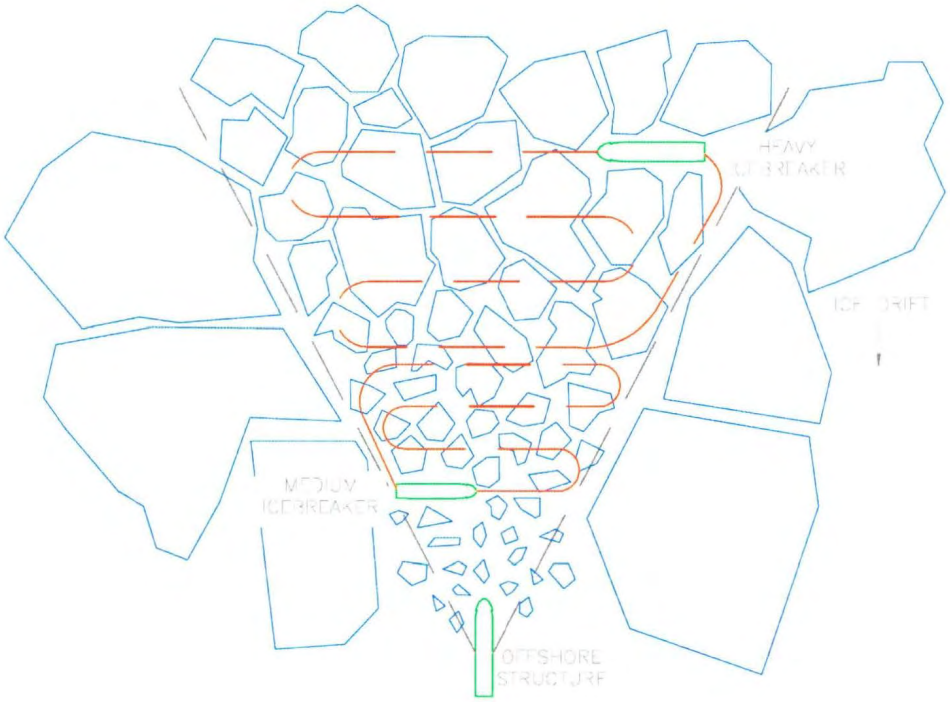

Figure 1. Physical Ice Management with Two Icebreakers
[After Daly and Colbourne 2012]

In recent operations, the smaller of the two icebreakers has been employed to direct propeller wash towards the ice floe and thereby direct it away from the offshore structure ((Edmond et al. 2011). Less conventional propulsion systems, such as azimuthing podded propulsors, which have the propulsor, shaft, and steering gear housed in a single unit, can generate thrust in any direction as the propeller azimuths around a central vertical axis. This has practical utility in ice management operations that employ propeller wash as a means of ice management.

Azimuthing podded propulsors offer a number of benefits in ice management. Azimuthing thrusters have been found to effectively clear ice from ports, around escorted vessels and offshore platforms. Further, the increased manoeuvrability means that the vessel can accurately position itself to manage only the ice that needs to be managed.

(Keinonen, 2008a). Figure 2 is a schematic diagram of using propeller wake wash as a means of ice management.

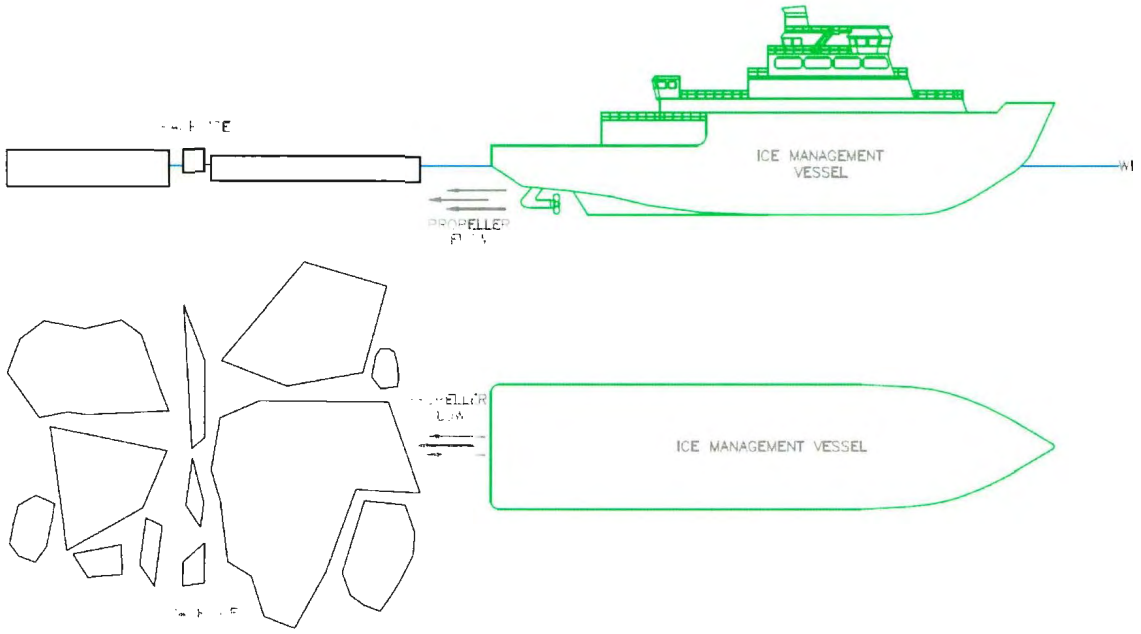

Figure 2. Schematic of Using Propeller Wake to Clear Ice

LITERATURE REVIEW

Assessments have been completed for iceberg management operations off the Newfoundland coast which evaluate the capabilities of physical management of icebergs, including management techniques, current practices at the time, and new developments in iceberg management operations (Anderson et al. 1986; Crocker et al. 1998). Both of these papers have found that azimuthing thruster wake was successfully used in practice for iceberg management of small ice masses. Anderson et al. (1986) also stated that high sea states cause the thruster wake to dissipate quickly and therefore reduce the effectiveness of this technique. This study does not specify ice coverage or sea state with regards to the limitations. More recent reviews of ice and iceberg management techniques have been

completed by Eik (2008), Keinonen (2008a), and Randell (2009).

There are a number of studies which focus on ice management operations for specific offshore sites. Eik and Gudmestad (2010) performed an evaluation of iceberg management systems for an offshore site in the Barents Sea. This study included numerical simulations to obtain maximum ice loads on the offshore structure with and without ice management and found that the maximum load was significantly reduced with ice management. Edmond et al. (2011) outlines the initial ice and iceberg management plans for the Shtokman Field in the Barents Sea and explains the rationale behind the choices made for ice operations. These more recent reviews of ice management comment on the use of azimuthing propeller wake as a means of clearing ice away from offshore structures.

A guide to ice management operations is included in Appendix K – Ice Management Plan of the Revised Outer Continental Shelf Lease Exploration Plan for the Camden Bay region (Shell Offshore Inc., 2011). This plan outlines ice alert levels, the proper procedures for each level of alerts, and personnel responsible for each procedure. This ice management plan is designed to prevent exploration and drilling suspension, however, it also identifies an alert level that triggers the suspension of drilling operations in the event that ice management barriers fail. A broader guide to ice management operations is provided by Dunderdale and Wright (2005). While this guide is intended for operations on the Grand Banks, it presents past ice management operation experience from the Beaufort Sea and Sakhalin Island and provides general ice management operation needs, techniques, and hazards.

Full-scale ice management trials were conducted on two vessels with azimuthing thrusters (Keinonen and Lohi 2000) and the results showed that it was possible to break and clear ice with the propulsors' wake and that precise ice management could be achieved with this propulsion system. Although this study does not specify ice coverage, Keinonen (2008a) reports that azimuthing thrusters were able to create ice free channels in ice with thicknesses ranging from approximately 0.10m to approximately 1.25m in 10/10th ice coverage. This study further explains that when aided by another icebreaker to break up the ice floes, the azimuthing thruster was able to clear up to 2.25m thick ice in 9/10ths coverage. The vessels used for this study were a 25MW and a 15MW icebreaker, however, the power required for ice clearing with azimuthing thrusters is not reported. Keinonen also does not report information on sea states or weather conditions during these full-scale ice management operations. Studies that support the use of podded propulsor wake as a means of ice management include Nyman et al. (1999) and Keinonen (2008b). In addition, a number of papers discuss the use of azimuthing podded propulsors for ships operating in ice covered waters, including Wilkman et al. (2006), Hänninen et al. (2007), and Vocke et al. (2011).

The evolution of propeller wake has been studied in terms of downstream pressure and velocity field measurements (Felli et al. 2006; Johansson and George 2006), as well as downstream mean velocities and turbulence (Nystrom et al. 2007; Lam et al. 2010; Situ et al. 2010; Lam et al. 2011a,b). The purpose of these studies was to characterize the flow characteristics in terms of point velocities in the downstream wake and to quantify the potential for seabed scouring from the propeller jet. In an effort to investigate the

potential of seabed scouring, Lam et al. (2011c) presented a review of equations to predict downstream propeller wake velocities. This study was a comprehensive study of the equations to calculate axial, tangential, and radial components of velocity both within the zone of flow establishment (ZFE) and the zone of established flow (ZEF) for a propeller jet.

Propeller and ice interaction research began in the 1960s with work done by Jagodkin in which a model for the ideal milling situation was investigated. Since then, research has continued in order to gain a better understanding of the forces involved in this propeller and ice interaction. Jagodkin's load prediction model (1963) assumed the ice piece was approaching the propeller at the ship's speed and therefore his model was based on the steady state milling condition. Edwards (1976) later concluded that ice forces on propellers involve both ice milling and ice impact forces, however, his work focused on ice milling as he saw these forces as more important. Wind (1983) later proposed a model focusing on ice impact forces. Additional laboratory testing was performed by Sasajima and Mustamaki (1984) to investigate the effects of milling and contact forces of a propeller operating in the first quadrant. Later experiments expanded previous research by investigating the mechanics of ice failure (Belyashov and Shpakov 1983; Belyashov 1993; Veitch 1994 and 1995). Bose (1996), Doucet et al. (1996), and Walker (1996) performed theoretical and experimental work on the hydrodynamic effects of a propeller blockage. They investigated the hydrodynamic loads and cavitation effects on the propeller.

Laboratory testing of propellers operating in ice expanded in the 1990s and 2000s

to include highly skewed propellers and podded propulsion units, as well as off-design conditions. Searle et al. (1999) and Moores et al. (2001) performed an investigation into the loads on highly skewed propellers. Akinturk et al. (2004) measured forces on a podded propulsor operating in ice with a partial hull stern attached to the unit. Wang et al. (2007, 2008) performed model tests of a podded propulsor operating in ice at various thrust angles in order to investigate propeller performance. Additionally, propeller and ice interaction has been studied in detail at model-scale with regards to the ice contact loads on propeller blades with fairly accurate results when compared to full-scale operations (Spencer et al. 2001). Despite the extensive research of podded propulsors in ice, little effort was applied to cavitation effects of these operations and therefore Sampson et al. (2009) studied podded propeller and ice interactions under depressurized conditions.

A major question previous research does not address is what factors influence the effectiveness of using propeller wake to clear ice. From the literature review performed for this thesis, the only information on the capability of azimuthing thrusters to clear ice is from full-scale trials. No model experimentation has been performed to further investigate this ice management technique. Full-scale experiments do not provide a systematic approach to studying the extents of ice management with propeller wake since they are highly dependent on sea state and weather conditions. Controlled model-scale experimentation can provide further insight into the significant factors that influence the ability to clear ice with propeller wake and can be used as a foundation for further full-scale trials.

SCOPE OF WORK AND PROJECT OBJECTIVES

The focus of this study was on the interaction between the propeller wake wash and ice cover in order to provide insight into the factors that affect the effectiveness of a podded propulsor to clear ice. Model-scale experiments offer an effective means to control important variables in the investigations of ice management through the use of azimuthing propeller wash. An experimental program was undertaken to study four factors involved in ice management using wake wash. The experimental program was conducted at the National Research Council's Ocean, Coastal, and River Engineering facility (previously the Institute for Ocean Technology) in St. John's, NL over a two week period during July 2012.

The objectives of this thesis were:

1. To develop an experimental program to investigate the factors that influence ice management with podded propulsors,
2. To determine which of the factors studied are the most significant, and
3. To develop equations to provide an estimation of the level of ice clearing for areas in the ice field.

Four major milestones have been specified to help in the completion of the above objectives. These were:

1. To familiarize with the current techniques used for ice management,
2. To understand the techniques and applications of model-scale podded propeller experiments,
3. To design an experimental program to model podded propeller wash as a

means of ice clearing, and

4. To perform the designed model-scale experiments, analyze the data collected, and draw conclusions on the results.

CHAPTER 2 – THEORY

MOMENTUM THEORY

One-dimensional momentum theory, also known as axial momentum theory, was first introduced by Rankine as a means of analyzing flow over propeller blades. Rankine's analysis treats the propeller blades as a single actuator disk in a frictionless fluid and makes the assumptions that the flow into the disk is uniform and that there is no rotation in the flow exiting the disk. The theory was later expanded by Froude to introduce rotational velocity to the propeller slipstream (Carlton, 2007).

The delivered power from the propeller and the thrust can be calculated using momentum theory. The delivered power is equal to the increase in kinetic energy of the slipstream per unit time and can be calculated as shown in Equation 1. The propeller thrust is equal to the increase in axial momentum of the slipstream and can be calculated as shown in Equation 2 (Carlton, 2007).

$$P_d = \frac{\dot{m}}{2}(V_B^2 - V_A^2) \qquad (1)$$

$$T = \dot{m}(V_B - V_A) \qquad (2)$$

In these equations, $\dot{m}$ is the mass flow per unit time of the flow through the actuator disk, V_B is the downstream flow velocity, and V_A is the upstream flow velocity. These equations can be rearranged such that the delivered power can be calculated as shown in Equation 3. The delivered power is also equal to the work done by the thrust force on the propeller (Carlton, 2007) and this also shown in Equation 3.

$$P_d = \frac{1}{2}T(V_B + V_A) = TV_0 \qquad (3)$$

In this equation, V_0 is the maximum velocity at the face of the propeller and is also known as the efflux velocity. Rearranging the above equation shows that V_0 can be calculated as the mean of the upstream and downstream flow velocities (Equation 4).

$$V_0 = \frac{1}{2}(V_B + V_A) \qquad (4)$$

BLADE ELEMENT METHOD

Froude expanded upon momentum theory (Carlton, 2007) by introducing blade geometry to the analysis. This became known as Blade Element Momentum (BEM) theory. BEM theory separates the propeller blade into discrete blade elements and assumes that the change in momentum of fluid passing though a blade element is provided solely by the force on the blade element from an incident velocity. This incident velocity is comprised of both an axial velocity and a rotational velocity. The blade section experiences lift and drag from a combination of the blade element's zero lift angle and the incidence angle. From this, the thrust and torque for the blade element can be calculated as shown in Equation 5 and Equation 6, respectively.

$$dT = \frac{1}{2}\rho Z c W^2 (c_l \cos(\beta_a) - c_d \sin(\beta_a))dr \qquad (5)$$

$$dQ = \frac{1}{2}\rho Z c W^2 (c_l \sin(\beta_a) + c_d \cos(\beta_a))dr \qquad (6)$$

In these equations, ρ is the density of water, Z is the number of propeller blades, c is the chordlength of the blade element, W is the incident velocity, c_l is the lift coefficient, c_d is the drag coefficient, β_a is the advance angle, and r is the radius to the blade element. These elemental thrust and torques are then integrated across the propeller blade to obtain the propeller thrust and torque.

WAKE PLUME

When a vessel is stationary, the wake is a function of the rotating propeller. As the longitudinal distance from the propeller increases, the flow velocity decelerates while the ambient fluid is accelerated slightly. This is because high viscous shear eddies are generated which induce lateral mixing of the propeller wake (Lam et al. 2011a). The propeller wake is classified by two regions – the zone of flow establishment (ZFE) and the zone of established flow (ZEF). Figure 3 is a schematic drawing showing propeller wake discharge.

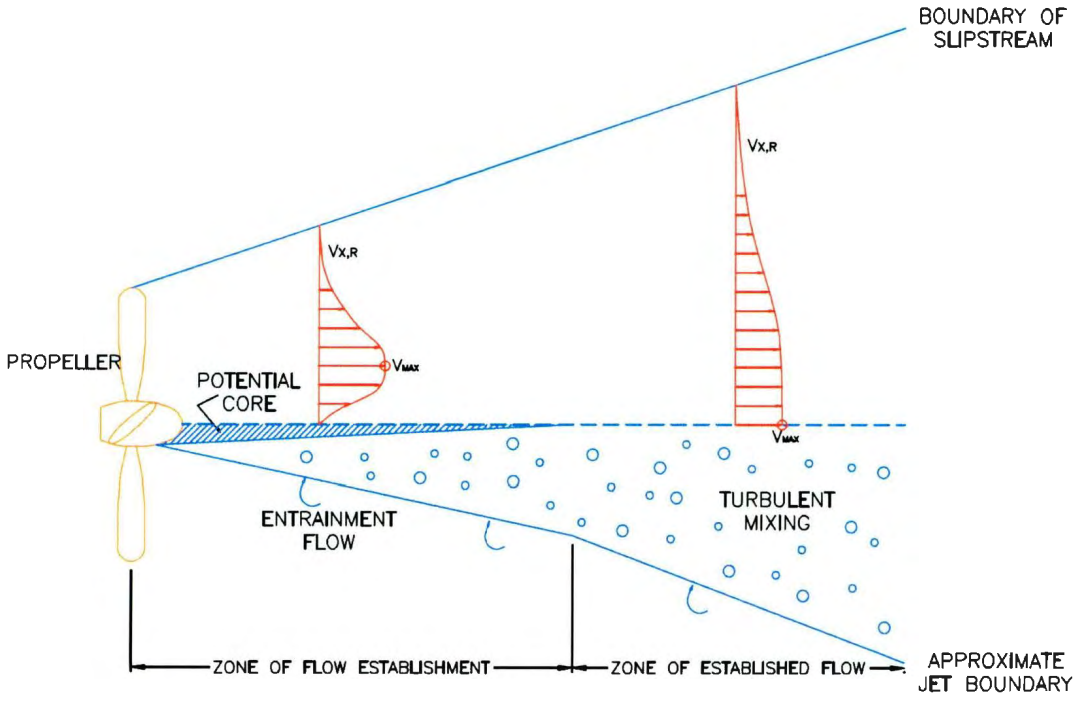

Figure 3. Schematic Diagram of Propeller Wake
[After Lam et al. 2011b, 2011c]

The ZFE is closest to the propeller face. In this region, there is a low velocity core along the axis of rotation of the propeller due to the lack of thrust generation by the propeller hub. In this zone, the axial velocity profiles have two peaks corresponding to the

rotation axis and the edge of the propeller hub (Lam et al. 2010). At a distance downstream, the rotating flow begins to mix and when the mixing with surrounding fluid reaches the axis of rotation of the propeller, the ZEF begins (Situ et al. 2010). At this point, the flow will only be mixing outwardly and there is one peak velocity, located at the axis of rotation (McGarvey 1996; Lam et al. 2010).

Decay within the propeller wake is proportional to the distance downstream for both momentum and energy decay (Lam et al. 2011a). However, in the axial direction, energy losses are typically faster when compared to momentum losses. Lam et al. (2011b) suggest an equation to determine the axial velocities for the ZFE that is an expansion of Stewart's (1992) finding that the axial velocity decays immediately from the propeller face. Stewart's decay equation for the ZFE is not valid at the efflux plane and therefore Lam et al. (2011b) proposed the linear equation shown below (Equation 7) to enable Stewart's equation to also predict axial velocity at $x/D_p=0$. Stewart (1992) also proposed a linear equation to predict the axial velocity decay in the ZEF, which is shown in Equation 8.

$$\frac{U_{max}}{U_0} = 1 - 0.1592\left(\frac{x}{D_p}\right) \tag{7}$$

$$\frac{U_{max}}{U_0} = 0.543 - 0.0281\left(\frac{x}{D_p}\right) \tag{8}$$

Equations for estimating the efflux velocity and viscous scaling effects are discussed further in Chapter 5.

CHAPTER 3 – EXPERIMENT DESIGN

DESIGN OF EXPERIMENTS – CENTRAL COMPOSITE DESIGN

There are numerous approaches to conducting experiments. The one-factor-at-a-time approach involves setting a baseline and range for all factors to be studied. The experiments then involve varying each factor, one at a time, over this range. While this method is commonly used in physical model testing, it does not consider interaction effects of the factors studied. Another method, which does account for interactions, is to use a factorial design where the factors are varied together rather than one at a time.

A factorial experiment involves varying factors between three levels—high, center, and low, however, this can be further expanded to include axial points and center points in order to generate a response surface of the results (Montgomery, 2009). A central composite design is one class of response surface experiment designs, and this was the approach used for this experimental program.

Central composite designs require five levels for each factor—low axial, low level (*-1*), center level (0), high level (*+1*), and high axial. For a rotatable design, the axial levels are set to (*-2*) and (*+2*) for the low axial and high axial levels, respectively. The factorial runs consist of experiments in which the factors are varied between a low level (*-1*), a center level (*0*), and a high level (*+1*). The axial points are tested with only one factor at a low (*-2*) or high (*+2*) axial level while the remainder are at the center level (*0*). Experiments at the center point are repeat experiments with all factors at the center level (*0*) in order to provide an estimate of experimental error (Montgomery, 2009; Lye, 2011).

FACTORS AND LEVELS

Four factors were chosen that were believed to have high significance in ice management operations. Additionally, for factors pertaining to the ship and podded propulsor unit, it was important to keep the ease with which the factors can be changed in mind. The four factors are presented in Table 1 with the corresponding levels for model-scale and full-scale values for a scale factor of 20 are shown for illustration. Three of the four factors, propeller shaft speed, inclination angle, and distance from the ice edge, pertain to the ship and can therefore be altered during ice management operations while only one, degree of ice cover, is dependent on the operating environment.

Altering the propeller shaft speed changes the amount of energy transferred to the propeller wash, and was therefore deemed a factor that should be tested in this program. The maximum propeller shaft speed of the podded propulsor unit is 16 RPS. The maximum propeller shaft speed used in the experimental program for this thesis was chosen as 15 RPS, which corresponds to approximately 200 RPM at full-scale. Likewise, the minimum propeller shaft speed was chosen as 5 RPS, which scales to approximately 67 RPM. This is a fairly low operating propeller shaft speed full-scale and therefore no lower rotational speeds were considered. The maximum and minimum rotational speeds are the axial levels for the experimental program and therefore the low, high, and center levels are spaced at equal intervals between the axial levels. Froude scaling was used as the means to determine the full-scale propeller shaft speeds and follows Equation 9.

$$\frac{V_{model-scale}}{V_{full-scale}} = \sqrt{\frac{l_{model-scale}}{l_{full-scale}}} \tag{9}$$

Table 1. Factors and Corresponding Levels

Model-scale					
Factor	**Low Axial (-2)**	**Low Level (-1)**	**Center Level (0)**	**High Level (+1)**	**High Axial (+2)**
RPS (x_1)	5	7.5	10	12.5	15
Inclination Angle (x_2)	-2.5 deg	0 deg	2.5 deg	5 deg	7.5 deg
Distance to Ice Edge (x_3)	0.1 m	0.4 m	0.7 m	1.0 m	1.3 m
Degree of Ice Cover (x_4)	15%	30%	45%	60%	75%
Full-scale ($\lambda = 20$)					
Factor	**Low Axial (-2)**	**Low Level (-1)**	**Center Level (0)**	**High Level (+1)**	**High Axial (+2)**
RPM	67.1	100.6	134.2	167.7	201.2
Inclination Angle	-2.5 deg	0 deg	2.5 deg	5 deg	7.5 deg
Distance to Ice Edge	2 m	8 m	14 m	20 m	26 m
Degree of Ice Cover	15%	30%	45%	60%	75%

The smallest achievable distance between the tip of the propeller hub and the ice edge was 0.1 m at model-scale. At this distance, the ice pieces were touching the side of the hull. Based on the wake velocity and decay studies by previous investigators, it was found that there are a number of estimations for the extent of the ZFE. Stewart et al. (1992) proposed a distance of $x/D_p < 3.25m$ and Lam et al. (2011b) proposed a distance of $x/D_p < 3.68m$ as the extent of the ZFE. When using these proposed distances, the

extent of the ZFE was determined as 0.65m and 0.74m for the Stewart and Lam estimations, respectively. Therefore, when choosing the distances to the ice edge, a distance of 0.7m was chosen as the centerpoint distance. Using this centerpoint and the minimum achievable distance of 0.1m, the change between each factor level was chosen as 0.3m which resulted in a maximum distance of 1.3m. The range of distance to the ice edge therefore included distances in which the ice edge is within the ZFE and ZEF. At full-scale, this maximum distance of 1.3m corresponds to approximately 26 m. It would seem that during ice management operations, one would want to be as close to the ice edge as possible in order to direct full force propeller wash into the ice field, rather than have the propeller wake dissipate in the open water between the ship and the ice. Studies of propeller wake modeling have shown, however, that the plume expands with increasing distance from the propeller (Situ et al. 2010). Because of this, it is possible that moving the ship away from the ice edge could allow a larger expanse of ice to be cleared due to the larger propeller wake plume. The strength of the plume must also be considered as the distance to the ice edge increases, because although the plume will be larger, the strength of the flow will be less due to energy losses.

Degree of initial ice cover is environment dependent and is therefore not easily controlled during ice management operations. This was included as a factor in order to study the ability of podded propeller wash to clear various concentrations. The interval chosen between levels was 15%, with a minimum concentration of 15%. This resulted in a maximum concentration of 75%. Ice coverage of 60% is generally considered the point at which ship manoeuvrability becomes hindered and ice breaking is necessary (Daley

and Colbourne. 2012). In the conditions where ice breaking is required, it would seem difficult to maneuver a vessel to make use of ice management with podded propulsors, and therefore the range of ice concentration studied seems appropriate for this type of ice management.

MEASURED RESPONSES

For the experimental program, responses were measured on the pod unit as well as for the ice field. The measured response of the ice field was directly used in the central composite design analysis while the podded propeller measurements were used to determine the delivered power of the propeller and make comparisons to the theoretical estimations of thrust and power.

Measurements from the pod unit included thrust, torque, propeller shaft speed, and the *Y*-component of the global dynamometer. These responses were then used to generate bollard condition open water curves for the podded propulsors, which will be further explained in Chapter 5.

The measured response for the ice field was the change in concentration of the ice cover. This was accomplished through the use of a Machine Vision recorder through which the video files were extracted and analyzed for the initial concentration of ice cover and the concentration of the ice cover once the propeller had stopped rotating. These two values were then subtracted to yield the change in concentration.

EXPERIMENTAL PLAN

For this program, a four factor, central composite, rotatable design was used with

six center points and no replication. This experiment setup yields 16 full-factorial runs, 8 axial point runs, and 6 center point runs, totaling 30 experiments to be performed in order to adequately study the four factors and the possible interaction effects. Using Design-Expert® Version 8 software for the experiment design, an experiment plan was developed with the desired parameters. The experiment plan for this program can be found in Appendix B.

When using the process of design of experiments, it is necessary to randomize the order in which the experiments are completed to reduce the influence of experiment runs on subsequent ones. The experiment plan is therefore in this randomized order (Appendix B).

CHAPTER 4 – EXPERIMENTATION

EXPERIMENTAL PODDED PROPULSOR AND PROPELLER

The podded propulsor used for this experimental program was designed and built by the National Research Council of Canada's Ocean, Coastal, and River Engineering Institute for research involving podded propulsors in ice (Liu, 2006; Wang et al. 2004). The model podded propulsor can be operated either in tractor or pusher mode. However, in these experiments it was operated in the tractor mode, in which the propeller is upstream of the pod strut. Figure 4 is a simplified drawing of the pod unit, without a propeller installed.

Figure 4. Podded Propulsor Unit

This pod unit contains a load cell installed at the propeller hub to measure thrust and a torque strain gauge on the shaft to measure the torque on the shaft. Additionally, there is a six-component global dynamometer to measure forces and moments on the pod unit in *X*-, *Y*-, and *Z*-coordinates. The dynamometer consists of one load cell in the *X*-direction, two load cells in the *Y*-direction, and three load cells in the *Z*-direction. Figure 5 indicates the locations of these load cells. The drive motor for the propeller is mounted above the global dynamometer and the propeller shaft speed is controlled through this. There is an additional motor mounted below the drive motor which controls the azimuthing position of the unit.

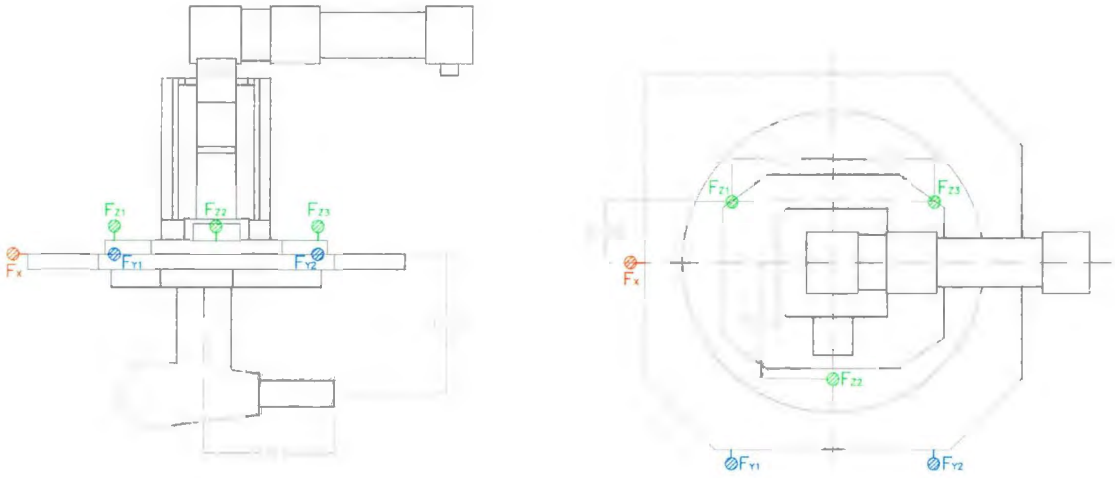

Figure 5. Global Dynamometer Load Cell Locations

For the purposes of this program, the pod unit was configured to measure propeller thrust, torque, and propeller shaft speed, as well as the *Y*-component of the global dynamometer to allow for a secondary thrust measurement. The *X*- and *Z*-components were not acquired since the pod unit was not azimuthing during experiments and therefore no loads would be experienced in those directions.

All data from the podded propulsor unit were collected through OCRE's data acquisition software, GDAC. This program was also used for calibrations of the podded propulsor unit.

CALIBRATIONS

Calibrations are a necessary procedure for experiments. From a calibration, the digital data can be accurately converted into physical values from output voltages. For this experimental program, the podded propulsor unit was calibrated for propeller thrust and torque, as well as the *Y*-component of the global dynamometer.

Injection calibrations were first conducted on each of the channels to be sampled during the experimental program, using the GDAC Calibration program. In this process, a sensitivity value, determined from a previous physical calibration of the podded propulsor unit, is used to inject a corresponding voltage into the specified channel. In doing so, the desired calibration slope is developed. The global dynamometer load cells were calibrated over a range from 30mV to -30mV while the thrust and torque dynamometers were calibrated over a range from 800mV to -800mV.

Once the injection calibration was completed, known loads were applied to the podded propulsor unit to obtain a calibration equation for the thrust, torque, and *Y*-component load cells. This calibration equation would then be used to convert the output voltage from the podded propulsor unit to a physical value. For propeller thrust and the *Y*-component of the global dynamometer, the physical unit was *N*, while the physical value for the propeller torque was *N-m*. There is a designated calibration stand for the podded propulsor unit that allows the pod unit to be rotated around a horizontal axis and therefore

allows calibrations in multiple configurations. An aluminum torque bar is installed in place of the propeller and was used to hang known weights for the applied load. By rotating the calibration stand and azimuthing the podded propulsor unit, calibrations were performed for compression and tension for the propeller thrust and *Y*-component and clockwise and counter clockwise for the propeller torque.

The process of conducting a thrust calibration involves applying loads to the pod unit in line with the direction of the propeller thrust. For thrust calibrations, the calibration stand was oriented such that the plate which houses the pod unit was in the vertical plane. The pod was then rotated to point up for compression calibrations and again rotated to point down for calibrations in tension. Known loads were applied in increasing and decreasing increments to cover the full range of expected loads on the pod unit. The output voltages from the pod thrust channel were then tared and then plotted against the known load. A regression line was fit to the data. The equation of this regression line is then the calibration equation used to convert the output voltage to a physical value with force units. Figure 6 shows the calibration stand set with the plate in the vertical plane and an applied load on the podded propulsor unit resulting in a tension force for thrust.

Figure 6. Thrust Tension Calibration

The process of conducting a torque calibration involves applying loads in the direction of propeller rotation at a known distance from the propeller shaft. For torque calibrations, the calibration stand was oriented such that the plate that houses the pod unit was in the horizontal plane. Like the thrust calibration, known moments were applied in increasing and decreasing increments to cover the full range of expected moments on the pod unit. The output voltages from the pod torque channel were then tared and then plotted against the known moment. A regression line was fit to the data. The equation of this regression line is then the calibration equation used to convert the output voltage to a physical value with moment units. Figure 7 shows the calibration stand set with the plate

in the horizontal plane and an applied moment on the podded propulsor unit resulting in a counter clockwise torque.

Figure 7. Counter clockwise Torque Calibration

Calibrations of the *Y*-component load cells of the global dynamometer were conducted simultaneously with the thrust calibrations. This is because when the calibration stand is set with the plate in the vertical plane, the *Y*-component load cells are also oriented in the vertical direction. The procedure for developing the calibration equation for this component is equivalent to that for the thrust; however, the voltages from the two load cells are summed prior to taring the data and plotting.

The time series plots of all calibrations are contained in Appendix A. This appendix also contains the raw data from the sampled channels as well as the spreadsheets used to create the plots necessary for obtaining the calibration equation. The final plots for the propeller thrust, torque, and *Y*-component of the global dynamometer

including the calibration equations are also displayed in Appendix A.

EXPERIMENTAL FACILITY

Experiments were conducted in the 90m ice tank of the National Research Council Ocean, River, and Coastal Engineering facility (NRC-OCRE) in St. John's, NL. Figure 8 shows the layout of this tank. Despite using the ice tank for the experimental program, synthetic ice was used in place of tank-grown ice in order to maintain consistency between experiments and reduce costs. The synthetic ice will be discussed further toward the end of this chapter.

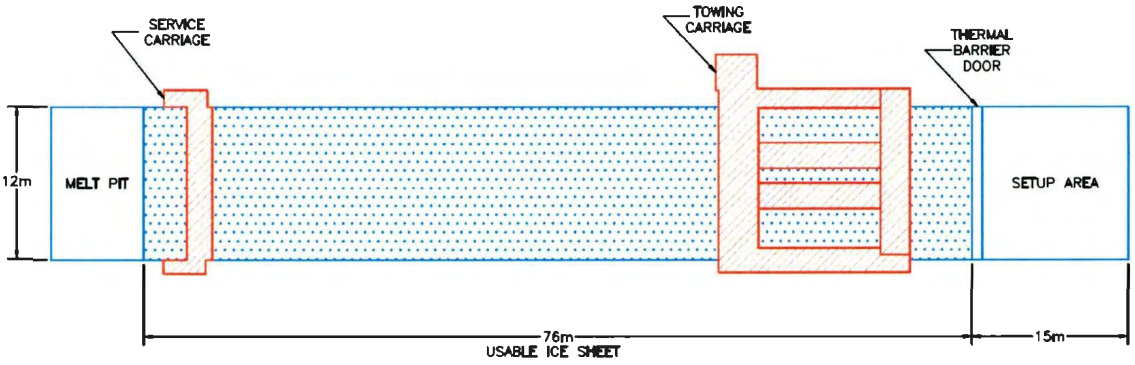

Figure 8. 90m Ice Tank at NRC-OCRE

A 4.0 m x 10.0 m pen was created mid-tank in order to contain the ice pieces during experimentation (Figure 9). The pen dimensions were chosen based on a review of wake studies, which found that the propeller wake diminished within a length of $50D_p$, where D_p is the propeller diameter (Johansson et al. 2006; Situ et al. 2010). Johansson et al. (2006) specified that the downstream axial velocity falls rapidly from 10% of the free-stream velocity at $x/D_p=10$ to approximately 2% at $x/D_p=50$. Situ et al. (2010) only commented that the axial velocity degraded badly at $x/D_p=50$. This length of $50D_p$ was

validated with preliminary tests using a 200 mm diameter propeller operated for 15 seconds.

The pen boundaries were constructed using 1"×1" wire mesh that extended approximately 40 cm below the water's surface to limit the influence of the mesh on the propeller wake wash. Foam floats were installed intermittently on the outside edges of the pen boundaries to keep the pen afloat. The corners of the pen boundary were attached to the ice tank walls and pulled taught to prevent the pen from moving during experimentation.

Figure 9. Ice Pen Boundaries

EXPERIMENTAL MODEL

The podded propulsor unit was installed in an existing Arctic icebreaker model. The icebreaker model houses two model podded propulsor units. However, for this study, only one podded propulsor unit was installed in the port side of the ship model and a plug

was installed in the starboard side to prevent water ingress. The propeller used for this program was a 200 mm diameter, left-handed propeller (Figure 10).

Figure 10. Propeller Installed on Pod Unit

The ship model was ballasted to the design waterline and was attached to a forward platform of the ice tank carriage. The model was oriented transversely across the tank with the propeller wake flowing down the tank length (Figure 11). The podded propulsor was rotated 90 degree to the typical ahead operating condition in order to minimize the effect of the ship's stern shape on the propeller wake and to achieve a minimum distance from the propeller to the ice edge of 0.1 m. Azimuthing angle was not a factor that was considered in this experimental program and therefore, it remained at 90 degrees to the ahead operating condition for the entirety of the program. Figure 12 shows the pod unit in the as-tested condition viewed from astern and from the port side of the ship model.

Figure 11. Arctic Icebreaker Model Installed on Carriage

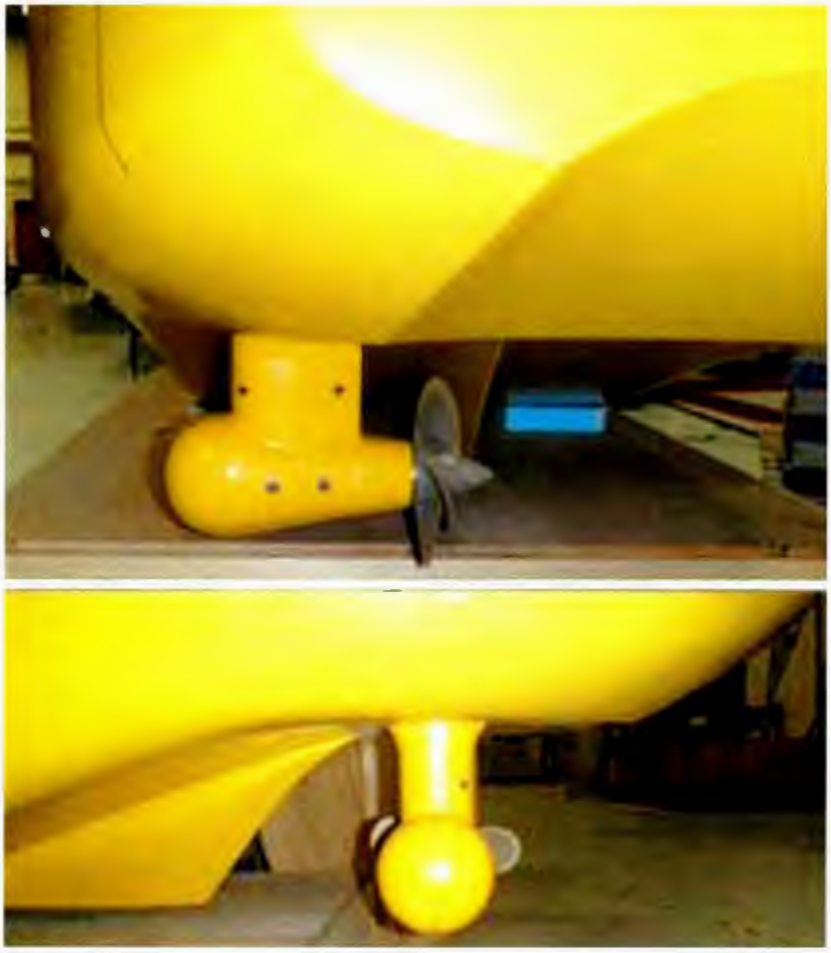

Figure 12. Pod Unit in As-Tested Condition

To achieve angles of inclination for the ship model, wedges were made for each desired angle. Depending on the experiment to be performed, the appropriate wedge was installed behind the mounting bracket on the starboard side of the model, which was the attachment point for ship model to the carriage, and ballast weight was adjusted in order to achieve the desired inclination angle. A bridle system was installed on the port side of the model and pulled tight for each desired inclination angle in order to prevent the angle from changing once the propeller generated thrust. Figure 13 shows the schematic diagram of the inclination angles tested. The bridle system can be seen in Figure 14.

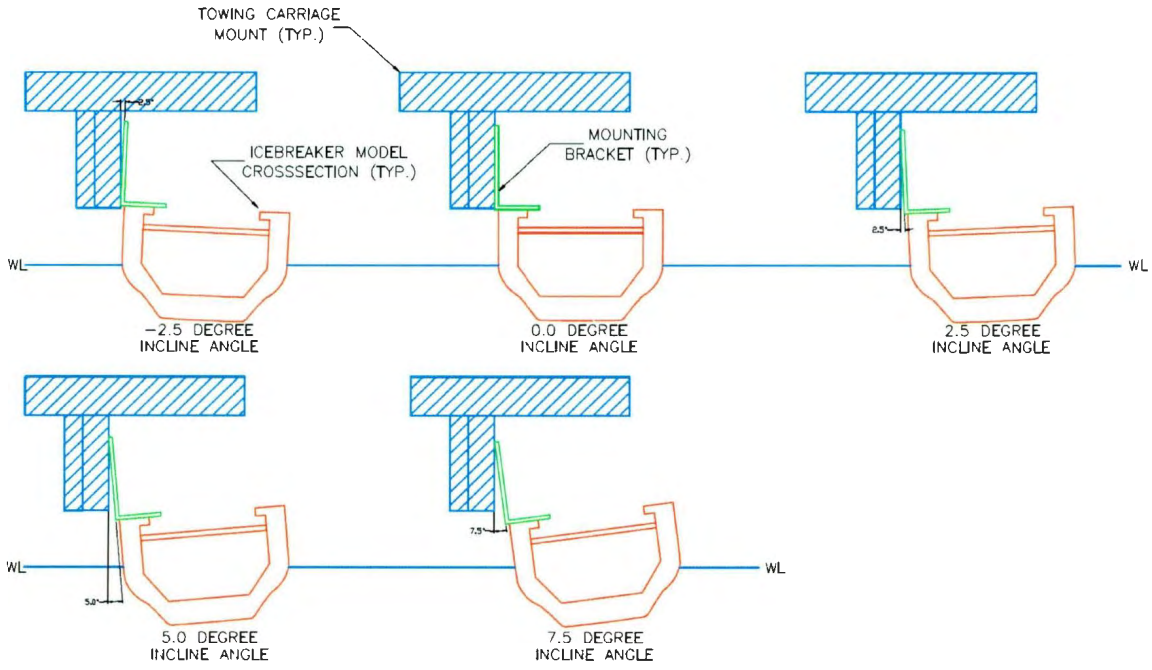

Figure 13. Schematic Diagram of Inclination Angles

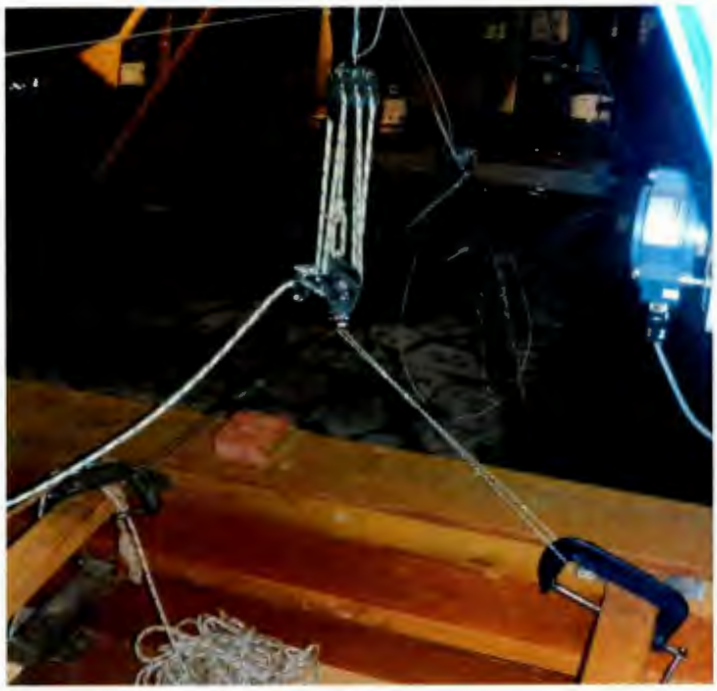

Figure 14. Bridle System

In order to achieve the desired distances between the propeller and the ice edge, the carriage, and therefore the ship model, was moved in relation to the ice edge. When the ice edge was touching the ship model's hull, the distance between the propeller and ice edge was 0.1m. This was the minimum distance obtainable without having the ice pieces protrude under the hull, and therefore was designated as the low axial point for the experiment design. For the remainder of the distances, the carriage was backed away from the ice pen to the desired distance from the ice edge.

SYNTHETIC ICE

Synthetic ice was used in order to maintain consistency between experiments. This option also reduced costs since there was no need to refrigerate the ice tank and grow multiple ice sheets. Sheets of polypropylene plastic were used as the synthetic ice

since the thickness and shapes of the pieces will remain constant throughout the test program.

The density of polypropylene sheets is approximately 0.9Mg-m^{-3} according to the polypropylene data sheet from the Professional Plastics supplier (Appendix B-3). Although the density of sea ice varies over a wide range, the average density reported by Timco and Frederking (1996) was 0.91Mg-m^{-3}. The similar densities between the polypropylene synthetic ice and sea ice means that both will have similar mass properties for a given volume.

Sheets were purchased with the dimensions of 4' x 8' x 0.5". In order to obtain the distribution that real ice follows when broken, an image of pack ice off of Fogo Island was scaled to the dimensions of the model test program and traced using CAD software (Figure 15). This CAD drawing was then used with a water-jet cutter to form the ice pieces.

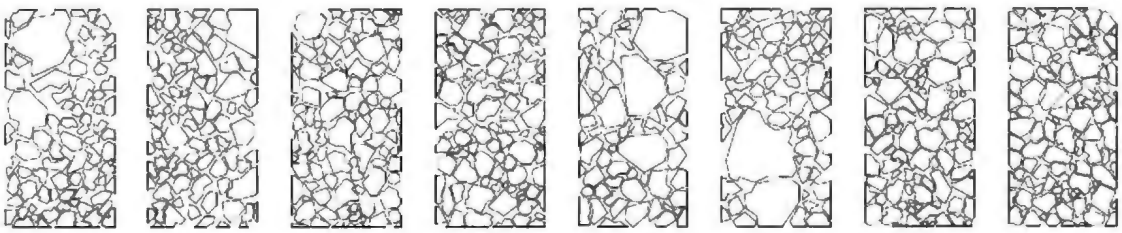

Figure 15. Ice Pieces to Cut from Polypropylene Sheets

The ice pieces were labeled with the concentrations in order to ensure that the same ice pieces were used for the various ice concentrations tested. All of the ice pieces labeled with 15 were placed in the ice pen for the 15% initial concentration experiments. For the experiments requiring 30% concentration, all of the ice pieces labeled with 15 and

all of the pieces labeled with 30 were placed in the pen. Likewise, for the 60% initial concentration, all of the ice pieces were placed in the pen—that is, all pieces labeled with 15, 30, 45, and 60 were in the pen (Figure 16).

Figure 16. Ice Pieces in Ice Pen for 60% Initial Ice Concentration Condition

EXPERIMENTAL PROCESS

The factors were adjusted as per the experiment plan prior to sampling data. For each run, a tare segment, or calm segment, was run for 15 seconds, followed by the propeller operating for 15 seconds. An additional 15 seconds of data were collected after the propeller was stopped. This yielded samples that were approximately 45 seconds in length. Although these last 15 seconds of data were not used during the analysis, they were used as a check to ensure that the instruments returned to their starting offsets and that there was no drift in the sampled data.

CHAPTER 5 –RESULTS

Discussed in this chapter are the results from the viscous scaling calculations, momentum theory calculations, model podded propulsor data, and ice management experiments. The viscous scaling calculations and momentum theory calculations were performed prior to experimentation to gain an understanding of the propeller flow characteristics. The measured data from the model podded propulsor were then used to calculate bollard condition thrust, torque, and delivered power. A comparison was also made of the measured podded propulsor data with the momentum theory calculations. The final section of this chapter presents the results from the ice concentration analysis and discusses the significant factors in each area of the ice field that was analyzed.

VISCOUS SCALING EFFECTS

When considering viscous effects, Verhey (1983) states that if the propeller Reynolds number, Re_{prop}, is greater than 7.104E04 and the flow Reynolds number, Re_{flow}, is greater than 3.103E03, then the scaling effects due to viscosity are negligible. This method of determining viscous scale effects has been used in a number of recent studies involving propeller wake decay (Situ et al. 2010; Lam et al. 2010; Lam et al. 2011b). Reynolds numbers are determined as shown in Equations 10 and 11.

$$Re_{prop} = \frac{nD_pL_m}{\nu} \tag{10}$$

$$Re_{flow} = \frac{D_pV_0}{\nu} \tag{11}$$

In these equations, n is propeller shaft speed, D_p is the propeller diameter, ν is the viscosity, L_m is a length term dependent on blade area ratio (Blaauw & van de Kaa, 1978),

and V_0 is the efflux velocity, or the maximum velocity at the propeller face (Fuehrer & Romisch, 1977). L_m and V_0 are calculated as shown in Equations 12 and 13, where β is the blade area ratio, N is blade number, D_h is the hub diameter, and C_t is the thrust coefficient.

$$L_m = \beta D_p \pi \left[2N\left(1 - \frac{D_h}{D_p}\right)\right]^{-1} \quad (12)$$

$$V_0 = 1.59 n D_p \sqrt{C_t} \quad (13)$$

The Reynolds numbers for both the propeller and flow were calculated for each rotational speed. The propeller characteristics for this thesis are presented in Table 2 and the results of the Reynolds number calculations are presented in Table 3. The flow Reynolds numbers are all greater than Verhey's value of 3.103E03. The Reynolds numbers due to the propeller are larger than Verhey's value of 7.104E04 except at the two lowest rotational speeds. The flow Reynolds number, however, is considered more significant than the propeller Reynolds number (Blaauw & van de Kaa, 1978; Verhey, 1983; Hamill & Johnston, 1993; McGarvey, 1996; Hamill et al. 2004). Appendix C contains the calculations that yield the values contained in Table 3.

Table 2. Propeller Characteristics for Viscous Scaling Calculations

D_h	46.5 mm
ν	1.14E-06 m^2/s
β	0.44
N	4
L_m	45.0 mm
C_t	0.17

Table 3. Viscous Scaling Effects

RPS	Re_{prop}	Re_{flow}
5	3.95E+04	1.15E+05
7.5	5.92E+04	1.72E+05
10	7.89E+04	2.30E+05
12.5	9.87E+04	2.87E+05
15	1.18E+05	3.45E+05

MOMENTUM THEORY CALCULATIONS

Using momentum theory, the thrust and delivered power for the propeller were calculated and used as predicted values in a comparison with the thrust and delivered power calculated from the pod unit measurements. The equation for efflux velocity from the wake scaling calculations (Equation 13) was used to determine V_0. Since the propeller was only rotating in place and not advancing, the upstream velocity, V_A, is equal to 0m/s. The downstream velocity, V_B, was then calculated rearranging Equation 4. Using these velocities, the propeller thrust was estimated using Equation 2. In this equation, the mass flow per unit time was calculated as the multiplication of the density of water, propeller disk area, and change in velocity. This resulted in an equation for propeller thrust as shown in Equation 14. The delivered power was calculated as shown in Equation 3. The results of these prediction calculations are included in Table 4.

$$T = 0.5\rho A(V_B^2 - V_A^2) \qquad (14)$$

Table 4. Momentum Theory Prediction Calculations for Model-Scale

RPS	V_0 (m/s)	V_A (m/s)	V_B (m/s)	T (N)	P_d (kW)
5	0.66	0	1.31	27.00	0.018
7.5	0.98	0	1.97	60.76	0.060
10	1.31	0	2.62	108.0	0.142
12.5	1.64	0	3.28	168.8	0.277
15	1.97	0	3.93	243.0	0.478

PODDED PROPULSOR UNIT ANALYSIS

Measurements from the podded propulsor unit included thrust, torque, and propeller shaft speed. The *Y*-component of the global dynamometer was also sampled as a redundancy to measuring thrust. Each measurement was sampled on a separate channel at 5000Hz through the self contained data acquisition unit on the podded propulsor. The time traces of each experiment are contained in Appendix C (C-2 through C-31). Each of the experiments was preceded by a 30 second calm run. The average of this segment was used to tare the data of the segment when the propeller was operating. The accumulated statistics file, which contains basic statistic values for the calm segment and the propeller operating segment for each of the experiments, can also be found in Appendix C (pages C-32 through C-43). The mean values for propeller shaft speed, thrust, torque, and *Y*-component of the global dynamometer for each of the propeller operating segments was then used to develop a plot of the bollard condition propeller data and to calculate the delivered power of the propeller.

A graph of the bollard condition propeller model-scale data was developed by plotting the thrust, torque, and the *Y*-component against the propeller shaft speed. The graph can be seen in Figure 17. The propeller torque is multiplied by a factor of 10 in

order to graph thrust and torque on the same scale. The difference between thrust and the *Y*-Thrust at higher propeller shaft speeds is believed to correspond to the dynamometer placement. The thrust dynamometer is located at the hub and is therefore measuring direct thrust from the propeller. The global dynamometer, however, is housed within the model and the measured loads are therefore affected by the flow over the hull and resistance on the pod unit strut.

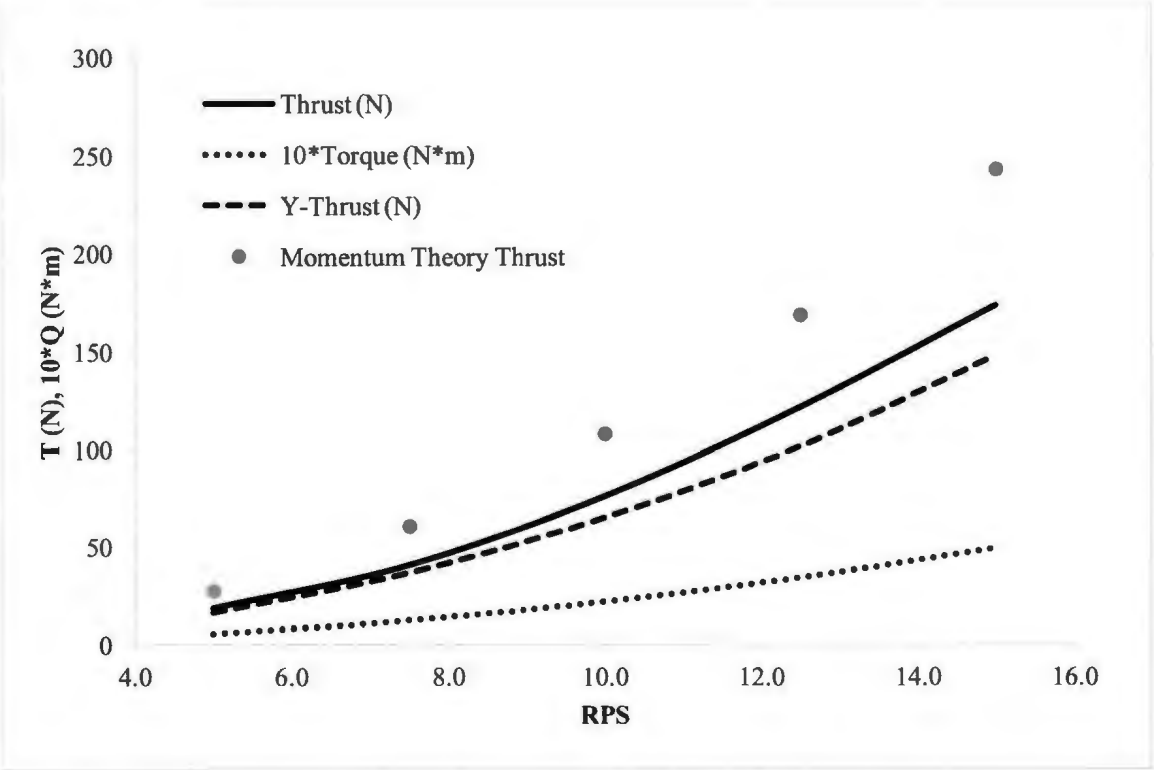

Figure 17. Model-scale Bollard Condition Data

Delivered power was calculated assuming a shaft transmission efficiency of 1.0 (Kerwin and Hadler, 2010; Hadler, 2011). The equation is shown in Equation 15, where n is propeller rotation speed, Q is propeller torque, and η_s is the shaft transmission efficiency. The graph of the delivered power corresponding to propeller shaft speed is

shown in Figure 18. This graph also displays a curve for the delivered power calculated using momentum theory, previously reported in Table 4.

$$P_d = 2\pi n Q \eta_s \qquad (15)$$

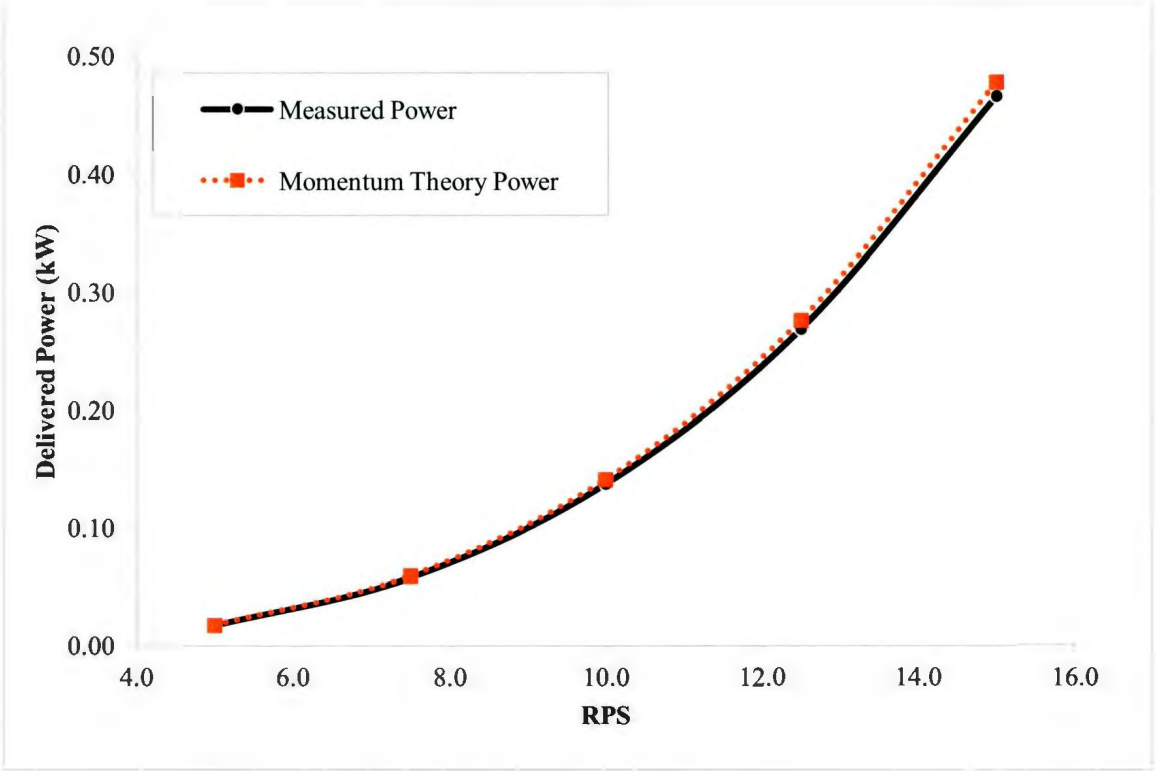

Figure 18. Model-scale Delivered Power

A comparison of thrust calculations from momentum theory and from the actual pod unit measurements (Figure 17) show that the percent difference between these values correspond to 32% to 40%, depending on the propeller shaft speed. Despite this, a comparison of delivered power calculations (Figure 18) shows good correlation between the two sets of values.

CALIBRATION UNCERTAINTY ANALYSIS

An uncertainty analysis was performed for the calibration stage of experimentation following the National Institute for Standards and Technology's guide for uncertainty in force measurements (Bartel, 2005). The expanded uncertainty, U, is determined as $2u_c$, where u_c is shown in Equation 16.

$$u_c^2 = u_f^2 + u_r^2 \tag{16}$$

In this equation, u_f is the uncertainty in the applied force and u_r is the uncertainty associated with assuming a linear fit of the regression equation. Since the applied force is calculated as the mass of an object multiplied by gravitational acceleration, the value u_f is then a summation of the uncertainty in the mass measurement and the value of gravitational acceleration. The value u_r is calculated following Equation 17, where d is the difference between the calculated and measured responses, k is the number of data points in the calibration, and m is the order of the regression polynomial plus one.

$$u_r^2 = \frac{\sum d^2}{k - m} \tag{17}$$

The calculated expanded uncertainties, U, for thrust, torque, and the Y-component of the global dynamometer are presented in Table 5. It was found in this analysis that the uncertainty associated with assuming a linear fit to the calibration data was far greater than that associated with the measured masses and calculation of gravitational acceleration. Therefore, the uncertainty is only reflective of u_r, with the significant figures shown in Table 5.

Table 5. Calibration Uncertainties

Calibration Condition	Uncertainty
Thrust	2.330 N
Torque	0.109 Nm
Y-Component of the Global Dynamometer	0.250 N

ICE CONCENTRATION ANALYSIS

The measured response was the change in ice concentration for specified areas in the ice field. Custom software, developed by NRC-OCRE, was used to calculate ice concentrations for the video acquired during each test. For each video analyzed, a mask must be placed on the video image such that bright areas are white and the remainder of the image is black. The software then counts the pixels that are white and divides by the total pixels in the image to yield the ice concentration. The image contrast can be adjusted to eliminate reflections from being included in the white pixels.

In the ice concentration analysis, four areas were defined that spanned the ice pen. Figure 19 provides a visualization of the areas used in the analysis, however this image does not show the exact area constraints. In the actual analysis, each rectangle was dimensioned as 0.65 m × 4 m. The turbulence on the water's surface from the operating propeller created additional glare, and therefore the start of Area 1 was positioned just beyond this turbulent region. Additionally, the end boundary of Area 4 was not defined at the actual pen boundary because it was known that ice would accumulate at the back of the pen. Because of this, it was possible for ice to clear beyond Area 4. Appendix D contains the boundary definitions used in the ice analysis.

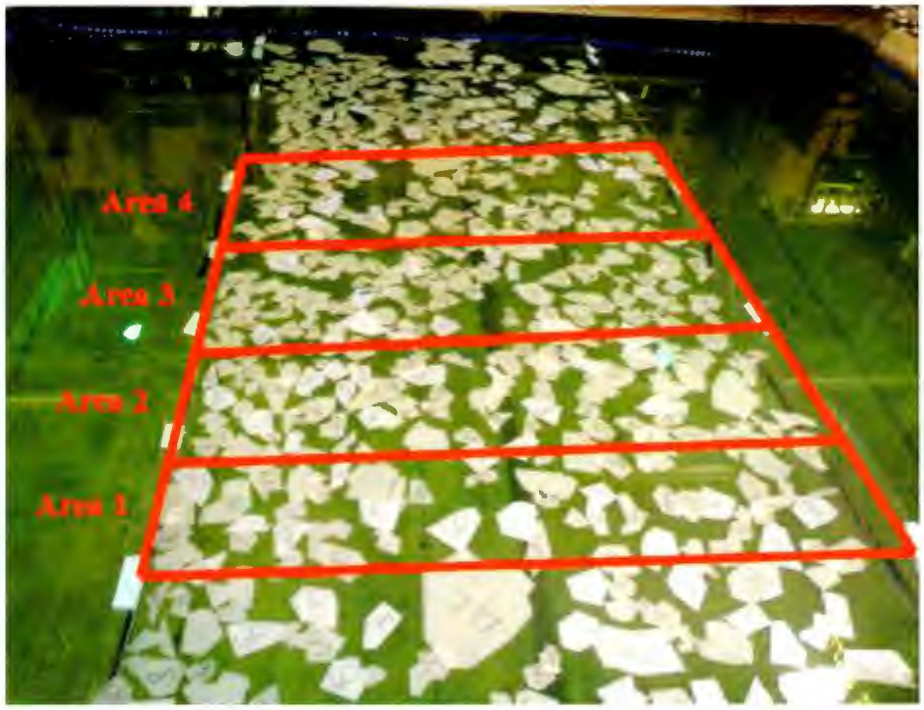

Figure 19. Example of Analysis Areas

The measured response for each defined area was the change in concentration, simply a subtraction of the final concentration from the initial. The resulting changes in concentration for the four analyzed areas are given in Table 6 along with the corresponding factors and levels. Plots of the changes in concentration for each analyzed area are shown in Figure 20, Figure 21, Figure 22, Figure 23, and Figure 24, each of which corresponds to an initial ice concentration. It is important to note that for theses plots, a change in concentration that is negative corresponds to an accumulation of ice and a positive change in concentration corresponds to ice clearing. Additionally, since the measured response is the change in concentration rather than the percent change in concentration, the maximum clearing for the areas depends on the initial concentration. For example, the maximum clearing for a 60% initial ice concentration is 60%.

Table 6. Experiment Runs and Associated Results for Each Area

Standard Order	Run Order	RPS (x_1)	Incline Angle (deg) (x_2)	Dist. to Ice Edge (x_3)	Degree of Ice Cover (x_4)	Y_{R1}	Y_{R2}	Y_{R3}	Y_{R4}
1	29	7.5	0	0.4 m	30%	9.81%	8.56%	18.08%	-22.97%
2	1	12.5	0	0.4 m	30%	17.25%	21.96%	27.42%	25.00%
3	25	7.5	5	0.4 m	30%	14.41%	19.95%	7.20%	-18.53%
4	9	12.5	5	0.4 m	30%	19.95%	28.53%	13.90%	19.25%
5	26	7.5	0	1 m	30%	3.87%	11.36%	15.09%	2.61%
6	10	12.5	0	1 m	30%	14.15%	26.63%	35.85%	19.83%
7	20	7.5	5	1 m	30%	1.95%	4.41%	3.30%	-2.54%
8	2	12.5	5	1 m	30%	23.25%	39.83%	42.76%	12.20%
9	21	7.5	0	0.4 m	60%	37.45%	15.74%	14.38%	-20.20%
10	3	12.5	0	0.4 m	60%	68.58%	62.41%	47.21%	11.83%
11	18	7.5	5	0.4 m	60%	32.97%	25.29%	19.93%	-6.20%
12	4	12.5	5	0.4 m	60%	40.77%	67.12%	61.53%	28.48%
13	14	7.5	0	1 m	60%	36.92%	22.31%	18.30%	-18.51%
14	16	12.5	0	1 m	60%	52.35%	56.97%	41.73%	25.95%
15	30	7.5	5	1 m	60%	30.22%	35.30%	14.55%	-13.43%
16	13	12.5	5	1 m	60%	39.89%	44.01%	57.77%	45.76%
17	5	5.0	2.5	0.7 m	45%	32.38%	23.60%	-5.38%	-14.27%
18	27	15.0	2.5	0.7 m	45%	23.47%	38.59%	55.84%	47.07%
19	12	10.0	-2.5	0.7 m	45%	66.64%	62.17%	41.65%	-17.12%
20	15	10.0	7.5	0.7 m	45%	21.35%	23.25%	30.36%	22.15%
21	11	10.0	2.5	0.1 m	45%	31.12%	44.53%	47.68%	15.39%
22	23	10.0	2.5	1.3 m	45%	8.52%	12.80%	18.05%	28.73%
23	7	10.0	2.5	0.7 m	15%	2.70%	10.31%	-0.52%	-2.57%
24	17	10.0	2.5	0.7 m	75%	40.76%	43.16%	42.43%	7.86%
25	6	10.0	2.5	0.7 m	45%	22.77%	24.63%	29.41%	-14.98%
26	8	10.0	2.5	0.7 m	45%	28.16%	28.00%	42.52%	12.51%
27	22	10.0	2.5	0.7 m	45%	34.69%	25.36%	28.87%	23.25%
28	19	10.0	2.5	0.7 m	45%	28.11%	24.11%	23.90%	-4.87%
29	24	10.0	2.5 deg	0.7 m	45%	31.02%	33.75%	33.38%	-5.78%
30	28	10.0	2.5 deg	0.7 m	45%	23.95%	16.96%	19.14%	14.27%

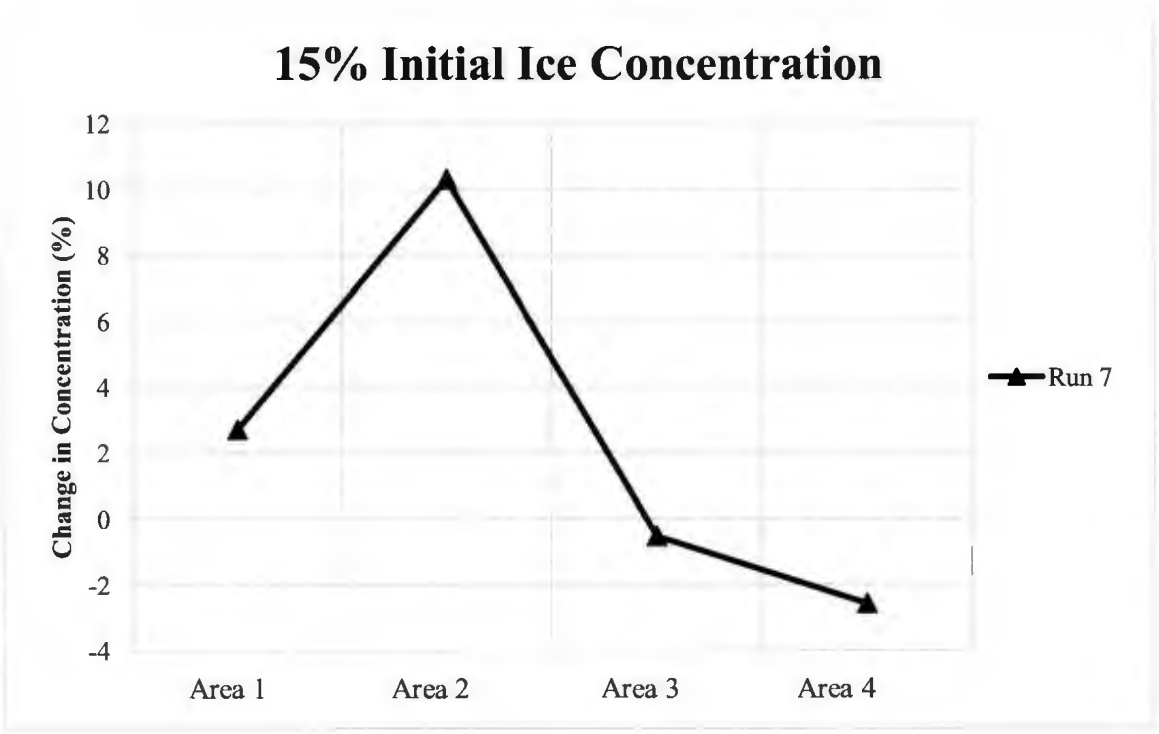

Figure 20. Change in Ice Concentration for 15% Initial Ice Concentration

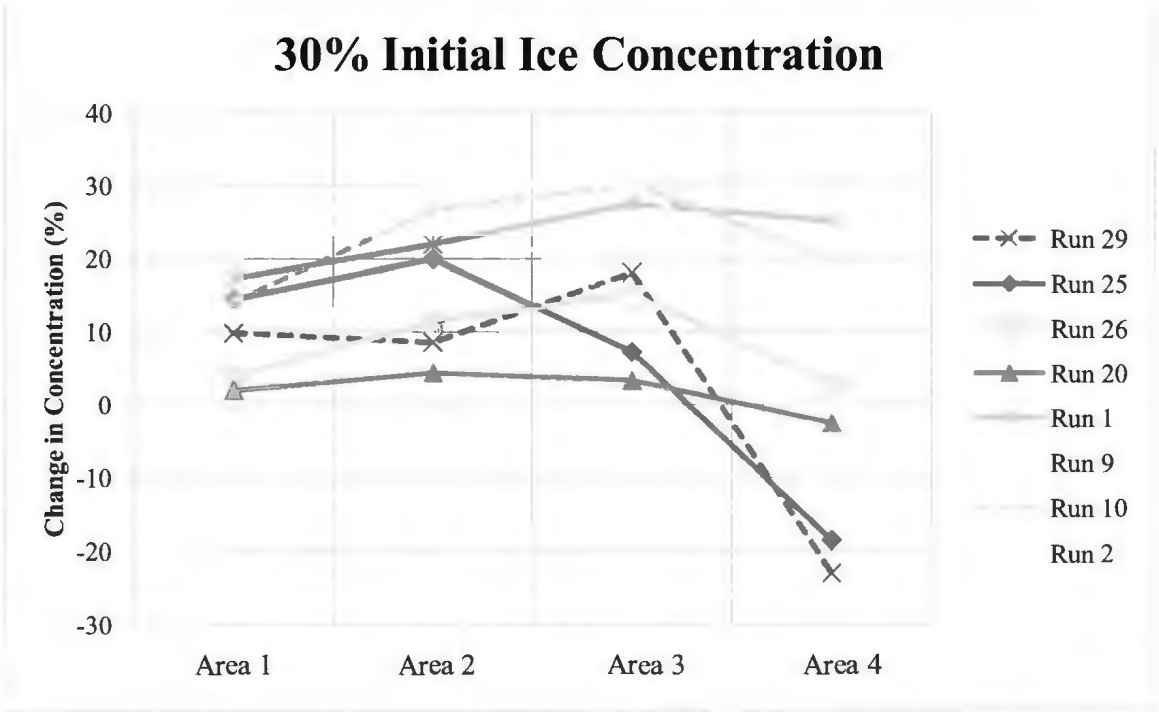

Figure 21. Change in Ice Concentration for 30% Initial Ice Concentration

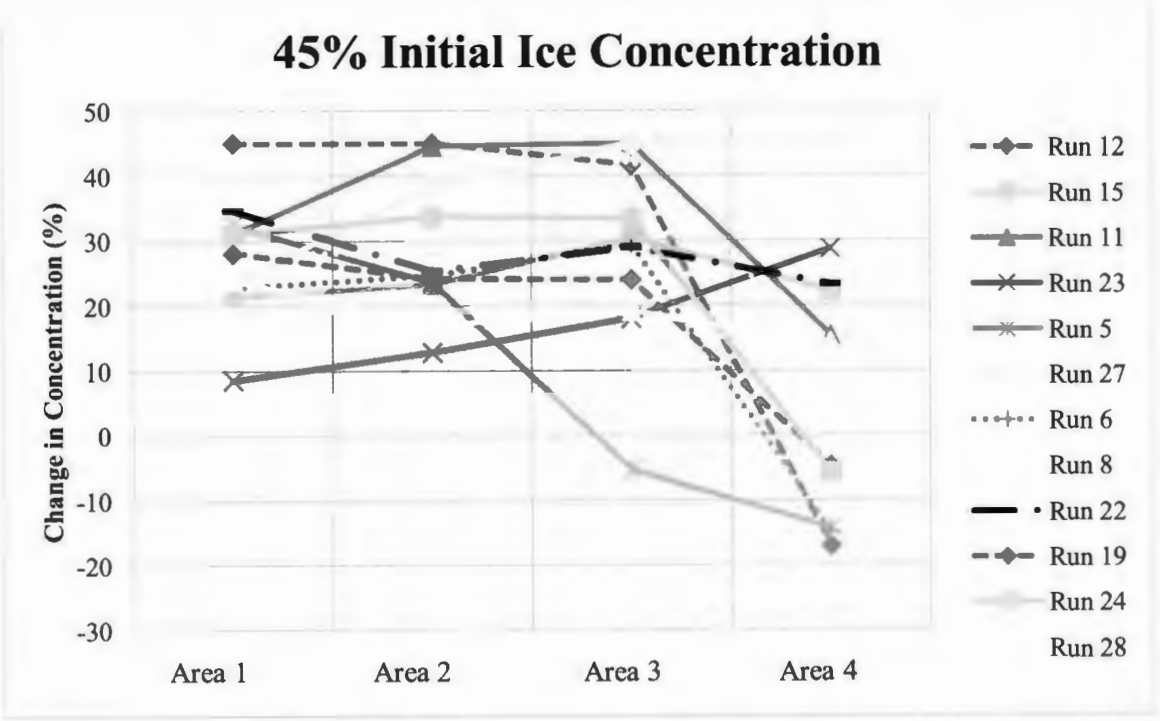

Figure 22. Change in Ice Concentration for 45% Initial Ice Concentration

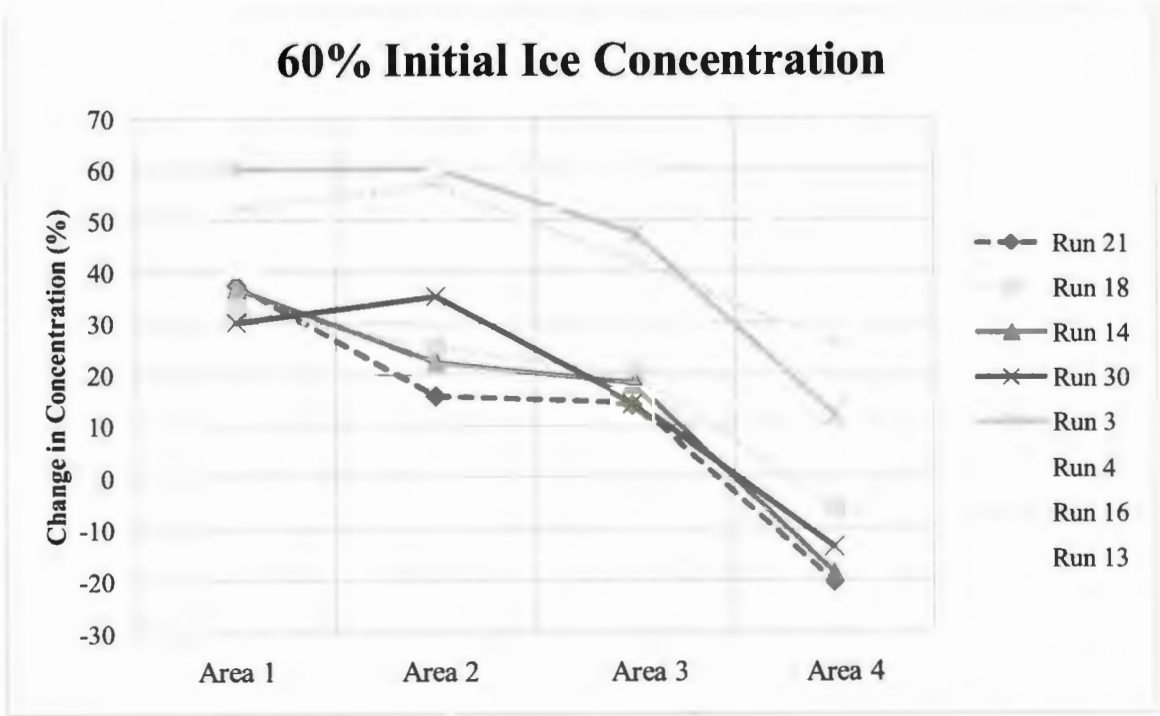

Figure 23. Change in Ice Concentration for 60% Initial Ice Concentration

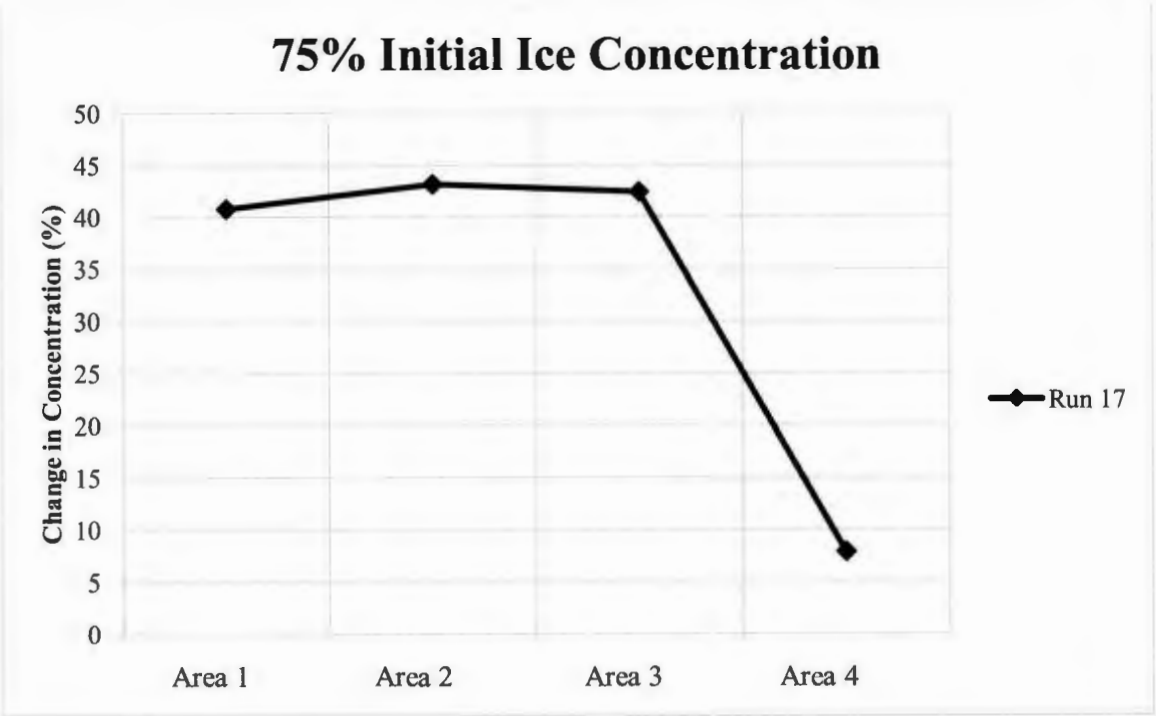

Figure 24. Change in Ice Concentration for 75% Initial Ice Concentration

Analysis Using Design-Expert® Software

In the analysis, the response for Area 1 is denoted as Y_{R1}; the response for Area 2 is denoted as Y_{R2}; the response for Area 3 is denoted as Y_{R3}; the response for Area 4 is denoted as Y_{R4}. Design-Expert® Version 8 software was used to analyze the ice concentration results and to generate the response surfaces.

In Area 1, closest to the propeller, there is a significant lack of fit in the analysis of variance model, indicating a high residual value. The residual is the difference between the observed response and the predicted response using the regression model (Montgomery, 2009). The high residual value seen in Area 1 is most likely due to the water circulation near the pod unit. The expansion of the wake plume in this area caused ice pieces that were cleared to recirculate back into the area later in the test. Therefore,

the changes in concentration were not consistent for this area, resulting in a significant lack of fit for the model.

In the analysis of Areas 2 and 3, it was determined that propeller shaft speed and initial ice concentration were significant factors in the analysis of variance model at the 95% confidence level. For Area 2, a square root transformation of the data was used to satisfy the equal variance assumption. The transformation is determined using a power function, in which the standard deviation is equal to the mean raised to a certain power, α. By transforming the data by a value of 1-α, the data are scaled to satisfy the equal variance assumption. The resulting prediction equation in terms of actual factors is shown in Equation 18 with respect to propeller shaft speed and Equation 21 with respect to delivered power. While the lack of fit is not significant for Area 2, the relatively high F-value, which is a ratio of the lack of fit variance to the pure error variance, of 3.37 suggests that there are somewhat inconsistent changes in concentration, as seen in Area 1. It would seem the recirculation of ice pieces influences the change in concentrations, however, the influence is most pronounced in Area 1. The ice pen boundary is not believed to have influenced the recirculation of ice pieces back into Area 1. The boundary was not rigidly supported on the surface in order to minimize the deflection of the ice pieces. It is believed that in real world operations, the boundary would be much more rigid, as it would be made of larger ice pieces, and therefore the recirculation seen in these operations would likely be even greater than what was seen in these model experiments.

In the analysis of Area 3, it was determined that no data transformation was

necessary to satisfy the equal variance assumption. As mentioned above, the propeller shaft speed and initial ice concentration were determined to be significant at the 95% confidence level. The resulting prediction equation in terms of actual factors is given in Equation 19 with respect to propeller shaft speed and Equation 22 with respect to delivered power.

Like Area 3, no transformation was necessary for the fit of data in Area 4. At the 95% confidence level, it was found that propeller shaft speed and model inclination angle were significant. The resulting prediction equation in terms of actual factors is given in Equation 20 with respect to propeller shaft speed and Equation 23 with respect to delivered power.

In the equations below, x_1 is the propeller shaft speed in revolutions per second, x_2 is the inclination angle in degrees, and x_4 is the initial ice concentration as a percent. It is important to note that theses equations correspond to model-scale.

$$\sqrt{Y_{R2}} = -1.18 + 0.37x_1 + 0.06x_4 \quad (18)$$

$$Y_{R3} = -53.1 + 5.66x_1 + 0.55x_4 \quad (19)$$

$$Y_{R4} = -66.8 + 6.85x_1 + 2.0x_2 \quad (20)$$

These equations are also presented in terms of power rather than propeller shaft speed. In these equations, x_{1p} is the delivered power of the propeller in kW, x_2 is the inclination angle in degrees, and x_4 is the initial ice concentration as a percent. Like Equations 18 through 20, above, Equations 21, 22, and 23 correspond to model-scale and the full-scale equations will be discussed in Chapter 6.

$$\sqrt{Y_{R2}} = 1.06 + 8.67x_{1p} + 0.06x_4 \quad (21)$$

$$Y_{R3} = -18.4 + 134.2x_{1p} + 0.55x_4 \quad (22)$$

$$Y_{R4} = -24.8 + 162.2x_{1p} + 2.0x_2 \quad (23)$$

When using an analysis of variance model, three assumptions are made. First is that the data follow a normal distribution; second is that the variances are equal for each sample; and third is that the experiment is performed randomly. In order to verify the assumptions, it is necessary to analyze the residuals. A normal plot of the residuals that follows a straight line fit verifies that the data are normally distributed. A plot of residuals against predicted values must be uniformly scattered and a plot of the residual against the run number must have no trend in order to validate that the experiments were performed randomly and that the assumption of equal variances is valid. For each of the three responses, the assumptions were validated by analyzing the residuals in the above mentioned plots, which are contained in Appendix E (pages E-1 through E-8).

The three dimensional response surfaces are shown Figure 25a, Figure 26a, and Figure 27a in terms of propeller shaft speed and Figure 28a, Figure 29a, and Figure 30a in terms of delivered power of the propeller. The two dimensional contour plots are shown in Figure 25b, Figure 26b, and Figure 27b in terms of propeller shaft speed and Figure 28b, Figure 29b, and Figure 30b in terms of delivered power of the propeller. The plot of Area 1 is not included, as the data from this area contained inconsistencies and could therefore not be used to draw definitive conclusions on the effectiveness of ice clearing. The plots for the Area 2 response are given in Figure 25 and Figure 28, Area 3 in Figure 26 and Figure 29, and Area 4 in Figure 27 and Figure 30. The contour plots are developed

by holding two factors constant while varying the remaining two. Since it was determined that only two factors were significant for each area, those factors were varied over the range from the *-1* level to the *+1* level, while the two non-significant factors were held constant at their center point values. For Areas 2 and 3, the range of change in concentration was from 0% to a maximum of approximately 50%. For Area 4, the range of change in concentration was from -20%, indicating that ice accumulated rather than cleared, to a maximum change in concentration of approximately 30%.

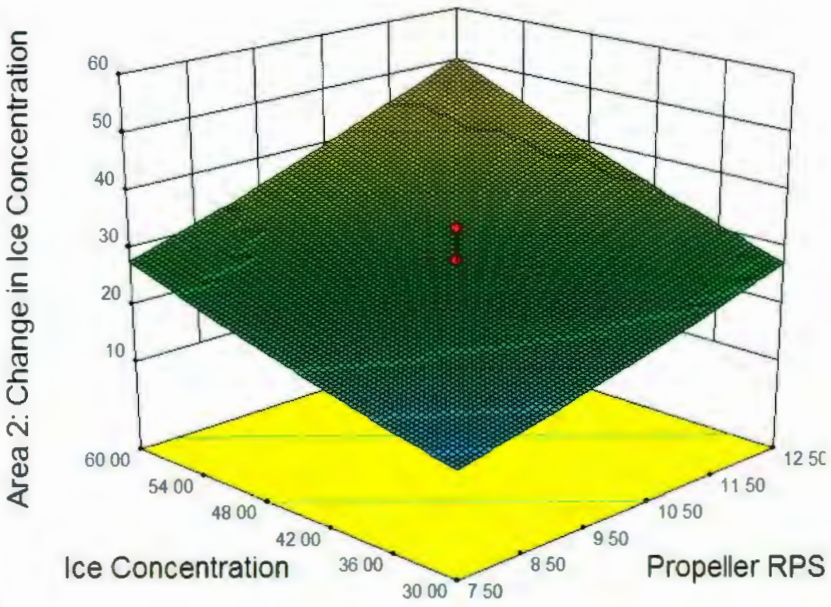

a)

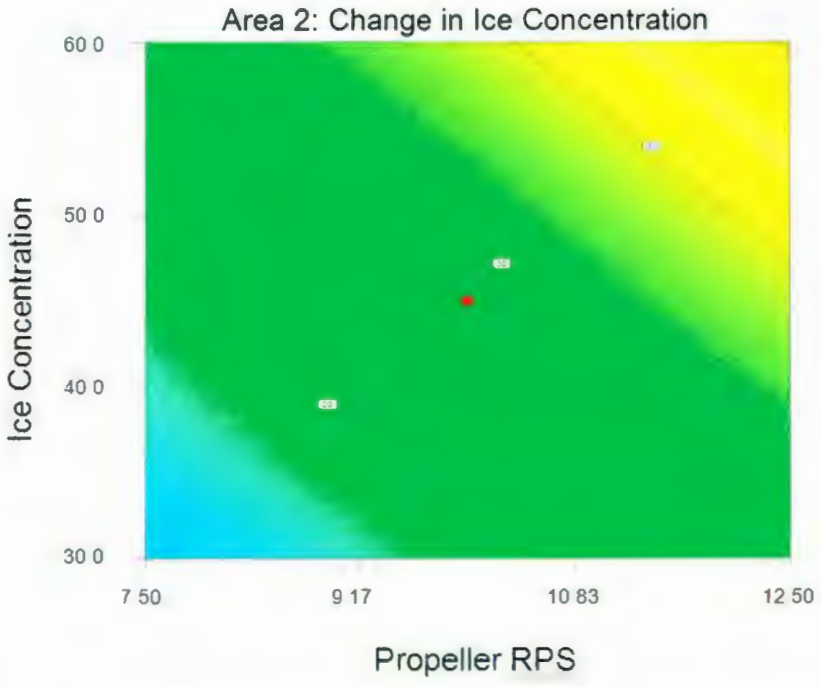

b)

Figure 25. Contour Plots of Area 2 with Propeller Shaft Speed

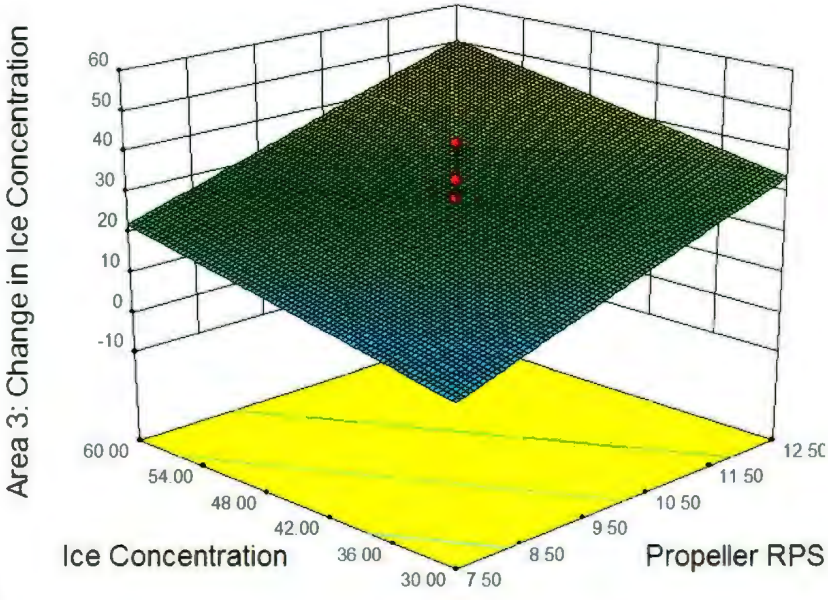

a)

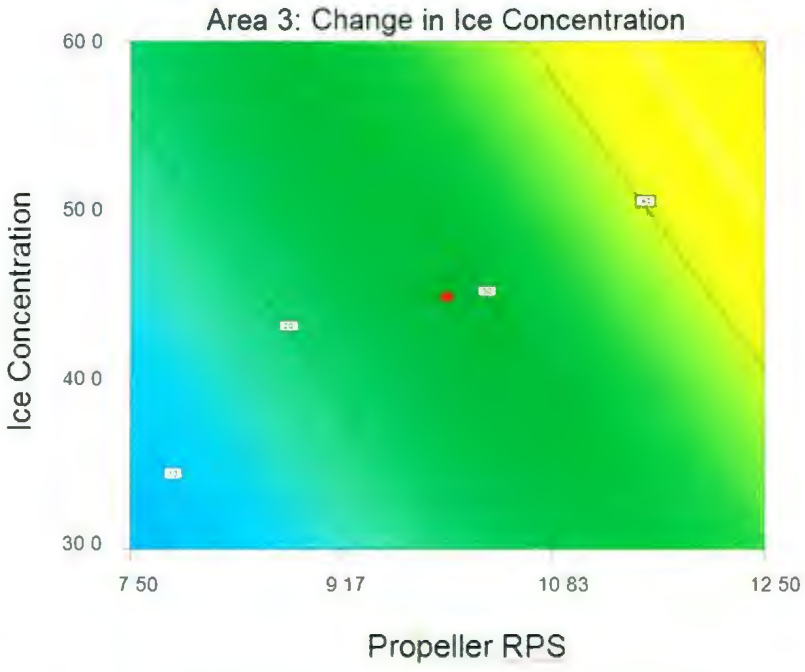

b)

Figure 26. Contour Plot of Area 3 with Propeller Shaft Speed

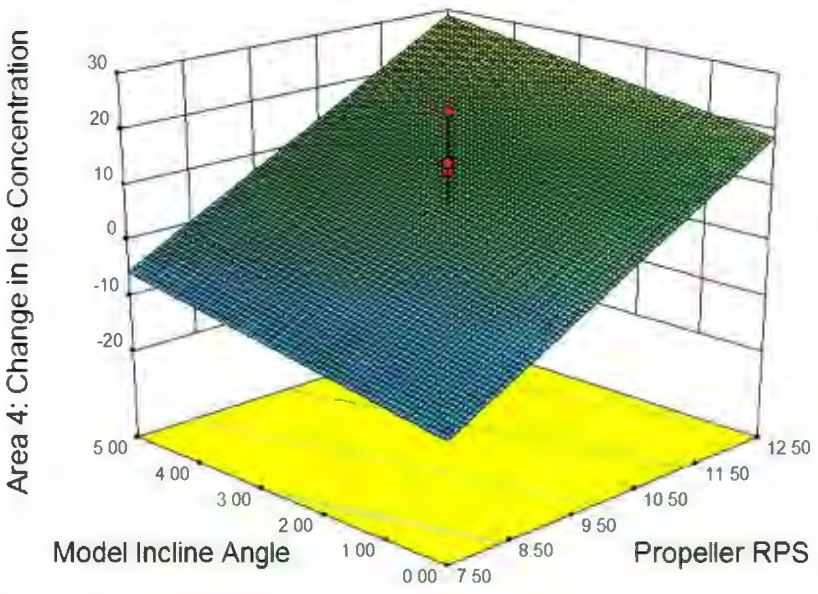

a)

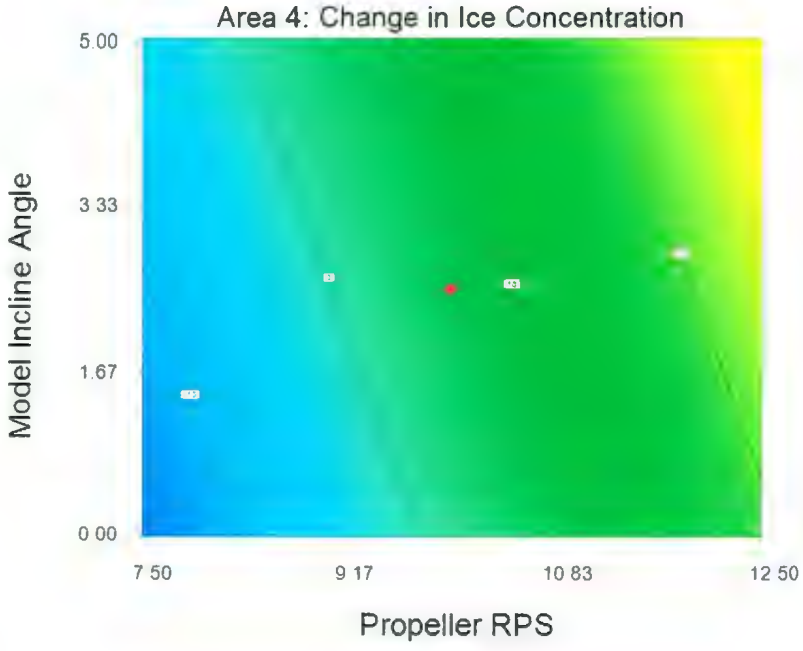

b)

Figure 27. Contour Plot of Area 4 with Propeller Shaft Speed

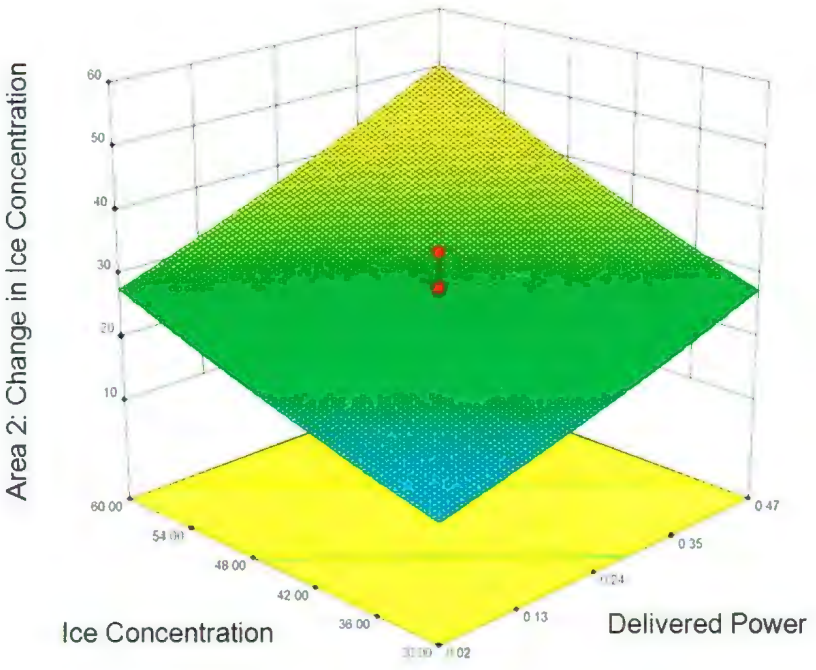

a)

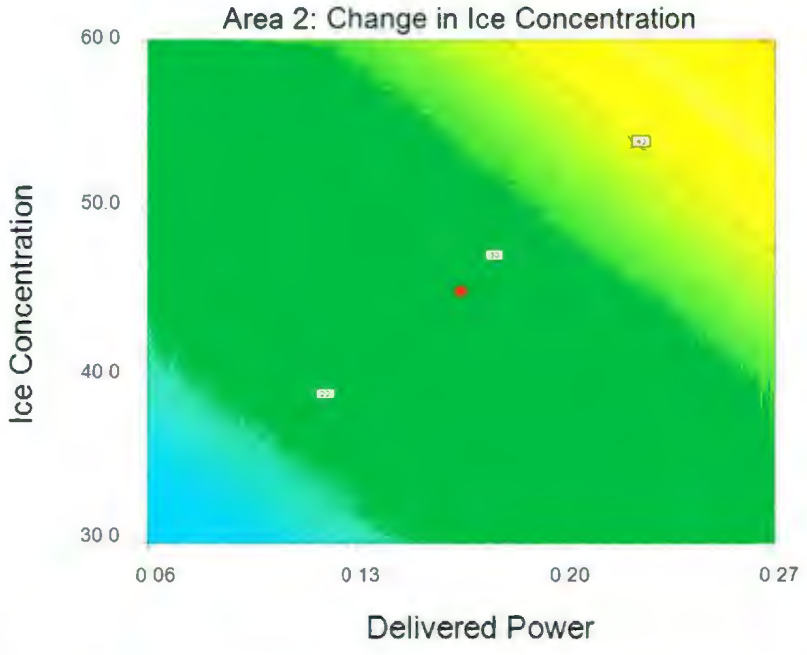

b)

Figure 28. Contour Plot of Area 2 with Delivered Power

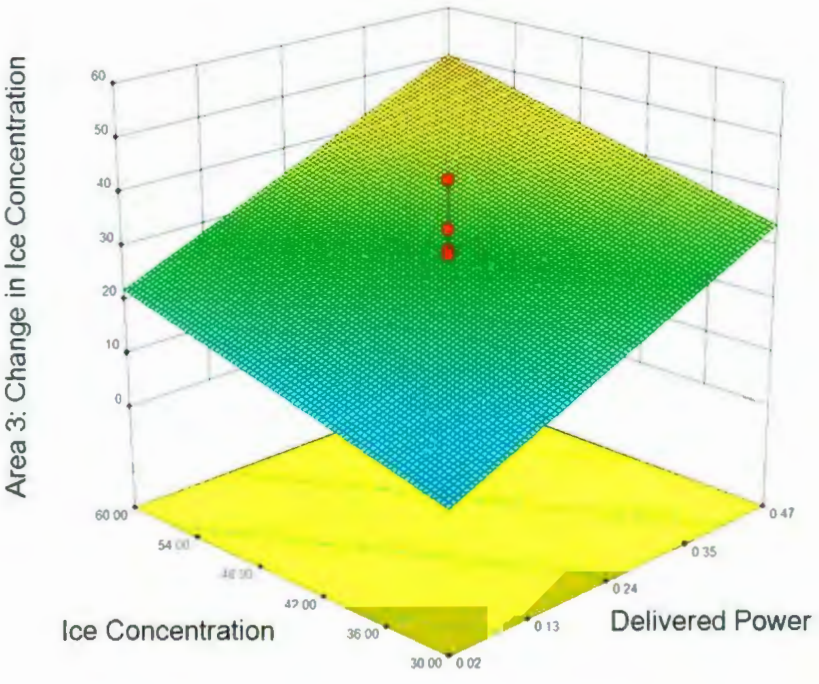

a)

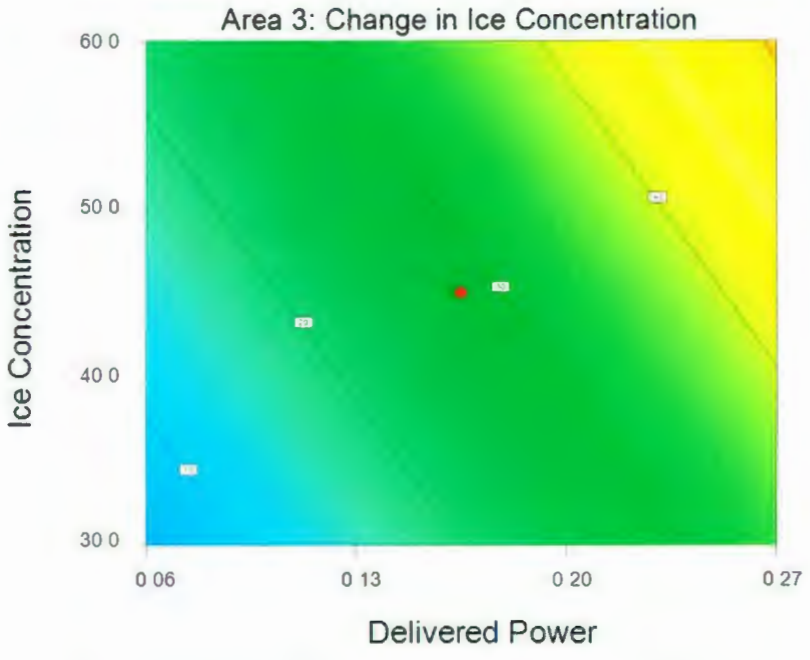

b)

Figure 29. Contour Plot of Area 3 with Delivered Power

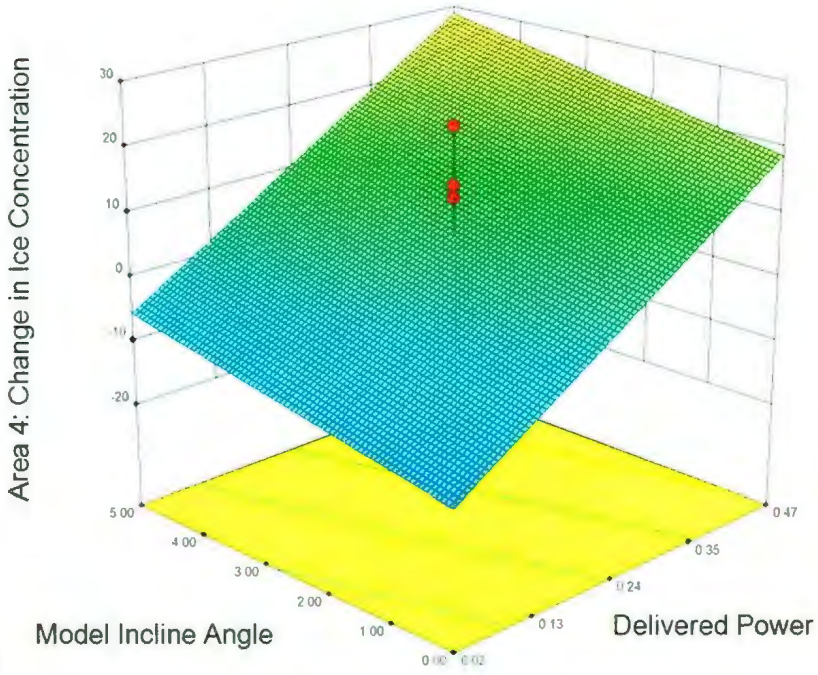

a)

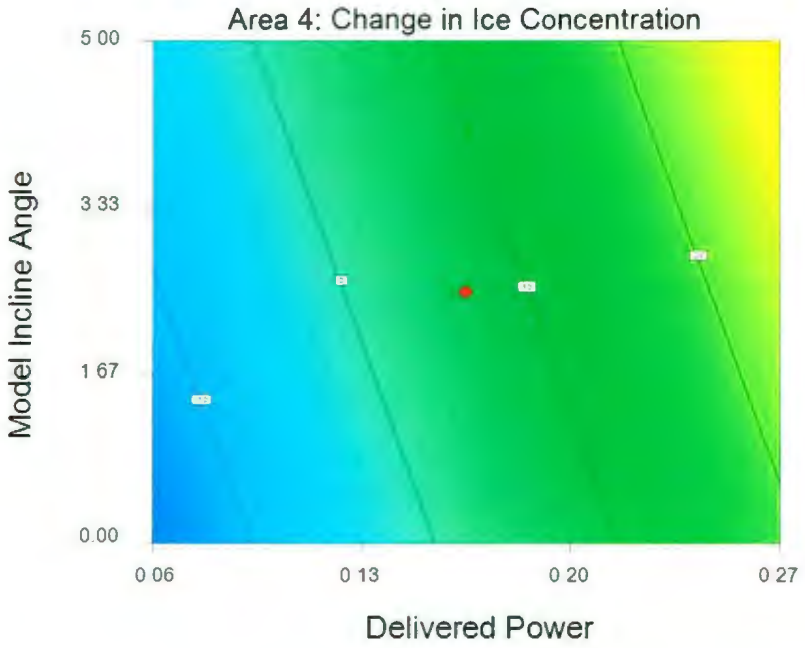

b)

Figure 30. Contour Plot for Area 4 with Delivered Power

CHAPTER 6 – DISCUSSION OF RESULTS AND CONCLUSIONS

EXPERIMENT CONCLUSIONS

The regions closest to the pod unit were the most turbulent as the wake plume expanded outward from the propeller. Because of this, ice pieces that cleared during the initial stages of the experiment recirculated back into Areas 1 and 2, causing scattered changes in concentration. The effect was most obvious in Area 1, where the lack of fit for the data in the analysis of variance model was significant. This means that the results resemble noise and this is a result of the scattered changes in concentration. Although there was a similar effect due to recirculation of ice pieces in Area 2, the influence was less than in Area 1. The lack of fit was determined to be insignificant; however, the relatively high F-value of 3.37 means that the lack of fit variance is higher than the pure error variance. The analysis of Areas 2 and 3 showed that propeller shaft speed and initial ice concentration were significant factors. The coefficients of the Area 2 prediction equation (Equation 18 and Equation 21) are small when compared to those of Area 3 (Equation 19 and Equation 22). This is likely due to the scattered changes in concentration, as described above. In both equations, the coefficient for the propeller shaft speed is greater than that of the initial ice concentration. This reveals that the propeller shaft speed, or propeller power, has the largest effect on how well the ice is cleared. In both regions, the 3D contour plots show that at the 60% initial ice concentration, approximately half of the ice was cleared away at 7.5 RPS and nearly all of the ice was cleared away at 12.5 RPS when the podded propulsor unit was run at speed for 15 seconds model-scale. A similar result is seen when analyzing the 30%

concentration: the change in concentration at the lower shaft speed is about half of the initial concentration and nearly all of the ice is cleared at the higher shaft speed.

It was interesting to find that for Area 4, the model inclination angle was significant, as well as the propeller shaft speed. It is evident from the 3D contour plot and from observation of the experiments that for low propeller rotation speeds, there is a negative change in concentration. The low propeller rotation speeds correspond to less energy into the ice field, meaning that ice pieces will travel at slow speeds and lose momentum through collisions with other ice pieces. Because of this, as the ice pieces were cleared from the regions closest to the propeller, the slow speed and loss of momentum caused them to stop in Area 4, causing the ice concentration to increase rather than decrease. At the higher propeller speed values, the energy input into the wake was higher, allowing the ice to clear out of Area 4 rather than accumulate.

From the 3D contour plots in Figure 27 and Figure 30, one can observe that increasing the inclination angle of the model increased the ability of the propeller wash to clear ice by about 10% for the full range of propeller rotation speeds. By increasing the inclination angle of the model, the propeller wash is directed more toward the water's surface. This is believed to have directed the strongest and fastest flow toward the ice pieces, which increased the velocity and momentum of the ice pieces, rather than directing it below the water's surface. This increased velocity and momentum caused the ice pieces to travel beyond Area 4 rather than accumulate.

The distance between the propeller and ice edge was not found to be a significant factor for the range investigated. From the results of these experiments, it would seem

that the position of the ice edge relative to the ZFE and ZEF has little effect on the ice clearing ability. It should be noted that the recirculation of ice pieces seen in Area 1 and 2, as explained above, may have decreased if larger distances between the propeller and ice edge had been tested. By increasing the distance, the turbulent region of the wake would have been in an ice free zone. Therefore, positioning the ice edge in the ZEF may result in more uniform clearing of all areas since there will be less recirculation of ice pieces near the ice edge.

Although dynamic azimuthing angle was not studied, it is believed that this factor may aid in reducing the recirculation of ice pieces in the areas closest to the propeller. It is expected that the length of the ice free channel would be consistent with the non-azimuthing experiments but the width of the ice free channel could be expanded by using dynamic azimuthing to effectively "sweep" the ice pieces away from the channel. Future experiments could investigate the influence of this factor on the ability to clear ice.

The results of the analysis show that the propeller rotation speed is the most significant factor in using propeller wash as a means of ice management. While high rotation speeds can effectively clear ice with low initial concentrations, the high speeds were also found to effectively clear the higher initial ice concentrations. It was also found that to effectively clear regions far downstream of the propeller, directing the propeller wash toward the water's surface transfers more kinetic energy into the ice pieces, causing them to carry their momentum farther downstream.

FULL-SCALE CONSIDERATIONS

The analysis described in Chapter 5 corresponds to model-scale, and therefore

Equations 18 through 23 are valid for the model-scale experiments performed. It is important to consider the full-scale applications of these equations, especially with regard to delivered power. Equations 21 through 23 have been scaled and are shown below in Equations 24, 25, and 26. In order to develop these equations, it was assumed that the same changes in concentration would result at full-scale as did at model-scale. Full-scale delivered power was calculated using the Equation 15, and the Froude scaled values of torque and propeller shaft speed measured during experimentation. This method of scaling is akin to directly multiplying the model-scale delivered power by the scaling factor raised to *3.5* ($\lambda^{3.5}$). In order to maintain a constant level of clearing between model- and full-scale, it is necessary to modify the coefficients of the power terms (x_{1p}). These coefficients are divided by $\lambda^{3.5}$, which in effect cancels out the scaling up of delivered power and maintains the change in concentration. Future studies on this ice management technique should validate this process of scaling the ice clearing prediction equations.

$$\sqrt{Y_{R2}} = 1.06 + 0.24x_{1p} + 0.06x_4 \qquad (24)$$

$$Y_{R3} = -18.4 + 3.76x_{1p} + 0.55x_4 \qquad (25)$$

$$Y_{R4} = -24.8 + 4.54x_{1p} + 2.0x_2 \qquad (26)$$

As explained above, the most significant factor in using azimuthing propeller wash to clear ice is the propeller rotation speed. From this conclusion, the higher the rotational speed, the more power will be imparted into the wake wash and therefore the more effectively ice will clear. In full-scale propeller operations, there is an upper limit to the propeller rotation speed. This is because the engines onboard the vessel have a maximum power output and therefore there is a maximum achievable shaft speed. In

addition to this maximum achievable shaft speed, there is the constraint of fuel consumption. Fuel consumption increases with propeller rotation speed since more power from the engines is required. Therefore, running at the highest power levels results in high fuel costs. Although a fuel cost analysis was outside the scope of this thesis, it is concluded that in a full-scale ice management operation, it will be necessary to find an optimum propeller shaft speed for each particular vessel and this optimum would balance fuel consumption and costs with propeller rotation speed and ability to clear ice.

In addition to propeller shaft speed, the inclination angle of the propeller was found to be significant in certain conditions. From Figure 21 and Figure 22, inclination angle appears to have a pronounced effect in the 30% and 45% initial ice concentrations. In these plots, the change in concentration increased, plateaued, or only slightly decreased in Area 4 for the runs with inclination angles greater than 0 degrees. In the 60% initial ice concentration condition (Figure 23), the 5 degree inclination angle (Run 13) only influenced the ability to clear ice in Area 4. Additionally, for the 60% initial ice concentration condition in Area 3 (Figure 23) a comparison of Run 4 and Run 13 shows that at a shaft speed of 12.5 RPS and a 5 degree inclination angle, the change in concentration for Area 3 is higher for the closer distance to the ice edge. Further, Figure 23 also shows that at 7.5RPS, a 0 degree inclination angle and 0.4m distance from the ice edge (Run 21) produced the same clearing as a 5 degree inclination angle and a 1m distance to the ice edge (Run 30). From this, it can be inferred that if a vessel is forced to increase the distance from the ice edge, increasing the inclination angle could produce the equivalent clearing, as if the vessel was closer with no inclination angle. Further, it would

seem advantageous to increase the inclination angle as the ice pieces clear and move farther downstream of the propeller face and this technique could be further investigated in future research.

In full-scale operations, an inclination angle can be achieved through ballasting the ship such that it is listed to a desired angle. Alternatively, new podded propulsor designs could incorporate a method to rotate about a horizontal axis in order to achieve a desired angle of inclination. This option, however, requires not only time for design work, but also time to either build a new ship with this new pod unit or retrofit an existing ship with the unit. In addition to cost and time, there is the issue of human factor limitations if a vessel is rolled significantly for ice management operations. This topic was outside the scope of this thesis and could be further investigated in future research.

WORKS CITED

Akinturk, A., Jones, S. J., Rowell, B., Duffy, D. (2004). Measuring podded propeller performance in ice. *1st International Conference on Technological Advances in Podded Propulsion,* Newcastle University, UK.

Anderson, K.G., McDonald, D., Mitten, P., Nicholls, S., Tait, D. (1986). Management of Small Ice Masses. *Environmental Studies Revolving Funds*, Report No. 042.

Bartel, T. (2005). Uncertainty in NIST Force Measurements. *Journal of Research of the National Institute of Standards and Technology, 110:6*, 589-603.

Belyashov, V. (1993). An Investigation on Fracture Mechanics and Ice Loading During Cutting Freshwater Ice by Indentors Simulating Propeller Blades. *Proceedings POAC*, 3-16.

Belyashov, V.A. & Shpakov, V.S., (1983). On Mechanics if Ice Crushing by Propeller Blades. *Ice Mechanics and Physics*. Academy of Sciences of the USSR, Moscow, 21-29.

Blaauw, H. G., van de Kaa, E. J. (1978). *Erosion of bottom and Sloping banks caused by screw rate of manoeuvring ships.* Delft Hydraulics Laboratory.

Bose, N. (1996). Ice Blocked Propeller Performance using a Panel Method. *Transactions of the Royal Institution of Naval Architects, 138,* .213-226.

Carlton, John. (2007). Marine Propellers and Propulsion. Oxford: Butterworth-Heinemann.

Crocker, G., Wright, B., Thistle, S., Bruneau, S. (1998). An Assessment of Current Iceberg Management Capabilities. Contract Report for: National Research Council Canada, Prepared by C-Core and B. Wright & Associated, Ltd..

Daley, C. D., Colbourne, B. (Winter Semester 2012). *Arctic ocean engineering, ENGR 9096 course notes.*

Doucet, J.M., Bose, N., Walker, D., and Jones, S. (1996) Cavitation Erosion in Blocked Flow with a Ducted Propeller. *Offshore Mechanics and Arctic Engineering, American Society of Mechanical Engineers.*

Dunderdale, P. Wright, B. (2005). Pack Ice Management on the Southern Grand Banks Offshore Newfoundland, Canada. Contract Report for: National Research Council of Canada, Prepared by Noble Denton Canada, Ltd.

Edmond, C., Liferov, P., Metge, M. (2011). Ice and Iceberg Management Plans for Shtokman Field. *Offshore Technology Conference*, Houston, TX.

Edwards, R.Y. (1976). Methods for Predicting Forces Encountered by Propellers during Interactions with Ice. *Proceedings, Third LIPS Propeller Symposium, Drunen.* 53-68.

Eik, K. (2008). Review of Experience within Ice and Iceberg Management. *Journal of Navigation, 61:4*, 557-572.

Eik, K., Gudmestad, O. (2010). Iceberg Management and Impact on Design of Offshore Structures. *Cold Regions Science and Technology*, i63, *15-28.*

Felli, M. Felice, F., Guj, G. (2006). Analysis of Propeller Wake Evolution by Pressure and velocity Phase Measurements. *Experiments in Fluids, 41*, 441-451.

Fuehrer, M., Romisch, K. (1977). Effects of modern ship traffics on islands and ocean waterways and their structures. *PIANC, 58*

Hadler, J. B. (Spring Semester, 2011). *NA IV: Propulsor design. course notes.*

Hänninen, S., Ojanen, M., Uuskallio, A., Vuorio, J. (2007). Recent Developments of podded propulsion in Arctic shipping. *Proceedings of the Recent Development of Offshore Engineering in Cold Regions. Volume 1 and 2,* 469-481.

Hamill, G. A., & Johnston, H. T. (1992). The decay of maximum velocity within the initial stages of a propeller wash. *Journal of Hydraulic Research, 31*(5), 605-613.

Hamill, G. A., McGarvey, J. A., Hughes, D. A. B. (2004). Determination of the efflux velocity from a ship's propeller. *Proceedings of the Institution of Civil Engineers: Marine Engineering, 157*(2), 83-91.

International Organization for Standardization. (2010). International Standard: Petroleum and Natural Gas Industries – Arctic Offshore Structures. ISO/FDIS 19906:2010(E).

Jagodkin, V.J. (1963). Analytical Determination of the Resistance Moment off a Propeller During its Interaction with Ice. *Problems of the Arctic and Antarctic. 13,* 79-81.

Johansson, P., George, W. (2006). The far downstream evolution of high-Reynolds-number axisymmetric wake behind a disk, part 1: Single point statistics. *Journal of Fluid Mechanics, 555*, 363-385.

Keinonen, A. J. (2008a). Ice management for ice offshore operations. *Offshore Technology Conference,* Houston, TX.

Keinonen, A. J. (2008b) Sakhalin Oil Production in Ice with Azimuth Ice Management Support. *ICETECH*, Banff.

Keinonen, A.J., Lohi, P. (2000). Azimuth and Multi Purpose Icebreaker Technology for Arctic and Non-Arctic Offshore. *Proceedings of the 10th International Offshore and Polar Engineering Conference*, Seattle, WA.

Kerwin, J., Hadler, J. B. (2010). The Principles of Naval Architecture Series: Propulsion The Society of Naval Architects and Marine Engineers.

Lam, W. H., Hamill, G. A., Robinson, D., Raghunathan, S. (2010). Observations of the initial 3D flow from a ship's propeller. *Journal of Ocean Engineering, 37*, 1380-1388.

Lam, W. H., Song, Y., Raghunathan, S., Hamill, G. A., Robinson, D. (2011a). Investigation of a ship's propeller jet using momentum decay and energy decay. *Canadian Journal of Civil Engineering, 38.*

Lam, W.H., Hamil, G.A., Song, Y.C. (2011b). Experimental Investigation of the Decay from a Ship's Propeller. *China Ocean Engineering, 25:2,* 265-284.

Lam, W.H., Hamil, G.A., Song, Y.C., Robinson, D.J., Raghunathan, S. (2011c). A Review of the Equations Used to Predict the Velocity Distribution within a Ship's Propeller Jet. *Journal of Ocean Engineering*, *38*, 1-10.

Liu, P. (2006). The design of a podded propeller base model geometry and prediction of its hydrodynamics. TR-2006-16, National Research Council Canada IOT.

Lye, L. (Fall Semester 2011). *Similitude, modeling, and experimental data analysis - ENGR 9516 course notes.*

McGarvey, J. A. (1996). The influence of the rudder on the hydrodynamics and the resulting bed scour of a ship's screw wash. Doctorate, Queen's University of Belfast.

Montgomery, D. (2009). Design and Analysis of Experiments (Eighth Edition) John Wiley & Sons, Inc.

Moores, C., Veitch, B., Bose, N., Jones, S., Bell, J., Carlton, J. (2001). Preliminary Blade Load Measurements on a Model Propeller in Ice. *20th International Conference on Offshore Mechanics and Arctic Engineering – OMAE01*. Rio de Janeiro.

Nyman, T. Riska, K., Soininen, H., Lensu, M., Jalonen, R., Lohi, P., Harjula, A. The Ice Capability of the Multipurpose Icebreaker Botanica – Full-Scale Results. *Proceedings of the Port and Ocean Engineering under Arctic Conditions Conference (*POAC), Helsinki.

Nystrom, E., Rehmann, C., ASCE, M., Oberg, K. (2007). Evaluation of Mean velocity and Turbulence Measurements with ADCPs. *Journal of Hydraulic Engineering, 133:12*, 1310.

Randell, C., Freeman, R., Power, D., Stuckey, P. (2009). Technological Advances to Asses, Manage and Reduce Ice Risk in Northern Developments. *Offshore Technology Conference*, Houston, TX.

Sampson, R., Atlar, M., Sasaki, N. (2009). Cavitation analysis of a double acting podded drive during ice milling. *Proceedings of the 7th International Symposium on Cavitation, 135.*

Sasajima, T. & Mustamaki E. (1984). Ice-milling Load Encountered by a Controllable Pitch Propeller. *Proceedings, 7th International Symposium on Ice, International Association for Hydraulic Research*. Hamburg, 281-295.

Searle, S., Veitch, B., and Bose, N. (1999). Ice-class Propeller Performance in Extreme Conditions. *Transactions of Society of Naval Architects and Marine Engineers, 107.*

Shell Offshore Inc. (2011). Appendix K: Ice Management Plan from the Revised Outer Continental Shelf Lease Exploration Plan for Camden Bay, Beaufort Sea, Alaska. Contract Report for: U.S. Department of the Interior.

Situ, R., Brown, R., Loberto, A. (2010). Experimental stud of the concentration field of discharge from a boat propeller. *Environmental Fluid Mechanics, 10*, 657-675.

Spencer, D., Jones, S. J. (2001). Model-Scale/Full-scale correlation in open water and ice for Canadian coast guard "R-class" icebreakers. *Journal of Ship Research, 45*(4), 249.

Stewart, D. (1992). Characteristics of a Ship's Screw Wash and the Influence of Quay Wall Proximity. *Ph.D. Thesis*. Queen's University of Belfast.

Taylor, R., Murrin, D., Kennedy, A., Randell, C. (2012). Arctic Development Roadmap: Prioritization of R&D. *Offshore Technology Conference,* Houston, TX.

Timco, G., Frederking, R. (1996). A Review of Sea Ice Density. *Cold Regions Science and Technology*, *24:1*, 1-6.

Veitch, B. (1994). Results of Ice Cutting Experiments with Cutting Tools Representing Propeller Blades. *Proceedings of the International Association of Hydraulic Research Ice Symposium*, 886-895.

Veitch, B. (1995). *Predictions of ice contact forces on a marine screw propeller during the propeller-ice cutting process.* Doctorate, Helsinki University of Technology, Ship Laboratory.

Verhey, H. J. (1983). *The stability of bottom and banks subjected to velocities in the propeller jet behind ships.* (No. 303). Netherlands: Delft University Hydraulic Laboratory.

Vocke, M., Ranki, E., Uuskallio, A., Niini, M., Wilkman, G. (2011). Experience from Vessels Operating in Ice in the Double Acting Principle. *Arctic Technology Conference*, Houston, TX.

Walker, D.L.N. (1996). The Influence of Blockage and Cavitation on the Hydrodynamic Performance of Ice Class Propellers in Blocked Flow. Doctorate, Memorial University of Newfoundland.

Wang, J., Akinturk, A., Bose, N., Jones, S. J., Song, Y., Chun, H., Kim, M. (2008). Experimental study on a model azimuthing podded propulsor in ice. *Journal of Marine Science and Technology, 13*(3), 244-255.

Wang, J., Akinturk, A., Fosterm, W., Jones, S. J., Bose, N. (2004). An experimental model for ice performance of podded propellers. *27th American Towing Tank Conference.*

Wang, J., Akinturk, A., Jones, S. J., Bose, N., Kim, M., & Chun, H. (2007). Ice loads acting on a model podded propeller blade. *Journal of Offshore Mechanics and Arctic Engineering, 129*(2), 236-244.

Wilkman, G., Arpiainen, M., Niini, M., Mattsson, T., Bercha, F., Bercha, S. (2006). Experience of Azipod Vessels in Ice. *Proceedings of the 7th International Conference on Performance of Ships and Structures in Ice, ICETECH06-134-RF.*

Wind, J. (1983). The dimensioning of high power propeller system for Arctic ice-breakers and icebreaking vessels. *Proceedings, Fifth LIPS Propeller Symposium, Drunen. 9.*

Appendix A

Podded Propulsor Calibrations

THRUST COMPRESSION CALIBRATION

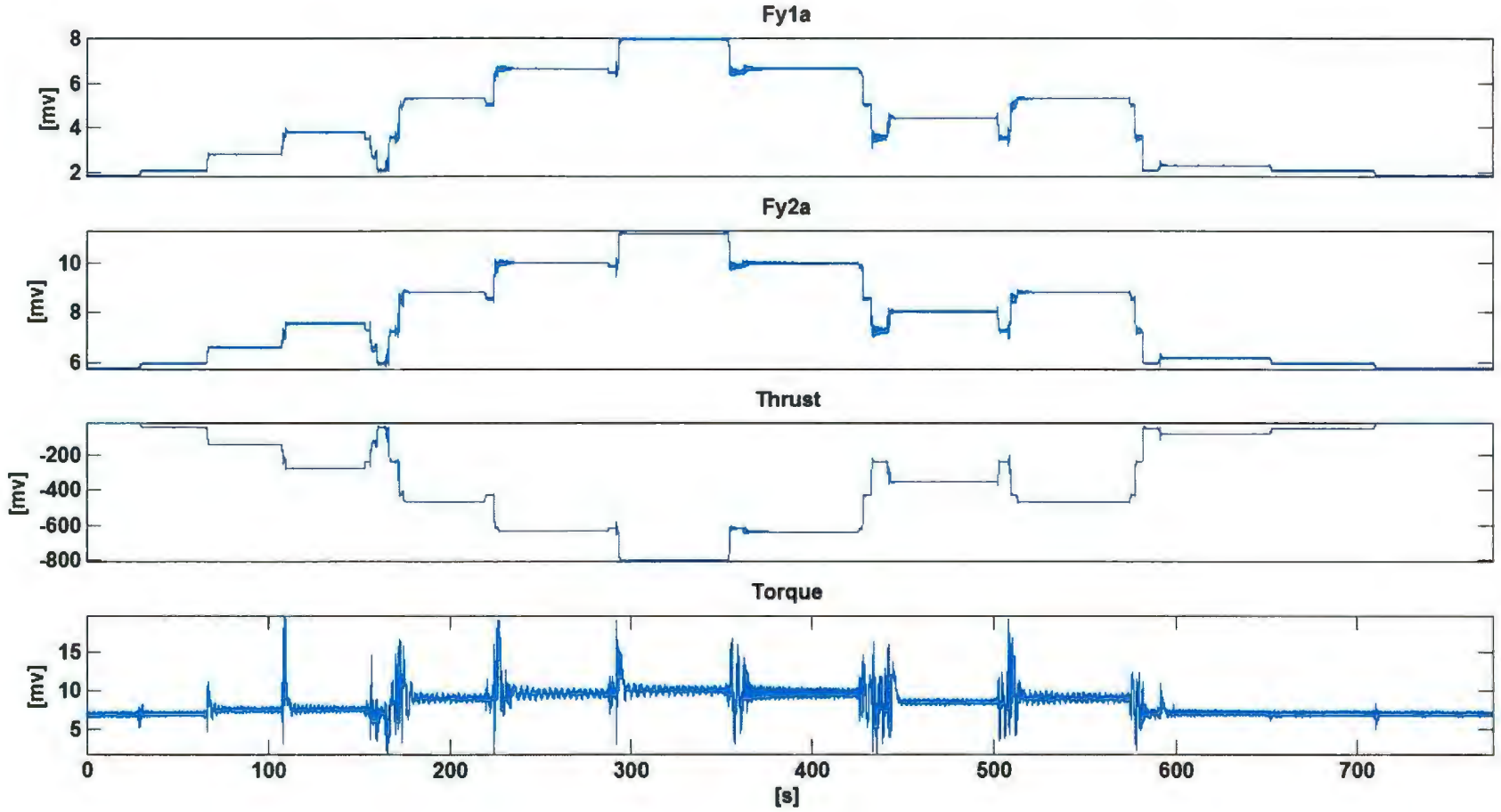

THRUST TENSION CALIBRATION

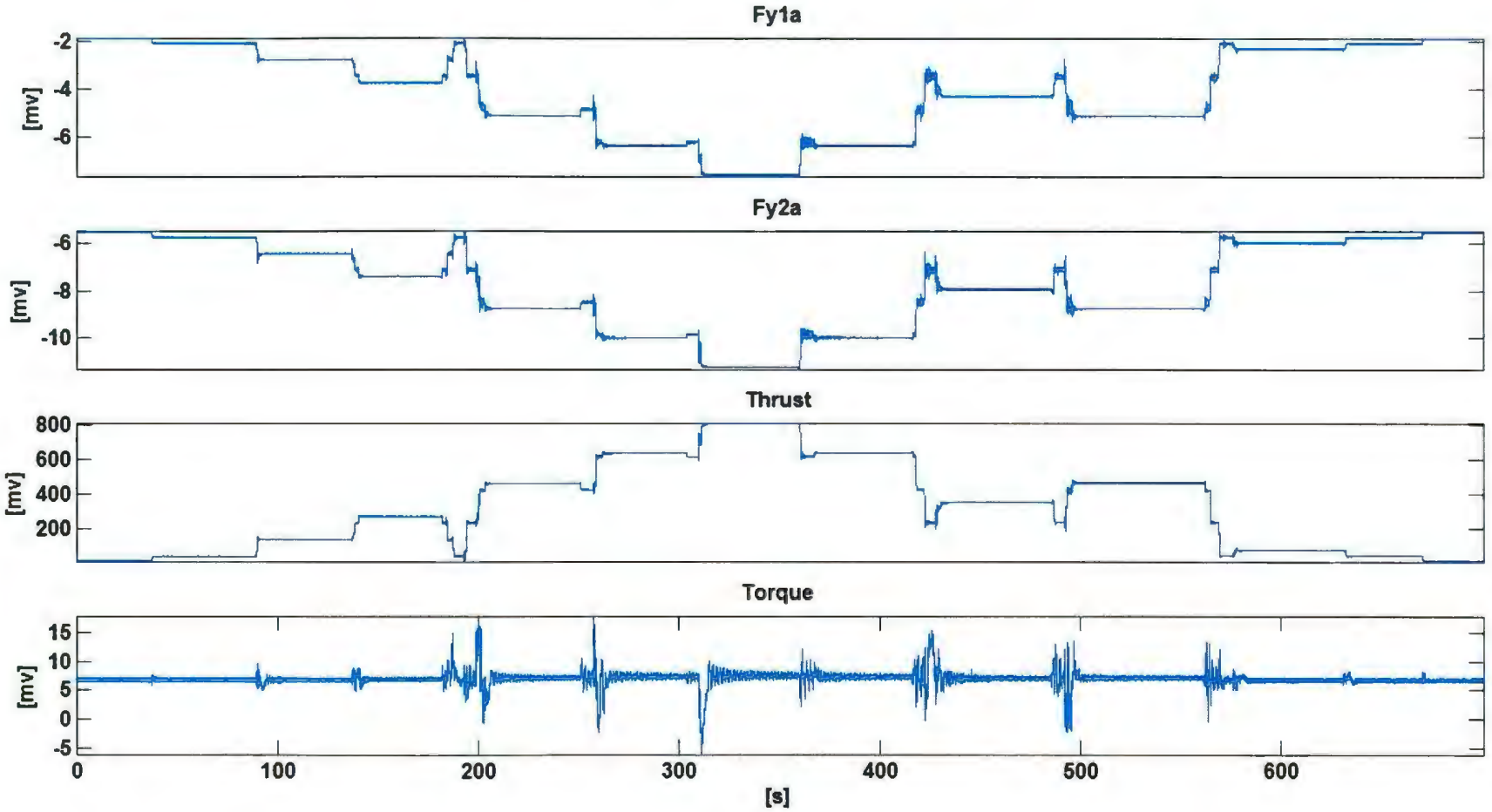

TORQUE COUNTERCLOCKWISE CALIBRATION

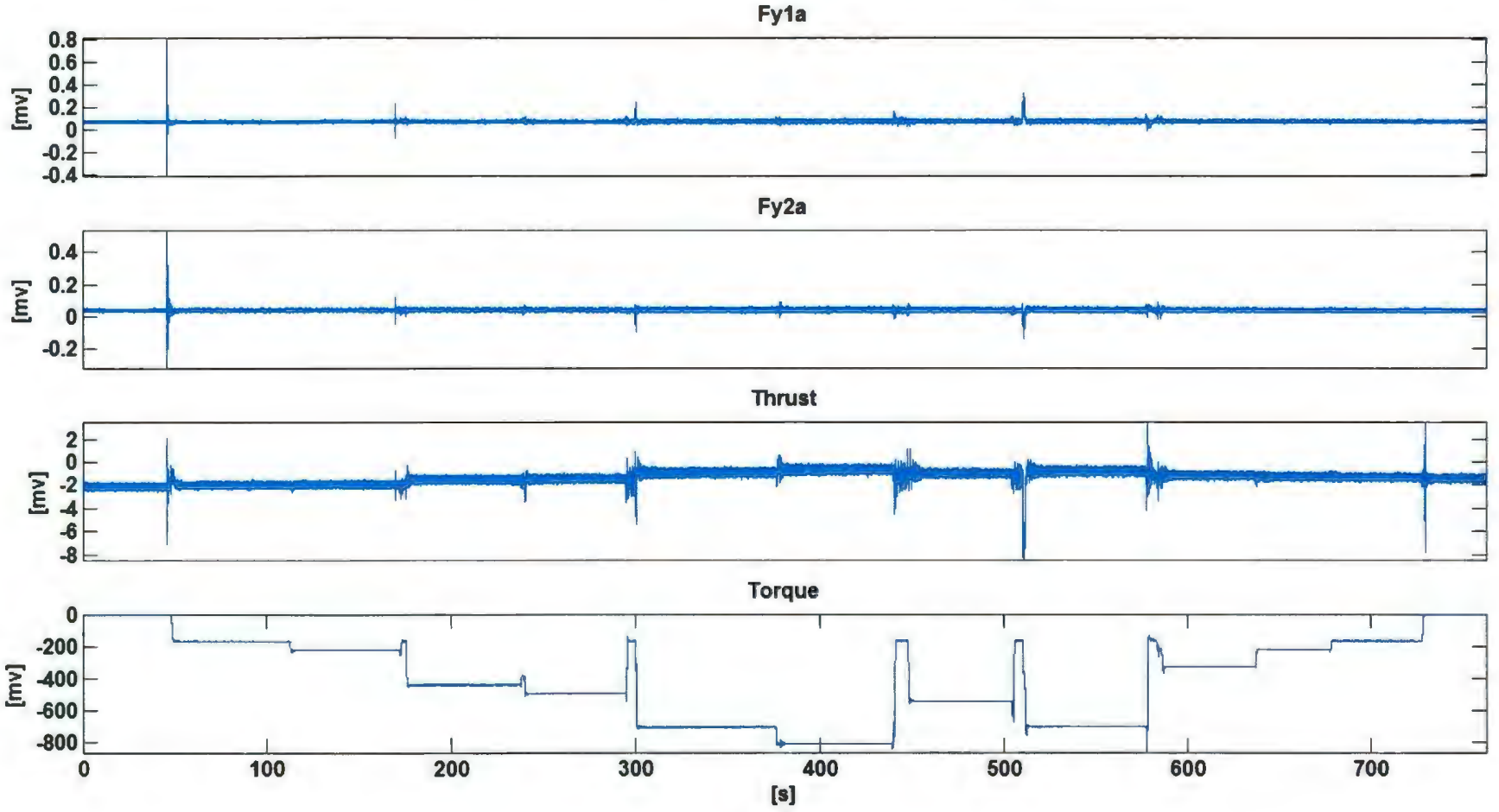

TORQUE CLOCKWISE CALIBRATION

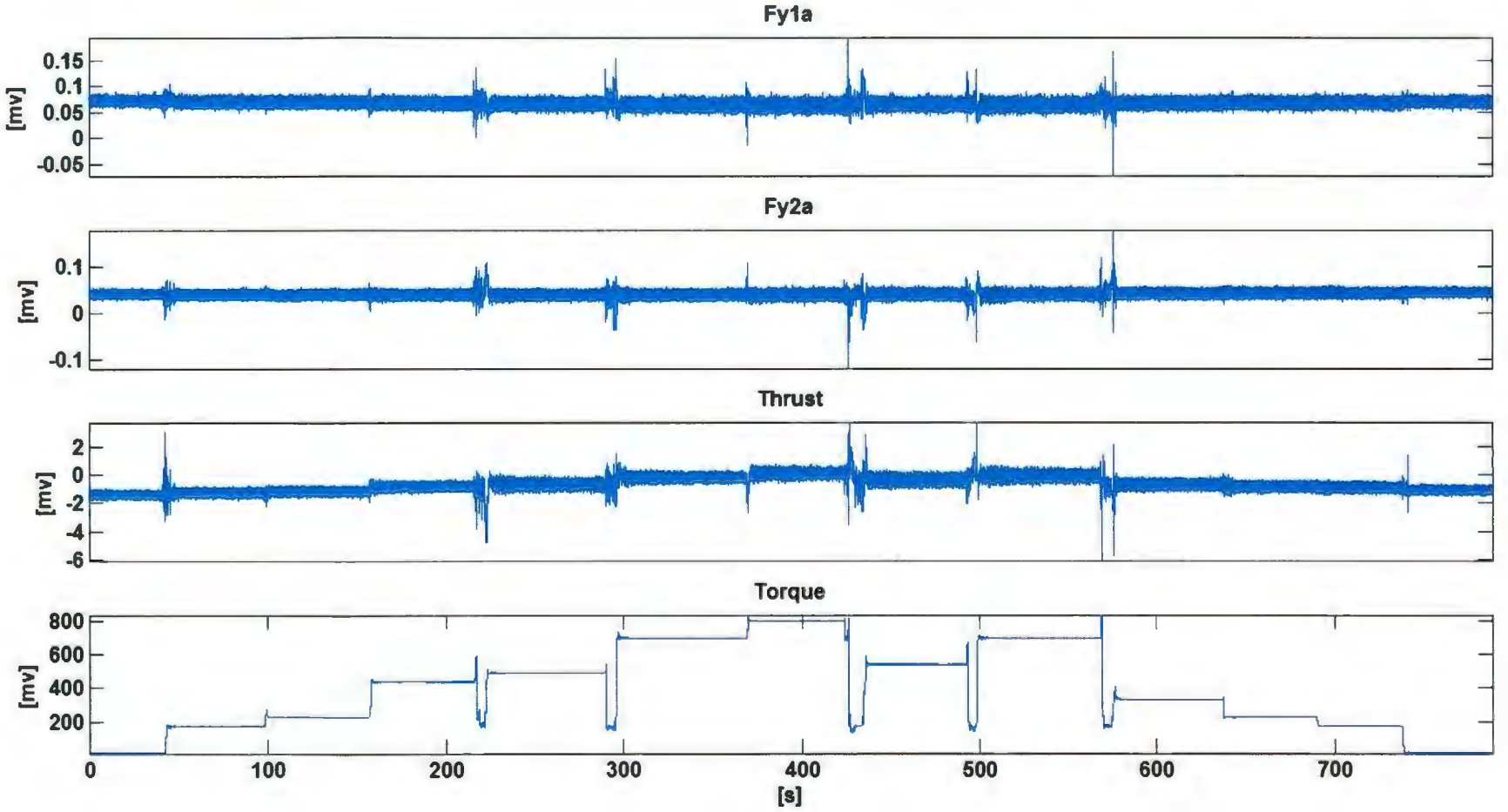

	Stat Type	Seg	Time 1 sec	Time 2 sec	Fxa mv	Fy1a mv	Fy2a mv	Fz1a mv	Fz2a mv	Fz3a mv	Thrust mv	Torque mv	Y-Force mv
POD_A_THRUST_COMPRESSION_001	mean	1	7.68	23.776	0.01001	1.87396	5.79769	1.88865	-3.7373	1.71877	-14.1	6.8728	7.67165
POD_A_THRUST_COMPRESSION_001	mean	2	51.58	61.086	0.00684	2.08481	5.99258	1.59745	-3.1723	1.45005	-42.459	6.95282	8.0774
POD_A_THRUST_COMPRESSION_001	mean	3	76.45	98.396	-0.0039	2.81906	6.63295	0.60834	-1.2566	0.53855	-138.56	7.50663	9.45201
POD_A_THRUST_COMPRESSION_001	mean	4	120.34	146.68	-0.0194	3.80041	7.57808	-0.7771	1.42795	-0.7375	-273.32	7.57536	11.3785
POD_A_THRUST_COMPRESSION_001	mean	5	186.18	213.984	-0.0411	5.31266	8.81909	-2.7603	5.2704	-2.5623	-464.1	9.01354	14.1318
POD_A_THRUST_COMPRESSION_001	mean	6	249.10	278.362	-0.0601	6.63585	9.97703	-4.5456	8.73471	-4.2051	-634.95	9.62139	16.6129
POD_A_THRUST_COMPRESSION_001	mean	7	306.16	342.008	-0.0801	7.95015	11.1429	-6.3317	12.1986	-5.8483	-800.83	10.0037	19.093
POD_A_THRUST_COMPRESSION_001	mean	8	380.78	420.286	-0.0593	6.64447	9.97393	-4.548	8.74163	-4.2052	-637.92	9.62366	16.6184
POD_A_THRUST_COMPRESSION_001	mean	9	453.21	496.369	-0.0263	4.43991	8.0506	-1.5746	2.97935	-1.4677	-352.37	8.50058	12.4905
POD_A_THRUST_COMPRESSION_001	mean	10	527.83	565.868	-0.0397	5.32044	8.81828	-2.763	5.28094	-2.5622	-466.91	9.01446	14.1387
POD_A_THRUST_COMPRESSION_001	mean	11	606.84	647.073	0.00457	2.31331	6.21082	1.27755	-2.55	1.15941	-75.346	7.09205	8.52413
POD_A_THRUST_COMPRESSION_001	mean	12	660.24	701.94	0.00738	2.08261	6.00054	1.59451	-3.165	1.45149	-44.6	6.98519	8.08315
POD_A_THRUST_COMPRESSION_001	mean	13	718.77	764.124	0.0098	1.87518	5.80113	1.88735	-3.7327	1.7209	-16.154	6.97065	7.67631

	Stat Type	Seg	Time 1 sec	Time 2 sec	Fxa mv	Fy1a mv	Fy2a mv	Fz1a mv	Fz2a mv	Fz3a mv	Thrust mv	Torque mv	Y-Force mv
POD_A_THRUST_TENSION__001	mean	1	8.27032	30.104	0.09011	-1.9022	-5.5363	-2.0219	3.35757	-1.2238	11.5996	6.7638	-7.4385
POD_A_THRUST_TENSION__001	mean	2	48.6295	85.6805	0.0909	-2.1042	-5.7403	-1.7197	2.7837	-0.9634	39.9076	6.79378	-7.8445
POD_A_THRUST_TENSION__001	mean	3	100.236	131.333	0.09434	-2.7955	-6.425	-0.7117	0.84684	-0.0654	136.158	6.80351	-9.2205
POD_A_THRUST_TENSION__001	mean	4	148.535	176.323	0.10081	-3.7585	-7.3894	0.69578	-1.8634	1.19381	270.544	6.95237	-11.148
POD_A_THRUST_TENSION__001	mean	5	212.713	243.809	0.11437	-5.1293	-8.7686	2.67623	-5.7268	3.0309	462.095	7.16561	-13.898
POD_A_THRUST_TENSION__001	mean	6	280.198	300.047	0.12368	-6.3676	-10.009	4.46539	-9.2007	4.66779	633.447	7.35927	-16.377
POD_A_THRUST_TENSION__001	mean	7	325.189	354.3	0.13248	-7.6039	-11.252	6.24828	-12.669	6.30693	803.608	7.56199	-18.856
POD_A_THRUST_TENSION__001	mean	8	381.427	409.215	0.12841	-6.3736	-10.008	4.45273	-9.1999	4.69071	634.522	7.30731	-16.381
POD_A_THRUST_TENSION__001	mean	9	444.943	476.04	0.11284	-4.3087	-7.9451	1.47523	-3.4124	1.95855	348.502	7.08151	-12.254
POD_A_THRUST_TENSION__001	mean	10	511.767	551.465	0.11716	-5.1342	-8.7694	2.67466	-5.7301	3.04263	463.227	7.15579	-13.904
POD_A_THRUST_TENSION__001	mean	11	586.531	626.229	0.10255	-2.3339	-5.9552	-1.4306	2.16667	-0.6222	72.0448	6.75592	-8.2891
POD_A_THRUST_TENSION__001	mean	12	639.461	665.264	0.10093	-2.1131	-5.7362	-1.7543	2.78661	-0.9079	41.3406	6.74353	-7.8493
POD_A_THRUST_TENSION__001	mean	13	677.174	695.699	0.10003	-1.9085	-5.5328	-2.0546	3.35956	-1.1717	12.8888	6.73412	-7.4413

	Stat Type	Seg	Time 1 sec Start Tim	Time 2 sec End Time	Fxa mv	Fy1a mv	Fy2a mv	Fz1a mv	Fz2a mv	Fz3a mv	Thrust mv	Torque mv	THRUST_ REPEAT mv
POD_A_TORQUE_CCW_001	mean	1	9.0028	42.13	0.1025	0.0707	0.0427	0.566861	2.217202	4.776465	-2.13327	-0.8301	0.113414
POD_A_TORQUE_CCW_001	mean	2	60.139	105.5	0.1005	0.0708	0.0426	0.766848	2.725609	4.497568	-1.98161	-164.19	0.113426
POD_A_TORQUE_CCW_001	mean	3	121.36	161.7	0.0999	0.0706	0.0427	0.831134	2.897585	4.408603	-1.91425	-219.07	0.113303
POD_A_TORQUE_CCW_001	mean	4	185.46	230.1	0.0968	0.0705	0.0432	1.095632	3.585044	4.036644	-1.51033	-436.3	0.113786
POD_A_TORQUE_CCW_001	mean	5	248.12	285.6	0.0965	0.0709	0.0435	1.15979	3.755995	3.946927	-1.44233	-489.44	0.114334
POD_A_TORQUE_CCW_001	mean	6	309.34	369.8	0.0929	0.0715	0.0432	1.419999	4.442694	3.57716	-0.93475	-701.08	0.114663
POD_A_TORQUE_CCW_001	mean	7	388.56	430.3	0.0918	0.0718	0.0428	1.542836	4.784028	3.402313	-0.68137	-804.34	0.114613
POD_A_TORQUE_CCW_001	mean	8	454.82	499.5	0.094	0.0719	0.0421	1.226409	3.928041	3.847539	-0.99591	-538.76	0.114
POD_A_TORQUE_CCW_001	mean	9	523.24	567.2	0.0925	0.0718	0.0427	1.42045	4.440034	3.577189	-0.83248	-699.34	0.114474
POD_A_TORQUE_CCW_001	mean	10	595.27	633.4	0.0945	0.0727	0.0415	0.981055	3.239326	4.196377	-1.18592	-326.67	0.114184
POD_A_TORQUE_CCW_001	mean	11	648.56	673.8	0.0942	0.0728	0.0404	0.856863	2.894397	4.370967	-1.28052	-218.67	0.113162
POD_A_TORQUE_CCW_001	mean	12	688.9	724.9	0.0943	0.0729	0.0403	0.792889	2.722448	4.460247	-1.32108	-164.24	0.113112
POD_A_TORQUE_CCW_001	mean	13	735.71	759.5	0.0947	0.0728	0.0393	0.602184	2.214144	4.72599	-1.42177	-1.7542	0.112083
POD_A_TORQUE_CW_001	mean	1	9.31	32.4	0.0955	0.0719	0.04	0.57474	2.214015	4.75541	-1.4109	12.2702	0.111894
POD_A_TORQUE_CW_001	mean	2	55.488	89	0.0922	0.0702	0.0388	0.286243	2.720808	4.927264	-1.26969	172.875	0.108948
POD_A_TORQUE_CW_001	mean	3	110.6	143.4	0.0913	0.0693	0.0386	0.1897	2.891655	4.988703	-1.17879	226.357	0.107918
POD_A_TORQUE_CW_001	mean	4	170.93	205.2	0.0887	0.0671	0.0377	-0.20483	3.575743	5.231797	-0.83158	438.454	0.104889
POD_A_TORQUE_CW_001	mean	5	239.45	277.4	0.0887	0.0661	0.0377	-0.30219	3.744531	5.295169	-0.70163	490.683	0.103742
POD_A_TORQUE_CW_001	mean	6	321.38	356.4	0.0867	0.0636	0.0372	-0.6905	4.437014	5.527892	-0.21346	695.667	0.100795
POD_A_TORQUE_CW_001	mean	7	404.05	415.2	0.085	0.0626	0.0374	-0.87361	4.774867	5.639445	0.061524	795.81	0.099986
POD_A_TORQUE_CW_001	mean	8	462.89	489	0.0884	0.065	0.0392	-0.40463	3.923504	5.356843	-0.40558	540.331	0.104139
POD_A_TORQUE_CW_001	mean	9	518.01	559.7	0.086	0.0636	0.038	-0.68868	4.437422	5.525809	-0.11733	694.829	0.101589
POD_A_TORQUE_CW_001	mean	10	592.49	629	0.0926	0.067	0.0407	-0.02488	3.234701	5.137359	-0.72534	331.294	0.107694
POD_A_TORQUE_CW_001	mean	11	651.33	683.4	0.0955	0.0681	0.0417	0.163508	2.8941	5.02692	-0.85403	225.8	0.1098
POD_A_TORQUE_CW_001	mean	12	701.23	725.1	0.0968	0.0687	0.0419	0.258819	2.722799	4.971087	-0.92057	172.689	0.110534
POD_A_TORQUE_CW_001	mean	13	750.39	780.9	0.0998	0.0701	0.043	0.543118	2.218565	4.798688	-1.10444	13.5864	0.113107

Thrust Calibration

Compression performed with Y load cell in tension - long sized cable

Compression Point 1 is long cable and torque bar, eyebolts, nuts, and d-links

	Point	Description	kg	N	mV	mV Tared
Tension Force: POD_A_TENSION_001	1	Tare	0.49	4.80	11.60	0.00
	2	Pan	1.48	14.49	39.91	28.31
	3	W12	6.48	63.53	136.16	124.56
	4	W12+W13+W9	13.48	132.19	270.54	258.94
	5	W15+W16+W9	23.48	230.26	462.10	450.50
	6	W15+W16+W17+W6	32.48	318.53	633.45	621.85
	7	W15+W16+W17+W18	41.48	406.80	803.61	792.01
	8	W15+W16+W17+W6	32.48	318.53	634.52	622.92
	9	W15+W12+W6	17.48	171.42	348.50	336.90
	10	W15+W16+W9	23.48	230.26	463.23	451.63
	11	W3+W4+W6	3.08	30.18	72.04	60.45
	12	Pan	1.48	14.49	41.34	29.74
	13	Tare	0.49	4.80	12.89	1.29
Compression Force: POD_A_THRUST_COMPRESSION_001	1	Tare	0.53	-5.23	-14.10	0.00
	2	Pan	1.48	-14.49	-42.46	-28.36
	3	W12	6.48	-63.53	-138.56	-124.46
	4	W12+W13+W9	13.48	-132.19	-273.32	-259.22
	5	W15+W16+W9	23.48	-230.26	-464.10	-450.00
	6	W15+W16+W17+W6	32.48	-318.53	-634.95	-620.85
	7	W15+W16+W17+W18	41.48	-406.80	-800.83	-786.73
	8	W15+W16+W17+W6	32.48	-318.53	-637.92	-623.82
	9	W15+W12+W6	17.48	-171.42	-352.37	-338.27
	10	W15+W16+W9	23.48	-230.26	-466.91	-452.81
	11	W3+W4+W6	3.08	-30.18	-75.35	-61.25
	12	Pan	1.48	-14.49	-44.60	-30.50
	13	Tare	0.53	-5.23	-16.15	-2.05

Pod A Thrust Calibration

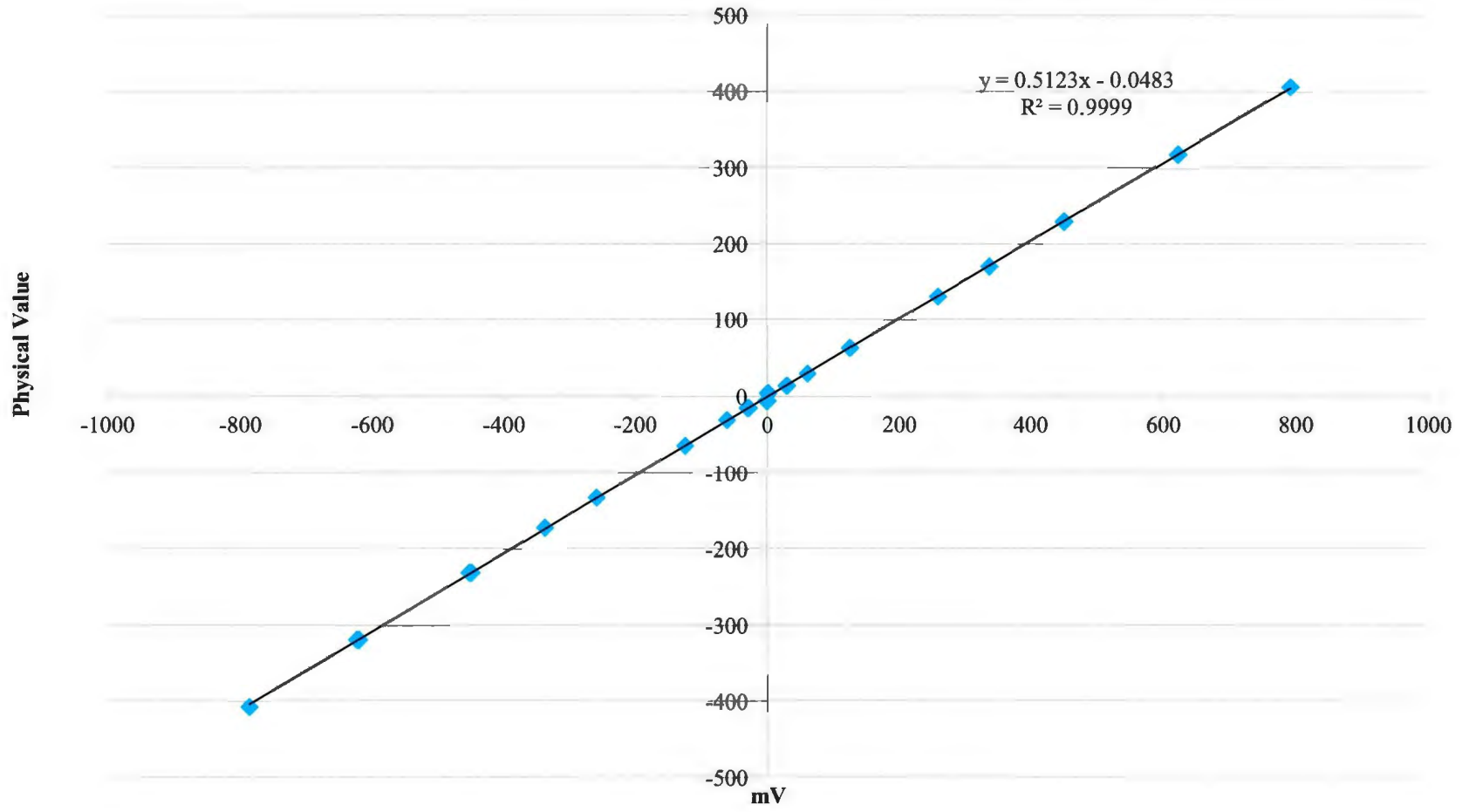

Torque Calibration

Moment Arm = 0.127 m (5 inches)

	Point	Description	Angle	Moment Arm	kg	N	Nm	mV	mV Tared
Clockwise Torque: POD_A_TORQUE_CW_001	1	Tare	0.62	0.1270	0.02	0.19	0.024	12.3	0.0
	2	Pan	1.59	0.1270	1.48	14.49	1.839	172.9	160.6
	3	W4	2.48	0.1269	1.98	19.39	2.461	226.4	214.1
	4	W4+W9	3.65	0.1267	3.98	39.01	4.944	438.5	426.2
	5	W6+W9	4.14	0.1267	4.48	43.91	5.562	490.7	478.4
	6	W12	5.25	0.1265	6.48	63.53	8.034	695.7	683.4
	7	W6+W12	5.89	0.1263	7.48	73.34	9.265	795.8	783.5
	8	W4+W6+W9	5.05	0.1265	4.98	48.82	6.176	540.3	528.1
	9	W12	5.63	0.1264	6.48	63.53	8.029	694.8	682.6
	10	W4+W6	4.36	0.1266	2.98	29.20	3.698	331.3	319.0
	11	W4	3.98	0.1267	1.98	19.39	2.457	225.8	213.5
	12	Pan	3.62	0.1267	1.48	14.49	1.836	172.7	160.4
	13	Tare	2.53	0.1269	0.02	0.19	0.024	13.6	1.3
Counter-Clockwise Torque: POD_A_TORQUE_CCW_001	1	Tare	0.92	0.1270	0.02	0.19	-0.024	-0.8	0.0
	2	Pan	1.75	0.1269	1.48	14.49	-1.839	-164.2	-163.4
	3	W4	2.13	0.1269	1.98	19.39	-2.461	-219.1	-218.2
	4	W4+W9	3.38	0.1268	3.98	39.01	-4.945	-436.3	-435.5
	5	W6+W9	3.86	0.1267	4.48	43.91	-5.564	-489.4	-488.6
	6	W12	5.07	0.1265	6.48	63.53	-8.037	-701.1	-700.3
	7	W6+W12	5.8	0.1263	7.48	73.34	-9.266	-804.3	-803.5
	8	W4+W6+W9	4.83	0.1265	4.98	48.82	-6.178	-538.8	-537.9
	9	W12	5.53	0.1264	6.48	63.53	-8.031	-699.3	-698.5
	10	W4+W6	3.99	0.1267	2.98	29.20	-3.700	-326.7	-325.8
	11	W4	3.61	0.1267	1.98	19.39	-2.458	-218.7	-217.8
	12	Pan	3.31	0.1268	1.48	14.49	-1.837	-164.2	-163.4
	13	Tare	1.91	0.1269	0.02	0.19	-0.024	-1.8	-0.9

Pod A Torque Calibration

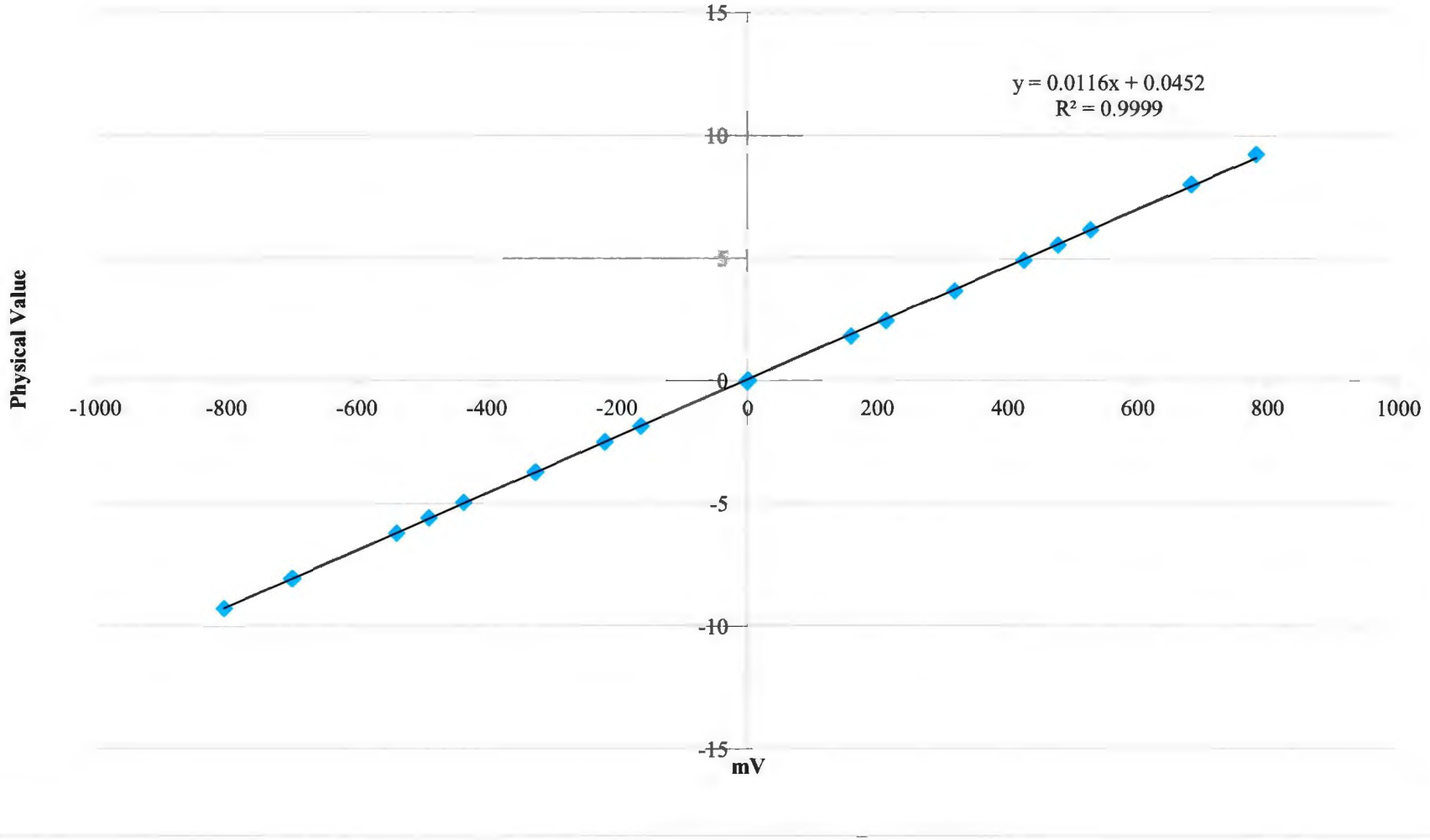

Y Force Calibration (Thrust Repeated)

Dist to Y1 and Y2 0.10414 m

					Thrust Repeated	
	Point	**Description**	**kg**	**N**	**mV**	**mV Tared**
Tension Force: POD_A_THRUST_COMPRESSION_001	1	Tare	0.53	5.23	7.67	0.00
	2	Pan	1.48	14.49	8.08	0.41
	3	W12	6.48	63.53	9.45	1.78
	4	W12+W13+W9	13.48	132.19	11.38	3.71
	5	W15+W16+W9	23.48	230.26	14.13	6.46
	6	W15+W16+W17+W6	32.48	318.53	16.61	8.94
	7	W15+W16+W17+W18	41.48	406.80	19.09	11.42
	8	W15+W16+W17+W6	32.48	318.53	16.62	8.95
	9	W15+W12+W6	17.48	171.42	12.49	4.82
	10	W15+W16+W9	23.48	230.26	14.14	6.47
	11	W3+W4+W6	3.08	30.18	8.52	0.85
	12	Pan	1.48	14.49	8.08	0.41
	13	Tare	0.5335	5.23	7.68	0.00
Compression Force: POD_A_THRUST_TENSION_001	1	Tare	0.49	-4.80	-7.44	0.00
	2	Pan	1.48	-14.49	-7.84	-0.41
	3	W12	6.48	-63.53	-9.22	-1.78
	4	W12+W13+W9	13.48	-132.19	-11.15	-3.71
	5	W15+W16+W9	23.48	-230.26	-13.90	-6.46
	6	W15+W16+W17+W6	32.48	-318.53	-16.38	-8.94
	7	W15+W16+W17+W18	41.48	-406.80	-18.86	-11.42
	8	W15+W16+W17+W6	32.48	-318.53	-16.38	-8.94
	9	W15+W12+W6	17.48	-171.42	-12.25	-4.82
	10	W15+W16+W9	23.48	-230.26	-13.90	-6.47
	11	W3+W4+W6	3.08	-30.18	-8.29	-0.85
	12	Pan	1.48	-14.49	-7.85	-0.41
	13	Tare	0.49	-4.80	-7.44	0.00

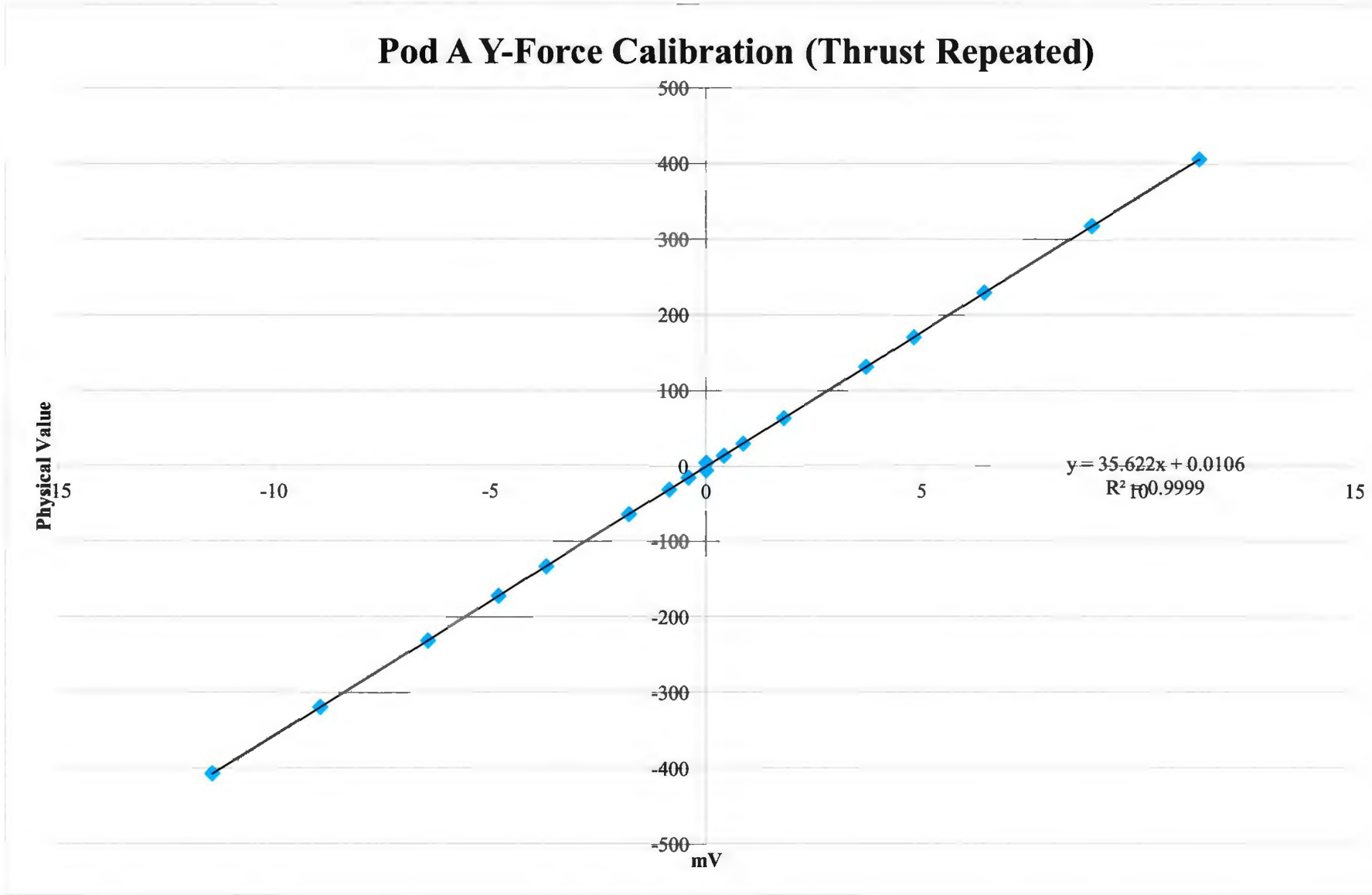
Pod A Y-Force Calibration (Thrust Repeated)
Physical Value
500
400
300
200
100
0
-100
-200
-300
-400
-500
-15
-10
-5
0
5
10
15
mV
y = 35.622x + 0.0106
R² = 0.9999

Appendix B

Experiment Data

Test Number	Prop RPM	Incline Angle	Distance to Ice Edge	Degree of Ice	Filename
Test 1	12.5 RPS	0 deg	0.4 m	3/10	Ice_Test_1_001
Test 2	12.5 RPS	5 deg	1 m	3/10	Ice_Test_2_001
Test 3	12.5 RPS	0 deg	0.4 m	6/10	Ice_Test_3_001
Test 4	12.5 RPS	5 deg	0.4 m	6/10	Ice_Test_4_001
Test 5	5.0 RPS	2.5 deg	0.7 m	4.5/10	Ice_Test_5_001
Test 6	10.0 RPS	2.5 deg	0.7 m	4.5/10	Ice_Test_6_001
Test 7	10.0 RPS	2.5 deg	0.7 m	1.5/10	Ice_Test_7_001
Test 8	10.0 RPS	2.5 deg	0.7 m	4.5/10	Ice_Test_8_001
Test 9	12.5 RPS	5 deg	0.4 m	3/10	Ice_Test_9_001
Test 10	12.5 RPS	0 deg	1 m	3/10	Ice_Test_10_001
Test 11	10.0 RPS	2.5 deg	0.1 m	4.5/10	Ice_Test_11_001
Test 12	10.0 RPS	-2.5 deg	0.7 m	4.5/10	Ice_Test_12_001
Test 13	12.5 RPS	5 deg	1 m	6/10	Ice_Test_13_001
Test 14	7.5 RPS	0 deg	1 m	6/10	Ice_Test_14_001
Test 15	10.0 RPS	7.5 deg	0.7 m	4.5/10	Ice_Test_15_001
Test 16	12.5 RPS	0 deg	1 m	6/10	Ice_Test_16_001
Test 17	10.0 RPS	2.5 deg	0.7 m	7.5/10	Ice_Test_17_001
Test 18	7.5 RPS	5 deg	0.4 m	6/10	Ice_Test_18_001
Test 19	10.0 RPS	2.5 deg	0.7 m	4.5/10	Ice_Test_19_001
Test 20	7.5 RPS	5 deg	1 m	3/10	Ice_Test_20_001
Test 21	7.5 RPS	0 deg	0.4 m	6/10	Ice_Test_21_001
Test 22	10.0 RPS	2.5 deg	0.6 m	4.5/10	Ice_Test_22_001
Test 23	10.0 RPS	2.5 deg	1.3 m	4.5/10	Ice_Test_23_001
Test 24	10.0 RPS	2.5 deg	0.7 m	4.5/10	Ice_Test_24_001
Test 25	7.5 RPS	5 deg	0.4 m	3/10	Ice_Test_25_001
Test 26	7.5 RPS	0 deg	1 m	3/10	Ice_Test_26_001
Test 27	15.0 RPS	2.5 deg	0.7 m	4.5/10	Ice_Test_27_001
Test 28	10.0 RPS	2.5 deg	0.7 m	4.5/10	Ice_Test_28_001
Test 29	7.5 RPS	0 deg	0.4 m	3/10	Ice_Test_29_001
Test 30	7.5 RPS	5 deg	1 m	6/10	Ice_Test_30_001

	Model Scale				Full Scale			
Level	RPS	Incline Angle	Distance to Ice Edge	Degree of Ice Cover	RPM	Incline Angle	Distance to Ice Edge	Degree of Ice Cover
-2	5.0	-2.5 deg	0.1 m	15%	67.1	-7.5 deg	2 m	15%
-1	7.5	0 deg	0.4 m	30%	100.6	0 deg	8 m	30%
0	10.0	2.5 deg	0.7 m	45%	134.2	7.5 deg	14 m	45%
1	12.5	5 deg	1.0 m	60%	167.7	15 deg	20 m	60%
2	15.0	7.5 deg	1.3 m	75%	201.2	22.5 deg	26 m	75%

15 seconds scales to 1.20 minutes

TYPICAL PROPERTIES of POLYPROPYLENE

ASTM or UL test	Property	Homopolymer	Co-Polymer	Flame Retardant
PHYSICAL				
D792	Density (lb/in^3) (g/cm^3)	0.033 0.905	0.033 0.897	0.035 0.988
D570	Water Absorption, 24 hrs (%)	<0.01	0.01	0.02
MECHANICAL				
D638	Tensile Strength (psi)	4,800	4,800	4,300
D638	Tensile Modulus (psi)	195,000	-	-
D638	Tensile Elongation at Yield (%)	12	23	28
D790	Flexural Strength (psi)	7,000	5,400	-
D790	Flexural Modulus (psi)	180,000	160,000	145,000
D695	Compressive Strength (psi)	7,000	6,000	-
D695	Compressive Modulus (psi)	-	-	-
D785	Hardness, Rockwell R	92	80	-
D256	IZOD Notched Impact (ft-lb/in)	1.9	7.5	0.65
THERMAL				
D696	Coefficient of Linear Thermal Expansion (x 10^{-5} in./in./°F)	6 2	6 6	-
D648	Heat Deflection Temp (°F / °C) at 66 psi at 264 psi	 210 / 99 125 / 52	 173 / 78 110 / 43	 106 / 41 57 / 14
D3418	Melting Temperature (°F / °C)	327 / 164	327 / 164	327 / 164
-	Max Operating Temp (°F / °C)	180 / 82	170 / 77	180 / 82
C177	Thermal Conductivity (BTU-in/ft^2-hr-°F) (x 10^{-4} cal/cm-sec-°C)	 0.76-0.81 2.6-2.8	 - -	 - -
UL94	Flammability Rating	HB	n.r.	V-O
ELECTRICAL				
D149	Dielectric Strength (V/mil) short time, 1/8" thick	500-660	475	500-650
D150	Dielectric Constant at 1 kHz	2.25	2.2-2.36	2.3
D150	Dissipation Factor at 1 kHz	0.0005-0.0018	0.0017	-
D257	Volume Resistivity (ohm-cm) at 50% RH	8.5 x 10^{14}	2 x 10^{16}	10^{15}
D495	Arc Resistance (sec)	160	100	-

Source: Professional Plastics Polypropylene Data Sheet
http://www.professionalplastics.com/professionalplastics/content/Polypro.pdf

Appendix C

Podded Propulsor Unit Analysis

Wake Scaling

D_p	200	mm	
D_h	46.5	mm	
ν	1.14E-06	m^2/s at 15C	
β	0.44	From scaling	
N	4		
L_m	45.03	mm	$\beta D_p \pi [2N(1-(D_h/D_p)]^{-1}$
C_t	0.17	From design J value	

RPS	V_0	Re_{prop}	Re_{flow}
5	0.66	3.95E+04	1.15E+05
7.5	0.98	5.92E+04	1.72E+05
10	1.31	7.89E+04	2.30E+05
12.5	1.64	9.87E+04	2.87E+05
15	1.97	1.18E+05	3.45E+05

RPS	**Re_{prop}**	**Re_{flow}**
5	3.95E+04	1.15E+05
7.5	5.92E+04	1.72E+05
10	7.89E+04	2.30E+05
12.5	9.87E+04	2.87E+05
15	1.18E+05	3.45E+05

TEST 1

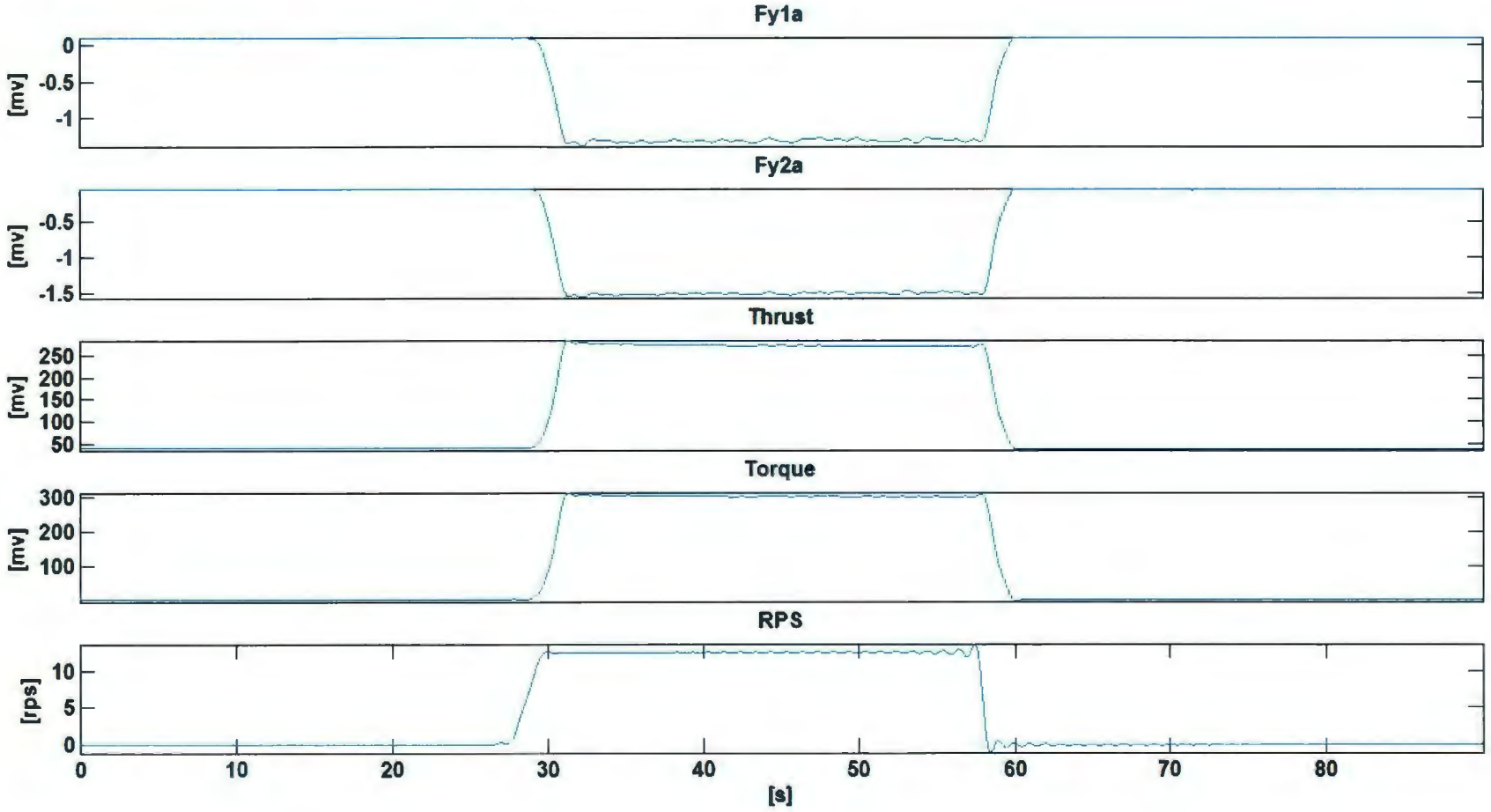
Fy1a
[mv]
0
-0.5
-1
Fy2a
[mv]
-0.5
-1
-1.5
Thrust
[mv]
250
200
150
100
50
Torque
[mv]
300
200
100
RPS
[rps]
10
5
0
0
10
20
30
40
50
60
70
80
[s]

TEST 2

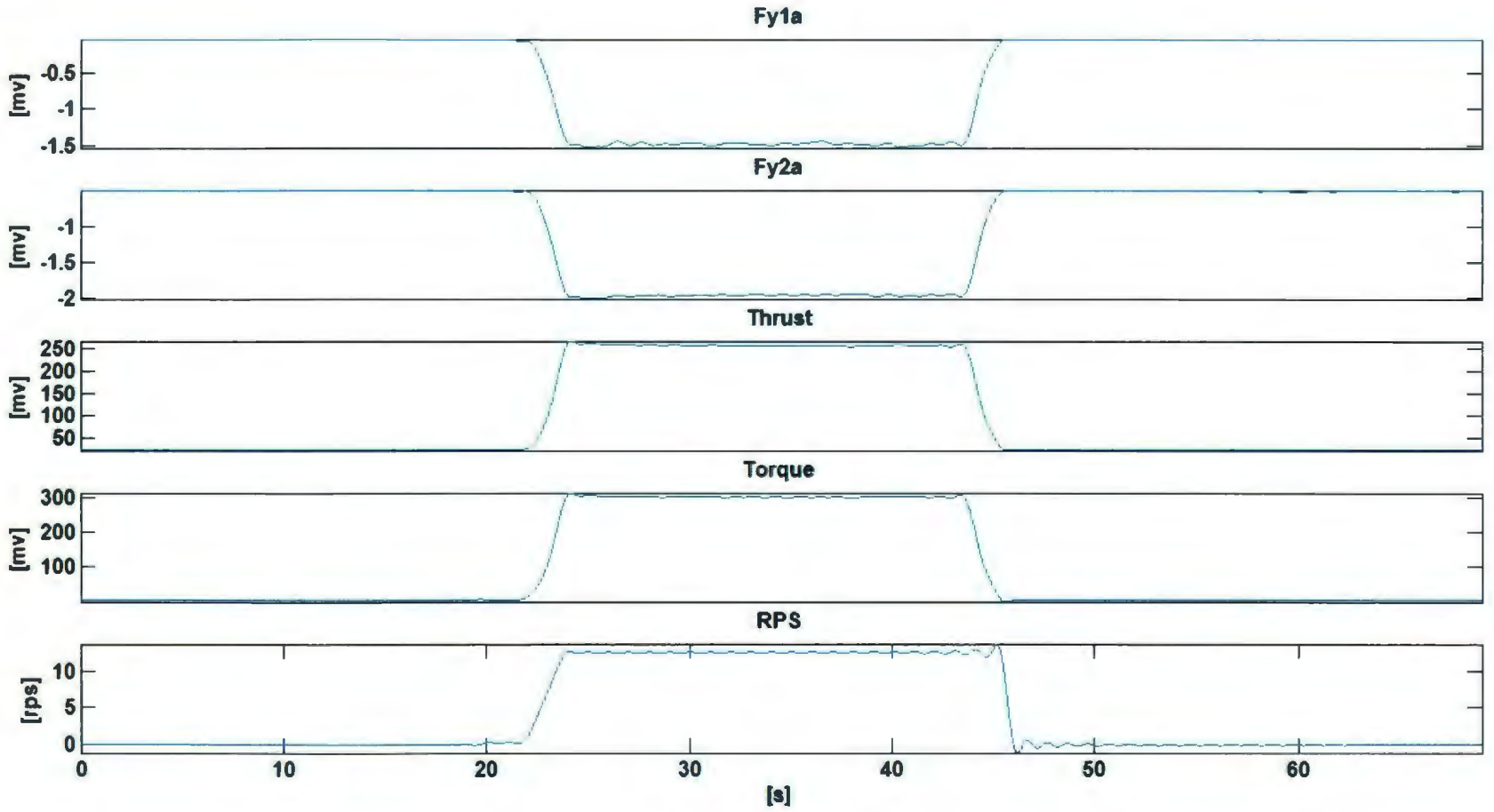
Fy1a
[mv]
-0.5
-1
-1.5
Fy2a
[mv]
-1
-1.5
-2
Thrust
[mv]
250
200
150
100
50
Torque
[mv]
300
200
100
RPS
[rps]
10
5
0
0
10
20
30
40
50
60
[s]

TEST 3

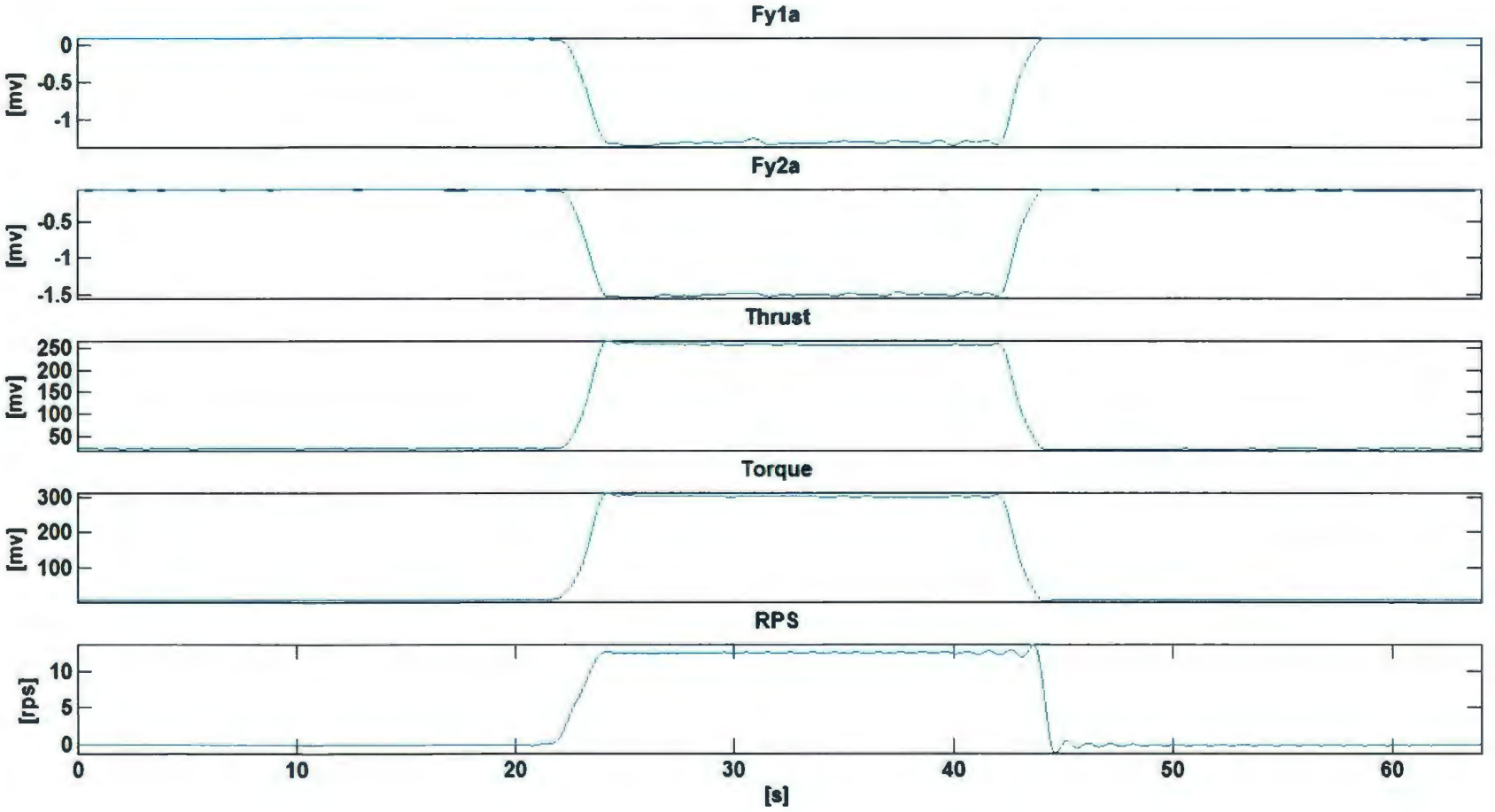
Fy1a
[mv]
0
-0.5
-1
Fy2a
[mv]
-0.5
-1
-1.5
Thrust
[mv]
250
200
150
100
50
Torque
[mv]
300
200
100
RPS
[rps]
10
5
0
0
10
20
30
40
50
60
[s]

TEST 4

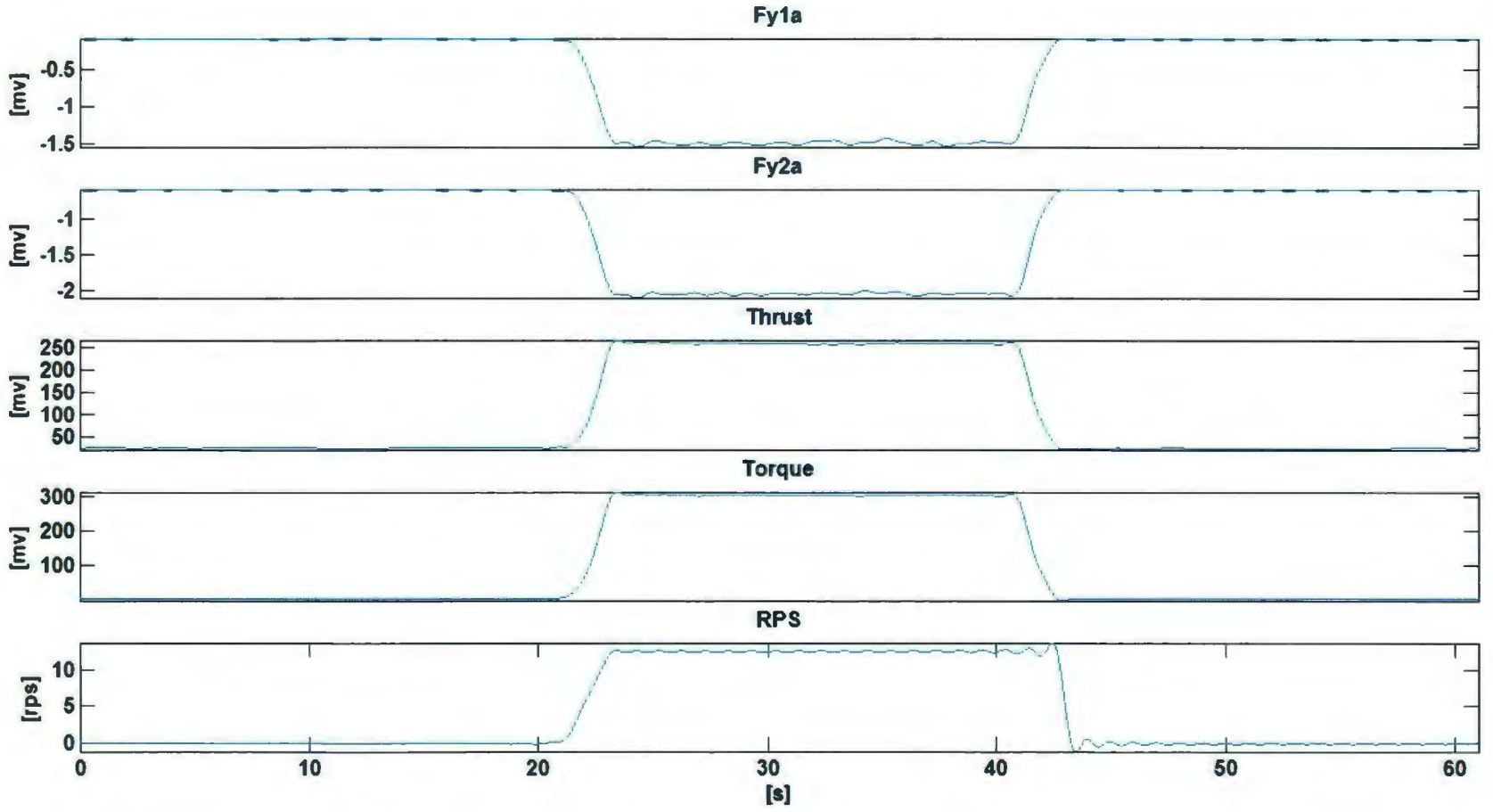
Fy1a
[mv]
-0.5
-1
-1.5
Fy2a
[mv]
-1
-1.5
-2
Thrust
[mv]
250
200
150
100
50
Torque
[mv]
300
200
100
RPS
[rps]
10
5
0
0
10
20
30
40
50
60
[s]

TEST 5

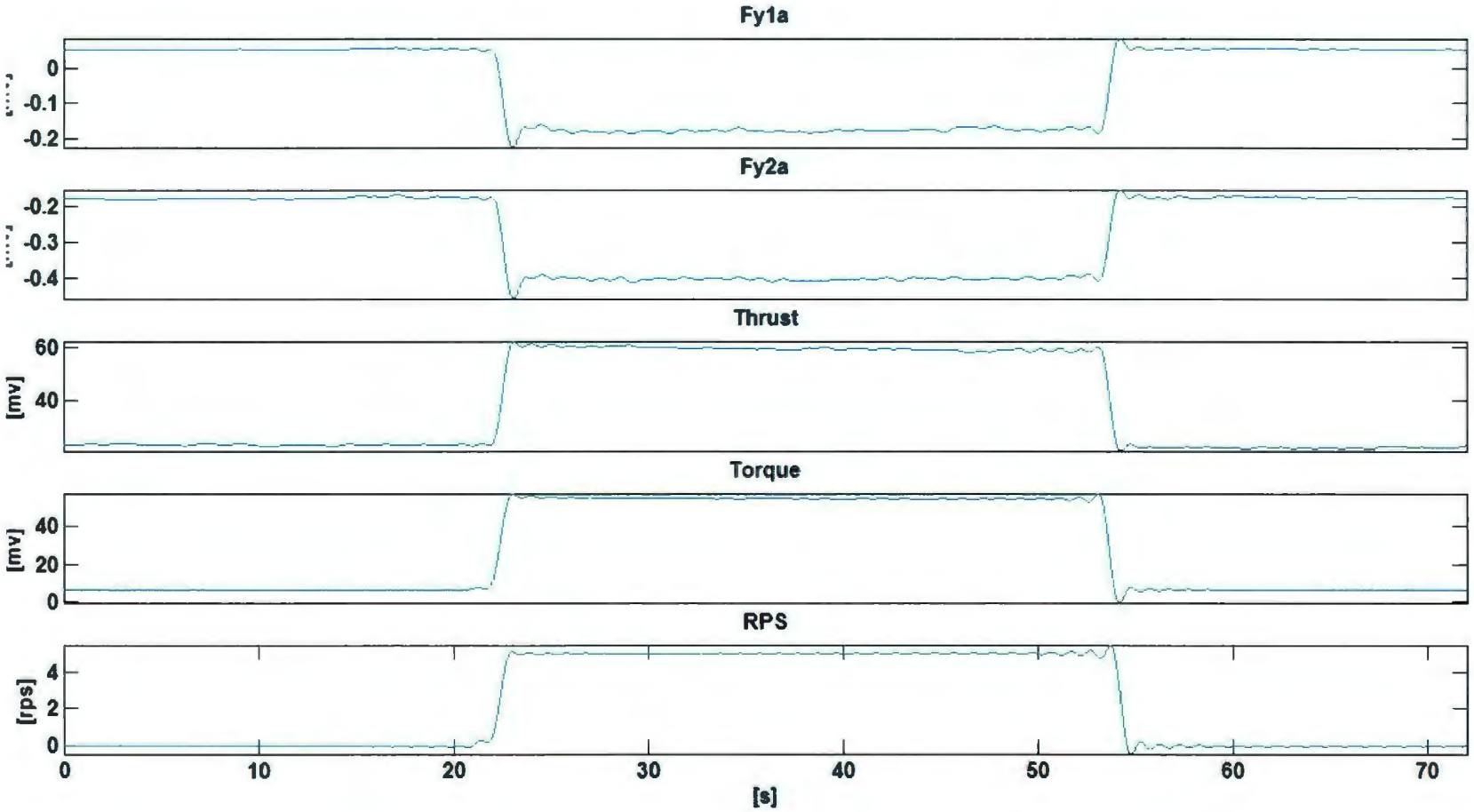
Fy1a
0
-0.1
-0.2
Fy2a
-0.2
-0.3
-0.4
Thrust
60
40
[mv]
Torque
40
20
0
[mv]
RPS
4
2
0
[rps]
0
10
20
30
40
50
60
70
[s]

TEST 6

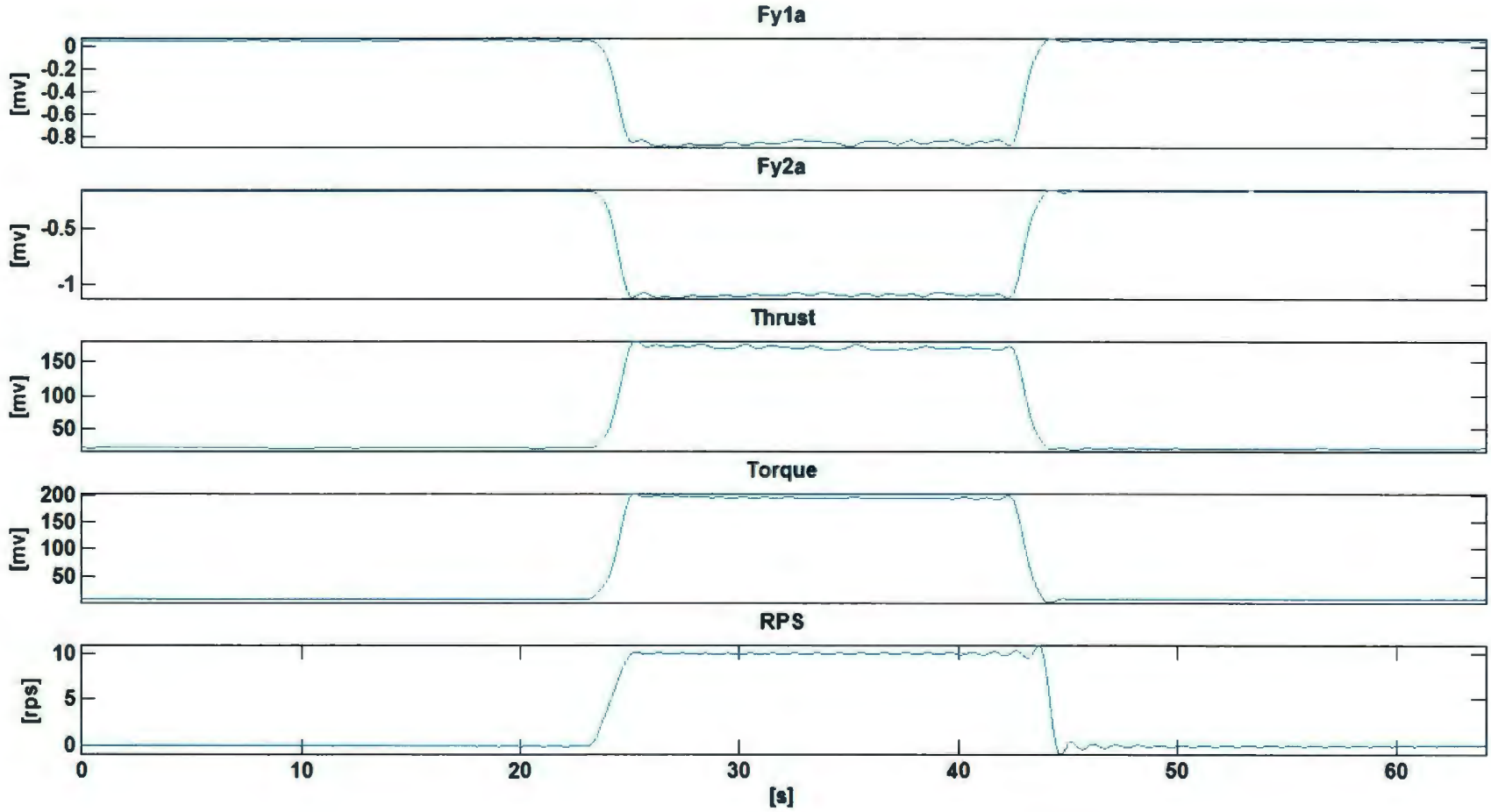
Fy1a
[mv]
0
-0.2
-0.4
-0.6
-0.8
Fy2a
[mv]
-0.5
-1
Thrust
[mv]
150
100
50
Torque
[mv]
200
150
100
50
RPS
[rps]
10
5
0
0
10
20
30
40
50
60
[s]

TEST 7

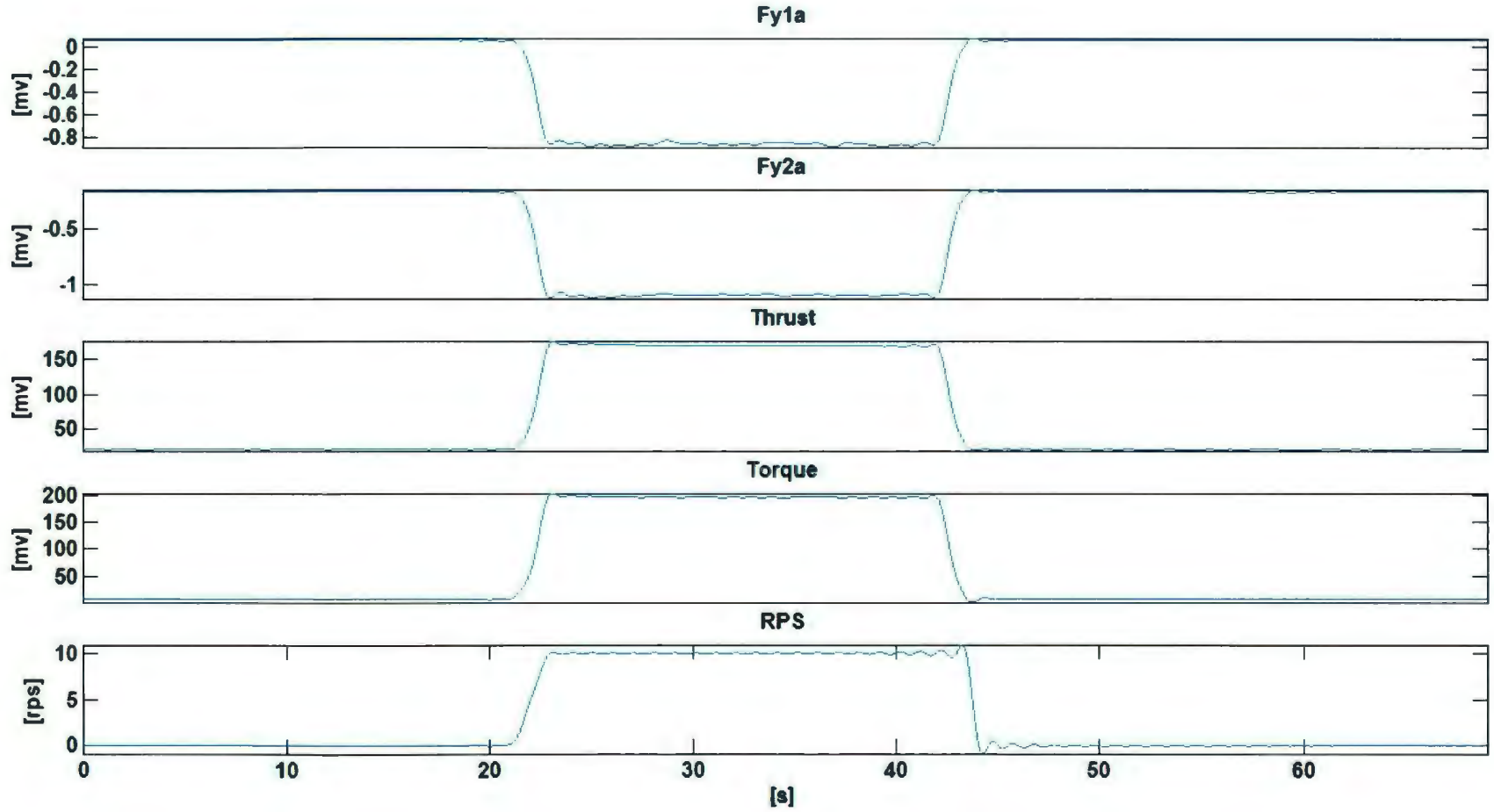
Fy1a
[mv]
0
-0.2
-0.4
-0.6
-0.8
Fy2a
[mv]
-0.5
-1
Thrust
[mv]
150
100
50
Torque
[mv]
200
150
100
50
RPS
[rps]
10
5
0
0
10
20
30
40
50
60
[s]

TEST 8

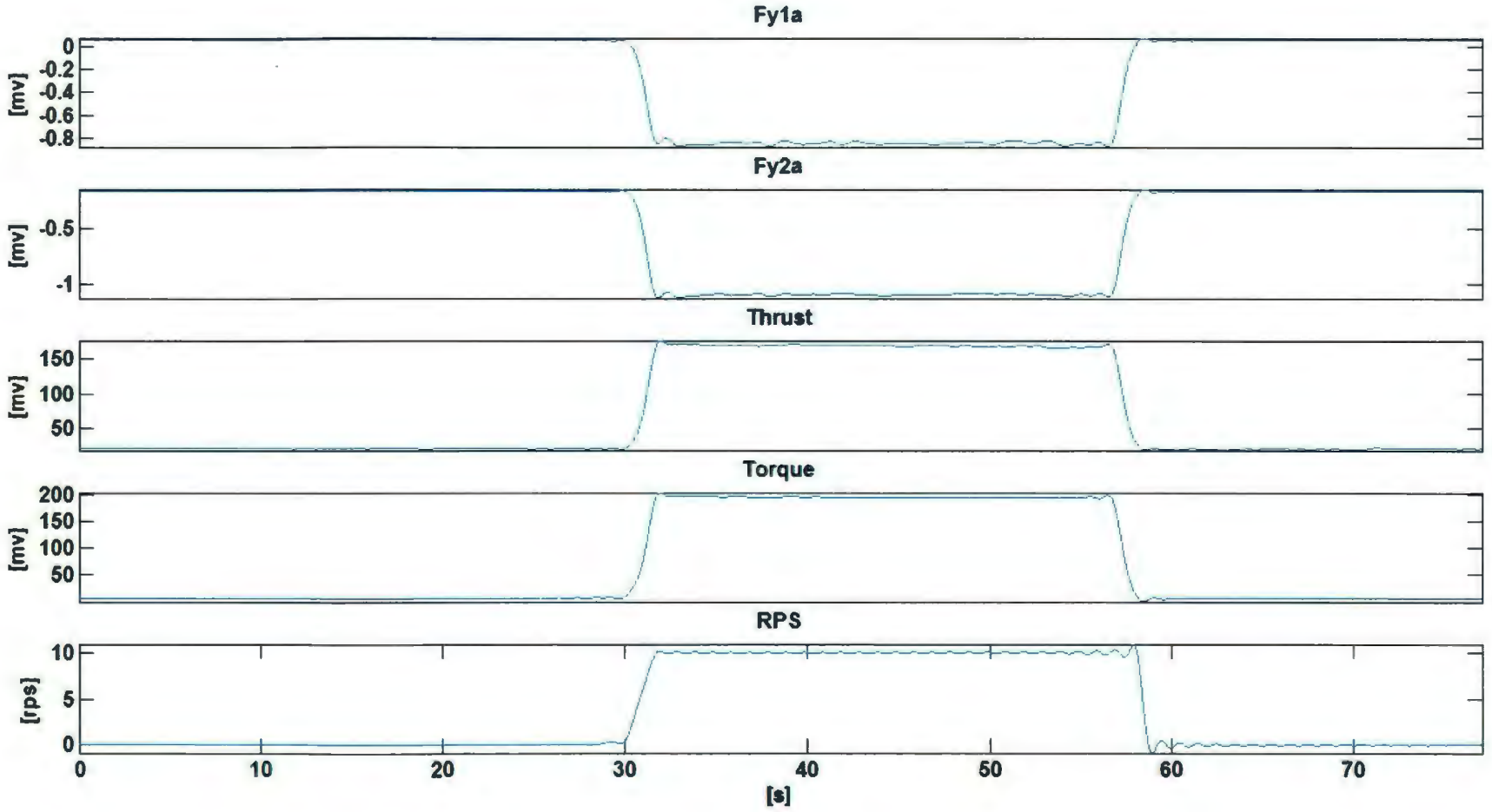
Fy1a
[mv]
0
-0.2
-0.4
-0.6
-0.8
Fy2a
[mv]
-0.5
-1
Thrust
[mv]
150
100
50
Torque
[mv]
200
150
100
50
RPS
[rps]
10
5
0
0
10
20
30
40
50
60
70
[s]

TEST 9

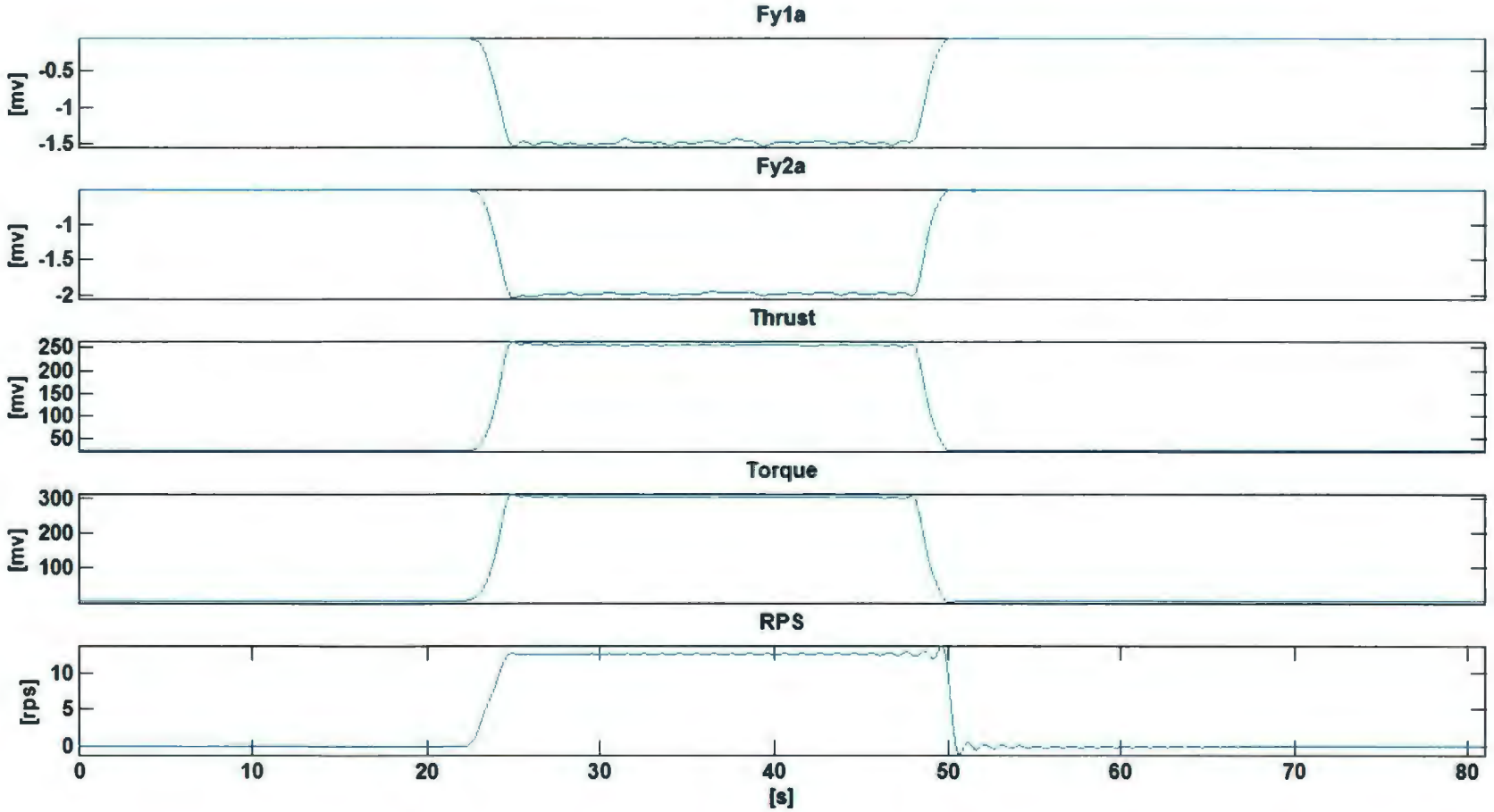
Fy1a
[mv]
-0.5
-1
-1.5
Fy2a
[mv]
-1
-1.5
-2
Thrust
[mv]
250
200
150
100
50
Torque
[mv]
300
200
100
RPS
[rps]
10
5
0
0
10
20
30
40
50
60
70
80
[s]

TEST 10

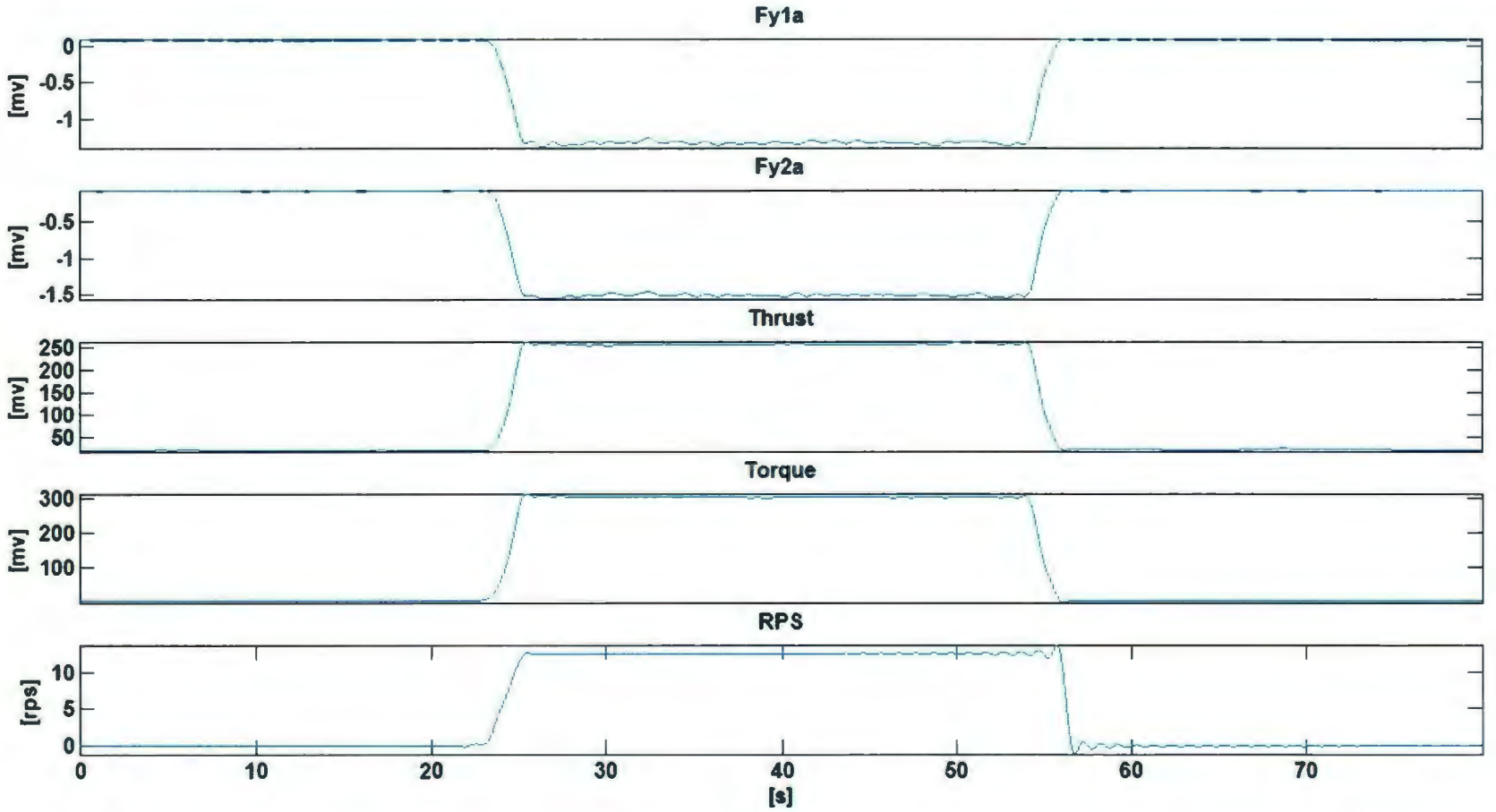
Fy1a
[mv]
0
-0.5
-1
Fy2a
[mv]
-0.5
-1
-1.5
Thrust
[mv]
250
200
150
100
50
Torque
[mv]
300
200
100
RPS
[rps]
10
5
0
0
10
20
30
40
50
60
70
[s]

TEST 11

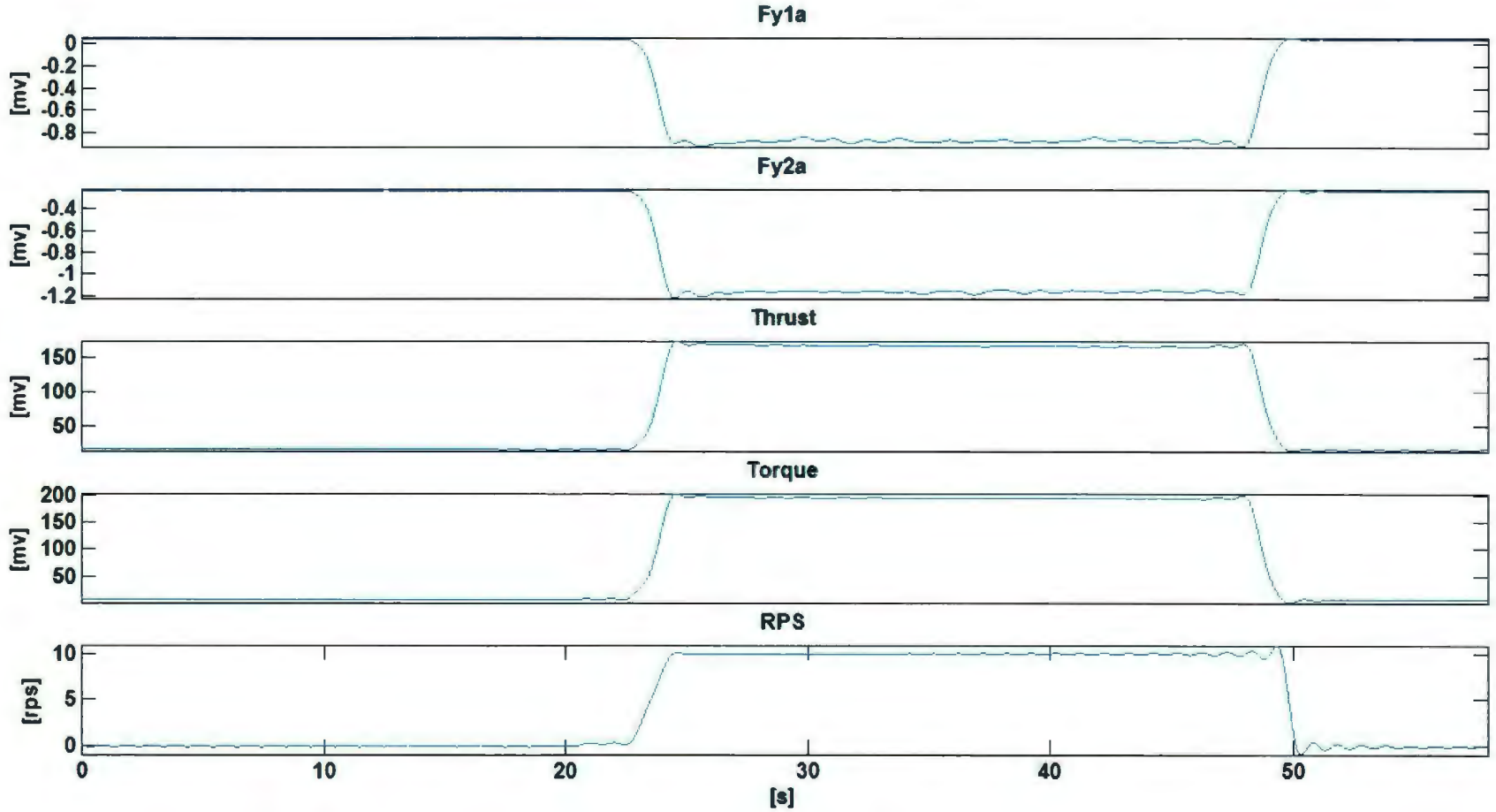
Fy1a
[mv]
0
-0.2
-0.4
-0.6
-0.8
Fy2a
[mv]
-0.4
-0.6
-0.8
-1
-1.2
Thrust
[mv]
150
100
50
Torque
[mv]
200
150
100
50
RPS
[rps]
10
5
0
0
10
20
30
40
50
[s]

TEST 12

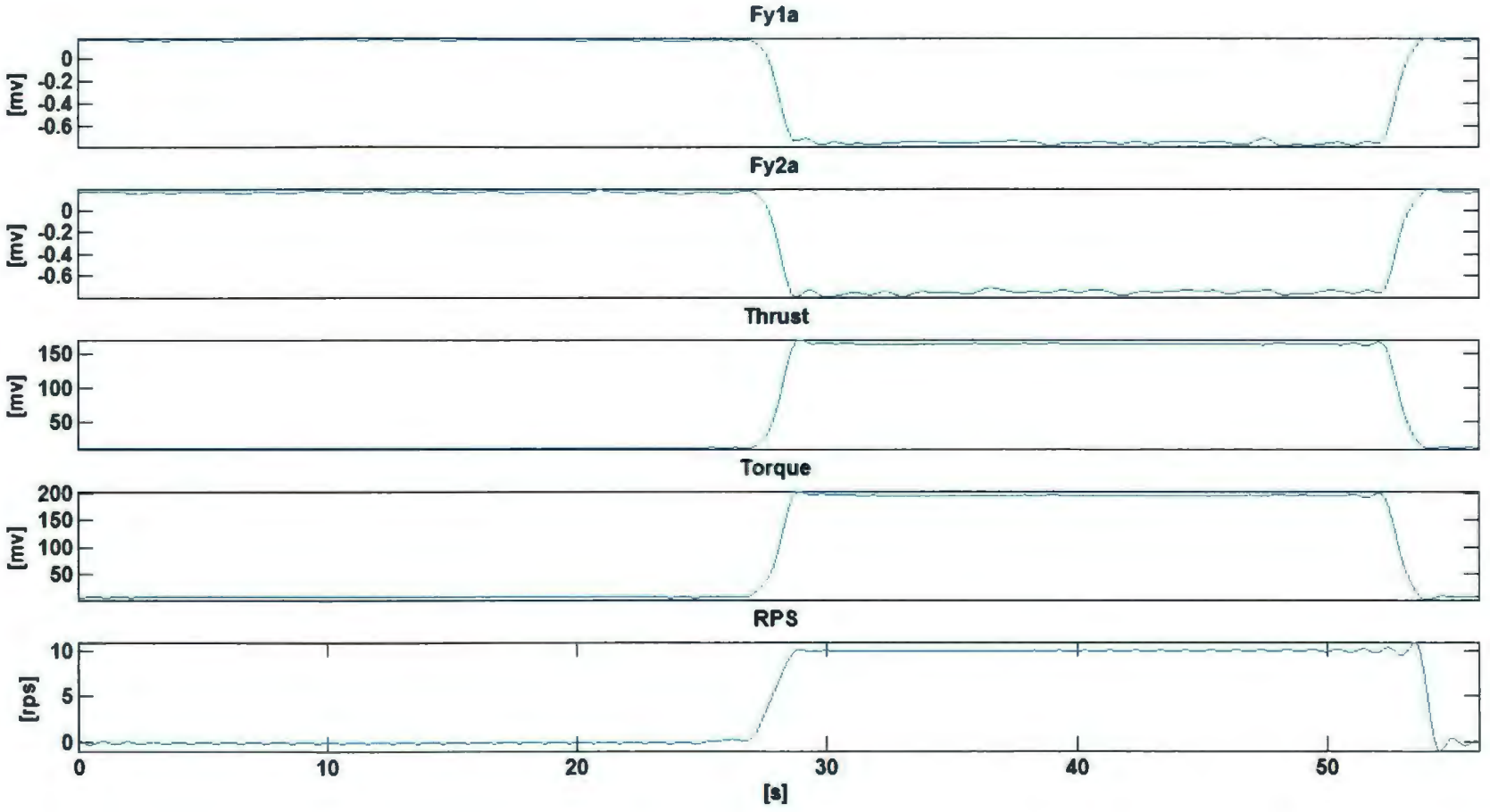
Fy1a
[mv]
0
-0.2
-0.4
-0.6
Fy2a
[mv]
0
-0.2
-0.4
-0.6
Thrust
[mv]
150
100
50
Torque
[mv]
200
150
100
50
RPS
[rps]
10
5
0
0
10
20
30
40
50
[s]

TEST 13

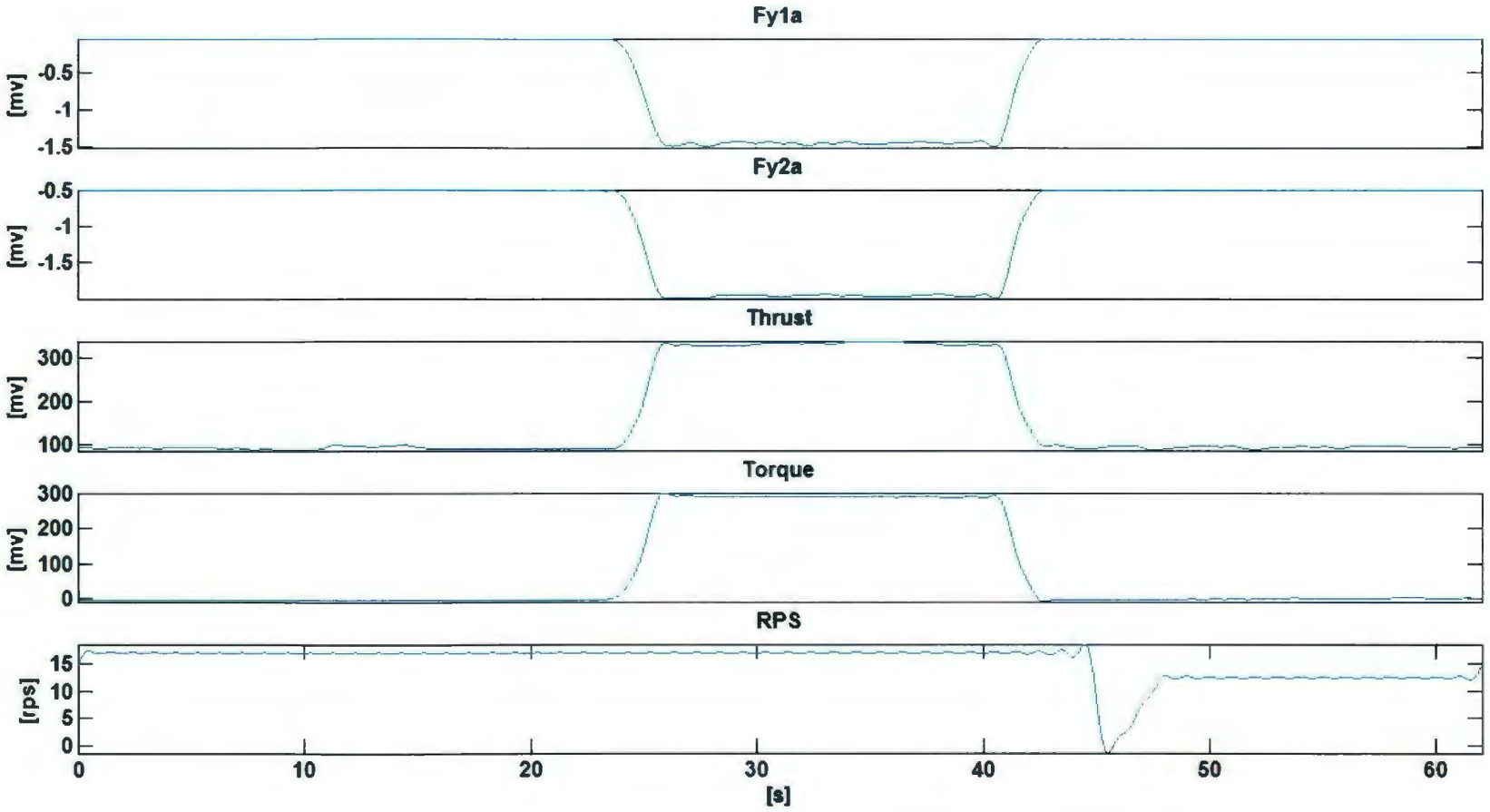
Fy1a
[mv]
-0.5
-1
-1.5
Fy2a
[mv]
-0.5
-1
-1.5
Thrust
[mv]
300
200
100
Torque
[mv]
300
200
100
0
RPS
[rps]
15
10
5
0
0
10
20
30
40
50
60
[s]

TEST 14

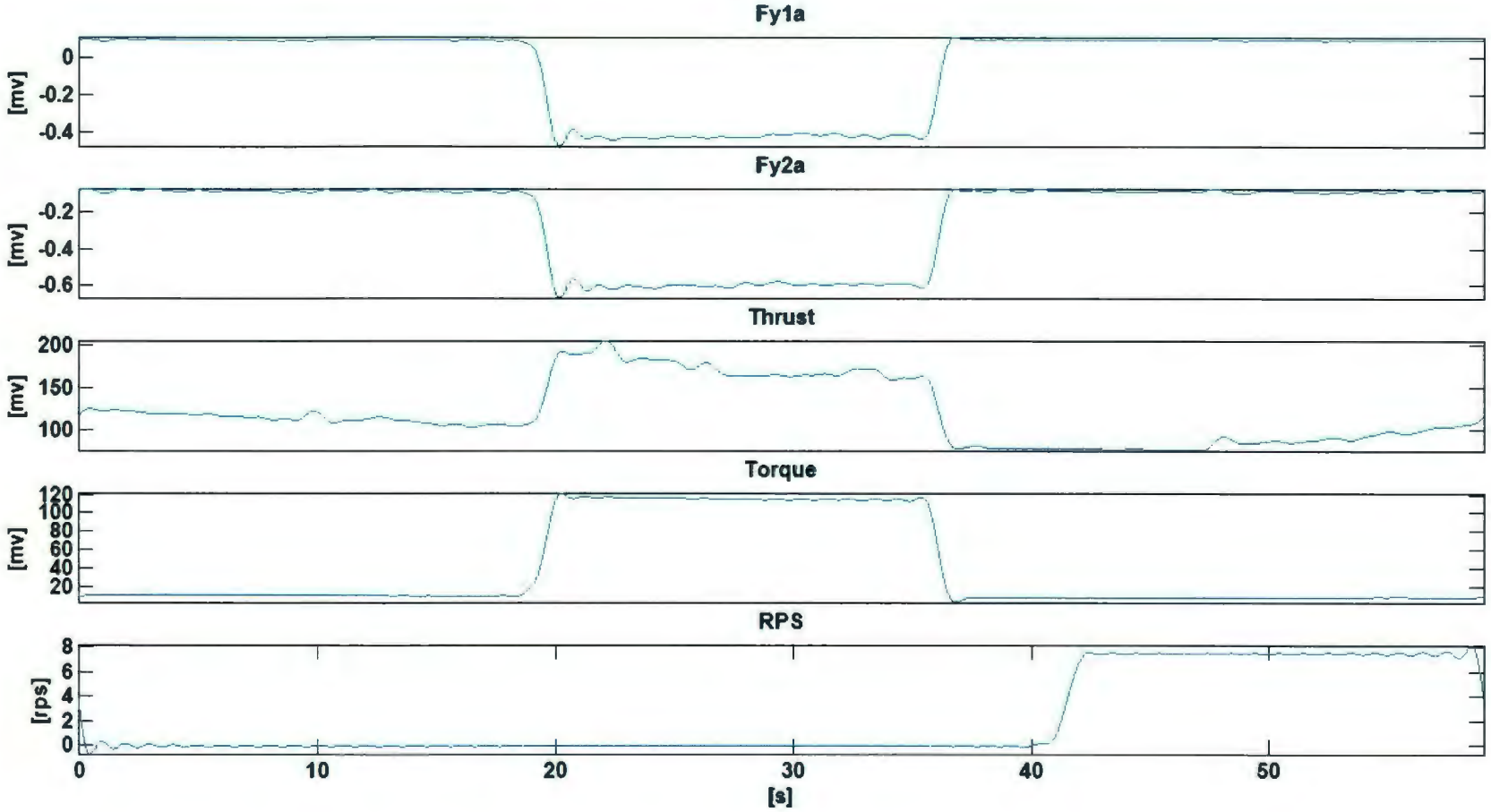
Fy1a
[mv]
0
-0.2
-0.4
Fy2a
[mv]
-0.2
-0.4
-0.6
Thrust
[mv]
200
150
100
Torque
[mv]
120
100
80
60
40
20
RPS
[rps]
8
6
4
2
0
0
10
20
30
40
50
[s]

TEST 15

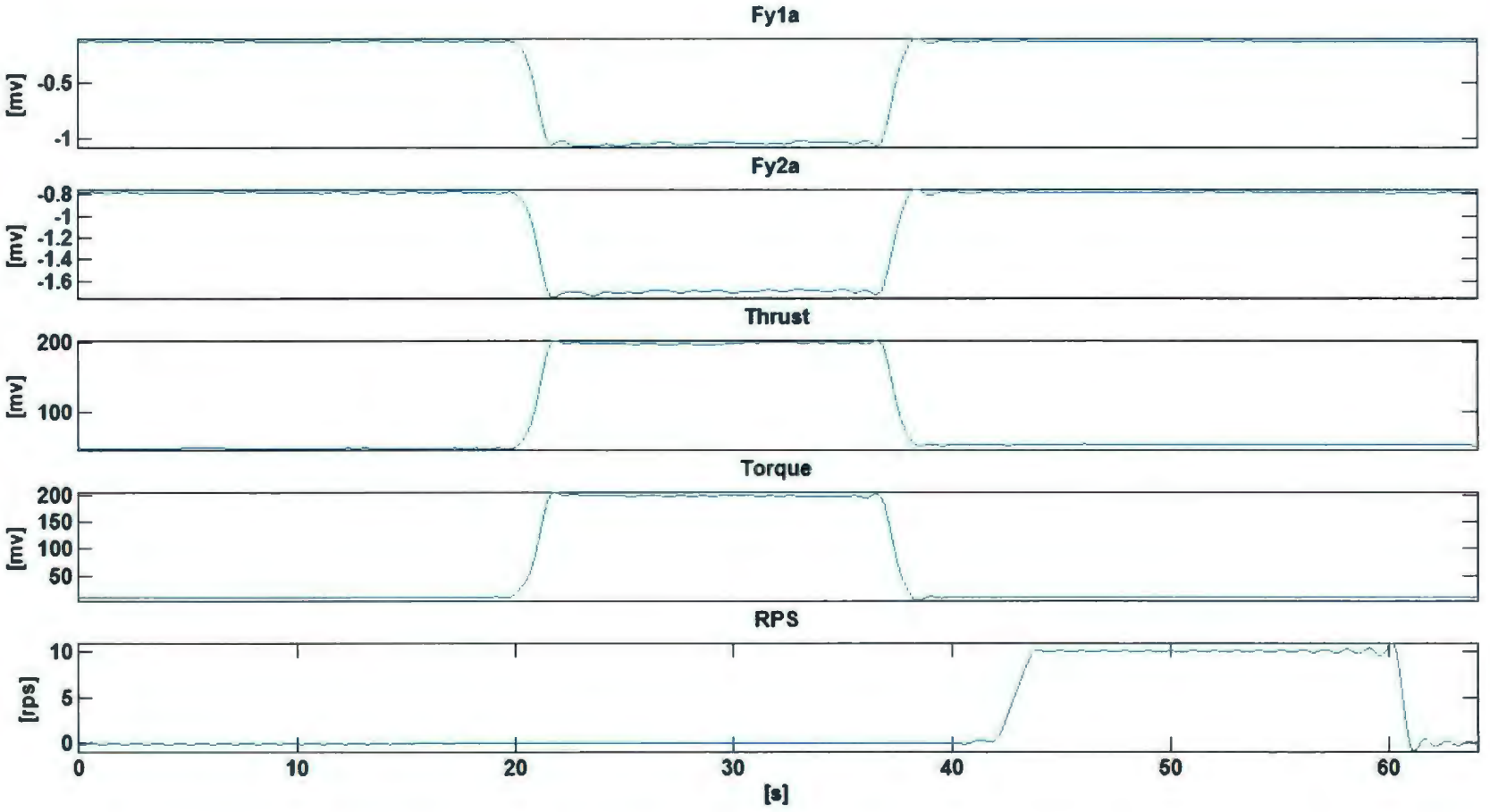
Fy1a
[mv]
-0.5
-1
Fy2a
[mv]
-0.8
-1
-1.2
-1.4
-1.6
Thrust
[mv]
200
100
Torque
[mv]
200
150
100
50
RPS
[rps]
10
5
0
0
10
20
30
40
50
60
[s]

TEST 16

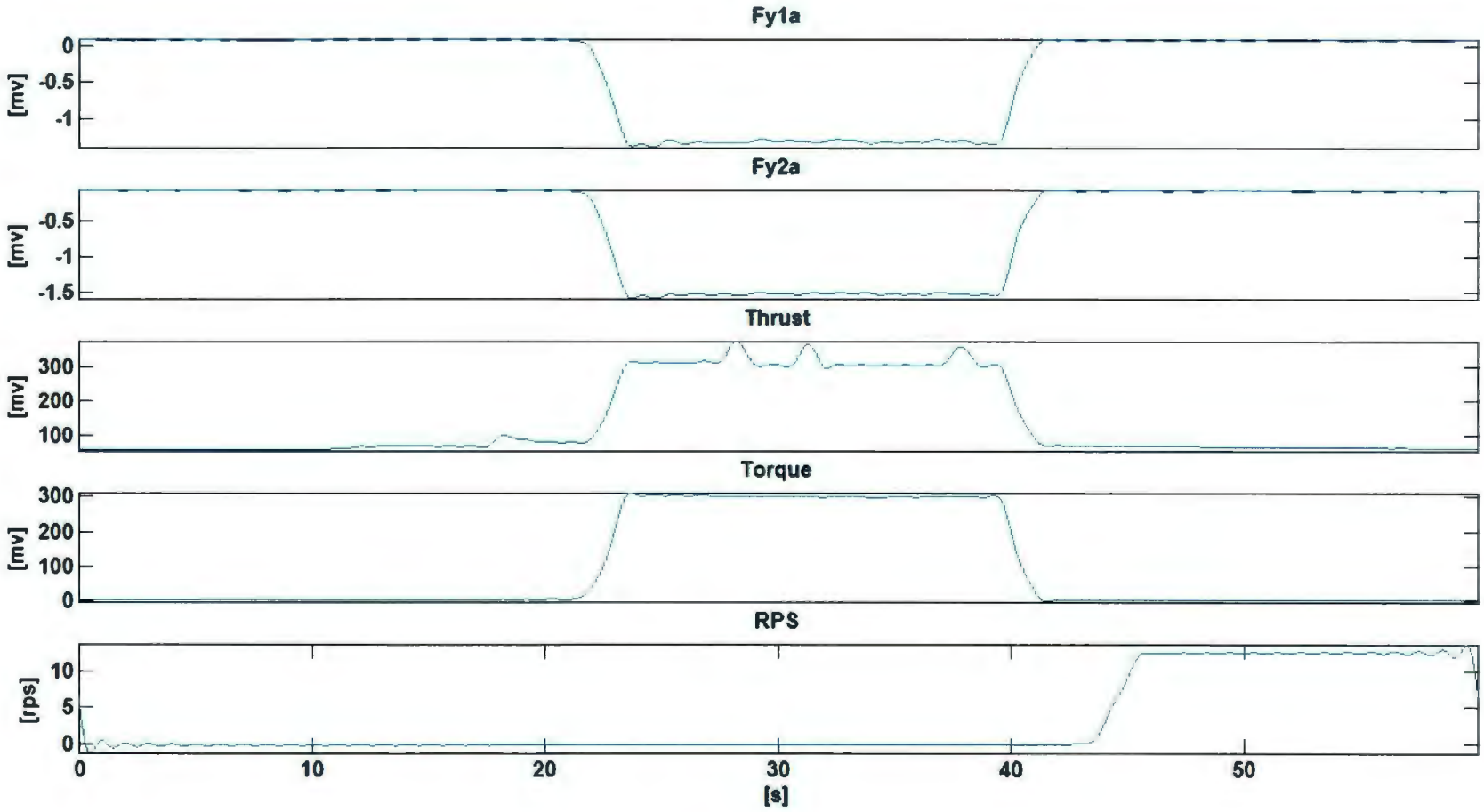
Fy1a
[mv]
0
-0.5
-1
Fy2a
[mv]
-0.5
-1
-1.5
Thrust
[mv]
300
200
100
Torque
[mv]
300
200
100
0
RPS
[rps]
10
5
0
0
10
20
30
40
50
[s]

TEST 17

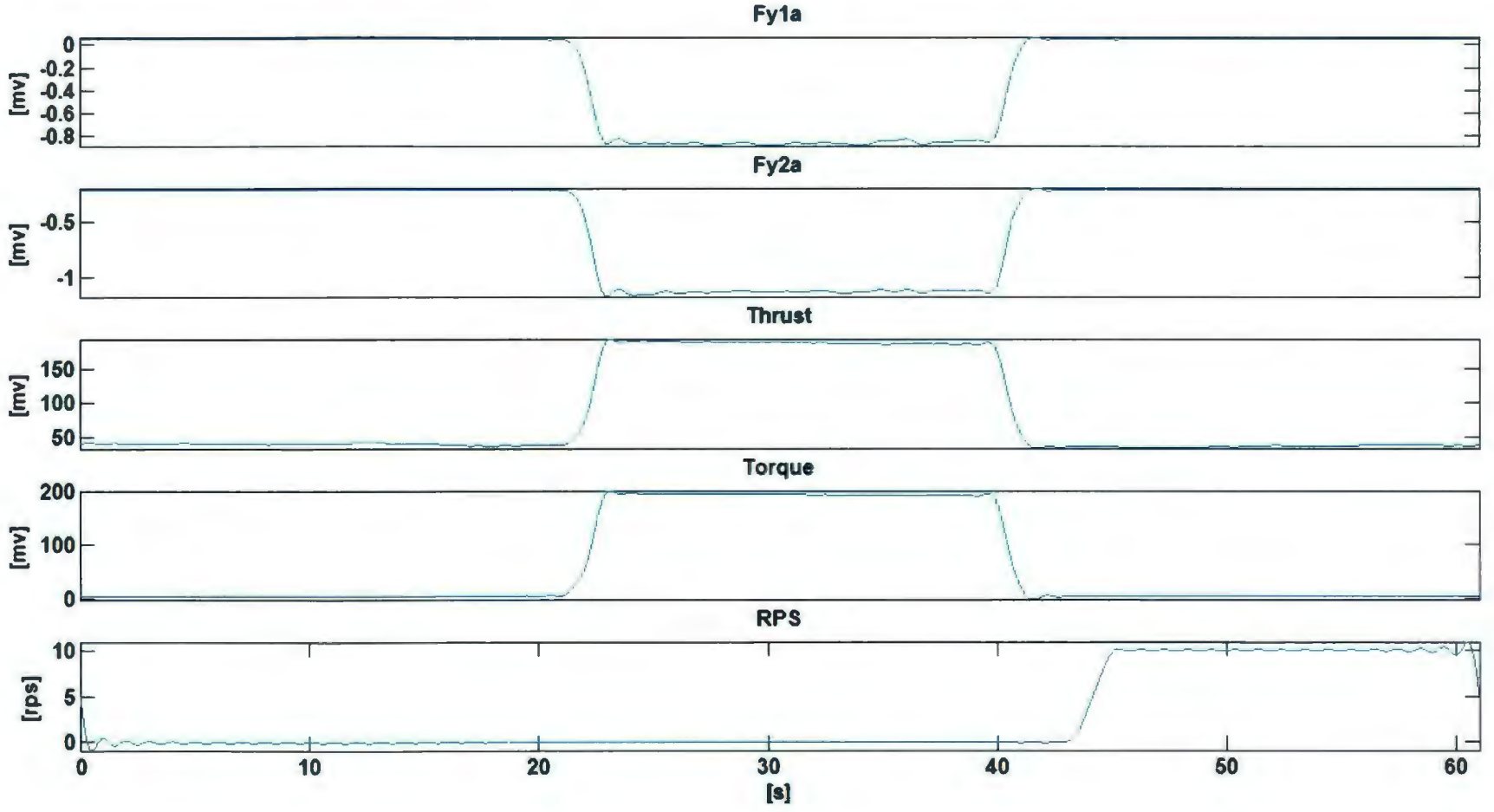
Fy1a
[mv]
0
-0.2
-0.4
-0.6
-0.8
Fy2a
[mv]
-0.5
-1
Thrust
[mv]
150
100
50
Torque
[mv]
200
100
0
RPS
[rps]
10
5
0
0
10
20
30
40
50
60
[s]

TEST 18

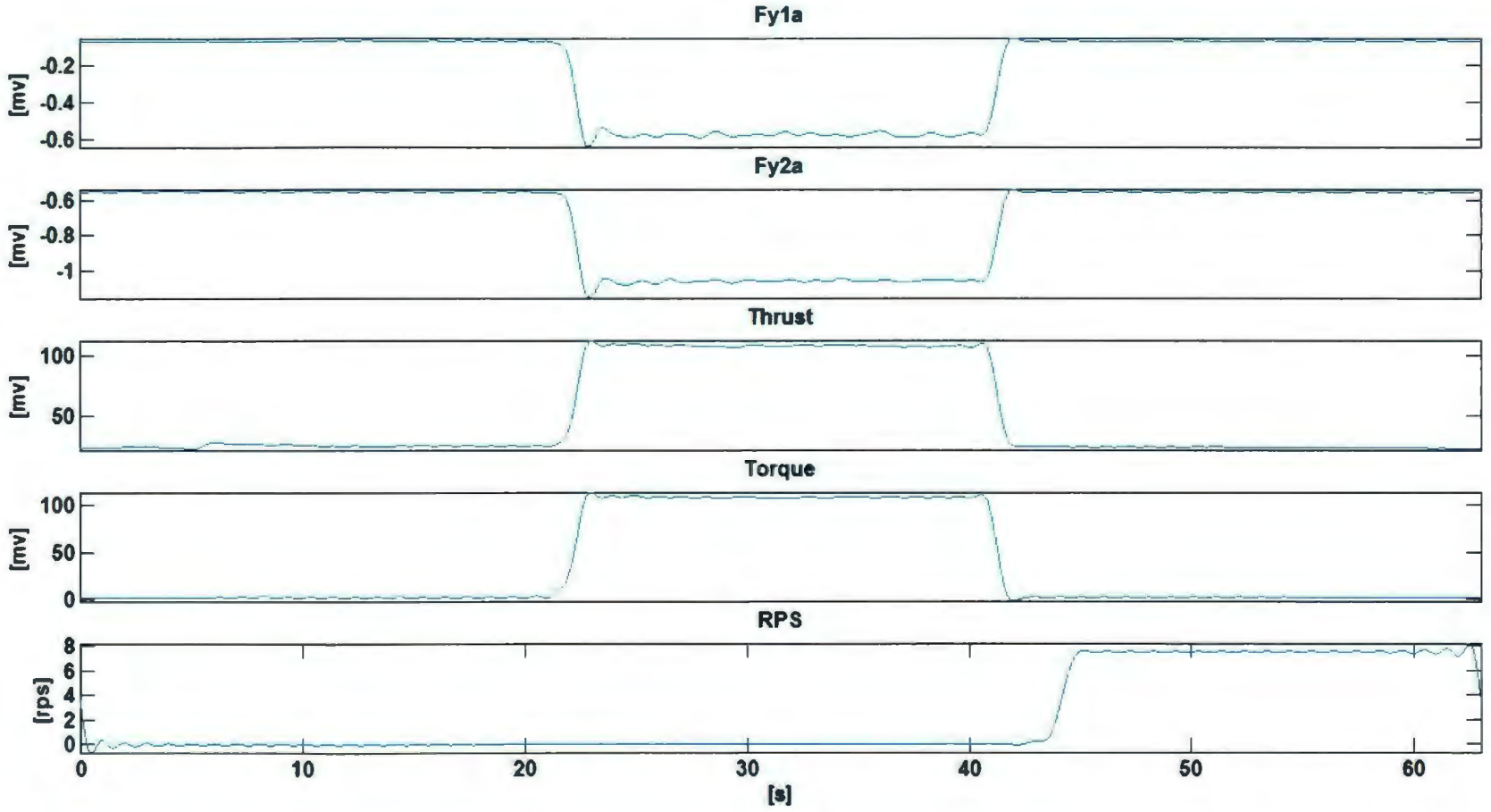
Fy1a
[mv]
-0.2
-0.4
-0.6
Fy2a
[mv]
-0.6
-0.8
-1
Thrust
[mv]
100
50
Torque
[mv]
100
50
0
RPS
[rps]
8
6
4
2
0
0
10
20
30
40
50
60
[s]

TEST 19

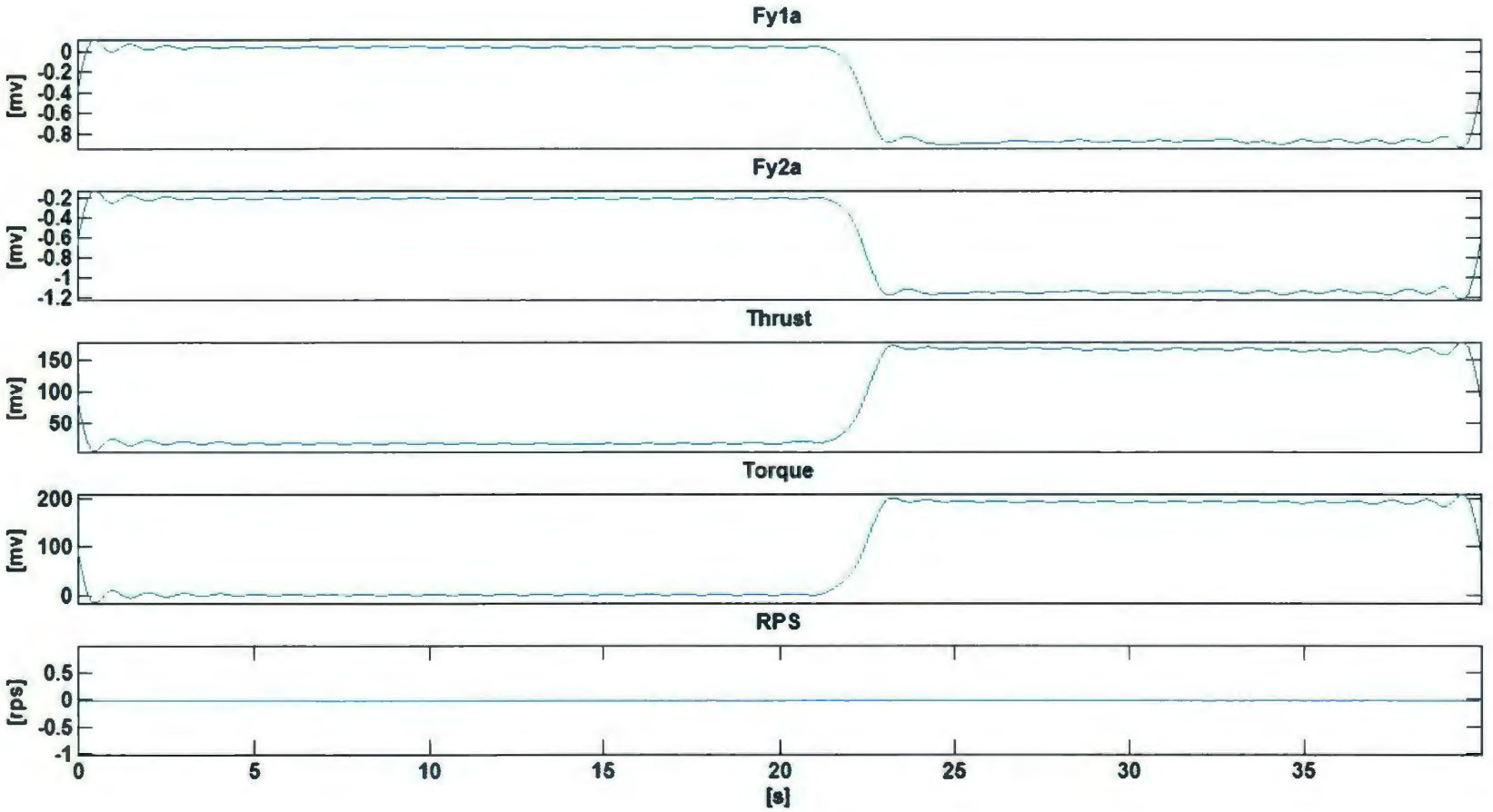
Fy1a
[mv]
0
-0.2
-0.4
-0.6
-0.8
Fy2a
[mv]
-0.2
-0.4
-0.6
-0.8
-1
-1.2
Thrust
[mv]
150
100
50
Torque
[mv]
200
100
0
RPS
[rps]
0.5
0
-0.5
-1
0
5
10
15
20
25
30
35
[s]

TEST 20

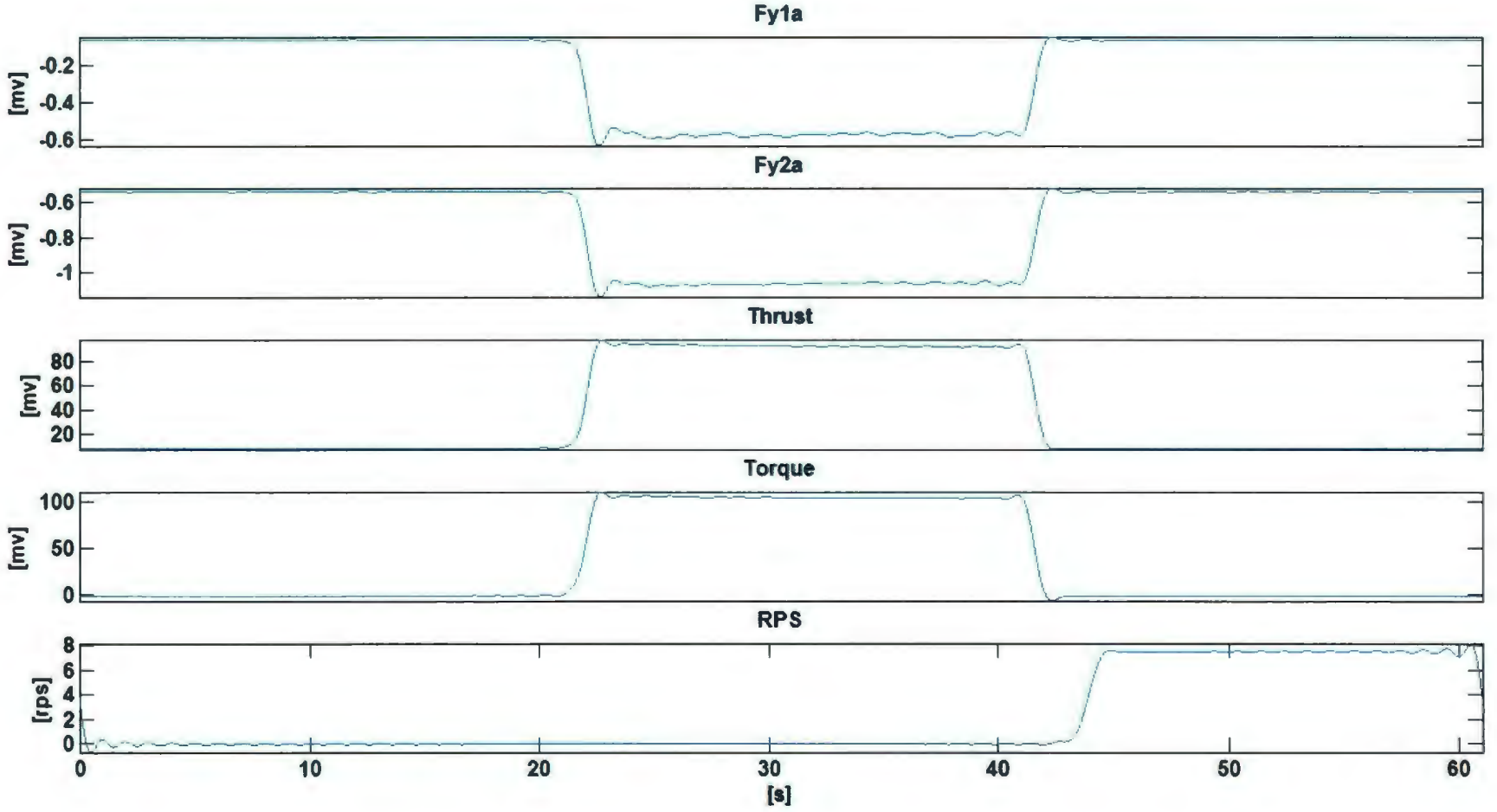
Fy1a
[mv]
-0.2
-0.4
-0.6
Fy2a
[mv]
-0.6
-0.8
-1
Thrust
[mv]
80
60
40
20
Torque
[mv]
100
50
0
RPS
[rps]
8
6
4
2
0
0
10
20
30
40
50
60
[s]

TEST 21

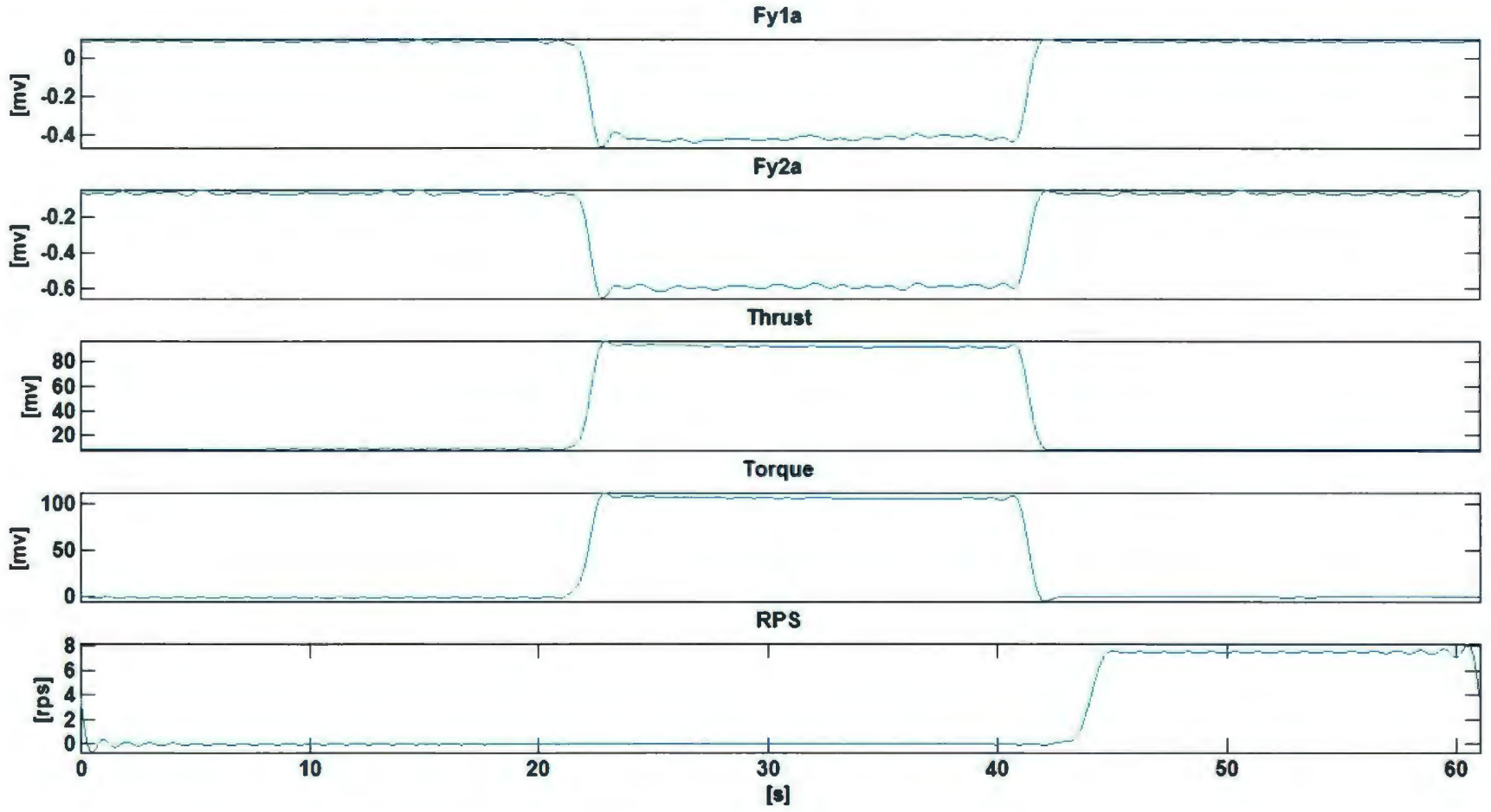
Fy1a
[mv]
0
-0.2
-0.4
Fy2a
[mv]
-0.2
-0.4
-0.6
Thrust
[mv]
80
60
40
20
Torque
[mv]
100
50
0
RPS
[rps]
8
6
4
2
0
0
10
20
30
40
50
60
[s]

TEST 22

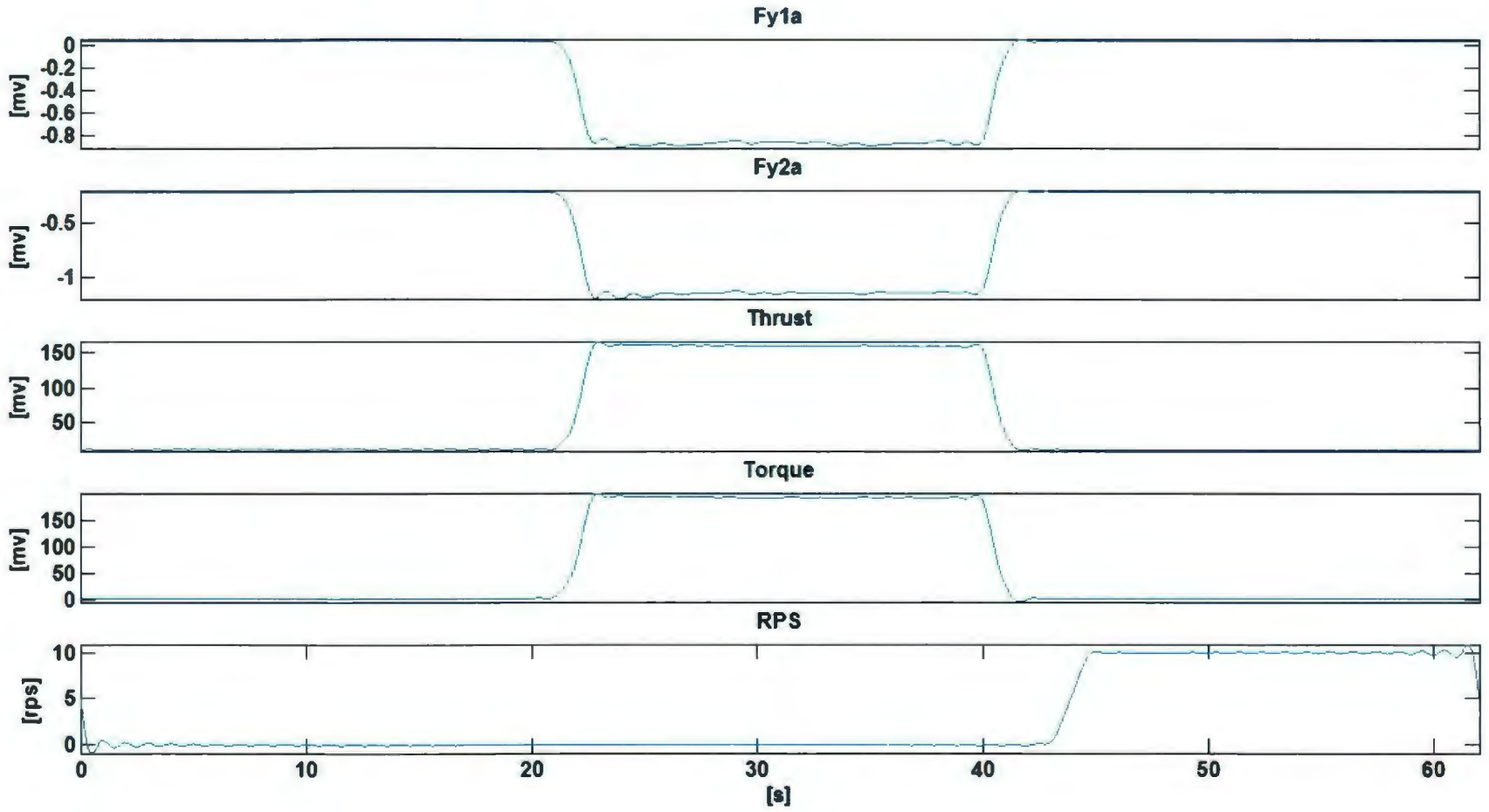
Fy1a
[mv]
0
-0.2
-0.4
-0.6
-0.8
Fy2a
[mv]
-0.5
-1
Thrust
[mv]
150
100
50
Torque
[mv]
150
100
50
0
RPS
[rps]
10
5
0
0
10
20
30
40
50
60
[s]

TEST 23

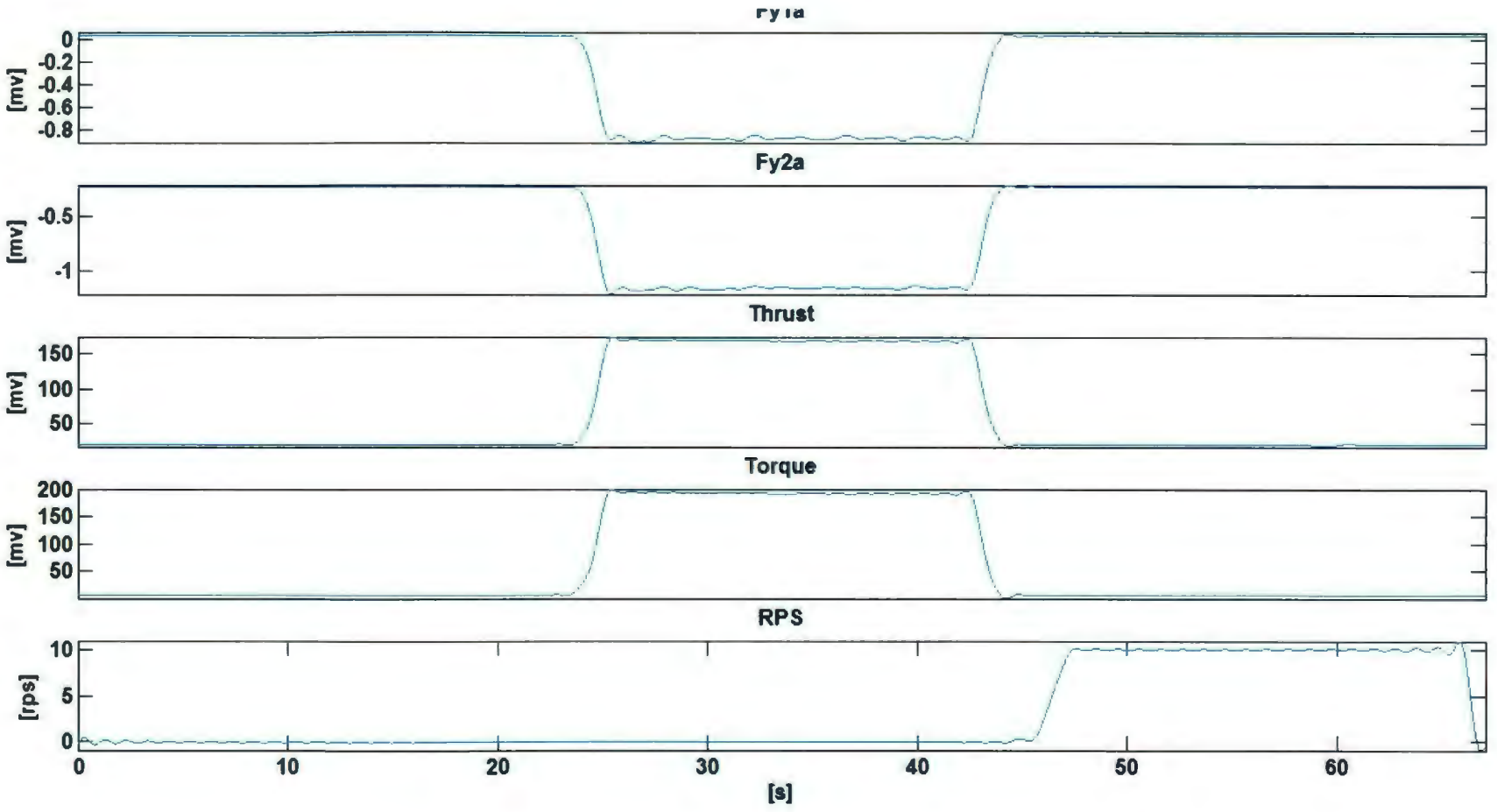
Fy1a
0
-0.2
-0.4
-0.6
-0.8
[mv]
Fy2a
-0.5
-1
[mv]
Thrust
150
100
50
[mv]
Torque
200
150
100
50
[mv]
RPS
10
5
0
[rps]
0
10
20
30
40
50
60
[s]

TEST 24

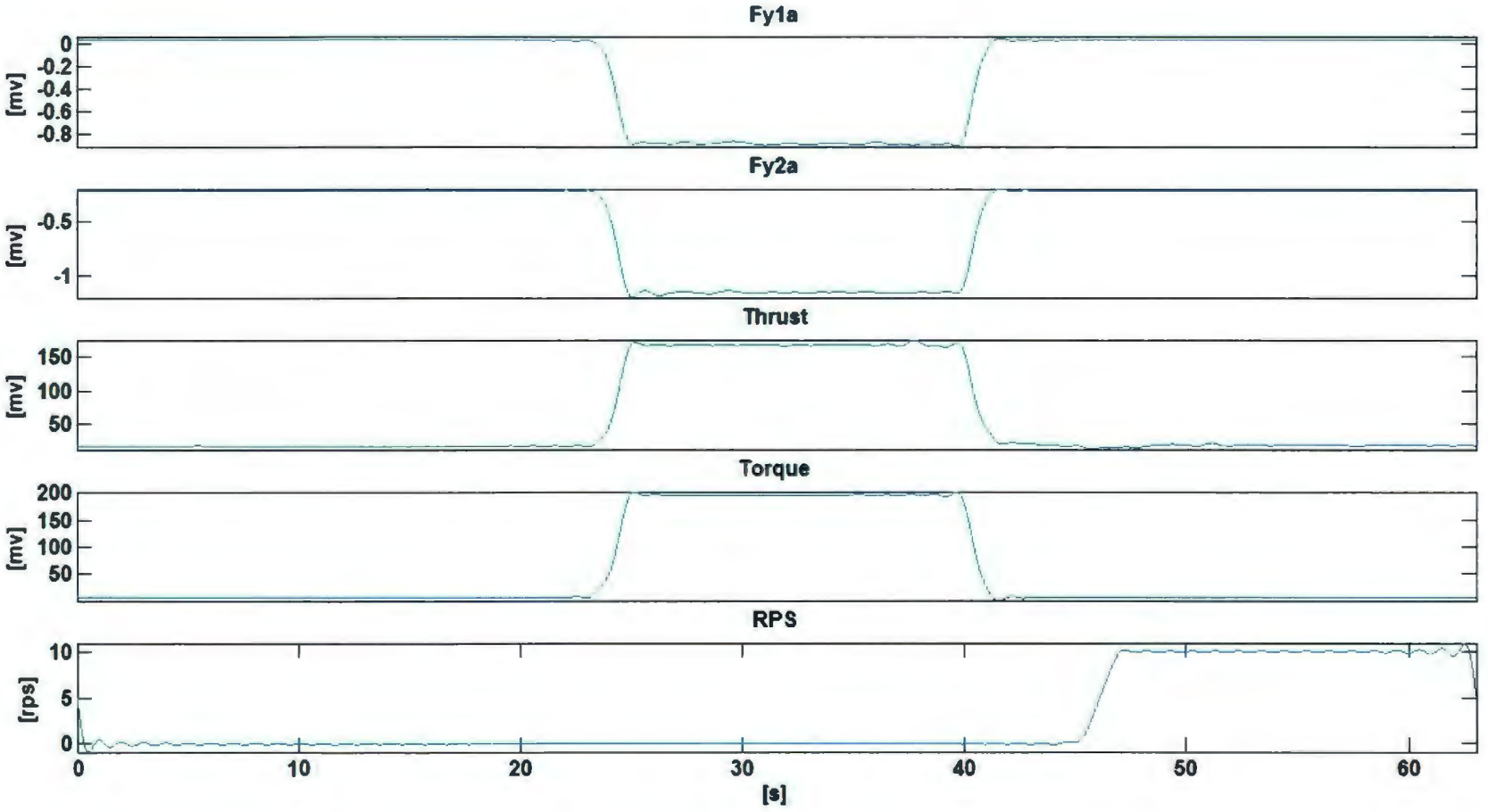
Fy1a
[mv]
0
-0.2
-0.4
-0.6
-0.8
Fy2a
[mv]
-0.5
-1
Thrust
[mv]
150
100
50
Torque
[mv]
200
150
100
50
RPS
[rps]
10
5
0
0
10
20
30
40
50
60
[s]

TEST 25

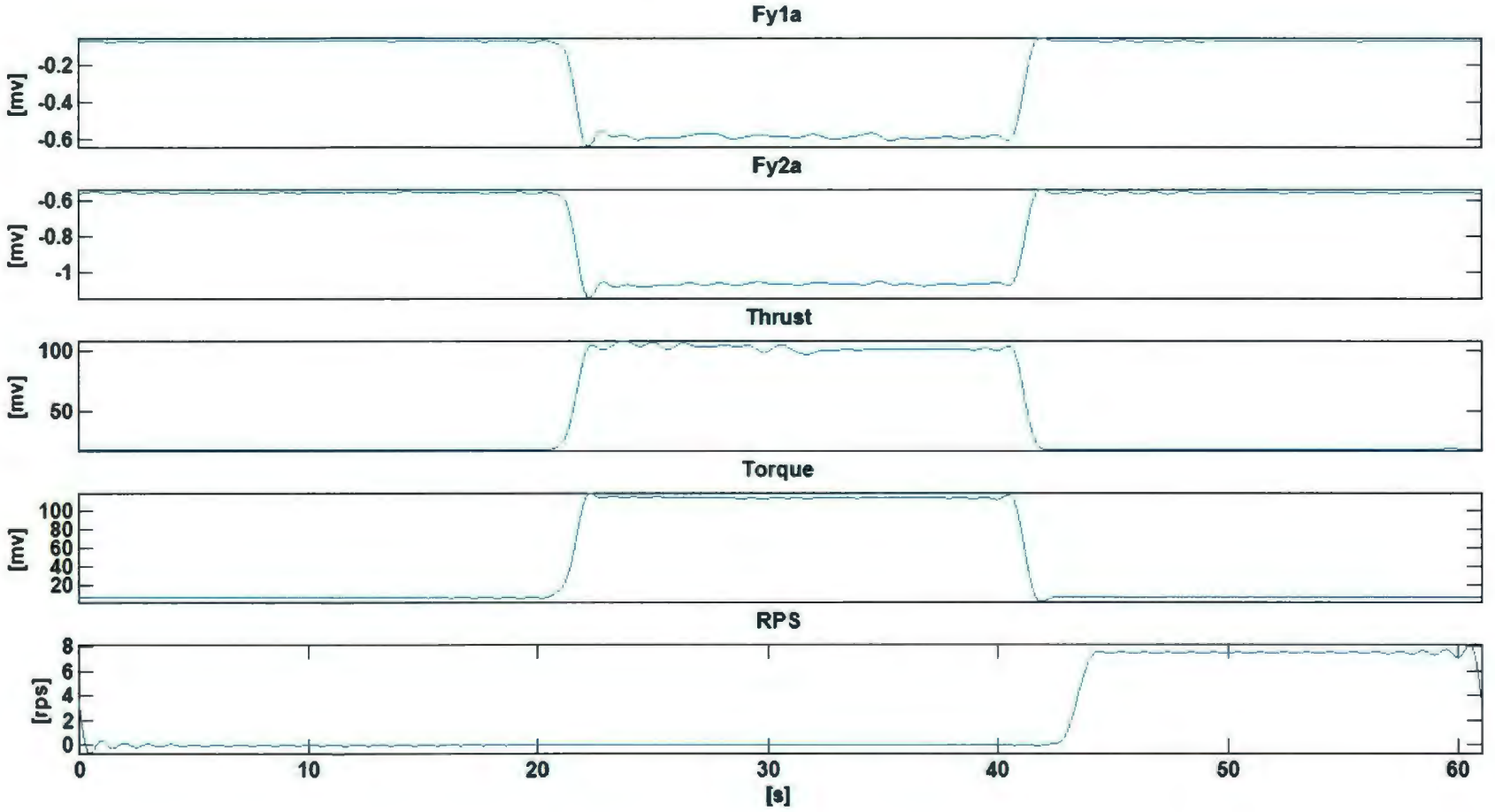
Fy1a
[mv]
-0.2
-0.4
-0.6
Fy2a
[mv]
-0.6
-0.8
-1
Thrust
[mv]
100
50
Torque
[mv]
100
80
60
40
20
RPS
[rps]
8
6
4
2
0
0
10
20
30
40
50
60
[s]

TEST 26

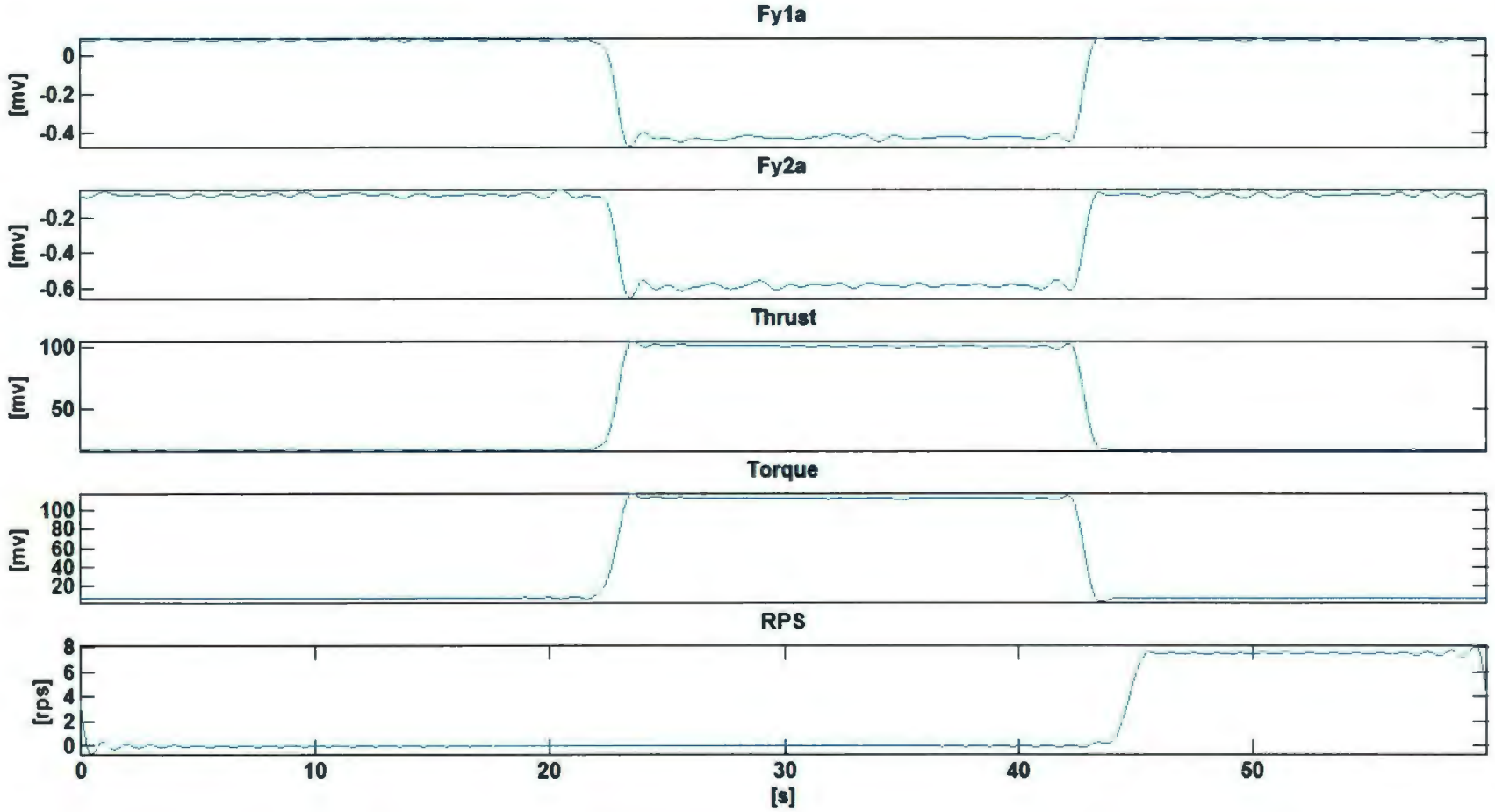
Fy1a
[mv]
0
-0.2
-0.4
Fy2a
[mv]
-0.2
-0.4
-0.6
Thrust
[mv]
100
50
Torque
[mv]
100
80
60
40
20
RPS
[rps]
8
6
4
2
0
0
10
20
30
40
50
[s]

TEST 27

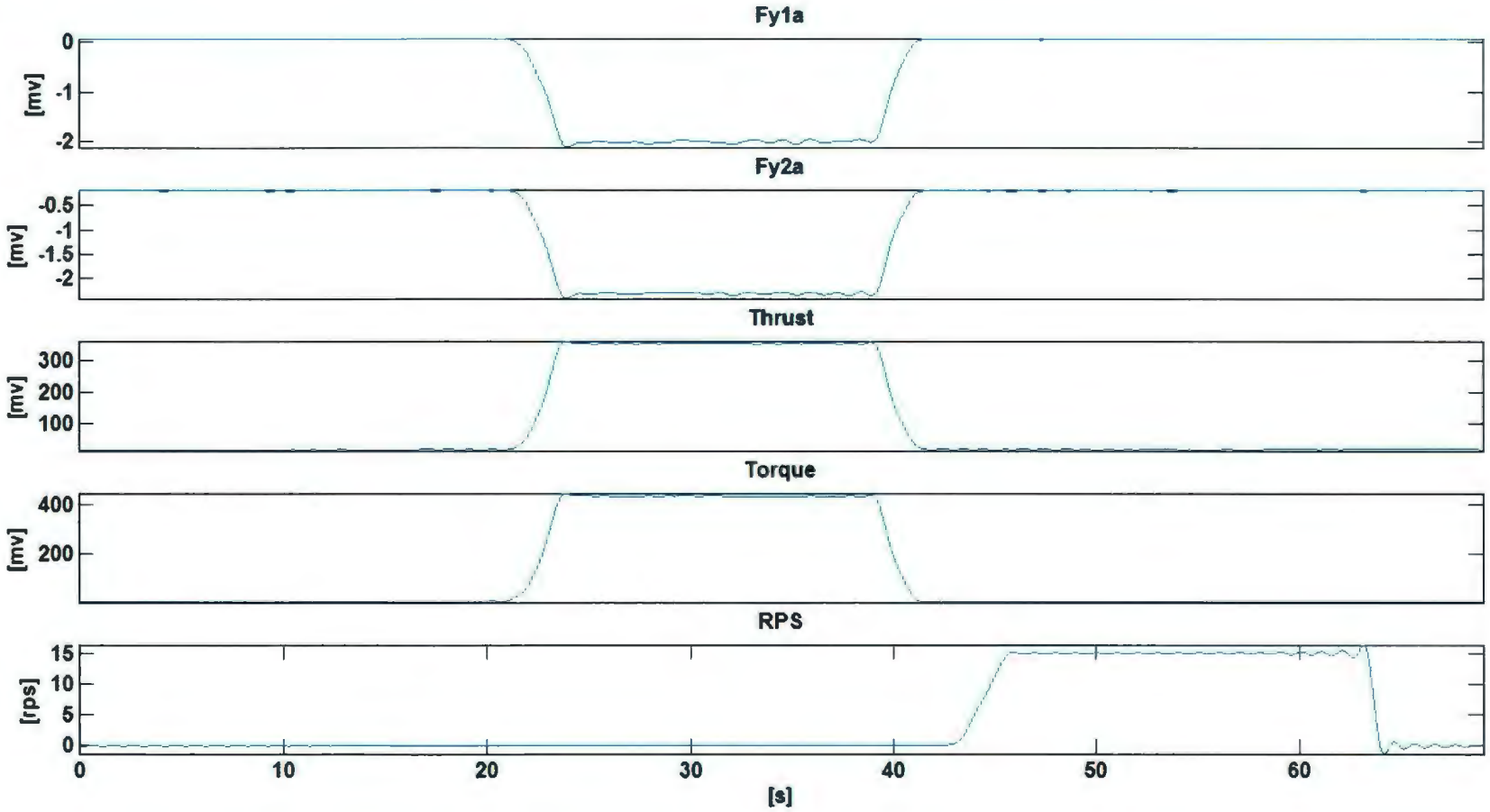
Fy1a
0
-1
-2
[mv]
Fy2a
-0.5
-1
-1.5
-2
[mv]
Thrust
300
200
100
[mv]
Torque
400
200
[mv]
RPS
15
10
5
0
[rps]
0
10
20
30
40
50
60
[s]

TEST 28

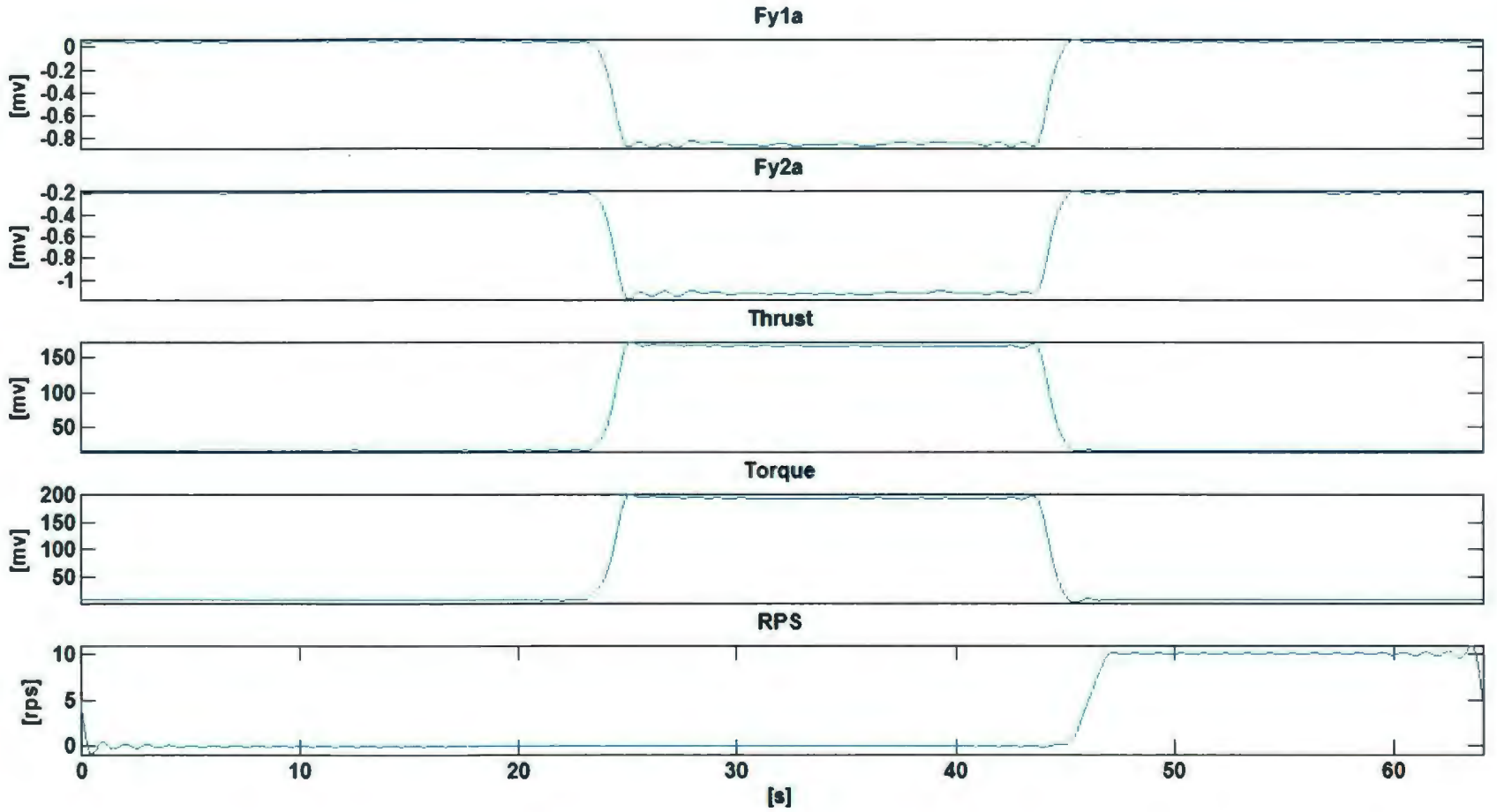
Fy1a
[mv]
0
-0.2
-0.4
-0.6
-0.8
Fy2a
[mv]
-0.2
-0.4
-0.6
-0.8
-1
Thrust
[mv]
150
100
50
Torque
[mv]
200
150
100
50
RPS
[rps]
10
5
0
0
10
20
30
40
50
60
[s]

TEST 29

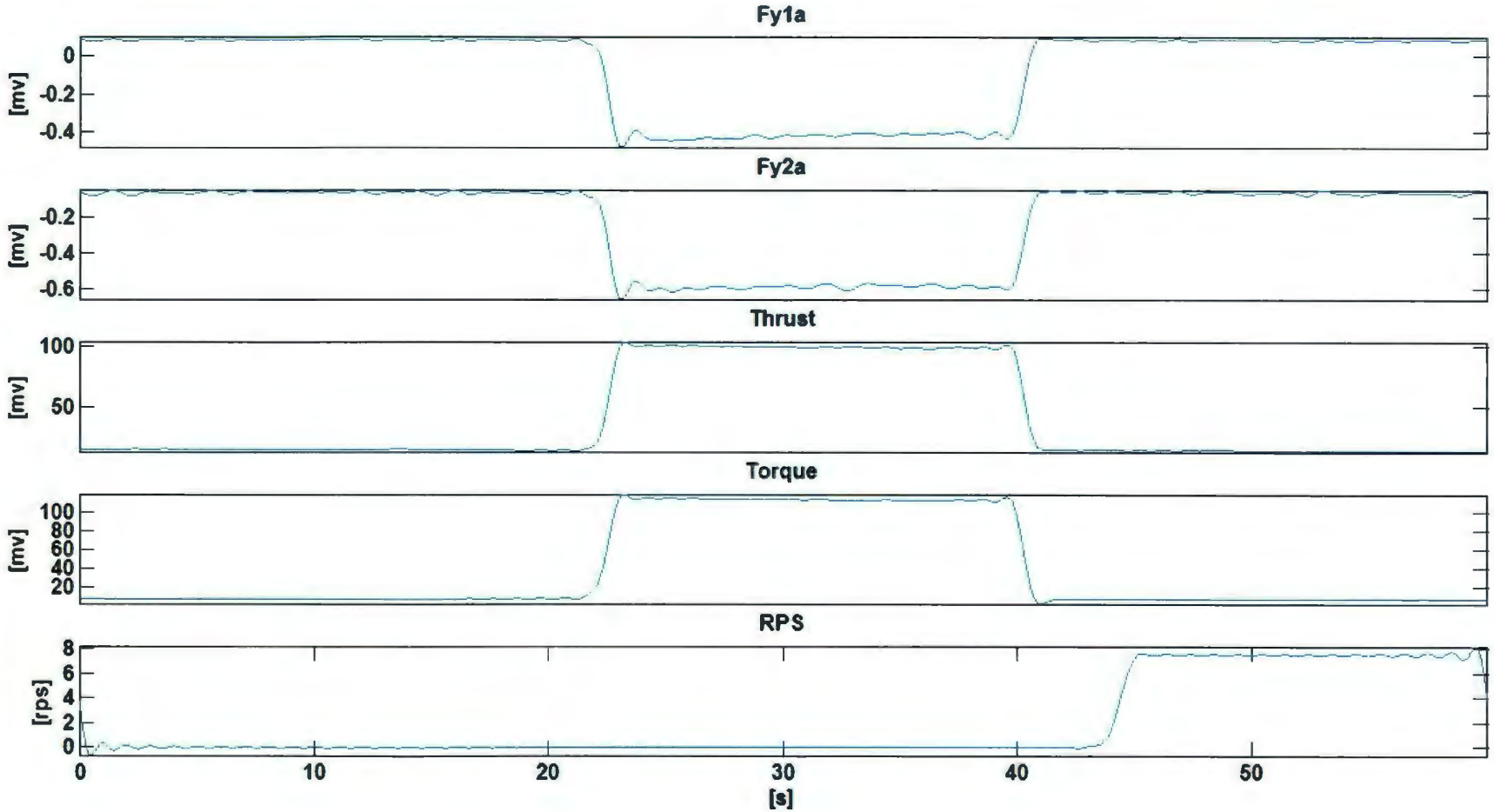
Fy1a
[mv]
0
-0.2
-0.4
Fy2a
[mv]
-0.2
-0.4
-0.6
Thrust
[mv]
100
50
Torque
[mv]
100
80
60
40
20
RPS
[rps]
8
6
4
2
0
0
10
20
30
40
50
[s]

TEST 30

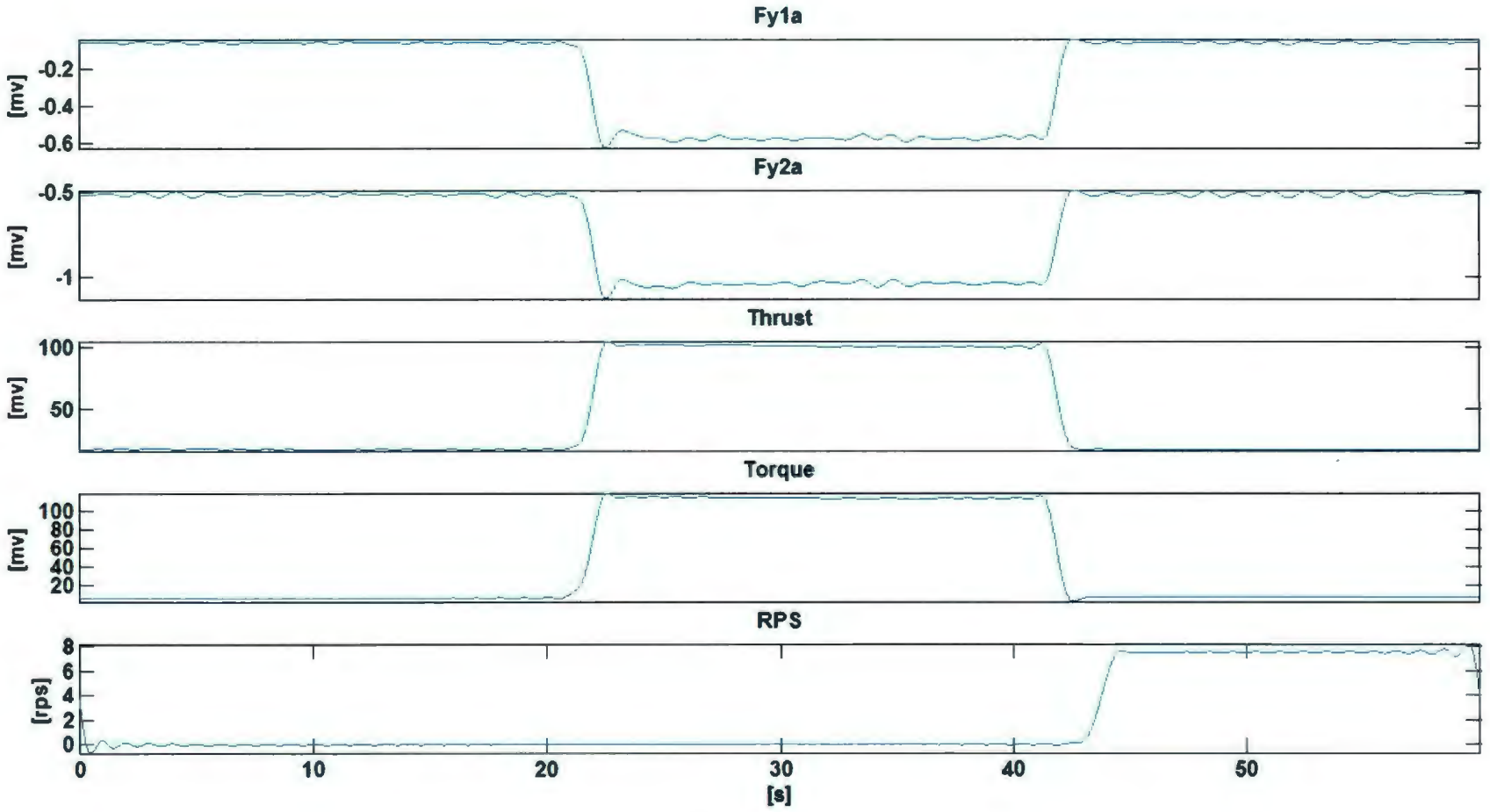
Fy1a
[mv]
-0.2
-0.4
-0.6
Fy2a
[mv]
-0.5
-1
Thrust
[mv]
100
50
Torque
[mv]
100
80
60
40
20
RPS
[rps]
8
6
4
2
0
0
10
20
30
40
50
[s]

	Stat Type	Segment	Time 1	Time 2	Azimuthin	RPS	DASPC23_	Fy1a	Fy2a	Thrust	Torque	DASPC55_	THRUST_R	CALCULAT	CALCULAT	CALCULATED_Y_THRUST
		Unit	sec	sec	deg	rps	volts	mv	mv	mv	mv	volts	mv	mv	mv	mv
		Descriptio	Time	Time												
Ice_Test_1_002	mean	1	2.59451	26.0727	-0.10055	-0.00041	-0.01234	-1.5E-16	-1.8E-17	-2.2E-14	-1.2E-14	-6.2E-17	4.5E-17	6.2E-14	4.3E-16	-5.8E-16
Ice_Test_1_002	stdv	1	2.59451	26.0727	2.89584	0.01459	0.00731	0.00123	0.00298	0.23996	0.19854	0.69411	0.00411	0.12293	0.0023	0.14635
Ice_Test_1_002	min	1	2.59451	26.0727	-23.9931	-0.02344	-0.04766	-0.00364	-0.00694	-0.70482	-0.51829	-0.98597	-0.01052	-0.36108	-0.00601	-0.37462
Ice_Test_1_002	max	1	2.59451	26.0727	12.95	0.02274	0.02783	0.00293	0.00763	0.45048	0.55738	0.99383	0.01053	0.23078	0.00647	0.37516
Ice_Test_1_002	abs_max	1	2.59451	26.0727	23.9931	0.02344	0.04766	0.00364	0.00763	0.70482	0.55738	0.99383	0.01053	0.36108	0.00647	0.37516
Ice_Test_1_002	mean	2	32.7929	50.2315	270.107	12.4998	0.05666	-1.40663	-1.43596	230.033	294.786	-0.01171	-2.84259	117.846	3.41952	-101.259
Ice_Test_1_002	stdv	2	32.7929	50.2315	1.2391	0.03361	0.69534	0.01763	0.01271	1.69345	1.33618	0.68874	0.02836	0.86755	0.0155	1.01036
Ice_Test_1_002	min	2	32.7929	50.2315	267.828	12.4198	-0.95473	-1.43681	-1.46	227.716	292.628	-0.9707	-2.89086	116.659	3.39448	-102.978
Ice_Test_1_002	max	2	32.7929	50.2315	272.508	12.5764	1.09893	-1.36528	-1.39939	234.778	298.528	0.99699	-2.77979	120.277	3.46292	-99.0217
Ice_Test_1_002	abs_max	2	32.7929	50.2315	272.508	12.5764	1.09893	1.43681	1.46	234.778	298.528	0.99699	2.89086	120.277	3.46292	102.978
	Stat Type	Segment	Time 1	Time 2	Azimuthin	RPS	DASPC23_	Fy1a	Fy2a	Thrust	Torque	DASPC55_	THRUST_R	CALCULAT	CALCULAT	CALCULATED_Y_THRUST
			sec	sec	deg	rps	volts	mv	mv	mv	mv	volts	mv	mv	mv	mv
			Start Time	End Time												
Ice_Test_2_001	mean	1	3.81521	19.3369	-0.24068	0.0001	-0.01206	-5.6E-16	-3.9E-15	-1.8E-13	-1.4E-13	-1.1E-16	4.9E-15	2.1E-14	1.7E-15	-1E-13
Ice_Test_2_001	stdv	1	3.81521	19.3369	3.88992	0.02321	0.00843	0.00216	0.00338	0.45567	0.20227	0.68888	0.00545	0.23344	0.00235	0.1942
Ice_Test_2_001	min	1	3.81521	19.3369	-24.2015	-0.04173	-0.041	-0.004	-0.00634	-1.50042	-0.64907	-1.0085	-0.00987	-0.76866	-0.00753	-0.3516
Ice_Test_2_001	max	1	3.81521	19.3369	13.1699	0.04392	0.03074	0.00585	0.00791	0.98131	0.53959	0.96465	0.0137	0.50272	0.00626	0.48808
Ice_Test_2_001	abs_max	1	3.81521	19.3369	24.2015	0.04392	0.041	0.00585	0.00791	1.50042	0.64907	1.0085	0.0137	0.76866	0.00753	0.48808
Ice_Test_2_001	mean	2	26.1195	37.4673	270.289	12.5005	0.03422	-1.41584	-1.44824	233.498	294.592	-0.00745	-2.86407	119.621	3.41726	-102.024
Ice_Test_2_001	stdv	2	26.1195	37.4673	1.21865	0.03772	0.70422	0.01553	0.00886	0.97394	1.02406	0.7015	0.02	0.49895	0.01188	0.71262
Ice_Test_2_001	min	2	26.1195	37.4673	268.132	12.4279	-0.94943	-1.44892	-1.4709	231.625	292.452	-1.00983	-2.90593	118.662	3.39244	-103.515
Ice_Test_2_001	max	2	26.1195	37.4673	272.477	12.576	1.01689	-1.37803	-1.42983	236.271	297.218	0.95625	-2.81396	121.042	3.44773	-100.239
Ice_Test_2_001	abs_max	2	26.1195	37.4673	272.477	12.576	1.01689	1.44892	1.4709	236.271	297.218	1.00983	2.90593	121.042	3.44773	103.515
	Stat Type	Segment	Time 1	Time 2	Azimuthin	RPS	DASPC23_	Fy1a	Fy2a	Thrust	Torque	DASPC55_	THRUST_R	CALCULAT	CALCULAT	CALCULATED_Y_THRUST
			sec	sec	deg	rps	volts	mv	mv	mv	mv	volts	mv	mv	mv	mv
			Start Time	End Time												
Ice_Test_3_001	mean	1	2.75235	19.2665	0.05824	-0.00063	-0.01268	6.6E-16	-3.1E-16	6.4E-14	-9.9E-16	-3.5E-16	2.6E-16	1.6E-14	-3.4E-16	2.6E-15
Ice_Test_3_001	stdv	1	2.75235	19.2665	1.57239	0.0228	0.00516	0.00119	0.00301	0.25164	0.25143	0.69556	0.00407	0.12892	0.00292	0.14509
Ice_Test_3_001	min	1	2.75235	19.2665	-5.13782	-0.03538	-0.03186	-0.00294	-0.01034	-0.51025	-0.64409	-0.95804	-0.01328	-0.2614	-0.00747	-0.47312
Ice_Test_3_001	max	1	2.75235	19.2665	6.45154	0.03444	0.01696	0.00305	0.0068	0.57851	0.60448	1.00796	0.00939	0.29637	0.00701	0.33461
Ice_Test_3_001	abs_max	1	2.75235	19.2665	6.45154	0.03538	0.03186	0.00305	0.01034	0.57851	0.64409	1.00796	0.01328	0.29637	0.00747	0.47312
Ice_Test_3_001	mean	2	25.1946	40.5594	269.927	12.5005	0.05034	-1.4113	-1.43791	233.635	295.775	0.04948	-2.84921	119.691	3.43099	-101.494
Ice_Test_3_001	stdv	2	25.1946	40.5594	1.90027	0.05501	0.69702	0.02071	0.01631	1.38031	1.40833	0.69129	0.03519	0.70713	0.01634	1.25358
Ice_Test_3_001	min	2	25.1946	40.5594	266.037	12.3423	-0.95984	-1.46297	-1.4812	231.531	293.677	-0.95948	-2.9437	118.613	3.40665	-104.86
Ice_Test_3_001	max	2	25.1946	40.5594	273.58	12.6653	1.02228	-1.35217	-1.40287	238.889	301.354	1.0071	-2.76224	122.383	3.49571	-98.3967
Ice_Test_3_001	abs_max	2	25.1946	40.5594	273.58	12.6653	1.02228	1.46297	1.4812	238.889	301.354	1.0071	2.9437	122.383	3.49571	104.86
	Stat Type	Segment	Time 1	Time 2	Azimuthin	RPS	DASPC23_	Fy1a	Fy2a	Thrust	Torque	DASPC55_	THRUST_R	CALCULAT	CALCULAT	CALCULATED_Y_THRUST
			sec	sec	deg	rps	volts	mv	mv	mv	mv	volts	mv	mv	mv	mv
			Start Time	End Time												
Ice_Test_4_001	mean	1	1.2396	19.2859	-0.07613	-0.00058	-0.01256	3.4E-17	-1.6E-15	6.5E-15	2.5E-14	2.8E-16	-7.3E-16	-2.3E-14	-1.1E-16	-7.5E-14

Ice_Test_4_001	stdv	1	1.2396	19.2859	2.118	0.02457	0.00463	0.00293	0.00511	1.00683	0.12388	0.69606	0.00803	0.5158	0.00144	0.28617
Ice_Test_4_001	min	1	1.2396	19.2859	-9.09663	-0.04174	-0.03308	-0.00615	-0.01057	-2.90625	-0.36834	-1.02141	-0.01672	-1.48887	-0.00427	-0.59572
Ice_Test_4_001	max	1	1.2396	19.2859	6.92803	0.04531	0.02771	0.00675	0.01195	1.79402	0.39763	0.9806	0.0187	0.91907	0.00461	0.6661
Ice_Test_4_001	abs_max	1	1.2396	19.2859	9.09663	0.04531	0.03308	0.00675	0.01195	2.90625	0.39763	1.02141	0.0187	1.48887	0.00461	0.6661
Ice_Test_4_001	mean	2	24.4172	40.1572	269.996	12.4981	0.02393	-1.41582	-1.4509	233.411	295.439	-0.00565	-2.86672	119.576	3.4271	-102.118
Ice_Test_4_001	stdv	2	24.4172	40.1572	1.72442	0.06524	0.69426	0.02271	0.01588	1.10075	1.11876	0.69227	0.0341	0.56392	0.01298	1.21471
Ice_Test_4_001	min	2	24.4172	40.1572	265.575	12.2887	-0.94705	-1.46937	-1.50763	230.643	291.107	-0.98286	-2.97686	118.158	3.37684	-106.042
Ice_Test_4_001	max	2	24.4172	40.1572	273.949	12.6827	1.04391	-1.35585	-1.40674	237.02	298.911	0.98806	-2.78966	121.425	3.46737	-99.3732
Ice_Test_4_001	abs_max	2	24.4172	40.1572	273.949	12.6827	1.04391	1.46937	1.50763	237.02	298.911	0.98806	2.97686	121.425	3.46737	106.042
	Stat Type	Segment	Time 1	Time 2	Azimuthin	RPS	DASPC23_	Fy1a	Fy2a	Thrust	Torque	DASPC55_	THRUST_R	CALCULAT	CALCULAT	CALCULATED_Y_THRUST
			sec	sec	deg	rps	volts	mv	mv	mv	mv	volts	mv	mv	mv	mv
			Start Time	End Time												
Ice_Test_5_001	mean	1	1.66729	20.586	-0.13725	-0.00013	-0.01323	-1.5E-17	2E-16	4.2E-14	1.6E-14	3.4E-16	-2.8E-16	-2.1E-14	2.2E-17	2.9E-16
Ice_Test_5_001	stdv	1	1.66729	20.586	3.1185	0.01343	0.01522	0.00124	0.00321	0.20846	0.02885	0.69428	0.0044	0.10679	0.00033	0.1567
Ice_Test_5_001	min	1	1.66729	20.586	-23.6056	-0.0369	-0.11777	-0.00199	-0.005	-0.55275	-0.11391	-0.95028	-0.00694	-0.28318	-0.00132	-0.24705
Ice_Test_5_001	max	1	1.66729	20.586	12.5661	0.04268	0.04753	0.0043	0.01026	0.34503	0.06076	1.02003	0.0145	0.17676	0.0007	0.51653
Ice_Test_5_001	abs_max	1	1.66729	20.586	23.6056	0.04268	0.11777	0.0043	0.01026	0.55275	0.11391	1.02003	0.0145	0.28318	0.00132	0.51653
Ice_Test_5_001	mean	2	25.758	47.9432	270.134	5.00043	0.02384	-0.22818	-0.22656	36.1554	47.6983	0.0236	-0.45474	18.5224	0.5533	-16.1987
Ice_Test_5_001	stdv	2	25.758	47.9432	1.53459	0.01392	0.69741	0.00472	0.00324	0.59594	0.24678	0.69644	0.00679	0.3053	0.00286	0.24178
Ice_Test_5_001	min	2	25.758	47.9432	266.783	4.96446	-0.96095	-0.23761	-0.23654	34.4645	47.1691	-0.95091	-0.47375	17.6562	0.54716	-16.8761
Ice_Test_5_001	max	2	25.758	47.9432	273.25	5.0387	1.0154	-0.21494	-0.2203	37.4922	48.3623	1.01516	-0.43875	19.2072	0.561	-15.6291
Ice_Test_5_001	abs_max	2	25.758	47.9432	273.25	5.0387	1.0154	0.23761	0.23654	37.4922	48.3623	1.01516	0.47375	19.2072	0.561	16.8761
	Stat Type	Segment	Time 1	Time 2	Azimuthin	RPS	DASPC23_	Fy1a	Fy2a	Thrust	Torque	DASPC55_	THRUST_R	CALCULAT	CALCULAT	CALCULATED_Y_THRUST
			sec	sec	deg	rps	volts	mv	mv	mv	mv	volts	mv	mv	mv	mv
			Start Time	End Time												
Ice_Test_6_001	mean	1	3.78071	20.5368	-0.02803	-0.00049	-0.01247	4.6E-16	7.5E-16	9.3E-15	-1.6E-14	2.6E-16	-9E-16	6.2E-14	-1.8E-16	1E-14
Ice_Test_6_001	stdv	1	3.78071	20.5368	1.08362	0.02285	0.00636	0.0009	0.00231	0.62905	0.0589	0.69323	0.00313	0.32226	0.00068	0.11143
Ice_Test_6_001	min	1	3.78071	20.5368	-4.71738	-0.04277	-0.03201	-0.00181	-0.00513	-2.05402	-0.23388	-0.96091	-0.00695	-1.05227	-0.00271	-0.24746
Ice_Test_6_001	max	1	3.78071	20.5368	3.83064	0.0451	0.00553	0.0025	0.00405	0.78984	0.24547	1.01126	0.00627	0.40463	0.00285	0.22328
Ice_Test_6_001	abs_max	1	3.78071	20.5368	4.71738	0.0451	0.03201	0.0025	0.00513	2.05402	0.24547	1.01126	0.00695	1.05227	0.00285	0.24746
Ice_Test_6_001	mean	2	26.102	40.6804	270.062	10.0015	-0.00606	-0.90786	-0.92569	148.962	189.534	-0.01551	-1.83354	76.3131	2.1986	-65.3144
Ice_Test_6_001	stdv	2	26.102	40.6804	2.38087	0.0448	0.69854	0.01632	0.01245	2.24853	1.16376	0.70085	0.02698	1.15192	0.0135	0.96113
Ice_Test_6_001	min	2	26.102	40.6804	265.224	9.87663	-0.95482	-0.94202	-0.95521	145.284	187.14	-0.96474	-1.89617	74.429	2.17082	-67.5455
Ice_Test_6_001	max	2	26.102	40.6804	274.818	10.1423	1.02482	-0.87958	-0.89678	153.726	193.261	1.00274	-1.78083	78.754	2.24183	-63.4366
Ice_Test_6_001	abs_max	2	26.102	40.6804	274.818	10.1423	1.02482	0.94202	0.95521	153.726	193.261	1.00274	1.89617	78.754	2.24183	67.5455
	Stat Type	Segment	Time 1	Time 2	Azimuthin	RPS	DASPC23_	Fy1a	Fy2a	Thrust	Torque	DASPC55_	THRUST_R	CALCULAT	CALCULAT	CALCULATED_Y_THRUST
			sec	sec	deg	rps	volts	mv	mv	mv	mv	volts	mv	mv	mv	mv
			Start Time	End Time												
Ice_Test_7_001	mean	1	1.72826	18.163	-0.00472	-0.00016	-0.01271	4.4E-16	-1.2E-15	-4.1E-14	3.2E-14	2.9E-16	9.8E-16	4.5E-15	-1.2E-15	-3.5E-14
Ice_Test_7_001	stdv	1	1.72826	18.163	1.11611	0.01042	0.00509	0.00129	0.00139	0.36344	0.18355	0.68848	0.00255	0.18619	0.00213	0.09076
Ice_Test_7_001	min	1	1.72826	18.163	-4.82261	-0.01907	-0.03158	-0.00302	-0.00327	-0.7278	-0.44928	-0.97909	-0.00601	-0.37285	-0.00521	-0.21402
Ice_Test_7_001	max	1	1.72826	18.163	3.96274	0.01881	0.00342	0.00264	0.0028	0.96842	0.42499	0.99981	0.00484	0.49612	0.00493	0.17249
Ice_Test_7_001	abs_max	1	1.72826	18.163	4.82261	0.01907	0.03158	0.00302	0.00327	0.96842	0.44928	0.99981	0.00601	0.49612	0.00521	0.21402

Ice_Test_7_001	mean	2	25.4673	40.5325	270.016	10.0012	0.05236	-0.9117	-0.92389	148.923	189.27	0.01439	-1.83559	76.2932	2.19553	-65.3874
Ice_Test_7_001	stdv	2	25.4673	40.5325	2.09386	0.05409	0.69643	0.01144	0.0082	0.78585	0.64503	0.69711	0.0174	0.40259	0.00748	0.61985
Ice_Test_7_001	min	2	25.4673	40.5325	265.832	9.86696	-0.94555	-0.938	-0.94614	147.075	187.359	-0.98043	-1.87328	75.3463	2.17336	-66.7298
Ice_Test_7_001	max	2	25.4673	40.5325	274.639	10.1511	1.02111	-0.87863	-0.90624	151.602	191.318	0.9851	-1.7857	77.6655	2.21928	-63.6101
Ice_Test_7_001	abs_max	2	25.4673	40.5325	274.639	10.1511	1.02111	0.938	0.94614	151.602	191.318	0.9851	1.87328	77.6655	2.21928	66.7298
	Stat Type	Segment	Time 1	Time 2	Azimuthin	RPS	DASPC23_	Fy1a	Fy2a	Thrust	Torque	DASPC55_	THRUST_R	CALCULAT	CALCULAT	CALCULATED_Y_THRUST
			sec	sec	deg	rps	volts	mv	mv	mv	mv	volts	mv	mv	mv	mv
			Start Time	End Time												
Ice_Test_8_001	mean	1	2.00141	26.3095	-0.03947	-0.00044	-0.01239	-8.6E-17	-3.4E-16	-5E-14	-8E-15	-3.2E-16	1.4E-16	1.3E-14	1.3E-16	1.5E-14
Ice_Test_8_001	stdv	1	2.00141	26.3095	1.59256	0.01334	0.00639	0.00109	0.00168	0.31946	0.19116	0.69106	0.00267	0.16366	0.00222	0.09525
Ice_Test_8_001	min	1	2.00141	26.3095	-5.95925	-0.02565	-0.03397	-0.00225	-0.00339	-1.12032	-0.45382	-1.00536	-0.0052	-0.57394	-0.00526	-0.1852
Ice_Test_8_001	max	1	2.00141	26.3095	5.06341	0.02459	0.01269	0.00298	0.00382	0.85427	0.45013	0.98045	0.00678	0.43764	0.00522	0.24159
Ice_Test_8_001	abs_max	1	2.00141	26.3095	5.95925	0.02565	0.03397	0.00298	0.00382	1.12032	0.45382	1.00536	0.00678	0.57394	0.00526	0.24159
Ice_Test_8_001	mean	2	34.8974	53.1648	270.069	10.0012	0.03295	-0.89611	-0.91528	147.489	187.213	-0.00883	-1.8114	75.5587	2.17167	-64.5256
Ice_Test_8_001	stdv	2	34.8974	53.1648	0.6796	0.03714	0.68943	0.01037	0.00671	0.75109	0.64922	0.69043	0.01461	0.38479	0.00753	0.52027
Ice_Test_8_001	min	2	34.8974	53.1648	268.315	9.91217	-0.94491	-0.92574	-0.93397	145.091	185.609	-0.98363	-1.85943	74.33	2.15307	-66.2367
Ice_Test_8_001	max	2	34.8974	53.1648	271.97	10.0962	1.02352	-0.87269	-0.90082	149.275	188.654	0.98211	-1.7753	76.4734	2.18838	-63.2397
Ice_Test_8_001	abs_max	2	34.8974	53.1648	271.97	10.0962	1.02352	0.92574	0.93397	149.275	188.654	0.98363	1.85943	76.4734	2.18838	66.2367
	Stat Type	Segment	Time 1	Time 2	Azimuthin	RPS	DASPC23_	Fy1a	Fy2a	Thrust	Torque	DASPC55_	THRUST_R	CALCULAT	CALCULAT	CALCULATED_Y_THRUST
			sec	sec	deg	rps	volts	mv	mv	mv	mv	volts	mv	mv	mv	mv
			Start Time	End Time												
Ice_Test_9_001	mean	1	0.95699	20.4031	0.06224	-0.00024	-0.01244	1.6E-16	8.5E-16	-2.2E-14	1.1E-14	-5.1E-16	1.8E-15	-1.7E-14	-2.4E-16	-4.3E-14
Ice_Test_9_001	stdv	1	0.95699	20.4031	1.61572	0.01779	0.00547	0.00099	0.00193	0.16506	0.13224	0.68916	0.0029	0.08456	0.00153	0.10327
Ice_Test_9_001	min	1	0.95699	20.4031	-5.44232	-0.0264	-0.03161	-0.00231	-0.00428	-0.45343	-0.42474	-0.96171	-0.00655	-0.23229	-0.00493	-0.23318
Ice_Test_9_001	max	1	0.95699	20.4031	6.76153	0.02602	0.01123	0.0023	0.00415	0.50658	0.46474	1.02238	0.00642	0.25952	0.00539	0.22862
Ice_Test_9_001	abs_max	1	0.95699	20.4031	6.76153	0.0264	0.03161	0.00231	0.00428	0.50658	0.46474	1.02238	0.00655	0.25952	0.00539	0.23318
Ice_Test_9_001	mean	2	26.3747	45.8208	269.979	12.5015	0.02875	-1.42083	-1.44628	233.379	295.237	0.02361	-2.86711	119.56	3.42475	-102.132
Ice_Test_9_001	stdv	2	26.3747	45.8208	1.4181	0.04504	0.69997	0.0195	0.01206	0.76986	0.89331	0.70026	0.02733	0.3944	0.01036	0.97369
Ice_Test_9_001	min	2	26.3747	45.8208	267.076	12.3735	-0.95154	-1.46284	-1.48243	231.738	293.28	-0.96368	-2.93321	118.719	3.40205	-104.487
Ice_Test_9_001	max	2	26.3747	45.8208	273.086	12.6409	1.01506	-1.36427	-1.41944	236.46	298.352	1.00192	-2.80213	121.138	3.46088	-99.8174
Ice_Test_9_001	abs_max	2	26.3747	45.8208	273.086	12.6409	1.01506	1.46284	1.48243	236.46	298.352	1.00192	2.93321	121.138	3.46088	104.487
	Stat Type	Segment	Time 1	Time 2	Azimuthin	RPS	DASPC23_	Fy1a	Fy2a	Thrust	Torque	DASPC55_	THRUST_R	CALCULAT	CALCULAT	CALCULATED_Y_THRUST
			sec	sec	deg	rps	volts	mv	mv	mv	mv	volts	mv	mv	mv	mv
			Start Time	End Time												
Ice_Test_10_001	mean	1	4.72589	20.4536	0.07012	-0.00057	-0.01291	-2.7E-16	-7.5E-17	-4.2E-14	-3.8E-14	-4.8E-16	2.8E-17	1.2E-13	1.1E-15	-9.5E-16
Ice_Test_10_001	stdv	1	4.72589	20.4536	1.54985	0.01853	0.00791	0.00185	0.00347	0.82892	0.25862	0.69549	0.00506	0.42465	0.003	0.18009
Ice_Test_10_001	min	1	4.72589	20.4536	-5.06388	-0.02849	-0.04338	-0.0043	-0.00701	-1.80154	-0.67519	-0.99113	-0.01126	-0.92293	-0.00783	-0.40121
Ice_Test_10_001	max	1	4.72589	20.4536	6.38505	0.02902	0.0122	0.00551	0.00863	1.70786	0.6275	0.9813	0.0141	0.87494	0.00728	0.50213
Ice_Test_10_001	abs_max	1	4.72589	20.4536	6.38505	0.02902	0.04338	0.00551	0.00863	1.80154	0.67519	0.99113	0.0141	0.92293	0.00783	0.50213
Ice_Test_10_001	mean	2	27.7882	52.0604	269.942	12.5012	0.02126	-1.41016	-1.42642	235.333	295.579	-0.01699	-2.83658	120.561	3.42871	-101.045
Ice_Test_10_001	stdv	2	27.7882	52.0604	1.45925	0.04247	0.69571	0.01853	0.01429	1.41296	0.793	0.69368	0.02906	0.72386	0.0092	1.0353
Ice_Test_10_001	min	2	27.7882	52.0604	266.73	12.3733	-0.95368	-1.46009	-1.46113	232.752	293.823	-0.99301	-2.89926	119.239	3.40835	-103.277
Ice_Test_10_001	max	2	27.7882	52.0604	273.421	12.6417	1.03358	-1.34509	-1.37989	240.422	297.61	0.97303	-2.72502	123.168	3.45228	-97.0706

Ice_Test_10_001	abs_max	2	27.7882	52.0604	273.421	12.6417	1.03358	1.46009	1.46113	240.422	297.61	0.99301	2.89926	123.168	3.45228	103.277
	Stat Type	Segment	Time 1	Time 2	Azimuthin	RPS	DASPC23_	Fy1a	Fy2a	Thrust	Torque	DASPC55_	THRUST_R	CALCULAT	CALCULAT	CALCULATED_Y_THRUST
			sec	sec	deg	rps	volts	mv	mv	mv	mv	volts	mv	mv	mv	mv
			Start Time	End Time												
Ice_Test_11_001	mean	1	6.93476	19.5982	0.16793	-0.0004	-0.01227	-3E-16	-5.1E-16	-5.4E-14	9.3E-14	-1.5E-17	8.5E-16	9.3E-15	-1.2E-15	-1.9E-14
Ice_Test_11_001	stdv	1	6.93476	19.5982	2.61281	0.02679	0.01049	0.00164	0.00194	0.28631	0.19329	0.68943	0.00346	0.14668	0.00224	0.12331
Ice_Test_11_001	min	1	6.93476	19.5982	-8.34084	-0.04168	-0.04604	-0.00438	-0.0042	-0.86534	-0.35486	-0.99992	-0.00851	-0.44331	-0.00412	-0.30315
Ice_Test_11_001	max	1	6.93476	19.5982	12.5192	0.04199	0.04724	0.00409	0.00537	0.44004	0.36963	0.9658	0.00936	0.22543	0.00429	0.33356
Ice_Test_11_001	abs_max	1	6.93476	19.5982	12.5192	0.04199	0.04724	0.00438	0.00537	0.86534	0.36963	0.99992	0.00936	0.44331	0.00429	0.33356
Ice_Test_11_001	mean	2	26.1767	44.1029	269.789	9.99998	0.03448	-0.89934	-0.92771	148.356	188.473	-0.01532	-1.82705	76.0028	2.18629	-65.083
Ice_Test_11_001	stdv	2	26.1767	44.1029	1.63746	0.02896	0.69353	0.01292	0.00901	0.92776	0.86012	0.69473	0.01913	0.47529	0.00998	0.68151
Ice_Test_11_001	min	2	26.1767	44.1029	266.834	9.91865	-0.95202	-0.92697	-0.95349	146.737	186.717	-0.9997	-1.86437	75.1734	2.16592	-66.4126
Ice_Test_11_001	max	2	26.1767	44.1029	272.664	10.076	1.01497	-0.86408	-0.91198	151.111	191.393	0.96665	-1.78298	77.4144	2.22016	-63.5132
Ice_Test_11_001	abs_max	2	26.1767	44.1029	272.664	10.076	1.01497	0.92697	0.95349	151.111	191.393	0.9997	1.86437	77.4144	2.22016	66.4126
	Stat Type	Segment	Time 1	Time 2	Azimuthin	RPS	DASPC23_	Fy1a	Fy2a	Thrust	Torque	DASPC55_	THRUST_R	CALCULAT	CALCULAT	CALCULATED_Y_THRUST
			sec	sec	deg	rps	volts	mv	mv	mv	mv	volts	mv	mv	mv	mv
			Start Time	End Time												
Ice_Test_12_001	mean	1	5.90168	24.1096	-0.06199	-0.00016	-0.01234	-2.7E-16	-1.2E-16	3.8E-15	-4.7E-15	-1E-15	4.7E-16	1.3E-14	-1.8E-16	2E-14
Ice_Test_12_001	stdv	1	5.90168	24.1096	2.46199	0.03545	0.00679	0.0025	0.00834	0.10403	0.08687	0.69422	0.01042	0.05329	0.00101	0.37119
Ice_Test_12_001	min	1	5.90168	24.1096	-9.57277	-0.0677	-0.04226	-0.00557	-0.01626	-0.36161	-0.32252	-0.9941	-0.02009	-0.18525	-0.00374	-0.71563
Ice_Test_12_001	max	1	5.90168	24.1096	7.40372	0.07065	0.02037	0.00768	0.02288	0.14361	0.28783	0.97376	0.03023	0.07357	0.00334	1.07701
Ice_Test_12_001	abs_max	1	5.90168	24.1096	9.57277	0.07065	0.04226	0.00768	0.02288	0.36161	0.32252	0.9941	0.03023	0.18525	0.00374	1.07701
Ice_Test_12_001	mean	2	32.4725	47.134	270.046	9.99926	0.00995	-0.90445	-0.91468	149.398	188.911	-0.02507	-1.81913	76.5367	2.19136	-64.8009
Ice_Test_12_001	stdv	2	32.4725	47.134	0.68786	0.02773	0.69298	0.00877	0.01506	0.49755	0.58385	0.69051	0.01911	0.2549	0.00677	0.68057
Ice_Test_12_001	min	2	32.4725	47.134	268.612	9.93143	-0.9593	-0.93175	-0.95571	148.543	187.744	-0.99074	-1.86245	76.0986	2.17783	-66.3442
Ice_Test_12_001	max	2	32.4725	47.134	271.388	10.0644	1.0159	-0.8874	-0.87714	151.134	190.845	0.97444	-1.77251	77.4261	2.2138	-63.1403
Ice_Test_12_001	abs_max	2	32.4725	47.134	271.388	10.0644	1.0159	0.93175	0.95571	151.134	190.845	0.99074	1.86245	77.4261	2.2138	66.3442
	Stat Type	Segment	Time 1	Time 2	Azimuthin	RPS	DASPC23_	Fy1a	Fy2a	Thrust	Torque	DASPC55_	THRUST_R	CALCULAT	CALCULAT	CALCULATED_Y_THRUST
			sec	sec	deg	rps	volts	mv	mv	mv	mv	volts	mv	mv	mv	mv
			Start Time	End Time												
Ice_Test_13_001	mean	1	5.12758	21.4772	-0.01378	16.9902	-10.0206	2.9E-16	-2.7E-15	6E-13	-1.2E-14	5.9E-16	-6.5E-16	3.3E-13	-6.1E-17	-6.2E-14
Ice_Test_13_001	stdv	1	5.12758	21.4772	0.7069	0.42042	0.24914	0.00112	0.0022	3.07254	0.31349	0.70154	0.00319	1.57406	0.00364	0.1135
Ice_Test_13_001	min	1	5.12758	21.4772	-2.01724	0.02155	-10.1095	-0.00312	-0.00549	-4.78484	-0.76147	-1.00656	-0.00838	-2.45127	-0.00883	-0.29839
Ice_Test_13_001	max	1	5.12758	21.4772	1.82357	17.0377	-0.02286	0.00307	0.00583	7.99222	0.70445	0.97478	0.00868	4.09442	0.00817	0.3091
Ice_Test_13_001	abs_max	1	5.12758	21.4772	2.01724	17.0377	10.1095	0.00312	0.00583	7.99222	0.76147	1.00656	0.00868	4.09442	0.00883	0.3091
Ice_Test_13_001	mean	2	27.3373	39.1747	0.03051	-0.00237	0.00107	-1.41385	-1.44588	241.394	294.947	-0.02735	-2.85973	123.666	3.42139	-101.869
Ice_Test_13_001	stdv	2	27.3373	39.1747	0.73549	0.05661	0.02753	0.01538	0.01166	3.28233	0.82118	0.69807	0.02358	1.68154	0.00953	0.83991
Ice_Test_13_001	min	2	27.3373	39.1747	-1.65175	-0.13424	-0.05982	-1.46018	-1.48084	236.169	293.25	-1.00716	-2.93936	120.99	3.4017	-104.706
Ice_Test_13_001	max	2	27.3373	39.1747	1.83736	0.12262	0.06645	-1.39066	-1.42077	247.414	296.526	0.97115	-2.82633	126.75	3.43971	-100.68
Ice_Test_13_001	abs_max	2	27.3373	39.1747	1.83736	0.13424	0.06645	1.46018	1.48084	247.414	296.526	1.00716	2.93936	126.75	3.43971	104.706
Ice_Test_13_001	mean	3	50.7777	59.6265	270.046	-4.49926	10.0481	-0.00101	-0.00063	2.37511	3.83456	0.0344	-0.00164	1.21677	0.04448	-0.05852
Ice_Test_13_001	stdv	3	50.7777	59.6265	2.72813	0.09179	0.71294	0.0009	0.00194	2.58152	1.45798	0.6978	0.00264	1.32251	0.01691	0.0939
Ice_Test_13_001	min	3	50.7777	59.6265	264.624	-4.65402	9.09547	-0.00313	-0.00587	-3.73781	1.43908	-1.01117	-0.00876	-1.91488	0.01669	-0.3121

Ice_Test_13_001	max	3	50.7777	59.6265	276.261	-4.33672	11.2179	0.00085	0.00287	5.96469	5.99921	0.96971	0.00321	3.05571	0.06959	0.11427
Ice_Test_13_001	abs_max	3	50.7777	59.6265	276.261	4.65402	11.2179	0.00313	0.00587	5.96469	5.99921	1.01117	0.00876	3.05571	0.06959	0.3121
	Stat Type	Segment	Time 1	Time 2	Azimuthin	RPS	DASPC23_	Fy1a	Fy2a	Thrust	Torque	DASPC55_	THRUST_R	CALCULAT	CALCULAT	CALCULATED_Y_THRUST
			sec	sec	deg	rps	volts	mv	mv	mv	mv	volts	mv	mv	mv	mv
			Start Time	End Time												
Ice_Test_14_001	mean	1	1.08743	16.3671	-0.01635	-0.00064	-0.01245	2.9E-16	-4E-16	-1.7E-13	5.8E-14	-2E-16	1.1E-16	6.7E-13	-1.4E-15	2.1E-17
Ice_Test_14_001	stdv	1	1.08743	16.3671	2.56678	0.06299	0.01032	0.00253	0.00591	4.9314	0.29525	0.69414	0.00828	2.52636	0.00342	0.29479
Ice_Test_14_001	min	1	1.08743	16.3671	-9.49815	-0.24838	-0.05814	-0.00617	-0.01446	-10.8612	-1.13984	-0.95432	-0.02055	-5.56419	-0.01322	-0.7319
Ice_Test_14_001	max	1	1.08743	16.3671	11.8554	0.32248	0.02619	0.00628	0.01319	8.71888	0.4517	1.05188	0.01907	4.46668	0.00524	0.6792
Ice_Test_14_001	abs_max	1	1.08743	16.3671	11.8554	0.32248	0.05814	0.00628	0.01446	10.8612	1.13984	1.05188	0.02055	5.56419	0.01322	0.7319
Ice_Test_14_001	mean	2	27.3529	34.7697	-0.05665	-8.5E-05	0.00022	-0.50774	-0.51031	50.8201	103.708	-0.01166	-1.01805	26.0351	1.20301	-36.2651
Ice_Test_14_001	stdv	2	27.3529	34.7697	1.59176	0.01492	0.00562	0.00817	0.00632	3.36434	0.47695	0.69833	0.01153	1.72355	0.00553	0.41083
Ice_Test_14_001	min	2	27.3529	34.7697	-3.04705	-0.0224	-0.01001	-0.52353	-0.53149	44.4975	102.275	-0.96015	-1.05028	22.7961	1.18639	-37.413
Ice_Test_14_001	max	2	27.3529	34.7697	2.87373	0.02272	0.01046	-0.49386	-0.49544	57.8623	104.628	1.01851	-0.99619	29.6429	1.21368	-35.4864
Ice_Test_14_001	abs_max	2	27.3529	34.7697	3.04705	0.02272	0.01046	0.52353	0.53149	57.8623	104.628	1.01851	1.05028	29.6429	1.21368	37.413
Ice_Test_14_001	mean	3	43.2461	55.5702	270.044	7.50221	0.01426	-0.00108	-0.00292	-29.2133	-1.82822	0.02431	-0.004	-14.966	-0.02121	-0.1424
Ice_Test_14_001	stdv	3	43.2461	55.5702	1.44901	0.04061	0.69205	0.00189	0.0055	6.58325	0.14423	0.69328	0.00723	3.3726	0.00167	0.25745
Ice_Test_14_001	min	3	43.2461	55.5702	266.212	7.40417	-0.97084	-0.00455	-0.01417	-38.1634	-2.14119	-0.97075	-0.01811	-19.5511	-0.02484	-0.64523
Ice_Test_14_001	max	3	43.2461	55.5702	273.374	7.61027	1.01768	0.00374	0.01323	-15.8797	-1.51657	1.01449	0.01697	-8.13515	-0.01759	0.60452
Ice_Test_14_001	abs_max	3	43.2461	55.5702	273.374	7.61027	1.01768	0.00455	0.01417	38.1634	2.14119	1.01449	0.01811	19.5511	0.02484	0.64523
	Stat Type	Segment	Time 1	Time 2	Azimuthin	RPS	DASPC23_	Fy1a	Fy2a	Thrust	Torque	DASPC55_	THRUST_R	CALCULAT	CALCULAT	CALCULATED_Y_THRUST
			sec	sec	deg	rps	volts	mv	mv	mv	mv	volts	mv	mv	mv	mv
			Start Time	End Time												
Ice_Test_15_001	mean	1	5.8979	17.5727	-0.04821	-0.00131	-0.01239	5.3E-16	7.9E-16	-6.1E-14	2E-13	2.5E-17	8.7E-15	7.9E-14	1.9E-15	-3.5E-13
Ice_Test_15_001	stdv	1	5.8979	17.5727	1.20222	0.02555	0.00459	0.00295	0.00534	0.35687	0.20089	0.69224	0.00824	0.18283	0.00233	0.29349
Ice_Test_15_001	min	1	5.8979	17.5727	-2.12434	-0.05201	-0.02019	-0.00768	-0.01352	-0.88734	-0.45601	-0.96426	-0.02118	-0.45458	-0.00529	-0.75453
Ice_Test_15_001	max	1	5.8979	17.5727	2.05264	0.04896	-0.00472	0.00572	0.0091	1.04834	0.41737	1.01377	0.0144	0.53706	0.00484	0.5131
Ice_Test_15_001	abs_max	1	5.8979	17.5727	2.12434	0.05201	0.02019	0.00768	0.01352	1.04834	0.45601	1.01377	0.02118	0.53706	0.00529	0.75453
Ice_Test_15_001	mean	2	23.7428	34.5103	0.01735	0.00116	-6.1E-05	-0.90525	-0.92056	150.994	188.892	0.05211	-1.82581	77.3545	2.19115	-65.039
Ice_Test_15_001	stdv	2	23.7428	34.5103	1.42339	0.01442	0.00607	0.01177	0.01054	1.22413	0.63213	0.69559	0.02014	0.62712	0.00733	0.71739
Ice_Test_15_001	min	2	23.7428	34.5103	-2.73687	-0.0205	-0.0117	-0.93342	-0.95546	148.73	187.589	-0.96435	-1.88888	76.1943	2.17603	-67.2859
Ice_Test_15_001	max	2	23.7428	34.5103	2.68091	0.02278	0.01206	-0.87735	-0.89896	153.058	190.766	1.01345	-1.7775	78.4115	2.21289	-63.3182
Ice_Test_15_001	abs_max	2	23.7428	34.5103	2.73687	0.02278	0.01206	0.93342	0.95546	153.058	190.766	1.01345	1.88888	78.4115	2.21289	67.2859
Ice_Test_15_001	mean	3	45.7012	53.928	269.989	10.0017	0.04428	-0.00125	-0.00091	5.12606	0.19136	0.05148	-0.00216	2.62608	0.00222	-0.07703
Ice_Test_15_001	stdv	3	45.7012	53.928	0.7484	0.04654	0.70743	0.00217	0.00392	0.3552	0.18173	0.70733	0.006	0.18197	0.00211	0.21369
Ice_Test_15_001	min	3	45.7012	53.928	268.146	9.92008	-0.9704	-0.00479	-0.00737	4.34264	-0.17327	-0.96514	-0.0121	2.22473	-0.00201	-0.43095
Ice_Test_15_001	max	3	45.7012	53.928	271.691	10.0783	1.01433	0.00359	0.00785	6.04029	0.5202	1.01263	0.01086	3.09444	0.00603	0.38687
Ice_Test_15_001	abs_max	3	45.7012	53.928	271.691	10.0783	1.01433	0.00479	0.00785	6.04029	0.5202	1.01263	0.0121	3.09444	0.00603	0.43095
	Stat Type	Segment	Time 1	Time 2	Azimuthin	RPS	DASPC23_	Fy1a	Fy2a	Thrust	Torque	DASPC55_	THRUST_R	CALCULAT	CALCULAT	CALCULATED_Y_THRUST
			sec	sec	deg	rps	volts	mv	mv	mv	mv	volts	mv	mv	mv	mv
			Start Time	End Time												
Ice_Test_16_001	mean	1	1.38941	10.3497	-0.13258	-0.00595	-0.01296	-2.1E-16	-9.3E-17	3.5E-14	-5E-14	-5.2E-16	1.1E-16	1.7E-13	4.1E-16	2.1E-15
Ice_Test_16_001	stdv	1	1.38941	10.3497	2.82733	0.1226	0.00933	0.0021	0.00484	0.74497	0.20323	0.69867	0.00683	0.38165	0.00236	0.24329

Ice_Test_16_001	min	1	1.38941	10.3497	-9.16692	-0.41411	-0.0384	-0.00424	-0.0095	-1.44365	-0.34445	-0.99364	-0.0135	-0.73958	-0.004	-0.48074
Ice_Test_16_001	max	1	1.38941	10.3497	6.99917	0.31293	0.00862	0.00604	0.01323	2.00653	0.32559	0.99508	0.01923	1.02794	0.00378	0.68509
Ice_Test_16_001	abs_max	1	1.38941	10.3497	9.16692	0.41411	0.0384	0.00604	0.01323	2.00653	0.34445	0.99508	0.01923	1.02794	0.004	0.68509
Ice_Test_16_001	mean	2	25.1511	36.9469	0.153	0.00555	0.00049	-1.41165	-1.43485	257.117	294.827	0.01637	-2.8465	131.721	3.41999	-101.398
Ice_Test_16_001	stdv	2	25.1511	36.9469	1.2532	0.02331	0.00614	0.0175	0.01079	18.7141	1.53828	0.70095	0.02507	9.58723	0.01784	0.8932
Ice_Test_16_001	min	2	25.1511	36.9469	-2.59331	-0.02787	-0.01293	-1.44822	-1.46018	238.293	292.689	-0.98023	-2.8998	122.077	3.3952	-103.297
Ice_Test_16_001	max	2	25.1511	36.9469	2.72106	0.03948	0.01301	-1.37533	-1.40585	317.159	298.404	0.99765	-2.78333	162.481	3.46149	-99.1478
Ice_Test_16_001	abs_max	2	25.1511	36.9469	2.72106	0.03948	0.01301	1.44822	1.46018	317.159	298.404	0.99765	2.8998	162.481	3.46149	103.297
Ice_Test_16_001	mean	3	46.9847	52.4289	270.264	12.5064	-0.03396	6.8E-05	-0.00019	9.52457	-0.77376	-0.02291	-0.00012	4.87944	-0.00898	-0.00436
Ice_Test_16_001	stdv	3	46.9847	52.4289	1.69547	0.04547	0.70485	0.00192	0.00479	1.39626	0.26509	0.71335	0.00647	0.7153	0.00308	0.23036
Ice_Test_16_001	min	3	46.9847	52.4289	267.353	12.4249	-0.97762	-0.00383	-0.01378	7.76333	-1.21802	-0.97872	-0.01574	3.97715	-0.01413	-0.56081
Ice_Test_16_001	max	3	46.9847	52.4289	273.173	12.5919	1.0054	0.00425	0.00719	12.529	-0.33357	0.99962	0.01143	6.41862	-0.00387	0.40702
Ice_Test_16_001	abs_max	3	46.9847	52.4289	273.173	12.5919	1.0054	0.00425	0.01378	12.529	1.21802	0.99962	0.01574	6.41862	0.01413	0.56081

	Stat Type	Segment	Time 1	Time 2	Azimuthin	RPS	DASPC23_	Fy1a	Fy2a	Thrust	Torque	DASPC55_	THRUST_R	CALCULAT	CALCULAT	CALCULATED_Y_THRUST
			sec	sec	deg	rps	volts	mv	mv	mv	mv	volts	mv	mv	mv	mv
			Start Time	End Time												
Ice_Test_17_001	mean	1	2.16209	18.3057	-0.03324	-0.00146	-0.0125	4.6E-17	-4.5E-16	-1.7E-13	-5.3E-14	-2E-16	-1.3E-15	1.4E-13	-1.3E-16	-6.5E-15
Ice_Test_17_001	stdv	1	2.16209	18.3057	1.17526	0.05566	0.00418	0.00117	0.00175	1.2993	0.25292	0.70054	0.00283	0.66563	0.00293	0.10065
Ice_Test_17_001	min	1	2.16209	18.3057	-4.70062	-0.19858	-0.02587	-0.00209	-0.00365	-4.07582	-0.68675	-0.9821	-0.00562	-2.08804	-0.00797	-0.20036
Ice_Test_17_001	max	1	2.16209	18.3057	4.20991	0.16739	0.00358	0.00243	0.00347	2.62701	0.42833	1.00123	0.00579	1.34582	0.00497	0.20642
Ice_Test_17_001	abs_max	1	2.16209	18.3057	4.70062	0.19858	0.02587	0.00243	0.00365	4.07582	0.68675	1.00123	0.00579	2.08804	0.00797	0.20642
Ice_Test_17_001	mean	2	24.1866	38.1393	0.04848	0.00099	-7.5E-05	-0.90756	-0.92974	145.19	188.589	0.00968	-1.83729	74.381	2.18763	-65.4481
Ice_Test_17_001	stdv	2	24.1866	38.1393	0.68354	0.01681	0.00307	0.01233	0.01075	1.504	0.9934	0.69904	0.02063	0.7705	0.01152	0.73482
Ice_Test_17_001	min	2	24.1866	38.1393	-1.91072	-0.02363	-0.00774	-0.92796	-0.96221	142.407	186.347	-0.97645	-1.87741	72.9549	2.16162	-66.8771
Ice_Test_17_001	max	2	24.1866	38.1393	2.10432	0.02625	0.00816	-0.86929	-0.90891	148.231	191.71	1.00149	-1.77852	75.9389	2.22384	-63.3543
Ice_Test_17_001	abs_max	2	24.1866	38.1393	2.10432	0.02625	0.00816	0.92796	0.96221	148.231	191.71	1.00149	1.87741	75.9389	2.22384	66.8771
Ice_Test_17_001	mean	3	46.3841	53.764	270.071	10.0023	0.03842	9.3E-05	-0.00038	-4.50906	-1.06784	0.05423	-0.00029	-2.30999	-0.01239	-0.01019
Ice_Test_17_001	stdv	3	46.3841	53.764	2.45499	0.04684	0.70985	0.00099	0.00149	0.84413	0.26121	0.6994	0.00235	0.43245	0.00303	0.08375
Ice_Test_17_001	min	3	46.3841	53.764	265.588	9.92766	-0.97241	-0.00221	-0.00388	-6.01912	-1.47917	-0.97899	-0.006	-3.0836	-0.01716	-0.21375
Ice_Test_17_001	max	3	46.3841	53.764	274.749	10.0778	1.00688	0.00208	0.00211	-2.5749	-0.54992	0.99966	0.0041	-1.31912	-0.00638	0.1462
Ice_Test_17_001	abs_max	3	46.3841	53.764	274.749	10.0778	1.00688	0.00221	0.00388	6.01912	1.47917	0.99966	0.006	3.0836	0.01716	0.21375

	Stat Type	Segment	Time 1	Time 2	Azimuthin	RPS	DASPC23_	Fy1a	Fy2a	Thrust	Torque	DASPC55_	THRUST_R	CALCULAT	CALCULAT	CALCULATED_Y_THRUST
			sec	sec	deg	rps	volts	mv	mv	mv	mv	volts	mv	mv	mv	mv
			Start Time	End Time												
Ice_Test_18_001	mean	1	2.53071	18.7273	-0.01093	-0.00056	-0.01258	-9.9E-16	-8.7E-15	-4.5E-15	-1.4E-14	4.4E-16	3.2E-15	-1E-13	7E-16	-1.5E-13
Ice_Test_18_001	stdv	1	2.53071	18.7273	1.33371	0.03938	0.00557	0.00139	0.00182	1.1276	0.2108	0.69755	0.00317	0.57767	0.00245	0.1129
Ice_Test_18_001	min	1	2.53071	18.7273	-5.11353	-0.14969	-0.03607	-0.00353	-0.00489	-3.3953	-0.45655	-0.99253	-0.00837	-1.73941	-0.0053	-0.29825
Ice_Test_18_001	max	1	2.53071	18.7273	4.23248	0.1244	0.00677	0.00379	0.0051	2.5861	0.5288	1.02353	0.00888	1.32486	0.00613	0.31632
Ice_Test_18_001	abs_max	1	2.53071	18.7273	5.11353	0.14969	0.03607	0.00379	0.0051	3.3953	0.5288	1.02353	0.00888	1.73941	0.00613	0.31632
Ice_Test_18_001	mean	2	24.2055	39.2707	-0.01767	0.00016	-3.7E-05	-0.50762	-0.51472	82.359	106.365	0.0279	-1.02235	42.1925	1.23383	-36.418
Ice_Test_18_001	stdv	2	24.2055	39.2707	1.15735	0.01194	0.00323	0.00867	0.00757	0.68803	0.53114	0.69709	0.01423	0.35248	0.00616	0.50692
Ice_Test_18_001	min	2	24.2055	39.2707	-3.59703	-0.01815	-0.01209	-0.52368	-0.53633	80.7353	105.477	-1.00131	-1.05664	41.3607	1.22353	-37.6397
Ice_Test_18_001	max	2	24.2055	39.2707	3.14774	0.01894	0.01027	-0.48526	-0.49908	84.6064	108.69	0.98141	-0.99264	43.3439	1.2608	-35.3597

Ice_Test_18_001	abs_max	2	24.2055	39.2707	3.59703	0.01894	0.01209	0.52368	0.53633	84.6064	108.69	1.00131	1.05664	43.3439	1.2608	37.6397
Ice_Test_18_001	mean	3	46.7139	55.1695	269.941	7.49928	0.06608	0.00016	-0.00067	-1.41021	-0.00443	0.0409	-0.00051	-0.72245	-5.1E-05	-0.01811
Ice_Test_18_001	stdv	3	46.7139	55.1695	1.99696	0.02956	0.71017	0.0013	0.00221	0.38909	0.14318	0.70874	0.00347	0.19933	0.00166	0.12378
Ice_Test_18_001	min	3	46.7139	55.1695	266.021	7.44872	-0.98512	-0.00293	-0.0059	-2.23296	-0.26171	-1.01073	-0.00882	-1.14394	-0.00304	-0.31423
Ice_Test_18_001	max	3	46.7139	55.1695	273.65	7.55012	0.99411	0.00313	0.004	-0.62455	0.23502	0.97211	0.00711	-0.31996	0.00273	0.25311
Ice_Test_18_001	abs_max	3	46.7139	55.1695	273.65	7.55012	0.99411	0.00313	0.0059	2.23296	0.26171	1.01073	0.00882	1.14394	0.00304	0.31423
	Stat Type	Segment	Time 1	Time 2	Azimuthin	RPS	DASPC23_	Fy1a	Fy2a	Thrust	Torque	DASPC55_	THRUST_R	CALCULAT	CALCULAT	CALCULATED_Y_THRUST
			sec	sec	deg	rps	volts	mv	mv	mv	mv	volts	mv	mv	mv	mv
			Start Time	End Time												
Ice_Test_19_001	mean	1	4.74478	18.9224	-0.00112	-0.00027	-0.01256	-3.2E-16	-4E-16	-9.8E-14	1.3E-14	-2.5E-16	-1.3E-16	6.4E-14	5.6E-17	-6.3E-14
Ice_Test_19_001	stdv	1	4.74478	18.9224	3E-05	7.1E-06	0.00033	0.00373	0.00391	0.54771	0.74477	0.69439	0.00757	0.28059	0.00864	0.26978
Ice_Test_19_001	min	1	4.74478	18.9224	-0.00112	-0.00027	-0.01257	-0.00951	-0.01014	-1.01375	-1.68432	-0.98936	-0.01965	-0.51934	-0.01954	-0.69983
Ice_Test_19_001	max	1	4.74478	18.9224	0	0	0	0.00944	0.00915	1.52608	1.96129	0.98987	0.0186	0.78181	0.02275	0.66244
Ice_Test_19_001	abs_max	1	4.74478	18.9224	0.00112	0.00027	0.01257	0.00951	0.01014	1.52608	1.96129	0.98987	0.01965	0.78181	0.02275	0.69983
Ice_Test_19_001	mean	2	25.3874	37.7125	0	0	0	-0.91853	-0.93723	150.401	190.699	-0.01716	-1.85576	77.0506	2.21211	-66.106
Ice_Test_19_001	stdv	2	25.3874	37.7125	0	0	0	0.01192	0.01056	1.50257	1.47862	0.69785	0.02097	0.76977	0.01715	0.74717
Ice_Test_19_001	min	2	25.3874	37.7125	0	0	0	-0.94932	-0.96289	146.213	186.482	-0.98677	-1.91169	74.905	2.16319	-68.0982
Ice_Test_19_001	max	2	25.3874	37.7125	0	0	0	-0.89535	-0.91417	152.889	194.243	0.99205	-1.81266	78.3251	2.25322	-64.5705
Ice_Test_19_001	abs_max	2	25.3874	37.7125	0	0	0	0.94932	0.96289	152.889	194.243	0.99205	1.91169	78.3251	2.25322	68.0982
	Stat Type	Segment	Time 1	Time 2	Azimuthin	RPS	DASPC23_	Fy1a	Fy2a	Thrust	Torque	DASPC55_	THRUST_R	CALCULAT	CALCULAT	CALCULATED_Y_THRUST
			sec	sec	deg	rps	volts	mv	mv	mv	mv	volts	mv	mv	mv	mv
			Start Time	End Time												
Ice_Test_20_001	mean	1	2.62334	18.5363	0.0313	0.00054	-0.01246	-2E-16	-4.1E-16	7.6E-14	2.5E-15	-4.4E-16	2.8E-15	-2.2E-14	6.7E-17	-3.5E-14
Ice_Test_20_001	stdv	1	2.62334	18.5363	1.74481	0.04104	0.00589	0.00129	0.00221	0.08922	0.12973	0.70071	0.00345	0.04571	0.0015	0.12278
Ice_Test_20_001	min	1	2.62334	18.5363	-5.29524	-0.1302	-0.03425	-0.0028	-0.00542	-0.30324	-0.40174	-0.98173	-0.00818	-0.15535	-0.00466	-0.29133
Ice_Test_20_001	max	1	2.62334	18.5363	5.05134	0.1294	0.00771	0.00325	0.00607	0.21081	0.38246	1.02718	0.00925	0.108	0.00444	0.32942
Ice_Test_20_001	abs_max	1	2.62334	18.5363	5.29524	0.1302	0.03425	0.00325	0.00607	0.30324	0.40174	1.02718	0.00925	0.15535	0.00466	0.32942
Ice_Test_20_001	mean	2	25.2821	38.6005	0.01264	-0.0005	-0.00014	-0.51129	-0.52532	83.4354	106.314	-0.03804	-1.03662	42.744	1.23324	-36.9263
Ice_Test_20_001	stdv	2	25.2821	38.6005	1.58473	0.01825	0.00155	0.0074	0.00595	0.64211	0.61758	0.69256	0.01162	0.32895	0.00716	0.41383
Ice_Test_20_001	min	2	25.2821	38.6005	-3.59003	-0.03169	-0.00509	-0.52948	-0.53622	82.0667	105.071	-0.99089	-1.06411	42.0428	1.21883	-37.9057
Ice_Test_20_001	max	2	25.2821	38.6005	3.89816	0.03127	0.00427	-0.49742	-0.50987	85.1779	108.211	0.99151	-1.00781	43.6366	1.25524	-35.9003
Ice_Test_20_001	abs_max	2	25.2821	38.6005	3.89816	0.03169	0.00509	0.52948	0.53622	85.1779	108.211	0.99151	1.06411	43.6366	1.25524	37.9057
Ice_Test_20_001	mean	3	45.8075	54.1099	270.006	7.49888	-0.02223	-0.00045	-0.00145	-0.45754	-0.51919	-0.03696	-0.0019	-0.2344	-0.00602	-0.06783
Ice_Test_20_001	stdv	3	45.8075	54.1099	1.42171	0.02177	0.70855	0.0014	0.00258	0.06267	0.04392	0.70915	0.00398	0.0321	0.00051	0.14173
Ice_Test_20_001	min	3	45.8075	54.1099	267.006	7.44946	-0.985	-0.00291	-0.00587	-0.56275	-0.6568	-1.0071	-0.00877	-0.2883	-0.00762	-0.31233
Ice_Test_20_001	max	3	45.8075	54.1099	273.4	7.54566	0.99741	0.0025	0.00414	-0.31053	-0.43686	0.98064	0.00664	-0.15908	-0.00507	0.23651
Ice_Test_20_001	abs_max	3	45.8075	54.1099	273.4	7.54566	0.99741	0.00291	0.00587	0.56275	0.6568	1.0071	0.00877	0.2883	0.00762	0.31233
	Stat Type	Segment	Time 1	Time 2	Azimuthin	RPS	DASPC23_	Fy1a	Fy2a	Thrust	Torque	DASPC55_	THRUST_R	CALCULAT	CALCULAT	CALCULATED_Y_THRUST
			sec	sec	deg	rps	volts	mv	mv	mv	mv	volts	mv	mv	mv	mv
			Start Time	End Time												
Ice_Test_21_001	mean	1	3.77645	18.8246	0.03262	0.0006	-0.01248	1.2E-15	-5.6E-16	1.5E-14	-9.2E-15	-2.8E-17	-1.5E-17	-2.1E-14	-1.3E-17	1.7E-15
Ice_Test_21_001	stdv	1	3.77645	18.8246	1.21554	0.03351	0.00245	0.00297	0.00694	0.12101	0.20036	0.70014	0.00959	0.06199	0.00232	0.34174
Ice_Test_21_001	min	1	3.77645	18.8246	-3.00808	-0.08588	-0.01965	-0.00796	-0.01301	-0.26521	-0.62747	-1.00104	-0.01949	-0.13587	-0.00728	-0.69417

Ice_Test_21_001	max	1	3.77645	18.8246	3.36799	0.09571	-0.00429	0.00825	0.0184	0.32061	0.49221	0.98536	0.02653	0.16425	0.00571	0.94504
Ice_Test_21_001	abs_max	1	3.77645	18.8246	3.36799	0.09571	0.01965	0.00825	0.0184	0.32061	0.62747	1.00104	0.02653	0.16425	0.00728	0.94504
Ice_Test_21_001	mean	2	24.7055	38.6582	-0.01837	-0.00063	-3.3E-05	-0.50997	-0.51954	83.9118	107.47	-0.01086	-1.02951	42.988	1.24665	-36.6732
Ice_Test_21_001	stdv	2	24.7055	38.6582	1.23642	0.01521	0.00475	0.01042	0.00967	0.59236	0.6304	0.69873	0.01806	0.30347	0.00731	0.64316
Ice_Test_21_001	min	2	24.7055	38.6582	-3.04069	-0.02458	-0.01313	-0.53123	-0.54427	82.6763	106.19	-1.00325	-1.06745	42.3551	1.23181	-38.0246
Ice_Test_21_001	max	2	24.7055	38.6582	3.33538	0.02342	0.01476	-0.48663	-0.49685	85.4825	109.326	0.97472	-0.98373	43.7927	1.26819	-35.0423
Ice_Test_21_001	abs_max	2	24.7055	38.6582	3.33538	0.02458	0.01476	0.53123	0.54427	85.4825	109.326	1.00325	1.06745	43.7927	1.26819	38.0246
Ice_Test_21_001	mean	3	46.557	53.7063	269.935	7.49992	0.02295	-7.3E-05	-8.4E-05	-0.63488	0.4966	-0.00516	-0.00016	-0.32525	0.00576	-0.00559
Ice_Test_21_001	stdv	3	46.557	53.7063	1.98026	0.02665	0.70623	0.00248	0.00563	0.11493	0.31708	0.70602	0.00786	0.05888	0.00368	0.27991
Ice_Test_21_001	min	3	46.557	53.7063	266.176	7.45165	-0.99142	-0.00491	-0.00984	-0.91193	-0.4132	-1.00286	-0.01466	-0.46718	-0.00479	-0.52209
Ice_Test_21_001	max	3	46.557	53.7063	273.414	7.55035	0.99197	0.00687	0.01646	-0.41585	0.83586	0.97505	0.02333	-0.21304	0.0097	0.83103
Ice_Test_21_001	abs_max	3	46.557	53.7063	273.414	7.55035	0.99197	0.00687	0.01646	0.91193	0.83586	1.00286	0.02333	0.46718	0.0097	0.83103
	Stat Type	Segment	Time 1	Time 2	Azimuthin	RPS	DASPC23_	Fy1a	Fy2a	Thrust	Torque	DASPC55_	THRUST_R	CALCULAT	CALCULAT	CALCULATED_Y_THRUST
			sec	sec	deg	rps	volts	mv	mv	mv	mv	volts	mv	mv	mv	mv
			Start Time	End Time												
Ice_Test_22_001	mean	1	2.95935	19.1332	0.02284	0.00062	-0.01243	-2.5E-17	-6.8E-16	2.2E-14	-5.4E-15	-2.4E-16	-6.7E-16	-2.7E-14	6.2E-16	-2E-14
Ice_Test_22_001	stdv	1	2.95935	19.1332	1.6255	0.05296	0.0078	0.0012	0.00161	0.1891	0.1921	0.70233	0.00277	0.09688	0.00223	0.09872
Ice_Test_22_001	min	1	2.95935	19.1332	-4.30308	-0.15028	-0.03338	-0.00227	-0.00338	-0.6288	-0.50854	-0.97754	-0.00564	-0.32213	-0.0059	-0.20077
Ice_Test_22_001	max	1	2.95935	19.1332	4.93753	0.17352	0.01124	0.00308	0.004	0.41377	0.52918	1.00107	0.00697	0.21197	0.00614	0.24843
Ice_Test_22_001	abs_max	1	2.95935	19.1332	4.93753	0.17352	0.03338	0.00308	0.004	0.6288	0.52918	1.00107	0.00697	0.32213	0.00614	0.24843
Ice_Test_22_001	mean	2	26.0481	37.0651	-0.03637	-0.00105	-0.00021	-0.91463	-0.92379	149.255	188.688	0.02056	-1.83842	76.4634	2.18878	-65.4884
Ice_Test_22_001	stdv	2	26.0481	37.0651	1.37738	0.02483	0.00532	0.01259	0.00734	0.55713	0.67158	0.70024	0.01759	0.28542	0.00779	0.62672
Ice_Test_22_001	min	2	26.0481	37.0651	-2.9366	-0.04171	-0.01036	-0.93882	-0.93569	148.203	187.415	-0.97612	-1.87182	75.9243	2.17402	-66.6781
Ice_Test_22_001	max	2	26.0481	37.0651	2.68795	0.03882	0.00955	-0.88681	-0.89945	150.509	190.15	1.00149	-1.78627	77.1058	2.20574	-63.6305
Ice_Test_22_001	abs_max	2	26.0481	37.0651	2.9366	0.04171	0.01036	0.93882	0.93569	150.509	190.15	1.00149	1.87182	77.1058	2.20574	66.6781
Ice_Test_22_001	mean	3	45.7966	53.5906	270.086	10.0012	0.00731	0.00016	-0.00041	-0.63289	-0.13134	0.0031	-0.00025	-0.32423	-0.00152	-0.00882
Ice_Test_22_001	stdv	3	45.7966	53.5906	1.5389	0.02449	0.70584	0.00103	0.00134	0.18588	0.23162	0.70454	0.0023	0.09523	0.00269	0.08181
Ice_Test_22_001	min	3	45.7966	53.5906	266.844	9.95099	-0.97579	-0.00159	-0.00267	-1.00199	-0.63231	-0.97584	-0.00408	-0.51332	-0.00733	-0.14542
Ice_Test_22_001	max	3	45.7966	53.5906	273.575	10.0515	1.00478	0.0022	0.00271	-0.30591	0.28924	1.00154	0.00472	-0.15672	0.00336	0.16809
Ice_Test_22_001	abs_max	3	45.7966	53.5906	273.575	10.0515	1.00478	0.0022	0.00271	1.00199	0.63231	1.00154	0.00472	0.51332	0.00733	0.16809
	Stat Type	Segment	Time 1	Time 2	Azimuthin	RPS	DASPC23_	Fy1a	Fy2a	Thrust	Torque	DASPC55_	THRUST_R	CALCULAT	CALCULAT	CALCULATED_Y_THRUST
			sec	sec	deg	rps	volts	mv	mv	mv	mv	volts	mv	mv	mv	mv
			Start Time	End Time												
Ice_Test_23_001	mean	1	5.22446	18.7131	0.02801	0.00088	-0.01267	1E-16	1.1E-16	7.3E-14	1.1E-13	5.4E-16	-2.3E-16	-8.5E-14	5.1E-16	-2.3E-14
Ice_Test_23_001	stdv	1	5.22446	18.7131	1.20256	0.03514	0.00358	0.00069	0.00058	0.17928	0.12588	0.69386	0.00119	0.09185	0.00146	0.04253
Ice_Test_23_001	min	1	5.22446	18.7131	-2.47104	-0.07871	-0.02011	-0.00124	-0.00143	-0.56252	-0.27474	-1.02493	-0.00244	-0.28818	-0.00319	-0.08699
Ice_Test_23_001	max	1	5.22446	18.7131	2.63874	0.08453	0.00121	0.00139	0.0014	0.30957	0.22939	0.96118	0.00271	0.15859	0.00266	0.09664
Ice_Test_23_001	abs_max	1	5.22446	18.7131	2.63874	0.08453	0.02011	0.00139	0.00143	0.56252	0.27474	1.02493	0.00271	0.28818	0.00319	0.09664
Ice_Test_23_001	mean	2	27.1989	40.3709	-0.02951	-0.00123	0.00018	-0.90358	-0.9287	148.52	188.367	0.01735	-1.83228	76.0865	2.18505	-65.2696
Ice_Test_23_001	stdv	2	27.1989	40.3709	1.41369	0.01763	0.00463	0.01266	0.00921	0.74181	0.89036	0.69278	0.01906	0.38003	0.01033	0.67907
Ice_Test_23_001	min	2	27.1989	40.3709	-3.40945	-0.02943	-0.01027	-0.93367	-0.95202	146.65	186.731	-1.01271	-1.88159	75.129	2.16607	-67.0259
Ice_Test_23_001	max	2	27.1989	40.3709	3.34934	0.02641	0.01152	-0.87318	-0.90784	150.218	190.95	0.96587	-1.78283	76.9569	2.21502	-63.5081
Ice_Test_23_001	abs_max	2	27.1989	40.3709	3.40945	0.02943	0.01152	0.93367	0.95202	150.218	190.95	1.01271	1.88159	76.9569	2.21502	67.0259

Ice_Test_23_001	mean	3	49.4899	58.799	269.979	10.0006	0.03487	-0.00085	-0.00109	-0.55448	0.39948	-0.01469	-0.00194	-0.28406	0.00463	-0.06907
Ice_Test_23_001	stdv	3	49.4899	58.799	1.18687	0.03804	0.70689	0.00081	0.00076	0.22963	0.1754	0.70851	0.00149	0.11764	0.00203	0.0529
Ice_Test_23_001	min	3	49.4899	58.799	267.614	9.93239	-0.97414	-0.00225	-0.00267	-1.42962	0.04664	-1.01002	-0.00483	-0.73239	0.00054	-0.17219
Ice_Test_23_001	max	3	49.4899	58.799	272.278	10.0703	1.00635	0.00094	0.00087	-0.01068	0.76216	0.96794	0.00144	-0.00547	0.00884	0.05145
Ice_Test_23_001	abs_max	3	49.4899	58.799	272.278	10.0703	1.00635	0.00225	0.00267	1.42962	0.76216	1.01002	0.00483	0.73239	0.00884	0.17219
	Stat Type	Segment	Time 1	Time 2	Azimuthin	RPS	DASPC23_	Fy1a	Fy2a	Thrust	Torque	DASPC55_	THRUST_R	CALCULAT	CALCULAT	CALCULATED_Y_THRUST
			sec	sec	deg	rps	volts	mv	mv	mv	mv	volts	mv	mv	mv	mv
			Start Time	End Time												
Ice_Test_24_001	mean	1	3.78118	20.1564	0.0262	0.00097	-0.01273	-1.3E-16	1.2E-15	6.7E-14	-1.6E-14	-8.3E-17	6.7E-16	-9.5E-14	1.4E-15	-5.5E-14
Ice_Test_24_001	stdv	1	3.78118	20.1564	1.24134	0.04208	0.00665	0.00133	0.00136	0.24051	0.22601	0.70027	0.00259	0.12322	0.00262	0.09239
Ice_Test_24_001	min	1	3.78118	20.1564	-3.12169	-0.11241	-0.03004	-0.00326	-0.00273	-0.49341	-0.52931	-0.96351	-0.00588	-0.25278	-0.00614	-0.20937
Ice_Test_24_001	max	1	3.78118	20.1564	3.48439	0.12563	0.00332	0.00324	0.0041	0.5669	0.52977	1.02563	0.00716	0.29042	0.00615	0.25518
Ice_Test_24_001	abs_max	1	3.78118	20.1564	3.48439	0.12563	0.03004	0.00326	0.0041	0.5669	0.52977	1.02563	0.00716	0.29042	0.00615	0.25518
Ice_Test_24_001	mean	2	26.8851	37.2461	-0.05656	-0.00125	0.00015	-0.92175	-0.9246	149.789	189.376	0.05168	-1.84634	76.7371	2.19676	-65.7704
Ice_Test_24_001	stdv	2	26.8851	37.2461	1.01535	0.01812	0.00483	0.00943	0.00583	0.65782	0.57727	0.70729	0.01339	0.337	0.0067	0.47707
Ice_Test_24_001	min	2	26.8851	37.2461	-1.99875	-0.02857	-0.00798	-0.93719	-0.93719	147.396	188.163	-0.96824	-1.86891	75.5111	2.18269	-66.5744
Ice_Test_24_001	max	2	26.8851	37.2461	1.84057	0.02573	0.00861	-0.90146	-0.90843	151.392	190.713	1.01172	-1.8122	77.5583	2.21227	-64.5542
Ice_Test_24_001	abs_max	2	26.8851	37.2461	1.99875	0.02857	0.00861	0.93719	0.93719	151.392	190.713	1.01172	1.86891	77.5583	2.21227	66.5744
Ice_Test_24_001	mean	3	49.1553	55.3481	270.008	9.99985	0.04548	-0.00039	-0.0004	1.48156	-0.16624	0.04638	-0.00079	0.759	-0.00193	-0.02802
Ice_Test_24_001	stdv	3	49.1553	55.3481	1.8038	0.04308	0.70717	0.00126	0.00135	1.05988	0.22765	0.70418	0.00255	0.54298	0.00264	0.0909
Ice_Test_24_001	min	3	49.1553	55.3481	266.946	9.9299	-0.97971	-0.00262	-0.00291	-0.45881	-0.56037	-0.98095	-0.0054	-0.23505	-0.0065	-0.19221
Ice_Test_24_001	max	3	49.1553	55.3481	273.264	10.0656	1.00497	0.00193	0.00237	4.40464	0.18782	1.00093	0.00419	2.25649	0.00218	0.1492
Ice_Test_24_001	abs_max	3	49.1553	55.3481	273.264	10.0656	1.00497	0.00262	0.00291	4.40464	0.56037	1.00093	0.0054	2.25649	0.0065	0.19221
	Stat Type	Segment	Time 1	Time 2	Azimuthin	RPS	DASPC23_	Fy1a	Fy2a	Thrust	Torque	DASPC55_	THRUST_R	CALCULAT	CALCULAT	CALCULATED_Y_THRUST
			sec	sec	deg	rps	volts	mv	mv	mv	mv	volts	mv	mv	mv	mv
			Start Time	End Time												
Ice_Test_25_001	mean	1	4.12239	17.3832	-0.00227	-0.00043	-0.01254	-3.7E-16	-6.8E-15	4.4E-14	4.4E-14	-2.9E-16	2E-15	-5.2E-14	-7.7E-16	5.5E-14
Ice_Test_25_001	stdv	1	4.12239	17.3832	1.6676	0.032	0.00519	0.00137	0.00247	0.13421	0.12201	0.70076	0.00382	0.06876	0.00142	0.13606
Ice_Test_25_001	min	1	4.12239	17.3832	-3.82183	-0.08397	-0.02718	-0.00369	-0.0062	-0.33269	-0.33624	-0.98925	-0.00989	-0.17044	-0.0039	-0.35225
Ice_Test_25_001	max	1	4.12239	17.3832	3.62912	0.08108	0.00163	0.00368	0.00654	0.39757	0.30227	1.00686	0.0102	0.20368	0.00351	0.36352
Ice_Test_25_001	abs_max	1	4.12239	17.3832	3.82183	0.08397	0.02718	0.00369	0.00654	0.39757	0.33624	1.00686	0.0102	0.20368	0.0039	0.36352
Ice_Test_25_001	mean	2	24.4172	39.4077	0.02299	0.00014	0.00012	-0.51486	-0.5181	84.1798	106.478	-0.01443	-1.03295	43.1253	1.23514	-36.7959
Ice_Test_25_001	stdv	2	24.4172	39.4077	1.87622	0.01328	0.00335	0.00923	0.00663	2.09424	0.45742	0.69745	0.01353	1.07288	0.00531	0.4821
Ice_Test_25_001	min	2	24.4172	39.4077	-4.69048	-0.0198	-0.00955	-0.53425	-0.53443	79.3337	105.287	-0.96541	-1.06311	40.6427	1.22132	-37.8703
Ice_Test_25_001	max	2	24.4172	39.4077	5.34089	0.02065	0.01124	-0.49392	-0.49975	89.2963	107.826	1.01788	-1.00051	45.7465	1.25078	-35.6403
Ice_Test_25_001	abs_max	2	24.4172	39.4077	5.34089	0.02065	0.01124	0.53425	0.53443	89.2963	107.826	1.01788	1.06311	45.7465	1.25078	37.8703
Ice_Test_25_001	mean	3	45.7499	53.3028	270.04	7.49866	0.01065	6.6E-05	-0.00101	-0.04	0.20371	0.01559	-0.00095	-0.02049	0.00236	-0.03376
Ice_Test_25_001	stdv	3	45.7499	53.3028	0.92348	0.03068	0.71286	0.00235	0.0047	0.07485	0.02929	0.71178	0.00703	0.03834	0.00034	0.25056
Ice_Test_25_001	min	3	45.7499	53.3028	267.597	7.44857	-0.96831	-0.00492	-0.01069	-0.18917	0.1514	-0.95415	-0.01557	-0.09691	0.00176	-0.55453
Ice_Test_25_001	max	3	45.7499	53.3028	272.912	7.54979	1.01199	0.00512	0.00924	0.1106	0.2825	1.02948	0.01434	0.05666	0.00328	0.51077
Ice_Test_25_001	abs_max	3	45.7499	53.3028	272.912	7.54979	1.01199	0.00512	0.01069	0.18917	0.2825	1.02948	0.01557	0.09691	0.00328	0.55453
	Stat Type	Segment	Time 1	Time 2	Azimuthin	RPS	DASPC23_	Fy1a	Fy2a	Thrust	Torque	DASPC55_	THRUST_R	CALCULAT	CALCULAT	CALCULATED_Y_THRUST
			sec	sec	deg	rps	volts	mv	mv	mv	mv	volts	mv	mv	mv	mv

			Start Time	End Time												
Ice_Test_26_001	mean	1	1.44612	18.7996	-0.05944	-0.0019	-0.01288	-2.9E-16	-4.3E-16	-1E-13	8.5E-14	2.7E-16	4.3E-17	4E-14	-4.1E-16	3.9E-16
Ice_Test_26_001	stdv	1	1.44612	18.7996	2.12008	0.05515	0.0086	0.00373	0.00725	0.2261	0.17915	0.69504	0.01065	0.11583	0.00208	0.37923
Ice_Test_26_001	min	1	1.44612	18.7996	-9.26103	-0.25146	-0.04878	-0.00953	-0.01989	-0.48385	-0.4977	-1.01801	-0.02848	-0.24788	-0.00577	-1.01434
Ice_Test_26_001	max	1	1.44612	18.7996	7.08999	0.19058	0.01552	0.00847	0.01712	0.59036	0.3939	0.96272	0.02443	0.30244	0.00457	0.87011
Ice_Test_26_001	abs_max	1	1.44612	18.7996	9.26103	0.25146	0.04878	0.00953	0.01989	0.59036	0.4977	1.01801	0.02848	0.30244	0.00577	1.01434
Ice_Test_26_001	mean	2	26.1719	40.066	0.02807	0.00129	0.00042	-0.51145	-0.51201	83.3335	106.114	-0.03152	-1.02346	42.6918	1.23092	-36.4577
Ice_Test_26_001	stdv	2	26.1719	40.066	1.58533	0.0188	0.00689	0.00842	0.00972	0.53228	0.40369	0.69751	0.01383	0.27269	0.00468	0.49252
Ice_Test_26_001	min	2	26.1719	40.066	-4.18761	-0.03387	-0.02065	-0.53308	-0.53566	82.1722	105.078	-1.01428	-1.05412	42.0968	1.21891	-37.55
Ice_Test_26_001	max	2	26.1719	40.066	4.09811	0.03536	0.01932	-0.49181	-0.48456	84.3699	107.01	0.96355	-0.99052	43.2227	1.24131	-35.2845
Ice_Test_26_001	abs_max	2	26.1719	40.066	4.18761	0.03536	0.02065	0.53308	0.53566	84.3699	107.01	1.01428	1.05412	43.2227	1.24131	37.55
Ice_Test_26_001	mean	3	47.8921	52.9393	270.014	7.50144	0.11267	-0.0012	-0.00124	-0.61136	-0.48223	0.0659	-0.00244	-0.3132	-0.00559	-0.08695
Ice_Test_26_001	stdv	3	47.8921	52.9393	1.50399	0.02695	0.69282	0.00437	0.01043	0.15822	0.14404	0.69273	0.01463	0.08106	0.00167	0.52098
Ice_Test_26_001	min	3	47.8921	52.9393	267.423	7.45154	-0.96714	-0.00972	-0.0194	-0.95969	-0.70936	-1.01323	-0.02734	-0.49165	-0.00823	-0.97381
Ice_Test_26_001	max	3	47.8921	52.9393	272.484	7.54947	1.01798	0.00644	0.01585	-0.26526	-0.22777	0.96391	0.02068	-0.13589	-0.00264	0.7365
Ice_Test_26_001	abs_max	3	47.8921	52.9393	272.484	7.54947	1.01798	0.00972	0.0194	0.95969	0.70936	1.01323	0.02734	0.49165	0.00823	0.97381
	Stat Type	Segment	Time 1	Time 2	Azimuthin	RPS	DASPC23_	Fy1a	Fy2a	Thrust	Torque	DASPC55_	THRUST_R	CALCULAT	CALCULAT	CALCULATED_Y_THRUST
			sec	sec	deg	rps	volts	mv	mv	mv	mv	volts	mv	mv	mv	mv
			Start Time	End Time												
Ice_Test_27_001	mean	1	3.68477	18.2282	0.00202	0.00036	-0.01257	3.9E-16	5.3E-16	1.4E-13	-1.4E-14	1.7E-16	1.3E-15	4.4E-15	9.6E-16	3.1E-14
Ice_Test_27_001	stdv	1	3.68477	18.2282	0.30745	0.03785	0.00106	0.00245	0.00526	0.85971	0.14468	0.70448	0.00756	0.44043	0.00168	0.26921
Ice_Test_27_001	min	1	3.68477	18.2282	-0.85366	-0.07924	-0.01421	-0.00658	-0.01385	-3.58386	-0.43826	-0.95431	-0.0204	-1.83601	-0.00508	-0.72667
Ice_Test_27_001	max	1	3.68477	18.2282	0.92619	0.08295	0.00096	0.00691	0.0122	1.51313	0.49232	1.0414	0.01906	0.77518	0.00571	0.67891
Ice_Test_27_001	abs_max	1	3.68477	18.2282	0.92619	0.08295	0.01421	0.00691	0.01385	3.58386	0.49232	1.0414	0.0204	1.83601	0.00571	0.72667
Ice_Test_27_001	mean	2	26.9021	36.6847	0.02286	-0.00095	6.9E-05	-2.04979	-2.10676	339.002	426.502	0.01357	-4.15655	173.671	4.94743	-148.065
Ice_Test_27_001	stdv	2	26.9021	36.6847	0.6317	0.02032	0.00315	0.02605	0.0159	0.9088	1.2743	0.6927	0.03891	0.46558	0.01478	1.38592
Ice_Test_27_001	min	2	26.9021	36.6847	-1.48106	-0.03061	-0.00666	-2.0956	-2.14741	337.037	423.483	-0.95997	-4.24154	172.664	4.9124	-151.092
Ice_Test_27_001	max	2	26.9021	36.6847	1.64187	0.02953	0.00729	-1.9974	-2.08137	340.663	428.952	1.0191	-4.07938	174.522	4.97585	-145.316
Ice_Test_27_001	abs_max	2	26.9021	36.6847	1.64187	0.03061	0.00729	2.0956	2.14741	340.663	428.952	1.0191	4.24154	174.522	4.97585	151.092
Ice_Test_27_001	mean	3	47.8368	55.6629	270.049	15.0002	0.03369	-2.2E-05	-3.5E-05	0.67231	0.07743	0.05253	-5.7E-05	0.34442	0.0009	-0.00202
Ice_Test_27_001	stdv	3	47.8368	55.6629	2.06354	0.05927	0.69266	0.00281	0.00485	0.12647	0.09898	0.69204	0.00732	0.06479	0.00115	0.26081
Ice_Test_27_001	min	3	47.8368	55.6629	266.706	14.8955	-0.98287	-0.00576	-0.01217	0.39047	-0.14024	-0.96383	-0.01694	0.20004	-0.00163	-0.60332
Ice_Test_27_001	max	3	47.8368	55.6629	273.465	15.0988	0.99535	0.00757	0.00717	0.94647	0.27934	1.01488	0.01436	0.48488	0.00324	0.51145
Ice_Test_27_001	abs_max	3	47.8368	55.6629	273.465	15.0988	0.99535	0.00757	0.01217	0.94647	0.27934	1.01488	0.01694	0.48488	0.00324	0.60332
	Stat Type	Segment	Time 1	Time 2	Azimuthin	RPS	DASPC23_	Fy1a	Fy2a	Thrust	Torque	DASPC55_	THRUST_R	CALCULAT	CALCULAT	CALCULATED_Y_THRUST
			sec	sec	deg	rps	volts	mv	mv	mv	mv	volts	mv	mv	mv	mv
			Start Time	End Time												
Ice_Test_28_001	mean	1	3.23628	19.206	-0.03971	-0.00165	-0.01242	2.3E-16	-5.9E-16	-1.7E-14	4.9E-14	8.1E-17	-1.6E-16	-5.9E-16	-1.9E-16	3.8E-14
Ice_Test_28_001	stdv	1	3.23628	19.206	1.1609	0.04615	0.00632	0.00105	0.00187	0.16617	0.20859	0.69928	0.00284	0.08513	0.00242	0.1013
Ice_Test_28_001	min	1	3.23628	19.206	-3.64994	-0.14424	-0.02829	-0.00245	-0.00605	-0.32295	-0.45689	-0.98948	-0.0085	-0.16545	-0.0053	-0.30269
Ice_Test_28_001	max	1	3.23628	19.206	3.17939	0.1259	0.00501	0.00263	0.00417	0.36118	0.43237	0.99259	0.0068	0.18503	0.00502	0.24229
Ice_Test_28_001	abs_max	1	3.23628	19.206	3.64994	0.14424	0.02829	0.00263	0.00605	0.36118	0.45689	0.99259	0.0085	0.18503	0.0053	0.30269
Ice_Test_28_001	mean	2	28.7636	42.0112	0.06287	0.00118	-1.7E-05	-0.89048	-0.93285	148.215	188.037	0.03903	-1.82334	75.9308	2.18123	-64.9509

Ice_Test_28_001	stdv	2	28.7636	42.0112	1.3914	0.01969	0.00594	0.01038	0.00816	0.42384	0.38567	0.69369	0.01707	0.21713	0.00447	0.60804
Ice_Test_28_001	min	2	28.7636	42.0112	-3.71734	-0.03625	-0.01431	-0.90842	-0.9503	146.826	186.502	-0.99	-1.85855	75.2187	2.16342	-66.2052
Ice_Test_28_001	max	2	28.7636	42.0112	4.31343	0.03653	0.01599	-0.86812	-0.90879	149.125	188.939	0.98756	-1.77781	76.3967	2.1917	-63.3293
Ice_Test_28_001	abs_max	2	28.7636	42.0112	4.31343	0.03653	0.01599	0.90842	0.9503	149.125	188.939	0.99	1.85855	76.3967	2.1917	66.2052
Ice_Test_28_001	mean	3	49.6331	55.6218	270.036	10.0022	0.01459	-0.00042	-0.0008	-0.8947	0.6689	-0.00017	-0.00122	-0.45836	0.00776	-0.04357
Ice_Test_28_001	stdv	3	49.6331	55.6218	1.96683	0.0401	0.69952	0.00173	0.00259	0.25414	0.2926	0.69895	0.00427	0.13019	0.00339	0.15214
Ice_Test_28_001	min	3	49.6331	55.6218	266.681	9.93975	-0.97815	-0.00389	-0.00596	-1.46602	0.12822	-0.99069	-0.00983	-0.75104	0.00149	-0.35032
Ice_Test_28_001	max	3	49.6331	55.6218	273.185	10.0666	1.00153	0.0025	0.0037	-0.42587	1.21126	0.9871	0.00592	-0.21817	0.01405	0.21071
Ice_Test_28_001	abs_max	3	49.6331	55.6218	273.185	10.0666	1.00153	0.00389	0.00596	1.46602	1.21126	0.99069	0.00983	0.75104	0.01405	0.35032
	Stat Type	Segment	Time 1	Time 2	Azimuthin	RPS	DASPC23_	Fy1a	Fy2a	Thrust	Torque	DASPC55_	THRUST_R	CALCULAT	CALCULAT	CALCULATED_Y_THRUST
			sec	sec	deg	rps	volts	mv	mv	mv	mv	volts	mv	mv	mv	mv
			Start Time	End Time												
Ice_Test_29_001	mean	1	2.4102	19.5935	-0.03928	-0.0013	-0.01276	1.3E-15	3.3E-16	-1.2E-13	3.9E-14	-1.3E-16	-2.5E-16	7.7E-15	-1.1E-15	-5E-15
Ice_Test_29_001	stdv	1	2.4102	19.5935	1.59003	0.0396	0.00789	0.00265	0.00611	0.34408	0.16217	0.69575	0.00865	0.17627	0.00188	0.30826
Ice_Test_29_001	min	1	2.4102	19.5935	-5.57193	-0.1488	-0.03959	-0.00707	-0.01694	-1.3669	-0.49741	-0.95847	-0.02279	-0.70026	-0.00577	-0.8119
Ice_Test_29_001	max	1	2.4102	19.5935	4.68728	0.1236	0.01027	0.00568	0.01218	0.92112	0.46271	1.02019	0.01785	0.47189	0.00537	0.636
Ice_Test_29_001	abs_max	1	2.4102	19.5935	5.57193	0.1488	0.03959	0.00707	0.01694	1.3669	0.49741	1.02019	0.02279	0.70026	0.00577	0.8119
Ice_Test_29_001	mean	2	25.4347	37.1738	0.03652	0.00066	8.8E-06	-0.50977	-0.52373	83.4978	106.289	0.04685	-1.0335	42.7759	1.23295	-36.8152
Ice_Test_29_001	stdv	2	25.4347	37.1738	1.15807	0.01203	0.00571	0.01053	0.01017	0.70171	0.76344	0.69706	0.01817	0.35948	0.00886	0.64728
Ice_Test_29_001	min	2	25.4347	37.1738	-2.28793	-0.01705	-0.01191	-0.53423	-0.55132	82.1004	104.872	-0.95653	-1.08555	42.0601	1.21652	-38.6696
Ice_Test_29_001	max	2	25.4347	37.1738	2.52929	0.01896	0.01149	-0.4945	-0.50428	84.8623	108.13	1.02101	-0.99903	43.4749	1.2543	-35.5873
Ice_Test_29_001	abs_max	2	25.4347	37.1738	2.52929	0.01896	0.01191	0.53423	0.55132	84.8623	108.13	1.02101	1.08555	43.4749	1.2543	38.6696
Ice_Test_29_001	mean	3	46.6445	52.4289	269.987	7.49972	0.0116	-0.0008	-0.00207	-1.00938	-0.89394	0.02865	-0.00287	-0.51711	-0.01037	-0.10233
Ice_Test_29_001	stdv	3	46.6445	52.4289	1.90366	0.03552	0.70989	0.00288	0.00634	0.45206	0.08679	0.71024	0.0091	0.23159	0.00101	0.32406
Ice_Test_29_001	min	3	46.6445	52.4289	266.503	7.44649	-0.97295	-0.00855	-0.01803	-1.69582	-1.03888	-0.9571	-0.02657	-0.86877	-0.01205	-0.94657
Ice_Test_29_001	max	3	46.6445	52.4289	273.952	7.55856	1.01116	0.00638	0.01188	-0.40521	-0.74439	1.02047	0.01826	-0.20759	-0.00863	0.65035
Ice_Test_29_001	abs_max	3	46.6445	52.4289	273.952	7.55856	1.01116	0.00855	0.01803	1.69582	1.03888	1.02047	0.02657	0.86877	0.01205	0.94657
	Stat Type	Segment	Time 1	Time 2	Azimuthin	RPS	DASPC23_	Fy1a	Fy2a	Thrust	Torque	DASPC55_	THRUST_R	CALCULAT	CALCULAT	CALCULATED_Y_THRUST
			sec	sec	deg	rps	volts	mv	mv	mv	mv	volts	mv	mv	mv	mv
			Start Time	End Time												
Ice_Test_30_001	mean	1	2.69375	16.8147	0.03286	0.00071	-0.01272	-3E-16	2.5E-15	2.7E-14	-4.4E-14	-4.7E-16	-1.3E-14	-9.5E-15	-9.9E-17	3.6E-14
Ice_Test_30_001	stdv	1	2.69375	16.8147	1.60207	0.04184	0.00838	0.00396	0.00753	0.22124	0.16358	0.69595	0.01146	0.11334	0.0019	0.4082
Ice_Test_30_001	min	1	2.69375	16.8147	-4.06913	-0.1113	-0.03665	-0.01024	-0.01814	-0.51243	-0.36867	-0.99224	-0.02837	-0.26252	-0.00428	-1.01065
Ice_Test_30_001	max	1	2.69375	16.8147	4.69837	0.12857	0.00849	0.0094	0.01699	0.39127	0.35614	0.98754	0.02638	0.20045	0.00413	0.93971
Ice_Test_30_001	abs_max	1	2.69375	16.8147	4.69837	0.12857	0.03665	0.01024	0.01814	0.51243	0.36867	0.99224	0.02837	0.26252	0.00428	1.01065
Ice_Test_30_001	mean	2	24.7542	39.7258	0.01025	-0.00071	5.2E-05	-0.51736	-0.52554	84.0997	107.485	0.03688	-1.0429	43.0843	1.24683	-37.1503
Ice_Test_30_001	stdv	2	24.7542	39.7258	1.55743	0.01778	0.00593	0.0086	0.01061	0.6969	0.73233	0.69784	0.0178	0.35702	0.00849	0.63414
Ice_Test_30_001	min	2	24.7542	39.7258	-4.10199	-0.03193	-0.01441	-0.53702	-0.55182	82.6638	106.054	-0.99198	-1.08866	42.3487	1.23023	-38.7803
Ice_Test_30_001	max	2	24.7542	39.7258	4.6655	0.03136	0.01333	-0.49458	-0.49907	85.4288	108.938	0.98551	-0.99553	43.7652	1.26368	-35.4628
Ice_Test_30_001	abs_max	2	24.7542	39.7258	4.6655	0.03193	0.01441	0.53702	0.55182	85.4288	108.938	0.99198	1.08866	43.7652	1.26368	38.7803
Ice_Test_30_001	mean	3	45.6804	52.4289	270.001	7.49897	-0.07126	-0.00056	-0.00046	-0.51592	0.8498	-0.08809	-0.00102	-0.26431	0.00986	-0.03639
Ice_Test_30_001	stdv	3	45.6804	52.4289	2.0123	0.02251	0.70434	0.00573	0.01094	0.17627	0.15342	0.70467	0.01664	0.0903	0.00178	0.59259
Ice_Test_30_001	min	3	45.6804	52.4289	265.421	7.45497	-0.9764	-0.01211	-0.02184	-0.86164	0.59139	-0.99116	-0.03394	-0.44142	0.00686	-1.20904

Ice_Test_30_001	max	3	45.6804	52.4289	273.941	7.54649	1.00371	0.0106	0.01895	-0.21813	1.12469	0.98634	0.02954	-0.11175	0.01305	1.05225
Ice_Test_30_001	abs_max	3	45.6804	52.4289	273.941	7.54649	1.00371	0.01211	0.02184	0.86164	1.12469	0.99116	0.03394	0.44142	0.01305	1.20904

Ice_Test_18_001	abs_max	2	24.2055	39.2707	3.59703	0.01894	0.01209	0.52368	0.53633	84.6064	108.69	1.00131	1.05664	43.3439	1.2608	37.6397
Ice_Test_18_001	mean	3	46.7139	55.1695	269.941	7.49928	0.06608	0.00016	-0.00067	-1.41021	-0.00443	0.0409	-0.00051	-0.72245	-5.1E-05	-0.01811
Ice_Test_18_001	stdv	3	46.7139	55.1695	1.99696	0.02956	0.71017	0.0013	0.00221	0.38909	0.14318	0.70874	0.00347	0.19933	0.00166	0.12378
Ice_Test_18_001	min	3	46.7139	55.1695	266.021	7.44872	-0.98512	-0.00293	-0.0059	-2.23296	-0.26171	-1.01073	-0.00882	-1.14394	-0.00304	-0.31423
Ice_Test_18_001	max	3	46.7139	55.1695	273.65	7.55012	0.99411	0.00313	0.004	-0.62455	0.23502	0.97211	0.00711	-0.31996	0.00273	0.25311
Ice_Test_18_001	abs_max	3	46.7139	55.1695	273.65	7.55012	0.99411	0.00313	0.0059	2.23296	0.26171	1.01073	0.00882	1.14394	0.00304	0.31423
	Stat Type	Segment	Time 1	Time 2	Azimuthin	RPS	DASPC23_	Fy1a	Fy2a	Thrust	Torque	DASPC55_	THRUST_R	CALCULAT	CALCULAT	CALCULATED_Y_THRUST
			sec	sec	deg	rps	volts	mv	mv	mv	mv	volts	mv	mv	mv	mv
			Start Time	End Time												
Ice_Test_19_001	mean	1	4.74478	18.9224	-0.00112	-0.00027	-0.01256	-3.2E-16	-4E-16	-9.8E-14	1.3E-14	-2.5E-16	-1.3E-16	6.4E-14	5.6E-17	-6.3E-14
Ice_Test_19_001	stdv	1	4.74478	18.9224	3E-05	7.1E-06	0.00033	0.00373	0.00391	0.54771	0.74477	0.69439	0.00757	0.28059	0.00864	0.26978
Ice_Test_19_001	min	1	4.74478	18.9224	-0.00112	-0.00027	-0.01257	-0.00951	-0.01014	-1.01375	-1.68432	-0.98936	-0.01965	-0.51934	-0.01954	-0.69983
Ice_Test_19_001	max	1	4.74478	18.9224	0	0	0	0.00944	0.00915	1.52608	1.96129	0.98987	0.0186	0.78181	0.02275	0.66244
Ice_Test_19_001	abs_max	1	4.74478	18.9224	0.00112	0.00027	0.01257	0.00951	0.01014	1.52608	1.96129	0.98987	0.01965	0.78181	0.02275	0.69983
Ice_Test_19_001	mean	2	25.3874	37.7125	0	0	0	-0.91853	-0.93723	150.401	190.699	-0.01716	-1.85576	77.0506	2.21211	-66.106
Ice_Test_19_001	stdv	2	25.3874	37.7125	0	0	0	0.01192	0.01056	1.50257	1.47862	0.69785	0.02097	0.76977	0.01715	0.74717
Ice_Test_19_001	min	2	25.3874	37.7125	0	0	0	-0.94932	-0.96289	146.213	186.482	-0.98677	-1.91169	74.905	2.16319	-68.0982
Ice_Test_19_001	max	2	25.3874	37.7125	0	0	0	-0.89535	-0.91417	152.889	194.243	0.99205	-1.81266	78.3251	2.25322	-64.5705
Ice_Test_19_001	abs_max	2	25.3874	37.7125	0	0	0	0.94932	0.96289	152.889	194.243	0.99205	1.91169	78.3251	2.25322	68.0982
	Stat Type	Segment	Time 1	Time 2	Azimuthin	RPS	DASPC23_	Fy1a	Fy2a	Thrust	Torque	DASPC55_	THRUST_R	CALCULAT	CALCULAT	CALCULATED_Y_THRUST
			sec	sec	deg	rps	volts	mv	mv	mv	mv	volts	mv	mv	mv	mv
			Start Time	End Time												
Ice_Test_20_001	mean	1	2.62334	18.5363	0.0313	0.00054	-0.01246	-2E-16	-4.1E-16	7.6E-14	2.5E-15	-4.4E-16	2.8E-15	-2.2E-14	6.7E-17	-3.5E-14
Ice_Test_20_001	stdv	1	2.62334	18.5363	1.74481	0.04104	0.00589	0.00129	0.00221	0.08922	0.12973	0.70071	0.00345	0.04571	0.0015	0.12278
Ice_Test_20_001	min	1	2.62334	18.5363	-5.29524	-0.1302	-0.03425	-0.0028	-0.00542	-0.30324	-0.40174	-0.98173	-0.00818	-0.15535	-0.00466	-0.29133
Ice_Test_20_001	max	1	2.62334	18.5363	5.05134	0.1294	0.00771	0.00325	0.00607	0.21081	0.38246	1.02718	0.00925	0.108	0.00444	0.32942
Ice_Test_20_001	abs_max	1	2.62334	18.5363	5.29524	0.1302	0.03425	0.00325	0.00607	0.30324	0.40174	1.02718	0.00925	0.15535	0.00466	0.32942
Ice_Test_20_001	mean	2	25.2821	38.6005	0.01264	-0.0005	-0.00014	-0.51129	-0.52532	83.4354	106.314	-0.03804	-1.03662	42.744	1.23324	-36.9263
Ice_Test_20_001	stdv	2	25.2821	38.6005	1.58473	0.01825	0.00155	0.0074	0.00595	0.64211	0.61758	0.69256	0.01162	0.32895	0.00716	0.41383
Ice_Test_20_001	min	2	25.2821	38.6005	-3.59003	-0.03169	-0.00509	-0.52948	-0.53622	82.0667	105.071	-0.99089	-1.06411	42.0428	1.21883	-37.9057
Ice_Test_20_001	max	2	25.2821	38.6005	3.89816	0.03127	0.00427	-0.49742	-0.50987	85.1779	108.211	0.99151	-1.00781	43.6366	1.25524	-35.9003
Ice_Test_20_001	abs_max	2	25.2821	38.6005	3.89816	0.03169	0.00509	0.52948	0.53622	85.1779	108.211	0.99151	1.06411	43.6366	1.25524	37.9057
Ice_Test_20_001	mean	3	45.8075	54.1099	270.006	7.49888	-0.02223	-0.00045	-0.00145	-0.45754	-0.51919	-0.03696	-0.0019	-0.2344	-0.00602	-0.06783
Ice_Test_20_001	stdv	3	45.8075	54.1099	1.42171	0.02177	0.70855	0.0014	0.00258	0.06267	0.04392	0.70915	0.00398	0.0321	0.00051	0.14173
Ice_Test_20_001	min	3	45.8075	54.1099	267.006	7.44946	-0.985	-0.00291	-0.00587	-0.56275	-0.6568	-1.0071	-0.00877	-0.2883	-0.00762	-0.31233
Ice_Test_20_001	max	3	45.8075	54.1099	273.4	7.54566	0.99741	0.0025	0.00414	-0.31053	-0.43686	0.98064	0.00664	-0.15908	-0.00507	0.23651
Ice_Test_20_001	abs_max	3	45.8075	54.1099	273.4	7.54566	0.99741	0.00291	0.00587	0.56275	0.6568	1.0071	0.00877	0.2883	0.00762	0.31233
	Stat Type	Segment	Time 1	Time 2	Azimuthin	RPS	DASPC23_	Fy1a	Fy2a	Thrust	Torque	DASPC55_	THRUST_R	CALCULAT	CALCULAT	CALCULATED_Y_THRUST
			sec	sec	deg	rps	volts	mv	mv	mv	mv	volts	mv	mv	mv	mv
			Start Time	End Time												
Ice_Test_21_001	mean	1	3.77645	18.8246	0.03262	0.0006	-0.01248	1.2E-15	-5.6E-16	1.5E-14	-9.2E-15	-2.8E-17	-1.5E-17	-2.1E-14	-1.3E-17	1.7E-15
Ice_Test_21_001	stdv	1	3.77645	18.8246	1.21554	0.03351	0.00245	0.00297	0.00694	0.12101	0.20036	0.70014	0.00959	0.06199	0.00232	0.34174
Ice_Test_21_001	min	1	3.77645	18.8246	-3.00808	-0.08588	-0.01965	-0.00796	-0.01301	-0.26521	-0.62747	-1.00104	-0.01949	-0.13587	-0.00728	-0.69417

Filtered Organized Data

			Voltage					Calculated		
	Point	Test #	RPS	Thrust	Torque	Y Thrust	Thrust (N)	Torque (N*m)	Y Thrust (N)	P_D (kW)
	1	Test 27	15.00	339.002	426.502	-4.157	173.671	4.947	-148.065	0.466
Average			15.00	339.002	426.502	-4.157	173.671	4.947	-148.065	0.466

			Voltage					Calculated		
	Point	Test #	RPS	Thrust	Torque	Y Thrust	Thrust (N)	Torque (N*m)	Y Thrust (N)	P_D (kW)
	1	Test 1	12.50	230.033	294.786	-2.843	117.846	3.420	-101.259	0.269

Average		7.50	79.455	106.278	-1.030	40.705	1.233	-36.688	0.058

			Voltage				Calculated		
Point	**Test #**	**RPS**	**Thrust**	**Torque**	**Y Thrust**	**Thrust (N)**	**Torque (N*m)**	**Y Thrust (N)**	**P_D (kW)**
1	Test 5	5.00	36.155	47.698	-0.455	18.522	0.553	-16.199	0.017
Average		5.00	36.155	47.698	-0.455	18.522	0.553	-16.199	0.017

Bollard Pull Graph

		RPS	Thrust (N)	Torque (N*m)	10*Torque (N*m)	Y Thrust (N)	Y Thrust Pos (N)
Model Scale	5	5.000	18.522	0.553	5.533	-16.199	16.199
	7.5	7.500	40.705	1.233	12.328	-36.688	36.688
	10	10.000	76.226	2.191	21.905	-65.265	65.265
	12.5	12.500	121.530	3.424	34.237	-101.667	101.667
	15	15.000	173.671	4.947	49.474	-148.065	148.065
		RPM	Thrust (kN)	Torque (kN*m)	10*Torque (kN*m)	Y Thrust (kN)	Y Thrust Pos (kN)
Full Scale	5	67.09	148.18	88.53	885.28	-129.59	129.59
	7.5	100.63	325.64	197.25	1972.52	-293.50	293.50
	10	134.17	609.81	350.48	3504.82	-522.12	522.12
	12.5	167.71	972.24	547.79	5477.94	-813.34	813.34
	15	201.25	1389.37	791.59	7915.88	-1184.52	1184.52

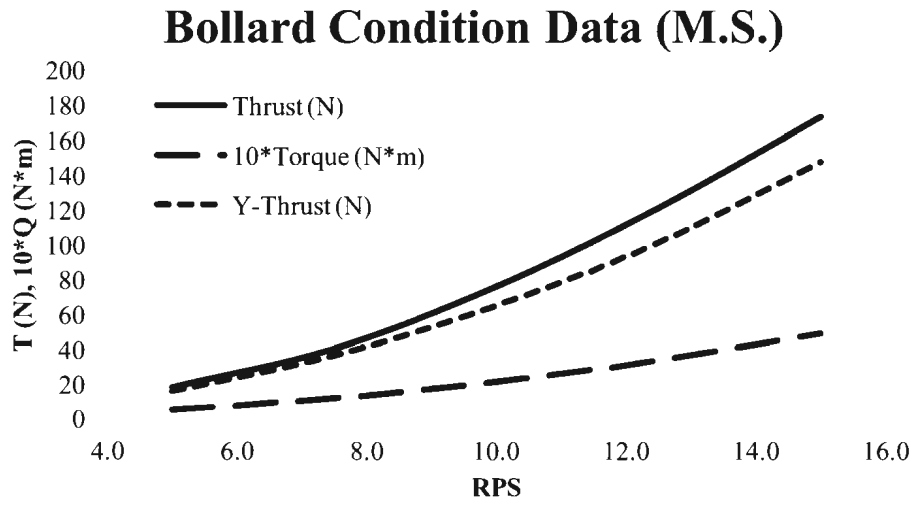

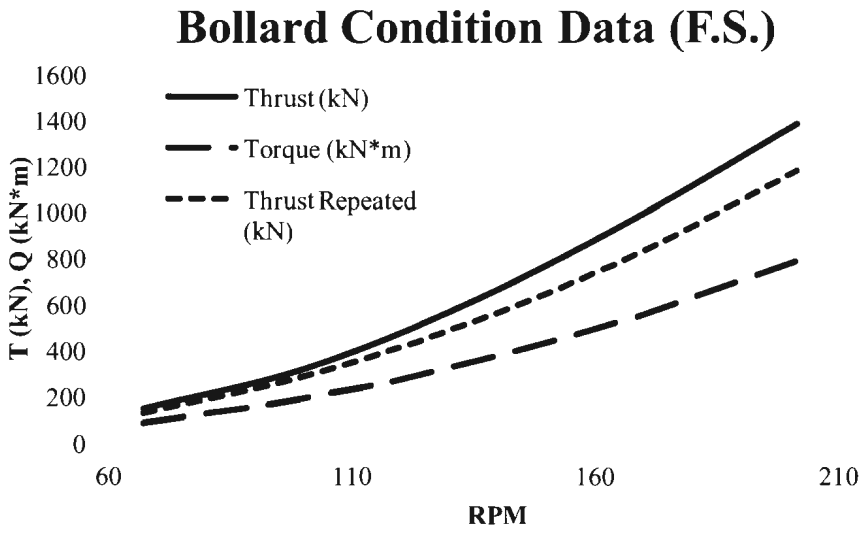

Power Graph

		RPS	P_D (kW)
Model Scale	5	5.000	0.017
	7.5	7.500	0.058
	10	10.000	0.138
	12.5	12.500	0.269
	15	15.000	0.466
		RPM	**P_D (MW)**
Full Scale	5	67.09	0.62
	7.5	100.63	2.08
	10	134.17	4.92
	12.5	167.71	9.62
	15	201.25	16.68

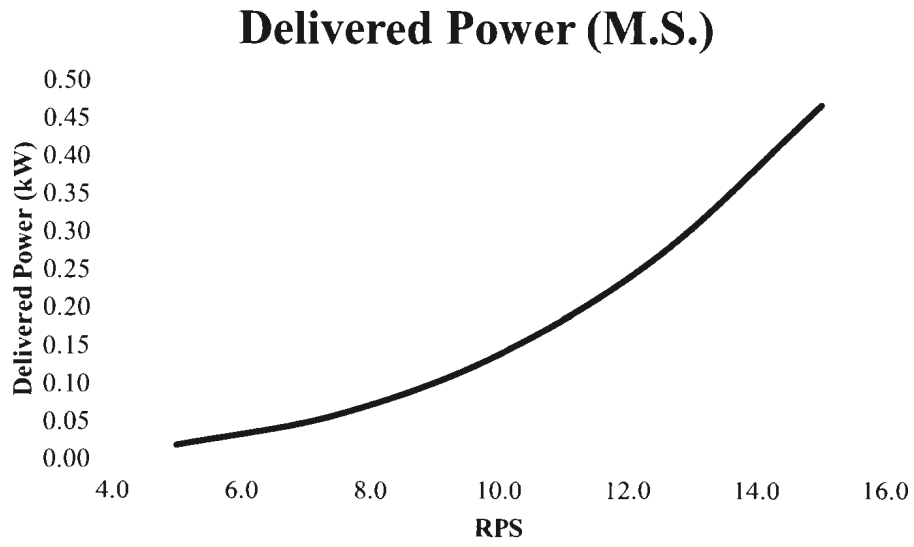

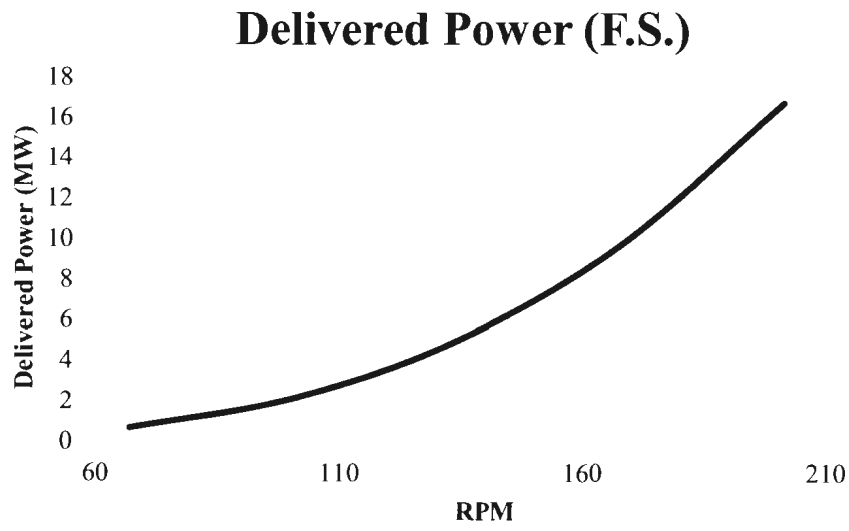

Appendix D

Ice Concentration Analysis

Regions for Test 1 through Test 12

```
[
[[330, 60], [815, 55], [1095, 1020], [0, 1020], [0, 770]],
[[35, 695], [1001, 695], [1047, 855], [0, 855], [0, 770]],
[[109, 535], [954, 535], [1001, 695], [35, 695]],
[[184, 375], [908, 375], [954, 535], [109, 535]],
[[258, 215], [861, 215], [908, 375], [184, 375]]
]
```

Regions for Test 13 through Test 30

```
[
[[190, 0], [750, 0], [820, 215], [890, 375], [1080, 1020], [0, 1020], [0, 770], [0, 400]],
[[0, 695], [985, 695], [1030, 855], [0, 855]],
[[0, 535], [940, 535], [985, 695], [0, 695]],
[[12, 375], [890, 375], [940, 535], [0, 535], [0, 400]],
[[90, 215], [820, 215], [890, 375], [12, 375]]
]
```

Appendix E

Central Composite Design Analysis

Area 1 Diagnostics:

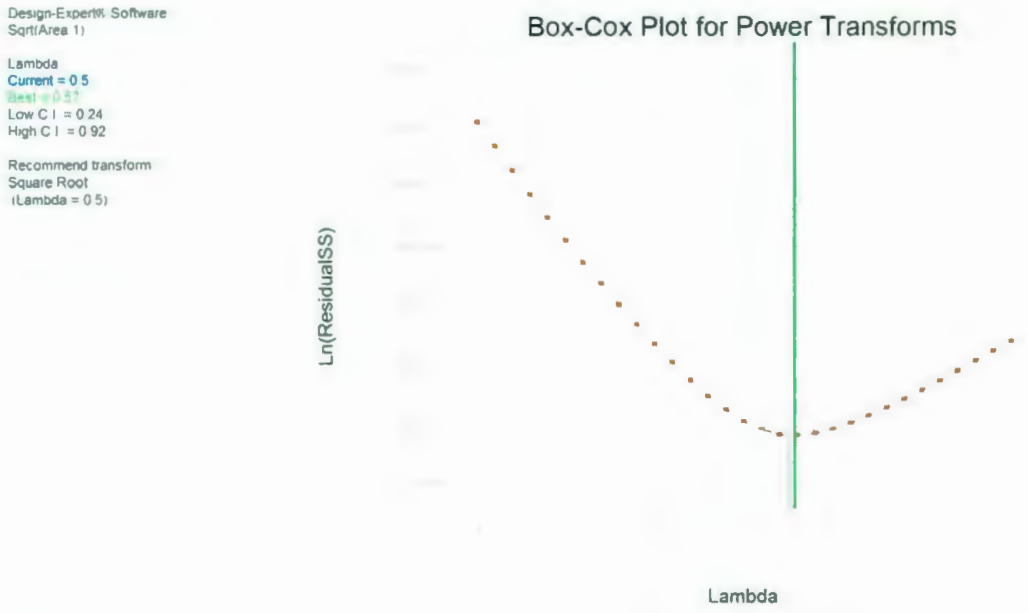

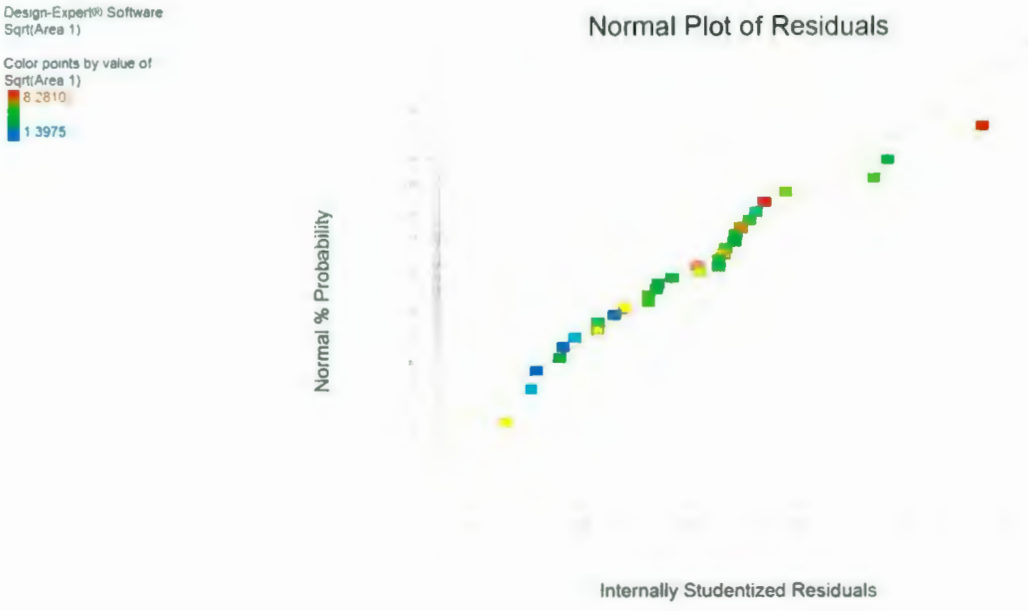

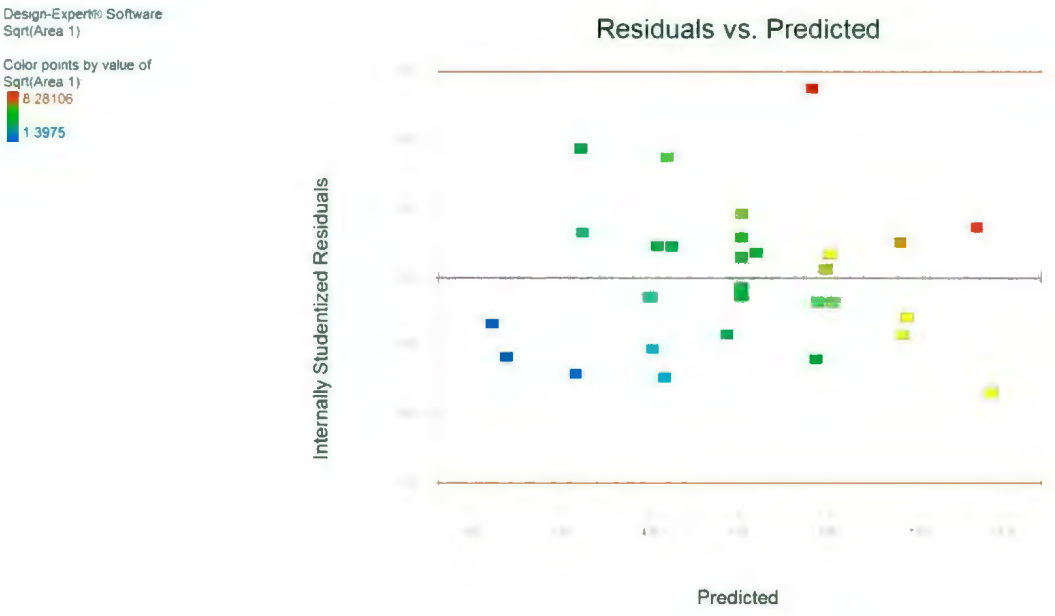
Design-Expert® Software
Sqrt(Area 1)
Color points by value of
Sqrt(Area 1)
8.28106
1.3975
Residuals vs. Predicted
Internally Studentized Residuals
Predicted

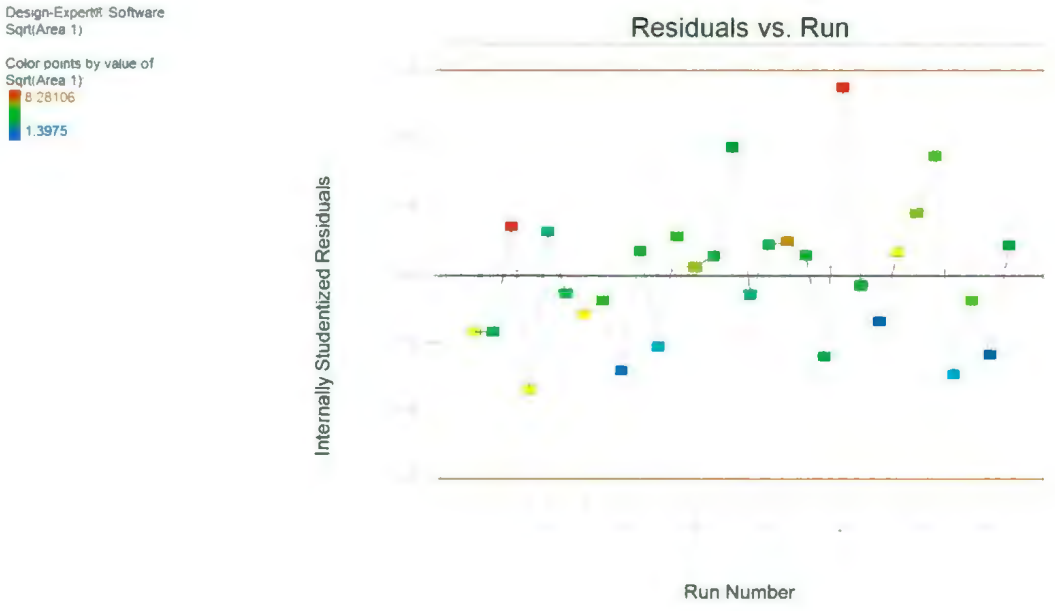
Design-Expert® Software
Sqrt(Area 1)
Color points by value of
Sqrt(Area 1)
8.28106
1.3975
Residuals vs. Run
Internally Studentized Residuals
Run Number

Area 2 Diagnostics:

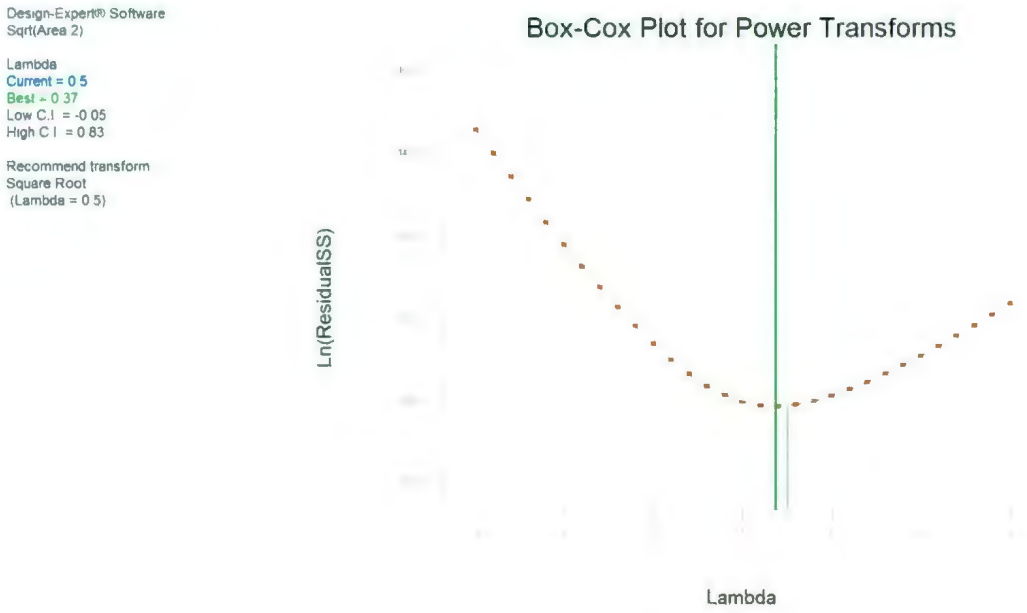

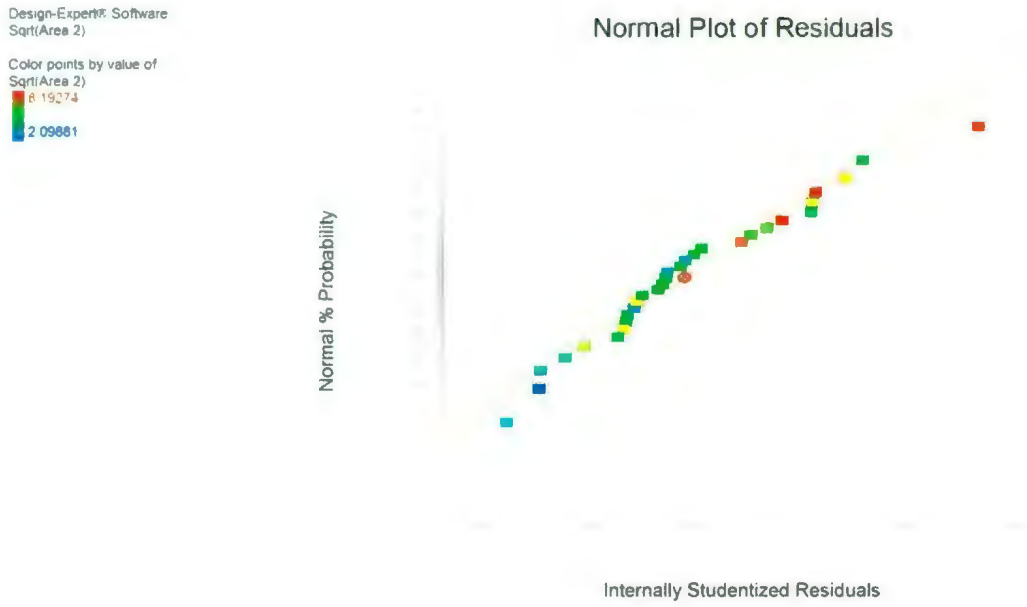

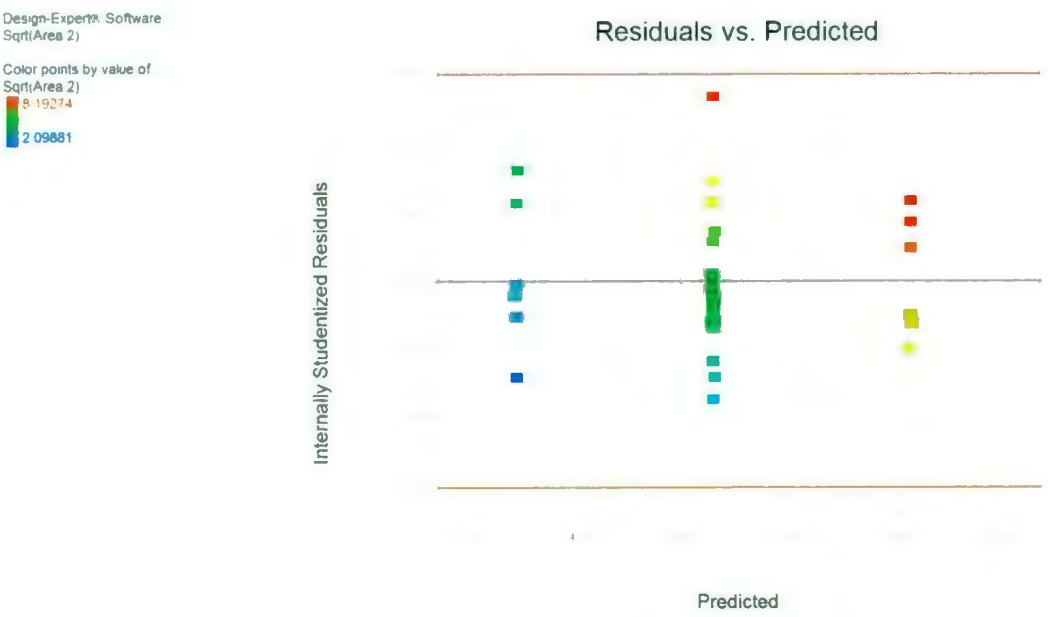
Design-Expert® Software
Sqrt(Area 2)
Color points by value of
Sqrt(Area 2)
8.19274
2.09881
Residuals vs. Predicted
Internally Studentized Residuals
Predicted

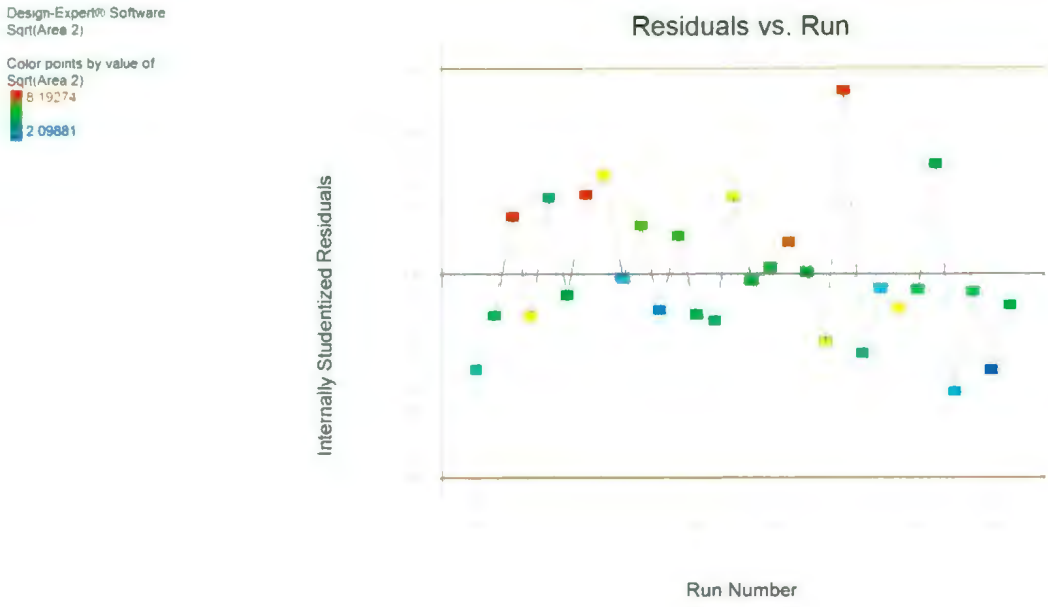
Design-Expert® Software
Sqrt(Area 2)
Color points by value of
Sqrt(Area 2)
8.19274
2.09881
Residuals vs. Run
Internally Studentized Residuals
Run Number

Area 3 Diagnostics:

Design-Expert® Software
Area 3

Lambda
Current = 1
Best = 0.84
Low C.I. = 0.51
High C.I. = 1.20

Recommend transform:
None
(Lambda = 1)

Box-Cox Plot for Power Transforms

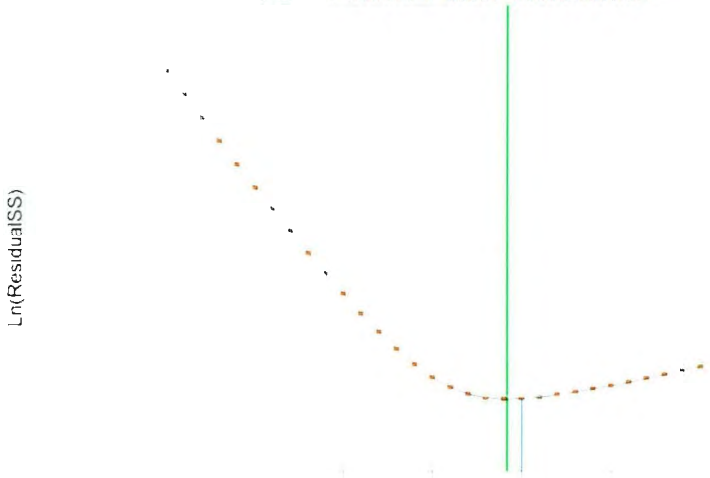

Design-Expert® Software
Area 3

Color points by value of
Area 3:
61.526
-5.384

Normal Plot of Residuals

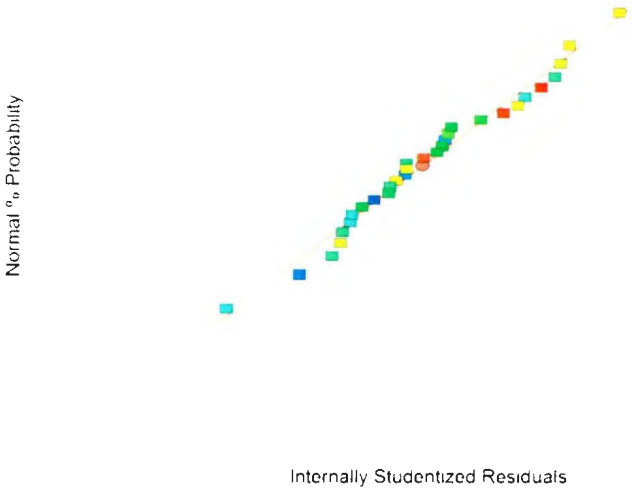

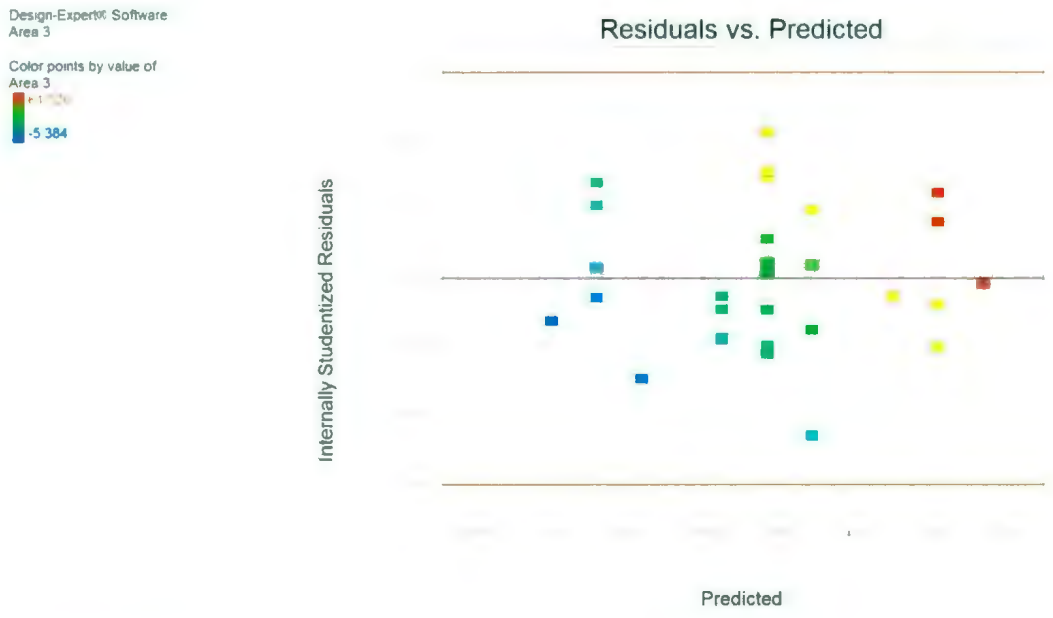
Design-Expert® Software
Area 3
Color points by value of
Area 3
-5.384
Residuals vs. Predicted
Internally Studentized Residuals
Predicted

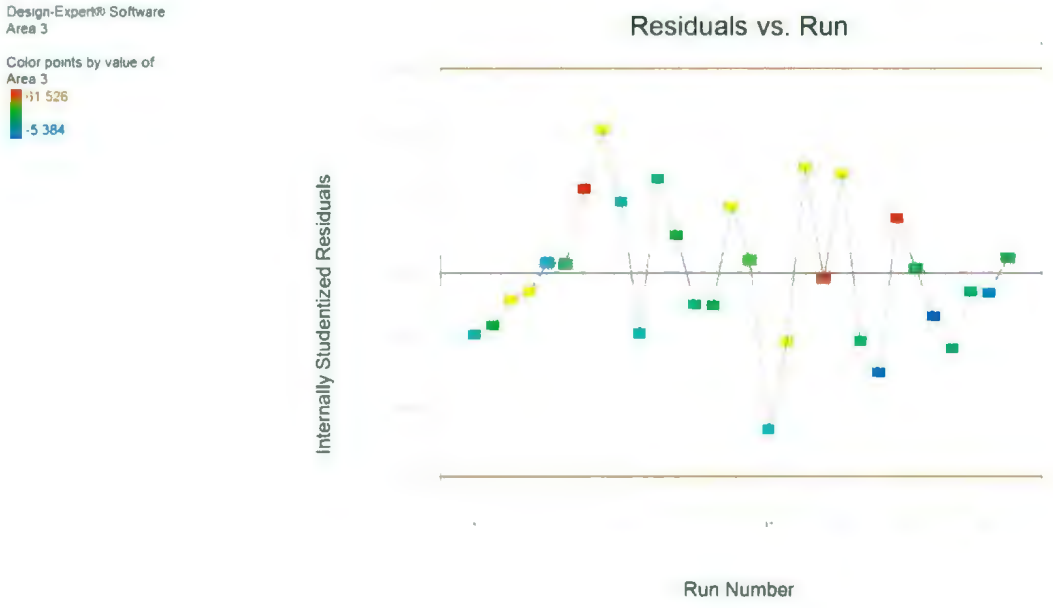
Design-Expert® Software
Area 3
Color points by value of
Area 3
31.526
-5.384
Residuals vs. Run
Internally Studentized Residuals
Run Number

Area 4 Diagnostics:

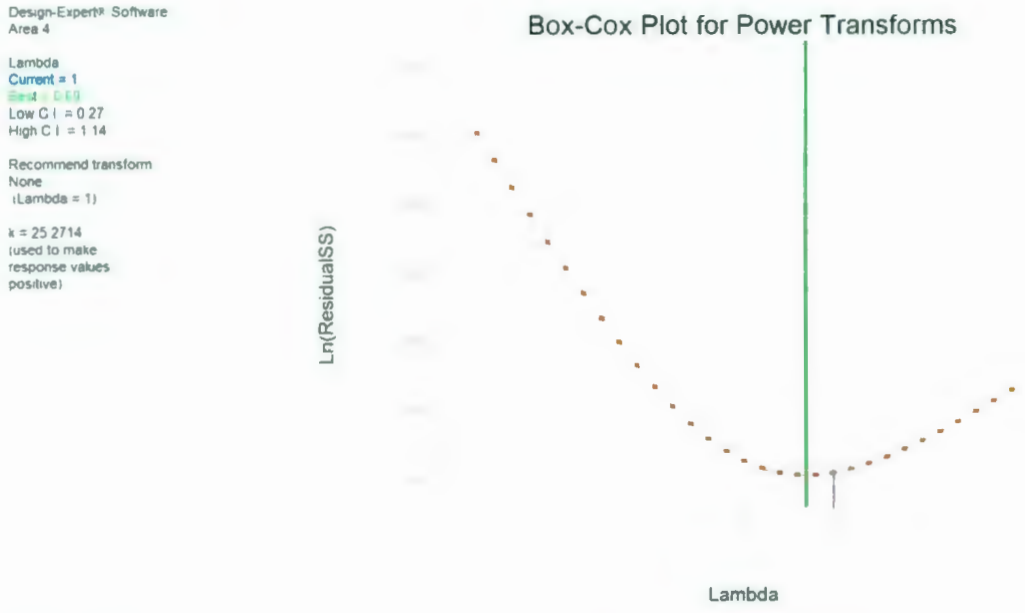

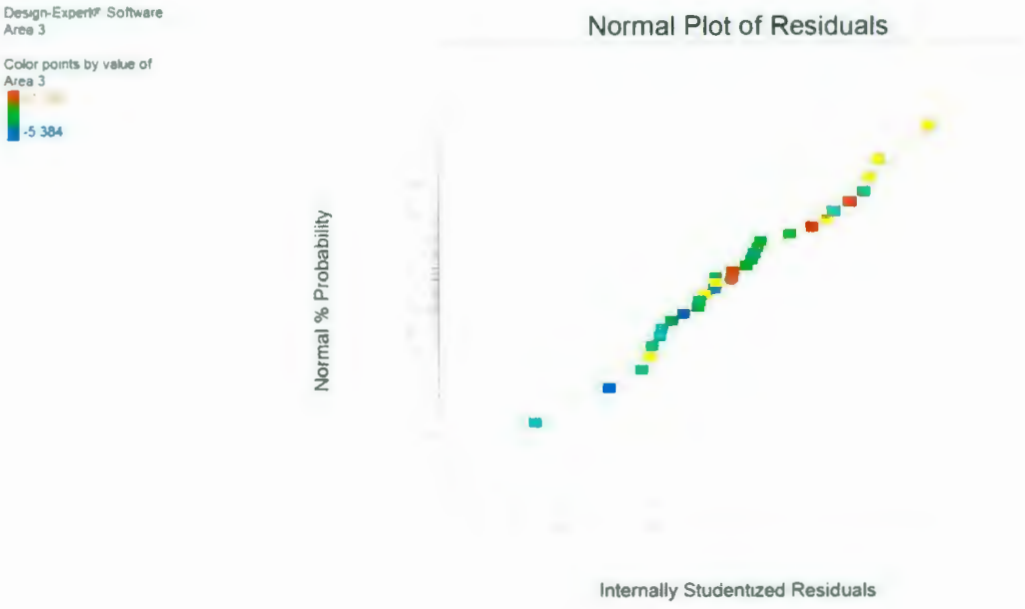

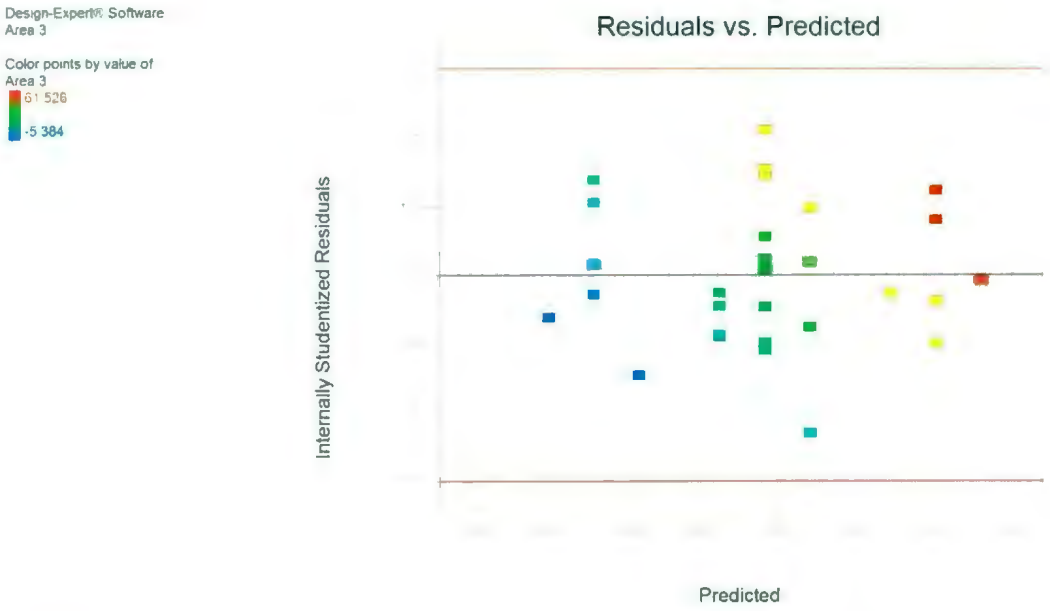
Design-Expert® Software
Area 3
Color points by value of
Area 3
61.526
-5.384
Residuals vs. Predicted
Internally Studentized Residuals
Predicted

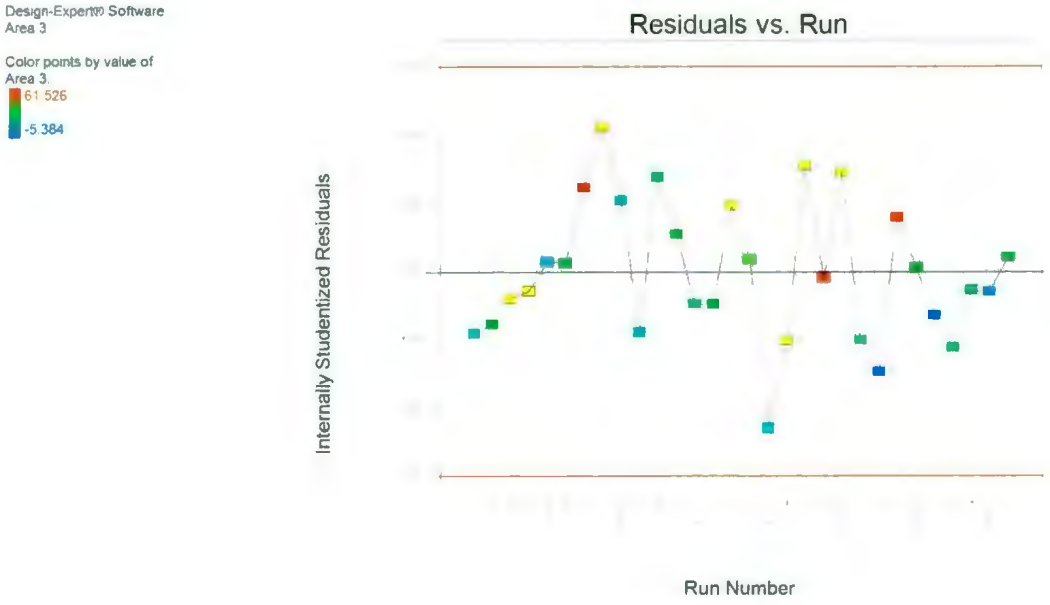
Design-Expert® Software
Area 3
Color points by value of
Area 3
61.526
-5.384
Residuals vs. Run
Internally Studentized Residuals
Run Number